Progressive collapse assessment of structures

By

David Ojonimi Stephen

Submitted in accordance with the requirements for the Degree of

Doctor of Philosophy

The University of Leeds,

School of Civil Engineering

January 2017

Intellectual Property and Publication Statements

The candidate confirms that the work submitted in his own, except where work which has formed part of jointly-authored publications has been included. The contribution of the candidate and the authors to this work has been explicitly indicated below. The candidate confirms that appropriate credit has been given within the thesis where references have been made to previous work of others.

Some of the works presented in Chapter 3 and Chapter 4 of the thesis have been published or currently being reviewed for publication as follows:

Stephen, O.D., D. Forth .J., Lam .D., Ye . J., Konstatinos .T., *Assessment of modeling techniques for progressive collapse evaluation*, Journal of construction steel facility (In view)

Stephen, D., J. Ye, and D. Lam. *Realistic Modelling of High Rise Steel Structures subjected to progressive collapse*. in Thirteenth International Conference on Civil, Structural amd Environmental Engineering Computing. 2011. Civil Comp Press,Stirlingshire UK.

Stephen, O.D., D. Lam, and V.V. Toropov, *Assessment of column removal time for progressive collapse evaluation of high rise structures*, in Research and Applications in Structural Engineering, Mechanics and Computation. 2013, CRC Press. p. 699-704.

Stephen, D., J. Ye, and D. Lam. *Progressive Collapse Evaluation of High Rise Steel Structures due to Sudden Loss of Structural Members*. in 10th International Conference on Advances in steel Concrete Composite and Hybrid Structures. 2012. Singapore.

The work directly attributed to the candidate includes the design, modelling, simulation and writing of the articles while the co-authors review the papers.

The right of David Ojonimi Stephen to be identified as Author of this work has been asserted in accordance with the Copyright, Designs and patents Act 1988.

This work is dedicated in memory of my late sister: Glory Ojima Stephen and in thanksgiving to my saviour Jesus Christ.

The Author

The author is a civil engineer with over ten years of professional research and industry-based experience in steel and reinforced concrete structures.

The author has worked as a design and a Resident Engineer on multiple projects with Jofa and Partners Consultants, Wuye, Abuja. He co-founded a multi-disciplinary consultancy firm: Structland Engineering Consultants, Samaru-Zaria before proceeding for a research degree at the University of Leeds.

He has published research works regarding the reliability-based assessment of structural engineering system using first order reliability method and co-authored some research works in building collapse.

The susceptibility of building structures to progressive collapse is the primary research interest of the author at the School of Civil Engineering, University of Leeds.

Acknowledgement

First of all, I will begin by acknowledging the word of God which gave me the courage to forge ahead amidst all challenges on a journey that seems no end.

Jeremiah 29: 11, the Lord says "for I know the plans I have for you, says the Lord. They are plans for good and not a disaster, to give you a future and a hope". I am forever grateful to the Almighty God.

I would like to express my deep appreciation to my main supervisor: Prof John Forth for his time and the courage in taking responsibility to supervise and ensure the completion of my work. In a special way, I wish to thank my first main supervisor; Prof. Dennis Lam for initiating this research work for his immeasurable continuous support despite his tight schedules.

Special thanks to my supervisory team: Prof. John Forth, Dr Konstantinos Tsavadaris and Prof. Dennis Lam for your unwavering guidance, advice and criticism. I would like to thank Dr Louis Fletcher, Dr Richardson and Prof. Basheer for their co-operation in teaching undergraduate students. Special thanks to Prof. Nigel Smith for the special intervention to support the last phase of my research degree.

I would like to thank my internal and external examiners: Dr Nikitas Nikolaos and Prof. Leroy Gardner respectively for their helpful criticism, guidance and valued opinions towards my thesis.

I would like to express my gratitude to all the individuals who at some point of my research were my primary supervisor: Prof. Dennis Lam, Prof Jianqiao Ye, Prof. Vassili Toropov and currently, Prof. John Forth for their guidance in making this study possible.

Special thanks to Evang. Edward Okaja for being a Father. I am grateful to Julie Oruo, Kenneth Ishiet, Rebekah Matheson, Joshua Ochepo, Faith and Abacha. I acknowledge your friendship in good and in bad times. In a special way, I wish to thank Retired General Salihu Ibrahim for his continual support. Also, special thanks to PTDF, Nigeria for partially sponsoring my research.

To my family, I am most grateful for the sacrifice made throughout the course of my career. Special and unwavering love to Sarah Ufedo-Ojo Stephen and Glory Ojima Stephen.

Abstract

The collapse of buildings over the last century as a result of abnormal loads has renewed interest in the field of structural engineering. Key events such as the disproportionate collapse of the Ronan Point building in London, the collapse of the Alfred Murray Building and the World Trade Centre are structural failures that have triggered more research into progressive collapse. Consequently, new design guidelines around the globe with a prescriptive recommendation for improving structural integrity based on tying force provision have been developed. However, in existing design guidelines and codes throughout the world, there is a lack of a codified modelling technique for progressive collapse. As a result of this limitation, researchers adopt different methods. Generally, during the progressive collapse, structural members experiencing significant displacements and rotations, while the beam-column connections are subjected to large tensile forces not envisaged at the conventional design phase.

Hence, this study presents an assessment of the effect of column removal time, the modelling techniques and the susceptibility of simple connections designed to Eurocode 3 Part: 1-8 to progressive collapse.

A computationally efficient approach and column removal time for progressive collapse assessment are proposed. The findings show that a braced framed system is likely to exhibit at least 35% progressive collapse when compared with a moment resisting frame system using the joint displacement and rotation criteria. Furthermore, the research shows that the UK tie provision in EN1991-1-7 underestimates the magnitude of the catenary force developed under the progressive collapse scenario. Consequently, the connection is disposed to progressive collapse with the shear force in the column and catenary action in the beam as the critical internal forces. Based on this assessment, five times the tensile force specified in EC3 for tensile force connection design checks is recommended. Shear force in the column and catenary force action in the beam are the internal governing forces that determine the maximum dynamic amplification factor of a simple connection. The work provides evidence that the tie beam-column web connection at the corner column is more critical under progressive collapse scenario as compared with the primary beam. Column web failure in yielding is attributed to the large catenary force developed in the tie beam connected to the web of the column.

Table of Contents

The Author ..... **iv**

Acknowledgement ..... **v**

Abstract ..... **vi**

Glossary of Terms ..... **xii**

List of Figures ..... **xiv**

List of Tables ..... **xx**

Chapter 1 General Introduction **1**

1.1 Preamble 1

1.2 Aim and Objectives 4

1.3 Scope of research 4

1.4 Thesis organization 5

Chapter 2 Literature Review **7**

2.1 Introduction 7

2.1.1 Airplane or Vehicular Impact 10

2.1.2 Natural gas explosions 10

2.1.3 Blast loading 11

2.1.4 Earthquake Excitations 12

2.1.5 Extreme Fire 12

2.1.6 Gross human error 13

2.2 Historic landmark building collapse 13

2.2.1 Ronan Point Building 13

2.2.2 Alfred Murrah Building Collapse 15

2.2.3 L' Ambiance Plaza 16

2.2.4 World Trade Centre 17

2.3 Progressive collapse codes and standards 18

2.3.1 General Service Administration 19

2.3.2 Department of Defense (DoD 2005) 20

2.3.3 ASCE Standard 7-05 21

2.3.4 British code provision 22

2.3.5 Canadian code provision 23

2.4 Progressive collapse modelling techniques 23

2.5 Progressive collapse assessment of frame structures 24

2.6 Mitigating progressive collapse 27
2.6.1 Indirect design approach – Tying Force Method 27
2.6.2 Direct design approach 31
2.6.3 Mitigating progressive collapse 31
2.6.4 Energy Based Approach 32
2.7 Research in connection behaviour and performance 32
2.7.1 Double web Angle connections 36
2.7.2 End plate connections (Header, Flush and extended) 36
2.8 Connection models 38
2.8.1 Polynomial Models 39
2.8.2 Power Models 40
2.8.3 Exponential model 40
2.9 Basic connection design review 40
2.10 Review of current state of art in connection design 41
Chapter 3 Progressive collapse modelling methods 43
3.1 Introduction 43
3.1.1 Research assumptions 45
3.2 Structural and material model 46
3.2.1 Study locations on the model 48
3.2.2 Load application (GSA 2003) 48
3.2.3 Removal of Load bearing elements 49
3.3 Concept of sudden column removal 50
3.3.1 Technique one: Sudden removal of internal forces 50
3.3.2 Technique two: Sudden application of gravity loading 51
3.3.3 Technique three: Balancing of gravity to reactive forces 53
3.3.4 Technique four: Opposite applied column forces 54
3.4 Results of column removal time (R_t) on structural response 55
3.4.1 Corner Column Removal Scenario (CCRS) 55
3.4.2 Results of Edge Column Removal Scenario (ECRS) 66
3.4.3 Results of Interior Column Removal Scenario (ICRS) 74
3.4.4 Summary of investigation 80
3.5 Relative evaluation of modelling techniques 81
3.5.1 Evaluation of modelling techniques at (ECRS) scenario 81
3.5.2 Evaluation of modelling techniques at (CCRS) scenario 83

3.5.3 Relative evaluation of modelling techniques (ICRS) 85
3.6 Chapter summary 86
Chapter 4 Assessment of moment resisting frame (MRF) 90
4.1 Introduction 90
4.2 Model description 91
4.2.1 Material description 92
4.2.2 Progressive collapse load combination 92
4.3 Time loading function 92
4.4 Scope of investigation 93
4.4.1 Position one: Corner column removal scenario 93
4.4.2 Position two: Linear static analysis (ECRS) 95
4.4.3 Position three: Static analysis response due to ICRS 96
4.4.4 Position four: Static analysis at EFCRS 98
4.5 Nonlinear static analysis (GSA 2003) 99
4.6 Dynamic analysis investigation 102
4.6.1 Position one: NLD assessment at CCRS 102
4.6.2 Position two: NLD assessment at ECRS 108
4.6.3 Position three: NLD assessment at ICRS 114
4.6.4 Position four: NLD assessment at EFCRS 118
4.7 Multiple column loss scenario (MCRS) 124
4.7.1 Scope of investigation 124
4.7.2 Main beam responses along the long span 126
4.7.3 Tie beam responses due to double column loss (DCRS) 130
4.7.4 Joint response due to multiple column loss 131
4.7.5 Adjacent column responses due to multiple column loss 132
4.8 Dynamic amplification factor 135
4.8.1 Structural member response criteria 136
4.8.2 Beam - column connection response criteria 138
4.9 Chapter summary 140
Chapter 5 Assessment of brace frame system (BFS) 142
5.1 Introduction: 142
5.2 Model description and scope of investigation 143
5.3 Linear static analysis 143
5.3.1 Position one: Static assessment due to CCRS 144

5.3.2 Position two: Assessment due to ECRS 145
5.3.3 Position three: Linear static assessment (ICRS) 147
5.3.4 Position four: Static assessment due to EFCRS 149
5.4 Nonlinear static analysis 151
5.4.1 Nonlinear static analysis at CCRS 151
5.4.2 Nonlinear static analysis at ECRS 153
5.4.3 Nonlinear static analysis at EFCRS 155
5.5 Nonlinear Dynamic analysis investigation 157
5.5.1 Position one: NLD assessment due to CCRS 157
5.5.2 Position two: NLD assessment due to ECRS 161
5.5.3 Position three: NLD assessment due to ICRS 165
5.5.4 Position four: NLD assessment due to EFCRS 174
5.6 Multiple column loss investigation 182
5.6.1 Scope of investigation 182
5.6.2 Catenary beam responses 183
5.6.3 Column responses 184
5.6.4 Joint responses 190
5.7 Chapter summary 191
Chapter 6 Comparison of BRF to MRF 193
6.1 Introduction 193
6.2 Relative comparison of MRF to BFS 194
6.2.1 Eight floor column removal scenario 194
6.2.2 Corner column removal scenario 194
6.2.3 Interior column removal scenario 195
6.2.4 Relative displacement responses 196
6.3 Chapter summary 198
6.4 Basis for chapter seven 200
Chapter 7 Finite element modelling of a typical connection 201
7.1 Introduction 201
7.2 Model validation 204
7.3 Case study connection description 205
7.3.1 Element types 206
7.3.2 Material properties 207
7.3.3 Boundary conditions 208

7.3.4 Contact modelling 208
7.3.5 Loading 209
7.4 Basic investigations 209
7.4.1 Mesh sensitivity analysis 209
7.4.2 Mesh verification analysis 211
7.4.3 Simple connections investigated as case studies 211
7.4.4 Effect of catenary force on connection response 212
7.4.5 Effect of shear force on connection response 213
7.5 Assessment of beam column connection control 216
7.5.1 Stress contours of model used as control 216
7.5.2 Stress contours in beams 219
7.5.3 Stress contours in the bolts 222
7.5.4 Stress contours in plates 227
7.5.5 Stress contours in nuts 231
7.5.6 Stress contours in column 233
7.6 Chapter summary 235
7.7 Basis for chapter eight 236
Chapter 8 Connection assessment under PC scenario 237
8.1 Introduction 237
8.2 Stress contours under progressive collapse scenario 238
8.2.1 Stress contours and column deformation 239
8.2.2 Stress contour in plates 244
8.2.3 Stress contours in beams 246
8.2.4 Stress contours in bolts 249
8.2.5 Stress contours in nuts 252
8.2.6 Chapter summary 255
Chapter 9 Closure to the thesis 256
9.1 Research findings 256
9.2 Proposals for future investigations 257
9.3 Limitations of research 257
9.4 Conclusion and recommendation 258

Glossary of Terms

AF	Axial force response
ASCE	American society of civil engineers
BFS	Braced frame System
BM	Beam
BR	Bracing
CBS	Concentric brace system
CCRS	Corner column removal scenario
CF	Catenary force
C'F	Column flange
CRS	Column removal scenario
COL	Column
D_y	Dynamic load combination
DL	Dead load
DAF	Dynamic amplification factor
DCR	Demand capacity ratio
DCRS	Double column removal scenario
E	Elastic modulus
EBS	Eccentric brace system
ECRS	Edge column removal scenario
EFCRS	Eight floor column removal scenario
F_y	Yield strength of steel
GSA	General Service Administration
G_k	Characteristic dead load
H	Storey height
ICRS	Interior column removal scenario
I	Moment of Inertia
LL	Live load
M_y	Moment about y-axis
M	Moment
MCRS	Multiple Column Removal Scenario
M_{max}	Maximum moment response

MRF	Moment Resisting Frame
M_{jRd}	Moment of resistance
Ms	Static moment response under double column loss
NLS	Nonlinear static analysis
N_s	Static load combination
N_d	Dynamic load combination
θ_y	Rotation about y-axis
P/ P'	Axial force in a member / Axial force after column removal
P_{max}	Maximum axial force response
Ps	Static axial force under double column loss
PC	Progressive collapse
PEEQ	Equivalent plastic strain
Q_{ce}	Ultimate unfactored capacity
Q_k	Imposed Load
Q_{ud}	Acting force demand
Rads	Radian
R_t	Column removal time
R_y	Joint rotational response about y-axis
s	Seconds
S_a	length of time to achieve equilibrium during modelling
S_t	Time at which equilibrium begins after column loss
SF	Shear force response
S_t	Stabilization period
T_i	Internal ties
T_p	Perimeter ties
TFM	Tying force method
V	Shear force
V'	Shear force response after column loss
VM	Von – Mises stress
V_{max}	Maximum shear force response
Vs	Static shear force under double column loss
Z	Section modulus

List of Figures

Figure 2-1 Air blast pressure time history FEMA 427 (2003) 11
Figure 2-2 Partial collapse of Ronan Point Building (Nair 2006) 14
Figure 2-3 Collapse of Alfred Murray Building in United States 16
Figure 2-4 Collapse of world trade centre in United States 18
Figure 2-5 Tie force of a typical frame structure (DoD 2009) 30
Figure 2-6 Illustration of UFC 4-023-03, 2004 tie provision 30
Figure 2-7 Types of joints (Díaz et al., 2011) 33
Figure 2-8 End plate connection types 37
Figure 3-1 3D model of steel building 46
Figure 3-2 Stress strain curve for steel and concrete (SAP 2000) 47
Figure 3-3 Floor plan study locations 48
Figure 3-4 Alternative Path Method (DoD 2009) 49
Figure 3-5 Removal of internal forces suddenly 50
Figure 3-6 Sudden application of gravity loads 52
Figure 3-7 Balancing of gravity to internal forces 53
Figure 3-8 Balancing gravity to internal forces suddenly 54
Figure 3-9 Corner column removal location (CCRS) 55
Figure 3-10 Displacement vs time (Function 1A) 56
Figure 3-11 Rotation vs time (Function 1A) 57
Figure 3-12 Displacement vs time (Function 1B) 57
Figure 3-13 Rotation vs time (Function 1B) 58
Figure 3-14 Displacement vs time (Function two) 59
Figure 3-15 Rotation vs time (Function two) 60
Figure 3-16 Displacement vs time (Function 3) 61
Figure 3-17 Rotation vs time at CCRS (Function3) 62
Figure 3-18 Displacement vs time (Technique four) 64
Figure 3-19 Rotation vs time (Technique four) 65
Figure 3-20 Edge column removal scenario (ECRS) 66
Figure 3-21 Displacement vs time at ECRS (Function 1A) 67
Figure 3-22 Rotation vs time at ECRS (Function 1A) 67
Figure 3-23 Displacement vs time at ECRS (Function 1B) 68
Figure 3-24 Rotation vs time (Function 1B) 68

Figure 3-25 Displacement vs time at ECRS (Function 2) 69
Figure 3-26 Rotation vs time at ECRS (Function 2) 70
Figure 3-27 Displacement vs time at ECRS (Function 3) 71
Figure 3-28 Rotation vs time at ECRS (Function 3) 72
Figure 3-29 Displacement vs time at ECRS (Function 4) 73
Figure 3-30 Rotation vs time at ECRS (Function 4) 73
Figure 3-31 Displacement vs. time at ICRS (Function 1A) 75
Figure 3-32 Displacement of Function 1B vs. time (Technique one) 75
Figure 3-33 Displacement vs time at ICRS (Function 2) 76
Figure 3-34 Rotation vs time at ICRS (Function 2) 76
Figure 3-35 Displacement vs time at ICRS (Function 3) 77
Figure 3-36 Rotation vs time at ICRS (Function 3) 78
Figure 3-37 Rotation vs time at ICRS (Function 4) 79
Figure 3-38 Displacement vs time at ICRS (Function 4) 79
Figure 3-39 Displacement responses for the four techniques 81
Figure 3-40 Relative rotational responses of four techniques 82
Figure 3-41 Displacement responses of techniques (CCRS) 84
Figure 3-42 Joint rotation of different techniques (CCRS) 84
Figure 3-43 Comparing modelling techniques at ICRC 86
Figure 3-44 Displacement responses of different techniques 87
Figure 3-45 Rotational responses of different techniques 88
Figure 4-1 3D elevation and plan view of the model 91
Figure 4-2 The step force function (Tsai and Lin 2009) 92
Figure 4-3 YZ and XZ elevation of model 94
Figure 4-4 XZ and YZ elevation of model at CCRS location 95
Figure 4-5 Elevation of XZ and YZ at ICRS 96
Figure 4-6 Eight floor column removal scenario (EFCRS) 98
Figure 4-7 Nonlinear hinge formation at maximum loads 100
Figure 4-8 Displacement response under load increment 100
Figure 4-9 Rotational response under load increment 101
Figure 4-10 Corner column removal scenario (CCRS) 102
Figure 4-11 Beam responses due to CCRS 104
Figure 4-12 Column responses with time due to CCRS 106
Figure 4-13 Joint response due to CCRS 107

Figure 4-14 Location of perimeter column removal location 108
Figure 4-15 Column responses vs time 110
Figure 4-16 Beam responses vs time (ECRS) 112
Figure 4-17 Joint response vs time (ECRS) 113
Figure 4-18 Descriptive labels of structural members 114
Figure 4-19 Column response vs time 116
Figure 4-20 Catenary force response in beams vs time 117
Figure 4-21 Joint Displacement response versus time 118
Figure 4-22 Eight floor column removal scenario (EFCRS) 119
Figure 4-23 Column response due to EFCRS 120
Figure 4-24 Beam response due to EFCRS 122
Figure 4-25 Joint responses vs time (EFCRS) 123
Figure 4-26 Deformed shape due to double column loss 124
Figure 4-27 Study locations for MCRS 125
Figure 4-28 Labels on multiple column removal scenario (MCRS) 125
Figure 4-29 Beam response to double column loss 127
Figure 4-30 Main beam responses due to DCRS 129
Figure 4-31 Tie beam response 130
Figure 4-32 Joint response for double column loss (DCRS) 132
Figure 4-33 Elevation showing double column removal locations 133
Figure 4-34 Moment response of adjacent columns verse time 135
Figure 4-35 Comparison of axial force response 136
Figure 4-36 Comparison of shear force response 137
Figure 4-37 Comparison of catenary forces in beams 138
Figure 4-38 Summary responses due to NLS and NLD. 139
Figure 5-1 Different type of bracing systems 142
Figure 5-2 Description of corner CCRS 144
Figure 5-3 Description of ECRS 146
Figure 5-4 Description of ICRS 148
Figure 5-5 3D elevation and labels of the structure 150
Figure 5-6 Beam responses at incremental loading (CCRS) 151
Figure 5-7 Column responses at incremental loads (CCRS) 152
Figure 5-8 Joint response due to CCRS 153
Figure 5-9 Nonlinear static column response under (ECRS) 155

Figure 5-10 Nonlinear static column response due to EFCRS 157
Figure 5-11 BM catenary force response due to CCRS 158
Figure 5-12 Force responses in columns due to CCRS 159
Figure 5-13 Shear force vs time in columns (CCRS) 159
Figure 5-14 Axial force responses in columns due to CCRS 160
Figure 5-15 Catenary force response in beams 161
Figure 5-16 Axial force response of the brace members 162
Figure 5-17 Axial force responses of columns due to ECRS 163
Figure 5-18 Column shear force response of BFS 163
Figure 5-19 Moment response in columns due to ECRS 164
Figure 5-20 Deformed shape and elevation planes due to ICRS 165
Figure 5-21 Shell element stress convention SAP 2000) 166
Figure 5-22 SAP 2000 stress definition along a shell (SAP 2000) 167
Figure 5-23 DAF vs number of storey using shell stresses 169
Figure 5-24 Catenary force response due to ICRS 170
Figure 5-25 Shear force response due to ICRS 170
Figure 5-26 Axial force response in columns due to ICRS 172
Figure 5-27 Shear force response in columns due to ICRS 172
Figure 5-28 Moment response in interior columns due to ICRS 173
Figure 5-29 Stress distribution and label description under ECRS 174
Figure 5-30 Principal stresses vs time at top of shell 175
Figure 5-31 Principal stresses vs time at bottom of shell 176
Figure 5-32 Principal shear stresses vs time at shell top surface 177
Figure 5-33 Catenary force (kN) vs time at EFCRS 178
Figure 5-34 Column axial force (kN) vs time 179
Figure 5-35 Column shear force (kN) vs time 179
Figure 5-36 Column moment (kNm) vs time response 180
Figure 5-37 Maximum joint displacement (mm) vs time 181
Figure 5-38 Maximum joint rotation (rads) vs time 181
Figure 5-39 Description of model and case study 183
Figure 5-40 Catenary force responses under double column loss 184
Figure 5-41 Column axial force response above removed column 184
Figure 5-42 Column shear force vs time 185
Figure 5-43 Moment response of columns vs time 186

Figure 5-44 Plan layout of double column assessment 187
Figure 5-45 Column axial force response (kN) 188
Figure 5-46 Shear force response (kN) 188
Figure 5-47 Moment force response (kNm) 189
Figure 5-48 joint responses due to multiple column loss 190
Figure 5-49 Rotational responses due to multiple column loss 191
Figure 6-1 Comparison of joint displacement response 197
Figure 6-2 Comparison of joint rotational response 198
Figure 7-1 Connection geometric deformation 204
Figure 7-2 Experimental and FEA under CRS. 205
Figure 7-3 3D representation of the control model 206
Figure 7-4 Mesh sensitivity analysis 210
Figure 7-5 Failure criteria checks (ABAQUS 2011) 211
Figure 7-6 Meshing of end plate beam column connection 212
Figure 7-7 Stress contours under catenary force 213
Figure 7-8 Connection response under shear force 214
Figure 7-9 Shear stress contours on plane x-y 215
Figure 7-10 Shear stress contour along x-z plane 215
Figure 7-11 Shear stress contour plots on y-z plane 216
Figure 7-12 VM stress state of the connection 217
Figure 7-13 Stress state contours under static conditions 218
Figure 7-14 Stress state contours under static conditions 218
Figure 7-15 VM stress state contour under initial conditions 219
Figure 7-16 Principal stress contour (S22) 220
Figure 7-17 Principal stress contour under static conditions (S11) 220
Figure 7-18 Stress vs strain components for main beam 221
Figure 7-19 Stress components vs strain for tie beam 221
Figure 7-20 VM stress state for the bolts at CF and CW 222
Figure 7-21 Principal stress state of bolts (x-x) 223
Figure 7-22 Principal stresses at C'F and CW respectively (y-y) 224
Figure 7-23 Principal stress state of bolts at C'F and CW (z-z) 225
Figure 7-24 Stress vs strain for bolts at column web 226
Figure 7-25 Stress vs strain for bolts at column flange 226
Figure 7-26 VM Stress contours in plates at C'F and CW 227

Figure 7-27 Principal stresses at C'F and CW (S11) 228
Figure 7-28 Principal stresses at C'F and CW (S22) 228
Figure 7-29 Stress components vs strain of plate at column web 229
Figure 7-30 Stress components vs strain of plate at the flange 230
Figure 7-31 Plastic strain distribution in plates 230
Figure 7-32 Von - Mises stress contours in bolts 231
Figure 7-33 Von- Mises stress contours in nuts at column web 232
Figure 7-34 Stress components vs strain in nuts at the flange 232
Figure 7-35 Stress components of the column 233
Figure 7-36 Stress components vs strain in column 234
Figure 7-37 Stress responses of connection used as control 235
Figure 8-1 VM stress plots with equivalent plastic strain 238
Figure 8-2 Buckling behaviour of column under PC scenario 240
Figure 8-3 Stress and strain contour plots (PC) 241
Figure 8-4 Tensile and shear stress components under PC 243
Figure 8-5 VM stress contours of the plates under PC 244
Figure 8-6 Tensile stress distribution (S11) under PC 245
Figure 8-7 Tensile stress response (S22) under PC 245
Figure 8-8 Plastic strain redistribution plots 246
Figure 8-9 VM stress contours of beams connecting the column 247
Figure 8-10 Plastic strain distribution under PC scenario 247
Figure 8-11 Tensile stress contours distribution (S11) in beams 248
Figure 8-12 Tensile stress contours distribution (S22) in beams 248
Figure 8-13 Von Mises stress redistribution for the bolts 250
Figure 8-14 Plastic strain distribution for the bolts 250
Figure 8-15 Tensile stress component (S22) 251
Figure 8-16 Component tensile strain in the bolts 252
Figure 8-17 VM stress response of the nuts under PC 253
Figure 8-18 Tensile stress component (S11) 253
Figure 8-19 Tensile stress component (S22) 254
Figure 8-20 Plastic strain contour plots in nuts 254

List of Tables

Table 4-1	**Section sizes for the investigation**	**92**
Table 4-2	**Redistribution of forces due to CCRS**	**94**
Table 4-3	**Removal of edge column (Column 31)**	**96**
Table 4-4	**Interior column removal scenario (COL 141)**	**97**
Table 4-5	**Static response due to EFCRS**	**99**
Table 4-6	**Static response under multiple column loss**	**133**
Table 5-1	**Member response under CCRS**	**145**
Table 5-2	**Member response due to ECRS**	**146**
Table 5-3	**Member response due ICRC**	**148**
Table 5-4	**Member responses due to EFCRS**	**150**
Table 5-5	**Stress redistribution and DAF for shell assessment**	**168**
Table 5-6	**Stress redistribution of shells due to EFCRS**	**177**

Chapter 1 General Introduction

1.1 Preamble

The planning and conceptual design stage of building structures require the right choice of structural frame configuration and construction materials in delivering an efficient building that meet clients requirements. These expectations are often challenging in a competitive design environment where an optimal performance of the structure at minimum cost is required. In high-rise structures, the steel frame structure is crucial in ensuring the overall safety of the occupants and the performance of the structure under service and abnormal conditions. The choice of the frame structure is often guided by time, cost, conservatism in adapting to new technologies, stakeholders involvement and building regulations. This important structural system of the building determines the overall performance of the structure under service conditions and abnormal loading conditions. At the conventional design phase of a high-rise building, estimation of characteristic dead, live and wind loads are done using design guidelines and engineering judgment to present an efficient design. The concept is based on the limit state design philosophy correlating the capacity to the demand response of the members. Over the last century, there has been catastrophic building collapse due to the failure of critical structural members causing death and injuries; a phenomenon tagged as "progressive collapse".

According to Edmund Burke (1729-1797) "Those who ignore history are bound (or doomed) to repeat it". Lessons learned from tragic building collapses created public concerns on structural safety and paved way for progressive collapse investigations. Consequently, major codes and design guidelines around the globe were reviewed, and new ones produced. This has led to a series of conference discussions, workshops and research interest in a progressive collapse. The subsequent paragraphs define terms associated with the progressive failure of building structures.

Progressive collapse: There is no unique definition accepted by all codified body and researchers on the term 'progressive and disproportionate collapse'. The design guideline (GSA 2003b) for progressive collapse assessment defines it as, "a situation where a local failure of a primary structural component leads to the collapse of adjoining members which,

in turn, leads to additional collapse". Other definitions of progressive collapse can be referenced in Gross and McGuire (1983).

Disproportionate collapse

Starossek and Haberland (2009) states that "if there is a pronounced disproportion between a comparatively minor event and the ensuing collapse of a significant part or even a whole of a structure, then this is a disproportionate collapse." This attempt is to define what constitutes 'disproportionate collapse'. Unfortunately, this definition is incomplete and subjective since the yardstick for relative comparison between the event, and the failure region isn't defined. In the existing literature, an attempt has been made by researchers to distinguish progressive collapse from disproportionate collapse as all disproportionate collapse are progressive; however not all progressive collapses are disproportionate (Agarwal and England 2008).

Structural robustness

The design guideline (EN1991-1-7:2006) defines Robustness as "The ability of a structure to withstand events like fire, explosions, impact or the consequences of human error without being damaged to an extent disproportionate to the original cause." On the other hand, GSA (2003) defines it as "Ability of a structure or structural components to resist damage without premature and/or brittle failure due to events like explosions, impacts, fire or consequences of human error, due to its vigorous strength and toughness." From the energy perspective, a significant amount of energy is induced on the structure within a short period if it is subjected to impact or blast. The ability of the structure to absorb and redistribute the energy safely depends on the degree of robustness of the entire structural system. In an attempt to dissipate such energy within a short period, the structure responds suddenly to the triggering event in seeking a new equilibrium state. Discussion on structural robustness can be found in Biondini et al. (2008) and Formisano et al. (2015).

Structural resilience

Structural resilience is the ability of the structural system to mitigate the effects of an extreme load and minimise the recovery needed to restore functionality. The three important considerations for building functionality focus on the system's ability to resist, adapt to, and to recover from exposure to different hazards. Consequently, resilience is a function of resistance, adaptation and recovery of a structural system after been subjected to hazards (Baker et al. 2008).

Rationale behind the study

This thesis addresses issues that have been neglected in previous studies on progressive collapse of structures. In a progressive collapse, building assessment are moving towards threat-independent load cases for design (e.g. single column removal with reduced gravity loads). One of the key observation in the guidelines and codes around the globe is that it recommends that all structures should not be susceptible to progressive collapse. On the contrary, there is no provision on how to explicitly carry out a quantifiable performance-based approach to achieving that recommendation. As a result, researchers adopt different modelling techniques to assess a structural performance under progressive collapse scenario. Another important consideration is to understand the behaviour and performance of simple connection under sudden column loss as observed by Ellingwood and Dusenberry (2005).

Hence, this thesis presents an assessment of beam-column connection designed to the provision of Eurocode 3 for progressive collapse scenario. A typical building model was evaluated for the effect of column removal period on structural response. The outcome of the studies resulted in a proposal which correlates column removal time to the period of the structure in the vertical vibration mode. Since different modelling techniques exist in literature, a comparison of commonly used methods was carried out and a recommendation made for progressive collapse evaluation. Following this, a moment resisting frame structure was compared to a braced frame structure under progressive collapse scenario. The critical response from the comparison of the structural configurations was used to evaluate beam-column connection designed to Eurocode 3. A discussion of the responses of simple beam-column behaviour designed to EC3 is presented and recommendations made for design considerations for progressive collapse.

1.2 Aim and Objectives

The aim of this research is to '*Assess the behaviour of steel structures due to progressive collapse*'

The objectives of the research are:

- To review the current research state in progressive collapse (Chapter 2).
- To investigate the effect of column removal time and modelling techniques on progressive collapse (Chapter 3).
- To determine the internal force redistribution and the dynamic effect of sudden loss of structural element on moment resisting frame structure (Chapter 4).
- To investigate the internal force redistribution of braced frame structure and to assess the dynamic effect of sudden column loss on brace system (Chapter 5).
- To compare the response of moment resisting frame (MRF) to the braced frame structure (BFS) (Chapter 6).
- To establish the state of stress of simple connection designed to the requirements of Eurocode 3 Part: 1-8 using ABAQUS finite element code (Chapter 7).
- To investigate the behaviour of simple connection under progressive collapse scenario (Chapter 8).
- To propose strategies for improving structural integrity under abnormal loading conditions (Chapter 9).

1.3 Scope of research

The assessment presented in this thesis is limited to a ten storey steel building structure having a regular span. The evaluation of the frame structure focuses on the joint displacement responses and the redistribution of internal forces as a result of sudden column loss. Geometric and material nonlinearity occurs on structures undergoing large deformation due to excessive load. To account for this, P-delta plus the large displacement is recommended in SAP 2000 manual. A damping factor of 5% and a column removal time of 2ms is assumed for this study (Fu 2012; Mark Adom-Asamoah and Ankamah 2016). Evaluation of the dynamic effects was limited to GSA 2003 provisions using SAP 2000, while the beam-column connection design was carried out using Eurocode 3 Part 1-8. Detail finite element assessment of the validated beam-column connection was carried out using the ABAQUS software.

1.4 Thesis organization

This thesis is structured into nine chapters with each chapter focusing on a particular objective. The scope of the research, aim and objective of the thesis are included in the introductory chapter. Each chapter begins with a brief introduction into what is expected and at the end of each chapter, brief highlights to the subsequent chapter are presented.

Chapter 1 This introductory chapter presents a basic information on the thesis structure, content, scope and research focus.

Chapter 2 This section critically reviews research in progressive collapse over the last century, important findings and progress made. Also, events that triggers progressive collapse and some historic building collapses are discussed. At the end of the literature review, a summary of knowledge gap is presented which holistically defines the basis for this research investigation.

Chapter 3 This section of the thesis addresses some of the key concerns in design codes and guidelines around the globe. That is, the column removal time for progressive collapse assessment and the modelling technique that captures the sudden column loss. The author has published the relative evaluation of modelling techniques and the impact of column removal time (Stephen et al. 2011; Stephen et al. 2013). Conclusion from chapter three is used in subsequent chapters to model sudden column loss.

Chapter 4 This chapter presents an assessment of moment resisting frame structure under column removal scenario. Part of the results were presented at an international conference and published in the conference proceedings (Stephen et al. 2012).

Chapter 5 This chapter presents an investigation into the behaviour of braced frame system under column removal scenario. A study on the internal force redistribution of the structure under instantaneous column loss scenario is presented.

Chapter 6 This chapter compares the response of the moment resisting frame structure in chapter 4 to that of braced frame system in chapter 5. Percentage increments in the internal forces were compared and a basis for connection design and assessment using finite element code was established.

Chapter 7 This chapter focuses on the validation of the simple connection designed to Eurocode 3 using ABAQUS finite element software. Detailed assessment of the control model is established in this section as a baseline study.

Chapter 8 This chapter presents an assessment of the beam column connection under progressive collapse scenario.

Chapter 9 This last chapter summarises and discusses the results of the investigations carried out. Recommendation for future work, conclusion and limitations were highlighted.

Chapter 2 Literature Review

2.1 Introduction

Structural safety has been the core consideration in the design of high-rise structures as compared to economy, aesthetics, durability and sustainability. To produce an effective design in a competitive environment considering limited resources, structural engineers incorporate structural optimization techniques to ensure the most efficient design at minimal cost. Safety factors in conventional design account for minimal variation in material strength and load estimation, however, this does not account for extreme loads such as blast or extreme fire.

Progressive collapse became an imperative field of structural engineering after the disproportionate collapse of Ronan Point Building in 1968, Alfred Murrah building in 1995, and the collapse of the World Trade Centre in 2001 (Stevens et al., 2011). Interest in this field of study was motivated by the disproportionate collapse of Ronan Point Building in 1968 due to a gas explosion. This event resulted in an immediate review of codes and the development of new building regulations and standards around the world (DoD 2005; GSA 2003; CEN 1994). Research works on progressive collapse and strategies to mitigate progressive collapse have been reviewed by Ellingwood (2006). A critical aspect of primary concern to the global engineering community is the disproportionate collapse of structures since all structural collapse are progressive.

In practice, structural designers are reluctant to perform nonlinear dynamic analysis due to its perceived complexity. To address this problem, the equivalent static option of predicting the dynamic response using conservative recommendations is a preferred choice. The guidelines GSA 2003 and UFC 2005 recommends an independent threat approach, which requires removal of a single column at a time with the expectation that the structure bridges over the removed column safely. That can only be achieved if the structure is capable of redistributing the resultant load from the removed column via the connections to other structural members. One of the most important considerations in mitigating progressive collapse is the performance of the connections, structural integrity provisions, the redundancy provision and the continuity between members. The strength, ductility and rotational stiffness of the connections significantly affect the deformation of the joint and the development of the catenary force in the beams.

Concept of progressive collapse: In recent times, high-rise structures are subjected to abnormal loads far beyond their design strength which often results in either partial or total collapse disproportionate to the initiating event. This is of primary importance to the engineering community engaged in investigating the complex mechanism in the chain transmission of failure from one structural member to another via connecting devices. The term progressive collapse can be described as a chain transfer of localised failure from one structural member to another resulting in partial or total collapse. The American Society of Civil Engineers (ASCE Standard 7-05), defines progressive collapse as "the spread of initial local failure from element to element resulting, eventually, in the collapse of an entire structure or a disproportionately large part of it (SEI/ASCE 7-05). The standard recommends that buildings should be designed "to sustain local damage with the structural system as a whole remaining stable and not being damaged to an extent disproportionate to the initial local damage."

Progressive collapse, as defined by Khandelwal et al. (2008) is a complex dynamic process wherein a collapsing system seeks alternative load paths to survive a loss of a critical structural member". Progressive and disproportionate collapses are events that are not common, however, whenever it occurs, it has catastrophic consequences. One of the earliest definitions to progressive collapse was by Ellingwood. B.R and Leyendecker E. V (1978) defines it as a chain reaction type of failure which follows damage to a relatively small portion of a structure. Nair (2006) defines progressive collapse as collapse of all or large part of a structure precipitated by failure or damage of a relatively small part of it. According to Kim and Kim (2009b), progressive collapse is a series of failures that leads to a partial or total collapse of a structure. According to Ellingwood (2006), "progressive collapse of a building is initiated by an event that causes local damage that the structural system cannot absorb or contain, and that subsequently propagates throughout the structural system, or a major portion of it, leading to a final damage state that is disproportionate to the local damage that initiated it." This definition is similar to the one presented by Yu et al. (2010) which states that "progressive collapse occurs when an initiating local failure spreads from element to element, eventually resulting in collapse of a disproportionately large or entire part of a structure.". On the other hand, Vlassis et al. (2006) stated that progressive collapse occurs in a structure that lacks continuity, ductility, and redundancy to resist an initial damage due to extreme loading. Dusenberry and Hamburger (2006) explains the mechanism of building collapse as a dynamic phenomenon in which kinetic energy is introduced into the structure while the inelastic strain energy accumulated within the structure strives to arrest the downward motion due to instantaneous loss of structural members.

The authors argued that the potential for structural collapse will be prevented if the energy absorbed by the structure exceeds the change in potential energy due to instantaneous column loss. In view of this argument, mathematical equations were derived from first principle correlating the strain energy, potential energy and kinetic energy. Collapse occurs if the remaining structural element lacks sufficient strain energy in arresting the motion of the structure to rest as it seeks a new equilibrium position. The energy-based approach is aimed at tracking the amount of energy released due to the collapsing mass relative to the amount of energy absorbed by the structure. Emphasis on the need to further investigate the stored strain energy for assessing the tendency of disproportionate collapse of structures was highlighted. One of the main advantages of this approach is that it does not require the load amplification factor to account for the dynamic effect because it can capture the dynamic effect approximately.

The British code (CEN 1994) does not consider progressive collapse explicitly, the provision was based on accidental actions on structures and the robustness of structures in mitigating accidental loads. Therein, it defines robustness as " the ability of a structure to withstand events like fire, explosions, impacts, or the consequence of human errors, without being damaged to an extent disproportionate to the original cause". This definition is not based on failure transmission as in ASCE Standard, but the performance of the structure in mitigating abnormal load due to unforeseen events relative to the triggering event.

This definition of progressive collapse incorporates the comparison between localized failure and the aftermath of the event. However, not all progressive collapse is disproportionate, and it is possible to have progressive collapse with the total collapse not been disproportionate to the localised failure. The National Institute of Standards and Technology (NIST) defines it as "the spread of local damage, from an initiating event, from element to element, resulting, eventually, in the collapse of an entire structure or disproportionately large part of it; this is also known as disproportionate collapse" NIST (2007).

It is important to note that some of the definitions given by various codes and standards stipulate what constitute disproportionate collapse by stating limits of the collapsing floor area.

Abnormal loads could result from extreme fire, bomb detonation, explosions and gross human error beyond far beyond the designed margin. It is no doubt that disproportionate collapse has catastrophic consequences at times leading to death.

This is a primary concern to the engineering community investigating the complex mechanism involves in chain transmission of failure from one structural member to another via connecting devices. Currently, engineers consider progressive collapse design criteria due to lessons learnt from previous structural failure because of its devastating consequences. Previous building collapses due to abnormal loading conditions has led to the code review and the development of new design guidelines. Some accidental loads are discussed below.

2.1.1 Airplane or Vehicular Impact

Accidental loads described in Eurocode 1, Part 1-7, Section 4 (CEN 1994) covers various aspects of unexpected impact due to vehicles, ship traffic, lift trucks, canal trucks, and helicopters. Effect of impact due to aircraft and vehicles on buildings is of primary concern in investigations of progressive collapse due to this form of actions. Studies on the impact of aeroplanes on concrete structures can be found in Arros and Doumbalski (2007).

At impact, a moving body such as a plane induces a significant amount of force on the structure over a short period. In order words, a moving body possesses momentum which when impacted on a building result in transmission of local failure from one point to another. Such a chain transmission of failure through structural members and connections could lead to a progressive collapse of the building. The mechanism of the impact on a structure is also a complex phenomenon. The kinetic energy of a moving object can be transferred into a different form of energy and elasto plastic deformation of the building structure and the colliding object. Vlassis et al. (2009) propose a new design-oriented methodology to assess the impact of falling floors on a lower level based on the kinetic energy of the impacting floors.

2.1.2 Natural gas explosions

As observed by Ellingwood (2006) the collapse of Ronan point building indicates that the gas pressure depends on two factors: compartment venting and resonance of air mass within the compartment. The gas pressure exerted does not exceed 17kPa, though less than 34kPa for abnormal loads recommended by most standards and guideline around the world.

2.1.3 Blast loading

Increase in terrorism has resulted in the death of thousands of people across the globe. This is a global challenge and researchers are seeking to develop a performance-based approach to which designs can perform optimally during such unforeseen events. The effect of a car bomb explosions could result in the sudden damage of a critical vertical load-bearing member which could potentially trigger a progressive collapse. A typical case in history was the collapse of Alfred Murrah building in which the column at the base supporting three other columns was destroyed due to a car bomb. Consequently, the transfer girder was subjected to loads beyond its carrying capacity triggering a complex load distribution mechanism resulting in the collapse of the building.

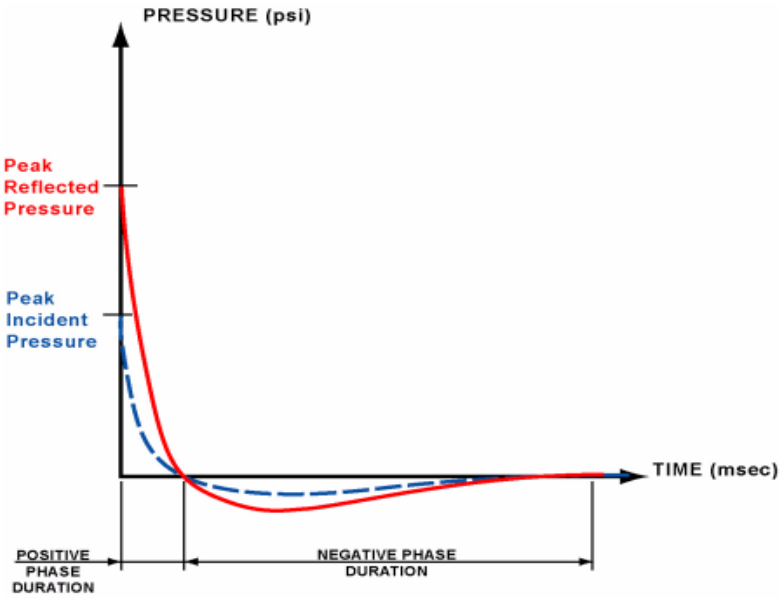

Figure 2-1 Air blast pressure time history FEMA 427 (2003)

Given this challenge, three basic approaches are used effectively to thwart terrorist activities on building. The three methods are gathering intelligence, access control and hardening. The research community is interested in the access control and hardening process. A typical pressure distribution plot from an explosive is shown in Figure 2-1. The positive phase duration indicates the arrival time at which a peak value of overpressure occurs over the ambient pressure. The pressure then decays to ambient level at a period where the curve intersects the time curve to the negative phase duration. Research work on the behaviour, response and mitigation of blast loads on the structural system can be found in the following: Choi et al. (2007) and Lee et al. (2007).

2.1.4 Earthquake Excitations

Some regions of the world experiences different earthquakes of varying magnitudes. The consequence of an earthquake is enormous; it causes injuries, death, fear and uncertainty. There is a fundamental difference between structural response due to earthquake and progressive collapse (Simões da Silva et al. 2001; Dusenberry and Hamburger 2006). Although to limit progressive collapse phenomenon, some studies (Bao et al. 2008; Khandelwal et al. 2008; Kim et al. 2009; Park and Kim 2010) show that structures are less prone to progressive collapse designed as a seismic structure. For a realistic simulation, some authors recommend the inclusion uncertain material properties in design concepts as noted by Park and Kim (2010). Some authors Jeong and Elnashai (2007); Hueste and Bai (2007) apply probabilistic concepts in earthquake engineering to assess structural susceptibility to progressive collapse.

2.1.5 Extreme Fire

Over the last three decades, there has been an improved understanding of the effect of extreme temperature and fire on the behaviour of structural members as found in Agarwal and Varma (2014). Given that, simplified analytical models were developed by researchers under fire conditions Simões da Silva et al. (2001).Structural design against fire is aimed to prevent structures from disproportionate collapse due to fire and to ensure that occupants and firefighters can safely escape from the building without been trapped inside. The protection of a structural building from fire is considered using the non-structural means of protection. Fire has an adverse effect on structural engineering systems because it reduces the stiffness and strength of structural members over a given period. This result in a loss in the load carrying capacity of a given structural member or a system when subjected to compartmental fire. Some researchers showed that advanced structural analysis can adequately replicate the behaviour of structures during fire Bennetts and Thomas (2002). The building regulation specifies the level of fire protection required as a function of time. This depends on the functionality of the building, its height, and considerations for sprinklers or not. Series of full-scale fire test carried out at Cardington (UK) is currently used as a basis for validating current research works. The findings from the experiment indicate that composite frame structures possess reserve strength through large deformation and catenary action in a slab with the development of tensile membrane behaviour in slabs (Fu 2012;

Abruzzo et al. 2006). Current research works focusing on the effect of fire on the progressive collapse of high-rise structures can be found in the following publications (Neal et al. 2012).

2.1.6 Gross human error

The earliest written code is dated to 2200 B.C, titled the Code of Hammurabi which was based on the principle of jungle justice and it states "If a building collapses and kills the occupant of the house, the builder shall be put to death". Gross human errors could occur at the planning, design and construction phase of the project. This could have a devastating effect on the performance of the building and in the worse scenario collapse. Human errors occur when a wrong concept, principle, or assumption is applied at the design stage to address an engineering problem. At times, poor technical workmanship and lack of strict supervision and quality control could result in the partial or total collapse of the building.

2.2 Historic landmark building collapse

A detailed technical review on some of the critical structural building collapse over the last century has been published in Nair (2006).

2.2.1 Ronan Point Building

This building is one of the most referenced structures in existing literature when describing the concept of progressive and disproportionate collapse. Interest in the progressive collapse was attributed to the partial collapse of Ronan Point Building in 1968 in London (Humay and Baldridge 2005; Nair 2006).

According to the paper published by Pearson and Delatte (2005), Ronan Point apartment building was constructed using Larsen – Neilson system developed in Denmark in 1948. The key advantage of this technology is that it limits wet works on site, saves construction time and to ensure quality control of precast structural load bearing members. The choice of this technology gained attention primarily because the demand for buildings in London was on the high side after the Second World War. Another key challenge faced in the construction industry is the migration of workers to factories where safer and easier jobs were available.

The building was a 22 storey building; the construction began on 25th July 1966 and was completed on 11 March 1968. Partial collapse of the building took place on the 16 May, 1968

which resulted in the death of four people with seventeen others been injured. The loss of lives would have exceeded this number if the residents were in at the time this event took place considering the magnitude of the disaster (Pearson and Delatte 2003; Pearson and Delatte 2005)

Griffiths (1968) presented a report attributing the collapse to a gas explosion which initiates progressive collapse. In that report, the nut has been fractured by over-tightening during the cause of installation and the hose linking the stove to the gas would have failed by a force of 1.6kN (360 pounds).

Furthermore, the technical report by Griffiths (1968), the collapse of Ronan point building, a wind of 100kPh (63mph) based on the code issued in 1952. These does not accurately represent the wind pressure of 170kPh (105mph) anticipated at two hundred feet above the ground every sixty years within the lifespan of the tower. The code was not reviewed to meet up with current requirements based on the publications made in 1963 by National Physical Laboratory Griffiths (1968). Further inquiry into the collapse of the building reveals the limitation of the structure in meeting up with fire requirements.

Figure 2-2 Partial collapse of Ronan Point Building (Nair 2006)

Figure 2-2 shows the collapsing section of Ronan Point Building from different views. The collapse of this building was attributed to lack of structural redundancy, lack of alternative load path and poor workmanship.

The structural integrity of the building was questionable considering the reports and test conducted after the partial collapse of the building. This resulted in a step by step demolition approach to study the damage further in May 1986. Considering the limitations of the code at that time to address progressive collapse, building codes were reviewed to account for unforeseen events and the Fifth Amendment to the building regulations in Britain in 1970 was introduced.

2.2.2 Alfred Murrah Building Collapse

One of the deadliest man-made disasters that created awareness on acts of terrorism in the United States is the collapse of Alfred Murray Federal Building on April 19, 1995. The design and construction of the building took place between 1974 and 1976; it is a nine storey reinforced concrete structure. The destruction was carried out by terrorists when a truck of bomb containing ammonium nitrate and fuel oil bomb was positioned at the base of the building which damaged three critical columns Osteraas (2006). The loss of the columns resulted in the failure of the transfer girder supporting other columns which uphold the floors above it. This chain transmission of failure led to the general collapse of the building (Nair 2004).

As reported by Corley et al. (1998) and Osteraas (2006), the structural form of Alfred Murray building was made up of a reinforced concrete ordinary moment resisting frame system with a dimension of approximately 220ft (67m) long in the east-west direction and 30.5m in the north-south direction. The floor height was 3.96m (13ft) from the third to the eight floors while the ninth floor has a floor height of 4.27m. The floor had a thickness of 152mm spanning one-way while the transfer girder had a width of 1220mm wide by 508mm deep beams. According to Osteraas (2006) the structural layout consists of columns on a 6.1 x10.7m grid supporting a beam and floor system.

Team experts from American Society of Civil Engineers (ASCE), Federal Emergency Management Agency (FEMA), US Army Corps of Engineers, General Service Administration (GSA), the National Institute of Standards and the Federal government engineers were deployed to critically examine the collapse of Alfred Murrah building due to blast loading. A detailed investigative report has been presented by some researchers Sozen et al. (1998).The findings indicate that the blast was equivalent to the detonation of 4000lbs of TNT, and the failure of the structure was attributed to a shear failure of critical columns resulting to progressive collapse mechanism as compared to the direct effect of the blast.

Progressive collapse would have been mitigated if spiral reinforcement were used in the critical columns on the first floor and continuous reinforcement used in all transfer girders.

Figure 2-3 Collapse of Alfred Murray Building in United States

The collapse of Alfred Murray Building was a typical illustration of progressive collapse due to an unforeseen event which induces abnormal loading condition on the structural system. (Nair 2004) argue that the failure was progressive, although disproportionate to the triggering event considering the magnitude of the destruction while others are of the opinion that it was progressive. Alfred Murray Building was not designed for energy absorption capabilities such that the amount of energy from the bomb detonation could be compared to the amount of energy to which it was originally designed for.

2.2.3 L' Ambiance Plaza

The collapse of L' Ambiance building in Bridgeport, Connecticut in 23 April 1987 occurred during the construction stage. It is a 16 storey building. The vertical load bearing members are steel columns which support pre-tensioned concrete slab. The building of the floor slabs requires a step by step positioning of the floor temporarily at intermediary levels. Unfortunately, local failure occurs at the top west wing which triggered progressive collapse due to the impact of falling slabs resulting in the collapse of the East wing. It is argued that the breakdown of the structure is disproportionate when the total collapse of the structure is compared to the initial local damage.

2.2.4 World Trade Centre

The collapse of the World Trade Centre (twin tower) on 11th September 2001 is one of the deadliest acts of terrorism that shocked the entire world within the last decade. The building collapse due to aircraft impact and extreme fire, although the north and south towers were able to withstand the impact for 102 and 56mins respectively during which some lives were saved (Wada et al., 2004). All tall buildings are subjected to some level of risk and uncertainties, designing tall buildings to withstand a gross terrorist attack such as the World Trade Centre collapse are practically impossible considering limited resources. Some researchers are of the view that the World Trade Centre performs optimally (Mlakar 2005); the impact of the aircraft on the building is within the safety margin of design Bažant and Zhou (2002). The collapse of the World Trade Centre does not fit into the definition of progressive collapse as argued by Mohamed (2006). Other notable research on the collapse of world trade centre can be found in literature (Usmani et al.,2003).

World Trade Centre 7

The collapse of World Trade Centre 7 is a typical example of progressive and disproportionate collapse as argued by Shankar Nair 2006. The building was a 47 story building close to the location of the twin tower. Progressive collapse began after the heated interior column lost its ability to withstand the gravity load it supports, with failure extending beyond the floor areas supported by the column. This resulted to total collapse of the structure.

Figure 2-4 Collapse of world trade centre in United States

If the collapse had been localised to the floors supported by the heated column alone, it should have been labeled progressive but proportionate. However, the failure of the interior column due to extreme fire resulted to total collapse of the structure with propagation of horizontal failure mechanism resulting in disproportionate collapse (Nair 2006).

2.3 Progressive collapse codes and standards

In recent times, series of design guidelines around the world are developed due to the catastrophic consequences of progressive collapse, particularly in the United States (GSA 2003; CEN 1994; DoD 2005). Currently, progressive collapse is considered in the planning, design and construction phase of new projects with high economic and political importance. Most of the design guidelines and codes propose different loading combinations; however, the universal concept found in all the provisions is the introduction of alternative paths in case of load redistribution due to loss of critical members. This provision is necessary if the prescriptive recommendations are insufficient in limiting progressive collapse. Also, a key structural member can be designed for specific load resistance. Current design guidelines incorporating progressive collapse are General Service Administration (GSA), and the Department of Defence Unified Facilities Criteria (UFC).These guidelines explicitly defined the loading conditions for progressive collapse and recommended the alternative load path method for structures susceptible to progressive collapse due to damage or loss of critical structural members. GSA and UFC requires that a single structural member is assumed

incapable of bearing the gravity load and the remaining structural system is checked to ensure it can safely redistribute the load of the removed member through alternative paths. This approach is threat independent and promotes ductility continuity and energy absorbing properties crucial to limiting progressive collapse.

Other standards such as ASCE 7 (ASCE 2002) titled "Minimum design loads for buildings and other structures" and ACI-318 (AC1 2002) do not explicitly define requirements for design against progressive collapse. However, references to structural integrity was made in the provision. Prescriptive recommendations are not found in these codes, which is a familiar code used for design. Other building codes such as the International Code Council 1997 (IBC 2003) do not mention the design requirements for progressive collapse.

In the UK, limited provision is made with respect to the design for progressive collapse. Detailed reviews in the provisions of codes and guidelines around the world can be found in literature (Ellingwood and Dusenberry 2005; Ellingwood 2006). The preceding sections review provision made by some specific codes to address progressive collapse.

2.3.1 General Service Administration

The General Service Administration (GSA), in its progressive collapse analysis and design guidelines for new federal office buildings and major modernization projects, is an independent threat approach used in assessing the potential for progressive collapse. The exemption of a building based on the guideline depends on the building occupancy, the building category (Steel or reinforced concrete, etc.) the number of stories, seismic zones and the local structural attributes. To evaluate the potential for progressive collapse, the GSA recommends the load combination shown in Equation 2-1 and Equation 2-2 for static and dynamic analysis respectively.

$$N_s = 2(DL + 0.25LL) \quad \textbf{2-1}$$

$$N_d = (DL + 0.25LL) \quad \textbf{2-2}$$

Where $N_S,\ N_d, LL\ and\ DL$ stands for the applied static load combination, dynamic load combination, live and dead loads respectively. The acceptance criteria for static analysis are based on the demand capacity ratio defined by Equation 2-3

$$\text{DCR} = \frac{\mathbf{Q_{ud}}}{\mathbf{Q_{ce}}} \quad \textbf{2-3}$$

Where DCR is the demand-capacity ratio. The acceptance criterion is specified in Table 5.1 of GSA 2003 design guideline for steel structures. Q_{ud} is defined as the acting force demand determined in the member or joint either using the moment, axial force, shear or combined forces. Q_{ce} is defined as the expected ultimate unfactored capacity of the component which could either be a moment, axial, shear or a combined action of forces. The DCR value must be greater than 1.0, for an irregular structural layout (atypical structural configuration), the guideline recommends 25% reduction in the DCR. (i.e ¾ x DCR). The acceptance criteria for the demand-capacity ratio (DCR) range between 1.25 and 3.0. Table 2.1 and Table 2.2 of the guideline shows the acceptance criteria based on the maximum allowable ductility and/or rotation limits for different structural types. A DCR for brittle failure mode in reinforced concrete indicates failure, whereas for ductile behaviour in bending, this implies that the member could sustain load up to a DCR of 2 provided no collapse mechanism is developed, and the member/connection has adequate ductility to redistribute the loads. A DCR greater than one indicates that the structural element or connection has reached its ultimate capacity, although for brittle modes of failure such as shear in reinforced concrete, this will result in failure. GSA 2003 limits the number of storey building to ten if a linear static analysis is used as a basis for progressive collapse.

2.3.2 Department of Defense (DoD 2005)

This standard provides a step by step design guidelines on how to limit progressive collapse of new and existing structures that may or have been subjected to abnormal loads or unforeseen event. This guideline identifies two primary modes to progressive collapse: The provision of ties which depends on the catenary action of the structure and the flexural mode which requires the structure to bridge over any removed structural element. Furthermore, one of the necessary criteria to be considered in designing a building against progressive collapse is the level of protection required. The standard subdivides buildings into four level of protection: Very Low Level of Protection (VLLOP), Low Level of Protection (LLOP), Medium Level of Protection (MLOP), and High Level of Protection (HLOP). The standard recommends that all buildings exceeding three storey buildings must be designed against progressive collapse. The alternative path method requires that key vertical and horizontal elements are removed at critical locations to check the potential of progressive collapse during analysis. The analysis may be linear or nonlinear. The structural detailing of connections must meet the requirements in the code of practice for load redistribution.

2.3.3 ASCE Standard 7-05

This guideline requires that structural stability and strength analysis checks should be carried out to ensure the structure is capable of resisting abnormal loads in section 2.5 of the guideline. According to Ellingwood (2006), the partial collapse of Ronan Point Building in 1968 in London paved the way for the introduction of progressive collapse into the United States. ANSI standard A58.1 – 1972, under the General Design Requirements section of the code, were reviewed from time to time, and one of the latest edition is ASCE standard 7-05 (ASCE 2005a). ASCE 7-02 design guidelines recommend nine indirect design approaches aimed at improving structural integrity, which are:

- A good building layout
- Integrated system of ties
- Changing floor spans of slabs
- Load – bearing interior partitions
- Catenary action of floor slabs,
- Beam actions of the walls
- Redundant structural systems
- Ductile detailing and
- Compartmentalized construction.

The load combination in the commentary of section 2.5 of ASCE standard 7-05 (ASCE 2005a) is given by:

$$(0.9\ or\ 1.2)D + (0.5L\ or\ 0.2S) + 0.2W \qquad \textbf{2-4}$$

Where D, L, S, and W stands for nominal Dead, Live, Snow and Wind load respectively. The values are specified in section 3, 4, 6 and 7 of ASCE Standard 7-05. The second equation accounts for designs where key elements are taken into considerations, and the load combination is:

$$(0.9\ or\ 1.2)D + A + 0.5L + 0.2W \qquad \textbf{2-5}$$

Where A is the structural action due to the expected abnormal loads. The lateral force 0.2W in Equation (2-5) is to ensure lateral stability under progressive collapse scenario. The $0.5L$

corresponds to the average value of maximum live load while the factor 0.9 is used in situations where the dead weight contributes to the overall building stability otherwise a factor of 1.2 is used. The likelihood of Equation 2-4 been exceeded is approximately 5% (Ellingwood and Dusenberry 2005).

ACI Structural Integrity provision

This provision makes recommendations about structural integrity through the provision of ties; however, these ties are not aimed at preventing progressive collapse but provide minimal provision for structural detailing as observed by Mitchell and Cook (1984). That is, no prescriptive set of design criteria for mitigating progressive collapse provision is provided (Ruth et al. 2006).

2.3.4 British code provision

Prevention of progressive collapse became a subject of interest after the collapse of Ronan Point Building in 1968 with the UK taking the lead in introducing draft rules (BSI 1972; BSI, 1985; DETR 1994) and provisions to prevent accidental loading as specified in BS 6399 and Liu et al. (2005). Section 2 of Eurocode 1 states that "structures shall be designed in such a way that it will not be damaged by events like fire, explosions, impact or consequences of human errors, to an extent disproportionate to the cause". However, this provision does not explicitly define a performance-based approach to which such designs can be achieved. This is probably due to the inability to adequately define the unlikely event to which the structure may be subjected to over its design life. Furthermore, it is practically impossible for structural engineers to design a structure to withstand all known hazards because of limited resources. Because of the complexity of the problem, the provision of Eurocode 1CEN (1994) gives the engineer the choice of a design method as long as it satisfies the requirement of section 2 of the code. The design for progressive collapse in the UK requires the tying of members about the same horizontal level and members about the same vertical elevation. The structure would then be checked to ensure that localised damage does not result in disproportionate collapse. At the ultimate limit state for accidental design situations, EN 1990:2002 propose the following load combination (Equation 2-6)

$$\sum_{j\geq 1} G_{kj} + P + A_d + (\psi_{1,1} \text{ or } \psi_{2,1})Q_{k1} + \sum_{j\geq 1} G_{kj}\,\psi_{k,i} \qquad \textbf{2-6}$$

The variables G_{kj} represents the permanent action, P is the pre-stressing action, A_d is the design accidental action, $(\psi_{1,1}Q_{k1}\ or\ \psi_{2,1}Q_{k1})$ is the frequency or quasi-permanent value of the dominant variable action while $\psi_{2,i}Q_{ki}$ is the quasi –permanent values of other actions.

2.3.5 Canadian code provision

The Canadian code requires a structural capability in withstanding abnormal loading conditions through the provision of structural integrity throughout its service life Liu Y et al. (2010). According to Cagley 2000 cited in Mohamed (2006), the National Building Code of Canada (NBCC) was reviewed to incorporate minimum specification for tensile forces in ties and local resistance of structural members after the collapse of Ronan point building. The clause that treats structural integrity does not explicitly refer to progressive collapse, and the commentary does not give procedure for the design against progressive collapse in previous versions as reviewed by Dusenberry (2002).

2.4 Progressive collapse modelling techniques

The analysis of progressive collapse is a threat independent approach as recommended by current design guidelines (GSA 2003). It is required that a critical load bearing member is removed instantaneously, and the structure is further analysed to assess its ability to absorbed the energy due to dynamic forces such as inertia and damping. Some researchers have taken this analysis further by investigating the consequence of multiple column loss and its effect on structural response (Fu 2010). A progressive collapse is a dynamic event; the initial condition methodology was proposed by Buscemi and Marjanishvili (2005) using a single degree freedom system. This approach requires that the displacement of the undamaged structure is determined under normal loading conditions and applied to the damaged structure before progressive collapse assessment. This process is to ensure that the structure is in its undamaged state before simulating the column loss. The initial displacement of the structure is negligible, Kaewkulchai and Williamson (2004) proves that the structure can be modelled and analysed without considering the initial condition methodology initially proposed by Buscemi and Marjanishvili (2005).

Researchers in existing literature adopt different modelling technique for progressive collapse assessment. The modelling technique and the column removal time used significantly affects the results, and the conclusion arrived for the study as observed by some researchers (Pujol and Paul Smith-Pardo 2009; Kim et al. 2009; Stephen et al. 2011; Liu et al. 2005). It is

observed that the dynamic amplification factor recommended in GSA 2003 also depends on the modelling technique used. Because of these challenges in existing literature, some researchers proposed a stepwise loading method and the application of this approach can be found in some published works of literature (Vlassis et al. 2009; Vlassis et al. 2008).

2.5 Progressive collapse assessment of frame structures

The last century saw a significant evolution in studies incorporating the behaviour of the beam–column connections in the analysis of frame structures. This trend arises because connections play a significant role in the survival time of high-rise structures under normal and abnormal loading conditions. Finite element programs such as ABAQUS (Lee et al. 2009), SAP 2000 (Marjanishvili 2004), LS-DYNA (Khandelwal et al., 2009; Möller et al., 2008), ADAPTIC (Izzuddin et al., 2008; Vlassis et al., 2008) and FEAP (Hartmann et al., 2008) are mostly based on a 2D sub-assembly (Kwasniewski, 2010). These finite element codes are popular commercial finite element application software for assessing progressive collapse.

For instance Jaspart (1988) proposed a manual approach in evaluating the collapse capacity of semi-rigid frame structures, taking the strength and stability into consideration. Jaspart and Maquoi (1990) present a study on the behavior of braced frame structures under semi-rigid connection conditions using the elastic and plastic design philosophies. Braham and Jaspart (2004) assessed the safety of frame structure assumed to have pinned connections.

Research works that integrate the nonlinear behaviour of connections with reference to semi-rigid frame structure can be found in the following literature: Bayo et al. (2006), Galvão et al. (2010), Cabrero and Bayo (2005), Ashraf et al. (2007), da S. Vellasco et al. (2006), da Silva et al. (2008), Hadianfard and Razani (2003). These studies were aimed at proposing an analytical approach to semi frames structure incorporating the nonlinear connection behaviour.

A significant amount of analytical and experimental studies on the performance of structural frames due to a notional column removal scenario and blast effects have been accomplished in recent times. Xu and Ellingwood (2011), Elsanadedy et al. (2014) and Türker and Bayraktar (2011) carried out experimental and numerical studies on the behaviour of steel frame structure subjected to dynamic loading. Different configuration of bracing types: crossed, V-type, ʌ type and K types were used. Their study concluded that bracing significantly increases the stiffness of the structural system. Also, cross bracing relative to

other bracing types exhibits higher stiffness as observed both experimentally and from the numerical simulations. Meng-Hao Tsai Tsai (2012) proposed a performance-based design approach for retrofitting regular building frames with steel braces against sudden column loss. The study using nonlinear dynamic analysis indicates that the proposed performance-based approach could be used for the conservative retrofit design of high-rise structures. Cross bracing of lateral resisting system has been shown to minimise the tendency of progressive collapse as shown in the studies carried out by Fu (2010). Also, the study reveals that the increase in slab reinforcement ratio increases the maximum dynamic deflection response which is a disadvantage. Studies carried out by (Alashker and El-Tawil, 2010) shows that floor systems significantly contribute to the structural response due to column removal. Fu (2010) and Fu (2012) provides a comprehensive parametric study on a 3D finite element structure under column removal scenario. The studies conclude that the cross-bracing system is less vulnerable to progressive collapse. The bracing system has been shown to improve progressive collapse resistance significantly (Mohamed, 2009; Khandelwal et al.,2009; Kim and Choi, 2004).

Some research works have been carried out using either a 2D or 3D frame structure in assessing progressive collapse based on the GSA (2003) recommendation. Detailed description of the advantages and disadvantages of the analytical method proposed by GSA 2003 can be found in Marjanishvili (2004). Marjanishvili and Agnew (2006) compared the analytical procedures in GSA (2003) using SAP 2000 finite element code and concluded that the DAF of 2.0 is non-conservative. Marjanishvili and Buscemi (2005) recommended that the initial state of the structure should be considered before modelling sudden column loss. Although, some researchers Kim et al. (2009), Pujol and Paul Smith-Pardo (2009) argue that adopting different assessment techniques in modelling unexpected column loss affects the outcome of the investigation. Lee et al. (2009) proposed collapse spectrum approach in assessing progressive collapse using a simply supported system. Other researchers adopt the equilibrium of column internal forces with gravity loading over a period to simulate progressive collapse (Ruth et al. 2006). The approximate approach that involves the immediate application of gravity loading has been adopted by some researchers for progressive collapse of a multi-storey building. Vlassis et al. (2008) established a quick assessment methodology for progressive collapse assessment based on collapse spectrum. Sudden column removal was modelled using downward step loading equivalent to the

reacting column forces. Other researchers also adopt this method of modelling sudden column loss (Ruth et al. 2006; Jinkoo Kim 2008).

The *remove command or model change* can be used in modelling sudden column loss as demonstrated in some research studies (Feng and Cai 2009). Codes and standards (DoD, 2005; GSA, 2003) around the world recommend sudden column loss for the assessment of structures due to progressive collapse. Kim and Kim (2009a) assessed the collapse resisting capacity of moment resisting frame structure. The studies show that the susceptibility to progressive collapse was highest when a corner column was removed; besides, an increase in the number of floors reduces the tendency to progressive collapse. Furthermore, the studies indicate that the linear static analysis is conservative relative to the nonlinear dynamic response although the perceived complexity of the nonlinear dynamic analysis is currently overcome due to the advancement in research software applications. The application of Pseudo-static response analysis is now implemented as an alternative approach to carrying out progressive collapse evaluation. Meng Hao Tsai (2012) proposed a retrofit design approach of steel frame structures based on column loss. This approach does not require the performance of dynamic analysis and analytical approach in estimating the forces in the additional braces were proposed. McKay et al. (2012) investigated the dynamic and nonlinear load increase factor used in GSA 2003 for assessing the nonlinear dynamic response of structures subjected to progressive collapse. These researchers argue that the dynamic amplification factor of 2.0 recommended in GSA design guideline is overly conservative. Given the study carried out by the author, the dynamic multiplier factor ranges from 1.05 to 1.75 for reinforced concrete and 1.2 to 1.8 for steel structures. Furthermore, the section property and the total deformation affect the dynamic response as well. Kim and Kim (2009a) studied the behavior of a moment resisting frame structure and shear braced wall structure to progressive collapse using the provision of GSA 2003 and DoD 2005. Ruth et al. (2006) proposed a dynamic amplification factor of 1.5 for a moment resisting frame structure for the economic design. However, it is important to note that the dynamic amplification factor significantly depends on the modelling technique and column removal time used for the assessment which is one of the objectives of Chapter three of this thesis. Vlassis et al. (2008) and Izzuddin et al. (2008) proposed a simplified approach to progressive collapse assessment of structures due to sudden column loss triggered by unforeseen events. Three stages of the investigation is proposed for this assessment framework: 1) determination of the nonlinear static response, 2) determination of the dynamic response

and 3) Ductility assessment. The proposed methodology offers a simplified approach in assessing the robustness of a structural system. Yang et al. (2015) investigate the behaviour of composite beam-column joints under middle column removal scenario using the component-based modelling. Parametric studies carried out show that progressive collapse resistance is enhanced by increasing the depth to span ratio of the beam.

2.6 Mitigating progressive collapse

All structures are susceptible to some level of risk associated with progressive collapse, therefore mitigating progressive collapse is crucial, considering the need to protect human lives and buildings from terrorism. Mitigating progressive collapse is one of the research areas currently undertaken by researchers all over the world. For instance, Ellingwood (2005) critically reviewed strategies and challenges mitigating progressive collapse and examined how structural integrity can be addressed effectively and economically. An extensive review on the implication of hazards, mitigating risk and ways of limiting progressive collapse due to multiple hazards can be found in the following published literature and discussions (Li et al., 2012; Duthinh et al., 2013; Fontaine and Steinemann, 2009; Godschalk, 2003; Li and Padgett, 2013; Prater and Lindell, 2000).

There are three techniques proposed for mitigating progressive collapse: the tie force approach, provision of alternative load path and the protection of critical elements from collapse (Abruzzo et al. 2006). Current practices used to mitigate progressive collapse focuses on ductility provision, redundancy provision, provision of local resistance, provision of ductility and continuity. These provisions are discussed briefly.

2.6.1 Indirect design approach – Tying Force Method

This approach falls into the category of prescriptive design rules stated in some design guidelines and codes (ASCE 07, BS 8110-1:1997, BS 5950). This approach is based on the provision of a least amount of strength, ductility and continuity as recommended in current design guidelines like DoD 2005, GSA 2003. The aim of this provision is to limit the tendency of progressive collapse through three key principles. These are effective detailing of tension ties (Horizontal and vertical), developing catenary action in event of loss of critical column, and ensuring ductility. Horizontal and vertical ties were introduced into the British code (BS5950-1, clause 2.4.5.3), BS8110-1 (clause 2.2.2.2)) to ensure that joints bear tension forces in the progressive collapse scenario. Alexander (2004) caution on the application of

ties based on the provision of BS5950 -1 (clause 2.4.5.3) in addressing robustness. The primary aim of the horizontal ties is to ensure that beams can span over a removed column through catenary action. According to Starossek and Haberland (2009) during the catenary action, the flexural loads is been transformed to tension loads which is very important in accounting for the loss of a structural element. However, it is believed that tying of structural elements will limit the tendency of disproportionate collapse. One of the key challenges to this assertion is that: the extent of ties resisting disproportionate collapse is not known. Report on the workshop held by the Joint Committee on Structural Safety (JCSS) and the International Association of Bridge and Structural Engineering (IABSE), stated that tying of structural members improves the robustness of structures. However, Faber M., (2006) reported that isolation and segmentation will be a better option.

According to Vlassis et al. (2008), the issue of interest focuses on the reliability of ties in resisting catenary action based on code provision. This limitation is because no allowance for ductility requirements at each level of its provision neither is it based on structural performance. Although Alexander (2004), argued that ties alone do not ensure the robustness of a building, its application should be done at ones discretion. A further observation made was that ties could drag down part of a building which may not have been affected by the collapse. Thus, it is a wise idea to introduce deliberately weak links particularly in buildings made up of L shape or those having a long length. Recent studies carried out further emphasize the underestimation of tie provision in UK design code (BS 8110 1997; EN1991-1-7:2006) in mitigating progressive collapse as presented by Tohidi et al., 2014 (Equation 2-7 and Equation 2-8).

$$P_1 = \frac{G_k+Q_k}{7.5}\frac{L_r}{5}F_t \qquad \textbf{2-7}$$

$$P_2 = \mathrm{F_t} \qquad \textbf{2-8}$$

Where $G_k$and $Q_k$are the characteristic dead and live loads respectively expressed in kN/m^2, L_r is the span, F_t is the lesser of (20 +4n_o) or 60kN/m where n_o is the number of floors. P_1 and P_2 is the tying force in kN. On the other hand, BS EN 1991-1-7 proposed two equations for internal and perimeter ties as shown in Equation 2-9 and Equation 2-10.

$$T_i = 0.8(G_k + \varphi Q_k)sL \text{ or } 75\text{kN whichever is greater} \qquad \textbf{2-9}$$

$$T_p = 0.4(G_k + \varphi Q_k)sL, \text{ whichever is greater} \qquad \textbf{2-10}$$

Where s the spacing of the ties, L is the span of the tie, φ is a factor which depends on the accidental design situation.

In recent times, researchers have tried to study the key principles related directly or indirectly to the provision of ties in resisting or limiting the likelihood of disproportionate collapse due to a failure of critical structural elements. For instance, Liu (2010) investigated the ways in which progressive failure can be prevented through a catenary action of connections. Yu et al. (2010) presents the effect of joints and composite floor slabs on the effective tying of steel structures for preventing progressive collapse. Three types of joints were investigated: rigid joints, semi-rigid joints and pin joints. They observed that rigid connections, a tensile capacity of concrete, tensile reinforcements within a joint and moment resisting decking profile increases the effectiveness of tying; thereby limiting the risk of progressive collapse. Though the study identifies factors that could limit progressive collapse, however, it provides no specific implementation rules. Studies carried out by Nethercot (2011) further questioned the link between increasing tying capacity and the actual resistance to progressive collapse.

Continuity provision in practice

Continuity is a strategy that is aimed at enhancing the overall performance of a structural engineering system by interconnecting the members together to increase efficient load redistribution in case of accidental loads. Some structural failure can be averted if the structures are linked together (Nair 2006). However, it is important to note that this provision has its merits and demerits depending on the case considered. For instance, poor continuity could localise the damage to only the members and floors directly affected by the accidental loads. That is, the damage is localised to the affected region of the building such that any damaged member does not redistribute the stresses to other parts of the structure. On the other hand, it has been observed that adequate provision for continuity could lead to horizontal progression of failure mechanism resulting to total collapse. The collapse of the World Trade Centre 7 located close to the twin tower was a typical example of how the horizontal progression of failure transmission could result in total collapse.

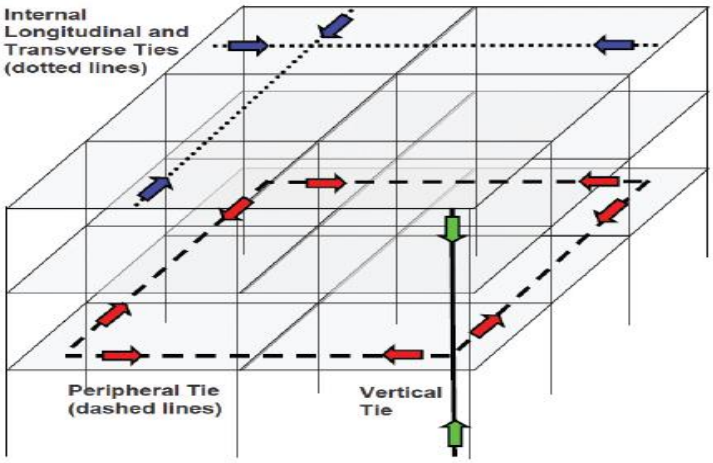

Figure 2-5 Tie force of a typical frame structure (DoD 2009)

Detail explanation of the collapse of the World Trade Centre 7 illustrating the concept of horizontal failure mechanism has been explained by Nair (2006). The design approach for mitigating progressive collapse in codes and design guidelines to enhance redundancy and local resistance is shown in Figure 2-5. The structural members of the building are linked together based on the tie force method; this approach improves the continuity, ductility and the development of alternative path for load redistribution. There are two types of ties: Horizontal and vertical ties. The use of horizontal ties such as internal, peripheral and ties to edge column, as shown in Figure 2-5 depends on the type of construction.

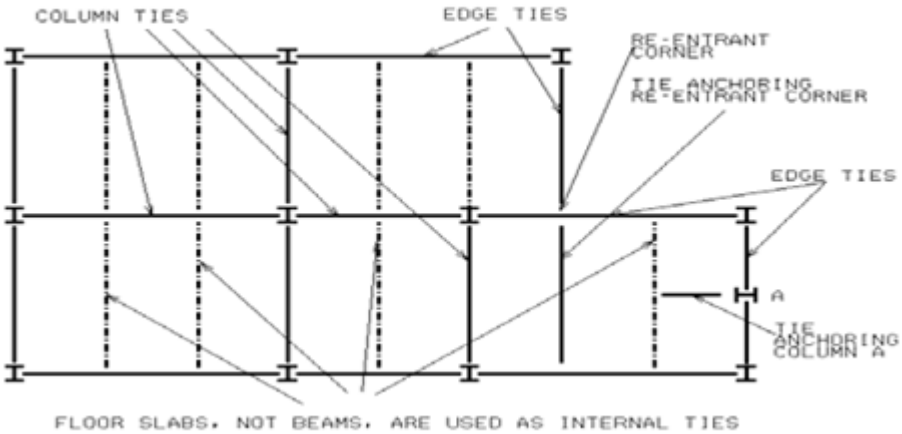

Figure 2-6 Illustration of UFC 4-023-03, 2004 tie provision

The vertical ties are used in columns and load bearing walls. The load path for the vertical ties must be continuous thought the height of the building. The internal ties should link one edge to another as shown in Figure 2-6.

2.6.2 Direct design approach

The direct design philosophy is based on two concepts: Provision of alternate load path and specific local resistance design. These two design approaches are often applicable when the prescriptive approach seems insufficient in limiting the tendency of progressive collapse. Since the code (GSA 2003, DoD 2005) recommends loss of a single column at a time, the structure is expected to bridge over the loss column through load redistribution via the joints without collapsing. This concept is referred to as the *alternate load path method*. The second design concept is to identify the key critical structural element within the structural system such that its failure or inability to resist gravity load may result in partial or total collapse when damaged. Such members are to be designed for a particular load; the current design guideline in the UK (Eurocode 1) recommends a pressure magnitude of $35kN/m^2$.

2.6.3 Mitigating progressive collapse

Tan and Astaneh-Asl (2003) demonstrate the application of cables in retrofitting existing structure using cables to prevent progressive collapse of floors. This hardening process requires that cables are placed inside the slab and anchored at its end. The concept from a structural perspective is that the cables should be capable of transferring the resultant load due to a missing column to other structural members through catenary action. The researchers demonstrate this idea using a single story building, and discovered that large deformations ranging from 40-60cm could be observed; however the pan-caking of the floors are mitigated. This investigation was carried out both experimentally and using a finite element code. However; the researcher did not consider how sudden the column removal affects the catenary action during the progressive collapse. Also, the catenary performance of the cables depends on the rigidity of the end constraints under axial tension when sudden column loss occurs.

Hadi and Alrudaini (2011) proposed a new redundant system for reinforced concrete building to prevent the potential of progressive collapse. In this approach, cables are connected to the ends of the beam and hanged to a braced frame steel structure on the top of the building. If there is column loss, the resultant loads will be transmitted to the braced steel building via the connecting cables. The result indicates that disproportionate collapse can be minimised based on this approach. However, this research work does not demonstrate

the extent at which the adjacent columns would be affected as a result of the additional stress due to the braced frame on the building.

2.6.4 Energy Based Approach

The energy-based method claimed by Powell (2005) is an approximate method for a multi-degree freedom system; however, it accurately predicts the maximum deflections for single degree freedom systems. This method has a correlation with the hazard potential analysis in vulnerability studies of structural engineering systems. The energy method is not common in research works related to disproportionate collapse; however, this is vital because structural collapse could be as a result of an impact, fire, and bomb detonations. These causes have one thing in common, the subject structural system to energy demand that could exceed the energy absorption capacity resulting in partial or total collapse. By implication, the induced energy often leads to strains as observed by Beeby (1999) and England et al. (2008). This idea or concept was suggested by Beeby (1999), in which he derived a simple energy equation based on strain energy principle in evaluating the amount of energy a rectangular beam can fail. To illustrate his idea, he assumed a failure of simply supported beam of an elastic-brittle material when subjected to a given stress when a load is applied at the midspan. However, the expression derived may differ when semi-plastic or plastic materials are used. Further advances were made by Dusenberry and Hamburger (2006), they conducted extensive research on the application of energy method in capturing the fundamental physics of collapse mechanism considering the limitations in the simplified analysis method. Two basic methods were adopted: Push-down analysis and flexural/catenary energy absorption analyses. The approach was based on physical phenomenon synonymous to building failure as compared to the forced based approach calibrated for the particular type of structure. Presently, none of the conventional approaches to the evaluation of disproportionate collapse potentials consider the influence of the stored strain energy in the structure at the time of the initiating events.

2.7 Research in connection behaviour and performance

Traditionally, the design of high-rise steel structures conservatively depends on the assumption that the connections are either pinned (braced frame structures) or rigid (Moment resisting frame structures). For ideal pin connections, moments are not transmitted via the connection because the connection is assumed to possess no rotational stiffness. Pin

connections resist only axial and shear forces. Moment resisting frames have a rigid joint; the connection is assumed to have an infinite amount rotational stiffness capable of transmitting shear, axial and moments. In fact, all connections possess a finite amount of rotational stiffness and are best described as semi-rigid connections. Joint classification based on this assumption is shown in Figure 2-7.

.

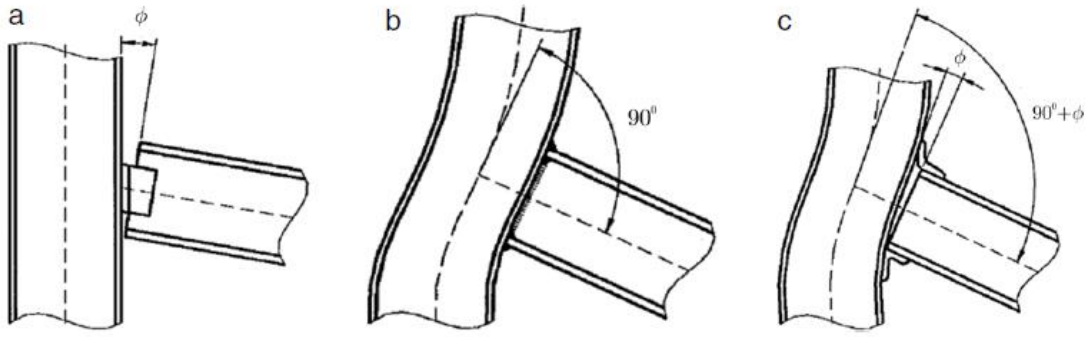

Figure 2-7 Types of joints (Díaz et al., 2011)

Where φ is the angular rotation between the beam and the column: (a) pinned; (b) rigid; and (c) semi-rigid. FEMA-273 proposed Equation 2-11 and Equation 2-12 to calculate the yield moment and yield rotation of steel beams and columns.

$$M_y = F_y Z \quad \textbf{2-11}$$

$$\theta_y = {}^{F_y Z}/_{6EI} \quad \textbf{2-12}$$

Where F_y is the yield strength of steel, Z is the Plastic section modulus, L is the member length, I is the moment of inertia about the bending axis and θ_y is the yield rotation. Over the last century, research effort has been intensified in developing a simplified and accurate methodology in predicting the behaviour of beam-column connections under different loading conditions. The challenge is to understand the complex interaction of the various connection components in stress redistribution particularly when subjected to abnormal loading conditions. Research in existing literature in connection studies incorporate the connection behaviour into the global assessment of high-rise steel structures using the moment-rotation (M-Ø) relationship.

In view of this, several models have been developed based on computational, experimental, informational and numerical studies to predict the mechanical behaviour of beam-column

connections based on the moment-rotation relationship (M-Ø). Extensive literature review on the current methodology in predicting these mechanical properties can be found in Kishi and Chen (1990), and Goverdhan (1983). These authors emphasise the need for further research in developing an accurate and simplified approach for predicting the M-Ø relationship. Jaspart and Maquoi (1990), Cabrero and Bayo (2005) and Aristizabal-Ochoa (2010) demonstrate the need to incorporate joint rotational behaviour in assessing the performance of high rise structures. Some researchers such as Bursi and Jaspart (1998) and Sherbourne and Bahaari (1997) applied advanced FE techniques to propose an approximate method in determining end plate stiffness, strength and ductility for a large variety of connection configurations. Currently, researchers have adopted various beam to beam or beam to column connection types in developing predictive correlation of semi-rigid connections relating the moment to the rotation behaviour (Chen and Kishi, 1989; Kishi and Chen 1990; Ang and Morris, 1984).

Studies of beam-column connections under cyclic loading over the few decades have been intensified following the Northridge earthquake in 1994 with particular reference to the behaviour of the connections under cyclic loading (Mashaly et al., 2011; Ghobarah et al., 1992; Garlock et al., 2003). The finite element analysis method has been employed over the last century in investigating the behaviour of connections under different loading scenario. The choice of the finite element approach for research and investigation of connections is based on the fact that some parametric studies are not possible in the confinement of the laboratory. Some of the extensive literature review and data collection on beam-column connections can be found in the works of Goverdham (1983) and Kishi and Chen (1990). As noted by Shi et al. (1996) not all practising professionals or researchers have access to connection database; therefore theoretical moment- rotation formulations incorporated into design software will be a preferred choice.

Simple connections such as flexible end – plate connections, angle web connection and bolted top and seat angle connection are commonly used in the construction industry to resist gravity loading. The design of these types of connections depends on the kind of frame structure, the loading conditions, and the joint restraints. Besides, the choice of suitable connections is also influenced by cost and the ease of fabrication.

Over the last 30 years, research interest in connection behaviour and performance has been a subject of great concerns, particularly after the 1994 Northridge and 1995 Kobe earthquake.

These events paved a way for more experimental and computational investigations on the behavior of connection (Qian et al., 2005; Lu et al., 2000). Some researchers attributed the failure of the connections due to these earthquakes to brittle damage and the lessons learnt were critically reviewed in existing literature Mahin (1998). The result of all these investigations shows that catenary action in beams and connections are crucial in mitigating progressive collapse. Current research works in assessing the behaviour of connections and performance under abnormal conditions are reviewed below.

Fin plate joints are commonly used in the construction industry because of the ease of fabrication, economy of construction and its simplicity. These joints are designed to resist shear force only as a primary force demand on the connections. However, when one or more columns are rendered incapacitated in resisting gravity load due to an unforeseen event, a large amount of tensile force are developed in the beam that subjects the bolting to tension. UK is the first to adopt continuity BS5950 (2001) through the tying of structural members to mitigate progressive collapse. However, relying solely on this recommendation to ensure efficient mitigation of progressive collapse is risky.

Attempts to improve the understanding of the catenary effect on connection behaviour and retrofitting approach has been intensified over the last few decades Liu (2010). Connection response under column removal scenario has been a research focus in recent times. Some studies can be found in the work done by Lew et al. (2012), Yang et al. (2015), Sadek et al. (2012), Yang and Tan (2012a). These studies present a correlation between the applied load and the corresponding displacement for a given connection type. Connection factors that significantly influence the load-deformation behaviour of a given frame structure was reviewed by Morris and Packer (1987), Cabrero and Bayo (2007), Cabrero and Bayo (2007). These authors carried out an experimental and theoretical investigation into the behaviour of 3D steel beam-column connections subjected to proportional loading. They proposed a model to determine the stiffness of a three-dimensional beam-column connection within the two principal axes. The behaviour of semi-rigid connections depends on its geometric configuration, material properties, applied forces, contact interactions between the components under a given load condition. The interaction of connection components under loading conditions is complex and still an ongoing research process. Joint failure triggers progressive collapse (Liu Y et al., 2010). The next subsection presents a brief review on double web angle connection.

2.7.1 Double web Angle connections

The components of double web angle connections are the column, beam, two angles, bolts, and nuts. Different configurations can be achieved using these connecting elements. Bolted top and bottom seated angle connection are made by bolting the top flange of the beam to the top flange of the column. Similarly, the bottom flange of the beam is bolted to an angle that is bolted to the column flange. Recent experimental and numerical studies (Yang and Tan, 2012b) demonstrate that significant deformation governs bolted angle connections. In addition, at the deformation stage, the connection possesses some level of tensile resistance contributing to the overall connection ductility and rotational capacity of the joint. Consequently, the authors recommend that the fracture of a beam-column component should govern the ultimate resistance of the connection. Kim et al. (2010) shows a hysteretic behavior of beam-column angle connections in steel frames. The top and seated angle connections were modeled by the component-based mechanical approach using the force-displacement formulations for angles, shear panel zone, nonlinear contacts and slippage. They attempt to predict the moment- rotation behavior of connections under cyclic loading conditions relative to experimental results. Garlock et al., (2003) carried out a series of experimental test to investigate how angle size and bolt gage length affect the connection stiffness, strength, energy dissipation capacity and resistance to low cycle fatigue. It was observed that angles had an inherent post-yield stiffness that is approximately linear and included geometric and material hardening.

2.7.2 End plate connections (Header, Flush and extended)

Bolted end plate connections have gained wide use in the construction industry because it requires less supervision, has a simplified geometry and a shorter assembly time relative to welded plate (Sherbourne and Bahaari,1994). The basic three forms of bolted end-plate connections are Header, Flush and Extended end plate connections as shown in a typical connection below (Figure 2-8).

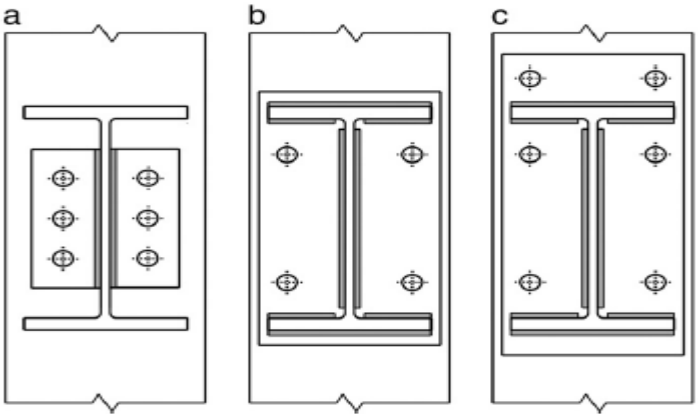

a) Header b) Flush c) Extended

Figure 2-8 End plate connection types

For header plate connection, the plate height depth is less than the depth of the beam. The flush end plate connection has an approximate plate height equal to the depth of the beam while the extended plate bolted connection has a plate height which exceeds the height of the beam. The choice among these options depends on the strength and stiffness requirement of the connections Bose et al. (1997). Predicting the behavior of bolted end-plate connection has been an area of research investigation over the last few decades.

This connection types are often designed to resist shear forces and are adopted for simple connection design in practice. The end plate thickness significantly affects the response of end plate connections. Studies carried out by Jenkins et al. (1986) and described in Shi et al. (1996), show that for connections having a thickness less than 15mm, yielding of the endplate is the determinant failure mode. Also, plastic deformation of the endplate significantly contributes to the ductility and rotational capacity of the connection while connections exceeding a thickness of 20mm, the failure mode are governed by bolt fracture. Some researchers (Sherbourne and Bahaari, 1997; Sherbourne and Bahaari, 1994) developed a simplified approach to 3D simulation of beam column end-plate connections using brick elements by assuming continuous connections between the nodes of the bolt head, nuts and the nodes of the plates. This approach simplifies the relative motions between the components of the connection. Adey et al. (2000) carried out 15 full scale experimental investigation into the behaviour of extended end plate connection under cyclic loading conditions. Effect of geometric parameters such as the beam size, bolt layout and end plate

thickness and stiffeners were assessed. It was observed that extension stiffeners improved the ability of the endplate to dissipate energy with an increase in connection rotation capacity at yield. In addition, plate thickness and stiffeners increase the flexural strength of the connections. After careful assessment of existing equations used in literature to predict the thickness of the plate, a new proposal was then made to predict the plate thickness required within 13% variation.

2.8 Connection models

Researchers are developing a numerical approach to predict connection response through simplified numerical models (Yu et al., 2009; Simões da Silva et al., 2001). Connection behaviour significantly depends on the geometric configuration, material properties and load application. The accurate numerical approach in predicting semi-rigid connection behaviour is a difficult task. However, developing numerical equations to reasonably predict connection behaviour through curve fitting data has been developed based on three common models: polynomial models, exponential models and power models (Abolmaali et al., 2005). According to Shi et al. (1996), these nonlinear moments formulation is widely accepted in existing literature because the parameters are based on experimental results. Nonetheless, Chen and Kishi (1989) observed that some of the numerical formulations are sophisticated in its application.

Models based on the initial stiffness as a critical parameter of the moment- rotation relationship are relatively easier to use although the key demerits of this model as observed by Chen and Kishi (1989) is its lack of suitability for a broad range of rotations. An extensive review on predicting the moment-rotation relationship based on derived equations from computational modelling and experimental investigations has been carried out Chen and Kishi (1989).

In recent times, there is an evolution on assessing the behaviour of connections in determining its moment-rotation relationship and improving the predictive empirical approach in existing works of literature. Mohamadi-Shooreh et al. (2013) developed a three parameter predictive model to determine the moment- rotation relationship of a beam to beam column connection. Mohamadi-Shoore and Mofid (2011) presented a comprehensive review of the various models in existing literature and equally proposed a predictive exponential model for a bolted end-plate connection.

Analytical models are based on the principle of structural analysis using equilibrium of forces, compatibility criteria, and material constitutive relations. The aim is to predict the rotational stiffness (K_j) and the moment-rotation of the connection $M_{j,Rd}$ of a joint due to its geometric and mechanical properties. Merits and demerits of the various types of models (Empirical, informational, mechanical and numerical) have been reviewed in the works of Díaz et al. (2011). Classification of joints based on strength, ductility and stiffness using experimental and theoretical data can be found in the works of Bjorhovde et al. (1990). The following subsections reviews the fundamental principles and application of some of the common models developed to predict the$M - \theta$ relationship in beam-column connection.

2.8.1 Polynomial Models

A typical polynomial model (Yee and Melchers, 1986) is based on a non- dimensional representation as shown in Equation 2-13. This model is used in predicting the moment-rotation behaviour of a given bolted connection based on some correlated geometric parameters. The disadvantage of this model as observed by Chen and Kishi (1989) was that the derivative of these expressions should represent the connections stiffness which may be negative or has some discontinuity which does not reflect the reality of the connection stiffness. The constants C1, C2, and C3 represent the curve fitting data as shown in Equation 2-13 while K is the standardised parameter that is a function of the geometrical and mechanical properties of the connection.

$$\theta_r = C_1 . (KM) + C_2 (KM)^3 + C_3 (KM)^5 \quad \textbf{2-13}$$

Based on the limitation of this model, Azizinamini A et al. (1985) proposed a new differential formulation to correlate the parameter K, geometric parameters (P_i) and the curve fitting parameter ∝ (Equation 2-14).

$$K = {P_1}^{\alpha_1} + {P_2}^{\alpha_2} + {P_3}^{\alpha_3} . \ . \ . \quad {P_n}^{\alpha_n} \quad \textbf{2-14}$$

The K value depends on the thickness of the plate (t_p), the thickness of the column flange (t_f), the depth of the beam and the inter-bolt spacing defining the depth of bolt connection (d_g). This model was used in the reliability based design approach carried out by Hadianfard and Razani (2003) to assess the behaviour of semi-rigid connections on steel frame structure. On the other hand, Prabha et al. (2010) used this approach to evaluate the behaviour of connection flexibility in steel rack. Other polynomial models in literature are found in Picard et al. (1976).

2.8.2 Power Models

The power model can be expressed in the form of a quadratic function with the form $y = ax^n$ where the variables y and x are related to the parameter n. However, the relationship between the moment and the rotation takes the form of a radical or fractional pattern. Ang and Morris (1984) power model was originally developed by Ramberg Osgood as shown in Equation 2-15.

$$\frac{\boldsymbol{\theta}}{\boldsymbol{\theta_y}} = \frac{|\mathbf{M}|}{\mathbf{M_y}} \left[\mathbf{1} + \left({}^{|\mathbf{M}|}/_{\mathbf{M_y}} \right)^{\mathbf{n-1}} \right] \qquad \textbf{2-15}$$

Where the variables $\theta, \theta_y, M, M_y, and\ n$ represents the variable rotation, characteristic rotation, variable moment, and shape parameter respectively. Richard R. M. and Abbot B. J. (1975) propose a three-parameter power model with three independent variables (Equation 2-16).

$$M = \frac{K_i \theta}{\left[1 + \left({}^{\theta}/_{\theta_0} \right)^n \right]^{\frac{1}{n}}} \qquad \textbf{2-16}$$

Where K_i is the initial connection stiffness; M_u is the ultimate moment capacity;θ_0 is a plastic reference rotation = ${}^{M_u}/_{R_{ki}}$; and n is the shape parameter.

2.8.3 Exponential model

The exponential function can be expressed as a correlation between two distinct variables in which one of the variables is expressed as a power of a constant base of a natural logarithm (e). This constant parameter has an approximate value of 2.7182, a typical expression using this model can be written as $y = e^x$. Other forms of exponential function are the inverse exponential function $(\ln x)$ and the indefinite integral ($y = e^x + c$). Chen, W. and Kishi, N. (1989) derived expressions for moment-rotation relationship using the exponential model.

2.9 Basic connection design review

Eurocode 3 EN 1993-1-8 (2005) presents a design methodology for different kinds of connections based on the geometric and mechanical properties of the components. This approach is known as the component based method. Three important considerations are

presented in Eurocode 3 which should be understood before the analysis of the frame structure. It is the moment of resistance, M_{jRd} rotational stiffness, $S_{j,ini}$ and rotation capacity $Ø_{cd}$ for a typical characteristic a joint. The rotational stiffness in Eurocode 3 is obtained by summing up the flexibilities of the necessary components. The code presents a predictive approach for determining the stiffness coefficient (k_i), from the beam-column connection components in order to obtain the overall stiffness of the connection.

2.10 Review of current state of art in connection design

This section reviews relevant current studies carried out to enhance the robustness of high-rise structures through structural configurations, connection improvement and various retrofitting method in mitigating progressive collapse within the last few decades. Lew et al. (2013) carried out an experimental investigation into the behaviour of moment connections under the column removal scenario. One of the tests had a welded unreinforced flange, bolted connections while the other has reduced beam section connection. The connections were subjected to vertically increasing monotonic loading; it was observed, that flexure dominated an initial elastic response. Increasing the vertical displacement resulted in the yielding of the connection with the development of axial tension in the beams which increase until the connection failed to a combined effect of bending and axial stress. It was then concluded that the rotational capacities of the specimens tested under monotonic displacement are approximately twice those recommended in seismic test data. Studies by Yang and Tan (2012b) indicate that increasing the numbers of bolt rows increases the load carrying capacity and rotational stiffness of the connection, although it has a negative consequence on the ductility performance of the connection. Given the investigations carried out, new proposals were made concerning the rotational capacities of simple connections incorporating catenary action resulting from progressive collapse. Aggarwal (1994) reveals that the flush end-plate connection has a lower moment-rotation as compared to the extended end-plate connection. Furthermore, the author argued that little research work has been done in flush end plate relative to the extended end plate and the design of flush end plate connection is based on traditional practices as against design criteria's as established for the extended end plate. Liu Y et al. (2010) studied the influence of semi-rigid connections and local joint damage on the progressive collapse of steel framework.

They stated that semi-rigid connections are more vulnerable to progressive collapse relative to the rigid frame structure, and axial capacity of members and connections play a significant

role in resisting progressive collapse. Since there are limited or no text results on the axial capacity of connections, the author limits its scope on structures and the gravity loads applied ignoring the effects of axial demands expected of the connections. They also discovered that the damage to the joint due to failed members affects progressive collapse of the structure and recommends further research work in this field. Limiting the progressive collapse of existing structures through strengthening is another important aspect of research investigation as observed by Liu (2010). Studies by Lui (2010) shows that retrofitting existing steel structures through the enhancement of beam-column connection will limit progressive collapse through catenary action. Maggi et al. (2005) investigated the parametric behaviour of endplate connection with a particular focus on the geometric behaviour of endplate and the bolt thickness. They authors suggest the need to ascertain the reliability of applying T-stub theory for extended endplate by using the equivalent T-stubs and the yield lines. Mohamadi-shooreh and Mofid (2008) presents a parametric study of end plate connection using a finite element method. The objective of the investigation was to assess the initial stiffness based on a wide range of geometric variables of the connection using regression analysis.

Chapter 3 Progressive collapse modelling methods

3.1 Introduction

This chapter describes four techniques for performing column removal analyses and investigates the influence of column removal time on a structural response. The duration of column removal is a parameter common to the four techniques evaluated in this chapter using a ten storey moment resisting frame structure. Preliminary investigations carried out by the author based on these objectives has been presented at international conferences and published in conference proceedings (Stephen et al., 2011; Stephen et al., 2012). Feedback from these conferences have been implemented in the thesis.

It is well known that the maximum dynamic response of a structure (deflection or rotation) depends on the "instantaneous" of the column removal, and the GSA already gives recommendations for the maximum column removal time. The recommendation states that:" While it is preferable to remove the column or wall section instantaneously, the duration for the removal must be less than one-tenth of the period associated with the structural response mode for the vertical motion of the bays above the column, as determined from the analytical model with the column or wall section removed" (GSA 2013). In a progressive collapse, most building codes are moving towards threat independent load cases for design (single column removal with reduced gravity loads).

There are six sections in this chapter; each section acts as a building block towards the objective of the research investigation. A brief description of each chapter is presented followed by a detailed introduction. The introduction is chapter specific which sets a background for the study. At the end of this chapter, basis for choosing a column removal time and a modelling technique for progressive collapse is established.

Section 3.2 This section of the chapter introduces a 3D model used for the investigation. The material properties, study location within the model and the applied loads are discussed under subsections within this section.

Section 3.3 This section critically reviews and explains the concept of a sudden column loss using four possible techniques including the approximate method. Each subsection explicitly describes a modelling technique concept and some researchers who adopt that approach.

Section 3.4 This section presents the results of the analysis of column removal time (R_t) within the range $0.001 \leq R_t \leq 5s$. Preliminary investigations show that $R_t \leq 0.001$ has less than 1% impact on the joint deformation response while column removal time greater than 5 has no significant effect on structural response (Stephen et al., 2013). Consequently, for the purpose of this studies, the range of column removal time is $0.001 \leq R_t \leq 5s$. The subsections within this section present the results using the edge, corner and interior locations using the four techniques described in section 3.3.

Section 3.5 This section compares the modelling technique and to assess how this modelling technique affects the response of the structure using the displacement and rotational response of the structure.

Section 3.6 This section summarises the findings and the conclusions from the results and equally establishes the basis for subsequent investigation of other chapters. Conclusions drawn from these studies determine the column removal time and the time history function to be used for the next chapter.

Introduction:

Over the last century, researchers in structural engineering have adopted different modelling techniques to model the removal of critical structural members. The method utilised depends on the finite element code used for the investigation. That is, various modelling techniques are used in existing literature to model a sudden column loss since no unified procedure is recommended and acceptable by all design codified bodies. Current codes and guidelines such as GSA 2003, DoD 2005 and Eurocode 1 did not explicitly define a modelling technique for progressive collapse assessment or a time-based assessment for sudden column loss.

Another important global recommendation in codes and design guidelines for progressive collapse assessment states that structures should be capable of bridging over loss columns. Therefore, to simulate the behaviour of structures under this condition, researchers adopt various modelling techniques and different column removal time for progressive collapse evaluation. Furthermore, there has been a constructive argument for and against the implementation of the dynamic amplification factor (DCR) recommended in GSA 2003. This ratio defines the maximum nonlinear dynamic response to a maximum nonlinear static response. The argument could be viewed from the application of different modelling techniques and the column removal time. The constructive evaluation of these arguments

requires a consistent modelling technique and column removal time lapse during research investigations.

Advancement in finite element analyses and the development of software applications capable of capturing complex engineering behaviour makes the finite element analysis method an attractive tool for engineering analysis. Some finite element analysis codes used for progressive collapse assessment are ABAQUS, LYS DYNA and, SAP 2000. These software applications can be used in modelling sudden columns loss for progressive collapse assessment. SAP 2000 can capture different ways of modelling sudden column loss and can be utilised for various techniques relative to other research softwares. It is user-friendly, specifically designed to suit structural engineering problems and is not a multidisciplinary research-based software application such as ABAQUS or LYS DYNA. Therefore, SAP 2000 is used for the purpose of these assessments.

This chapter focuses on two key issues identified by Kim et al. (2009) which mentions that the modelling technique and the time-lapse for column removal significantly affect the response of the structure. Therefore, in this chapter the extent at which these factors affect the response of the structure is evaluated. A time range given as $0.001 \leq R_t \leq 0.5$s was used for the assessment at three different locations within the structure with the column removal time treated as a random variable. At the end of this investigation, a correlation of column removal time to the period of response of the structure in the vertical vibration mode is proposed. In addition, modelling techniques at constant column removal time are compared. Based on these responses, a proposal is made for modelling sudden column loss for progressive collapse.

3.1.1 Research assumptions

The following reasonable assumptions are made from existing literature, design guidelines and software manuals:

- The column is removed over a period of 2ms with 5% proportional damping factor Fu (2010)
- The column removal time is less than a tenth of the period of the structure in the vertical mode under column removal scenario GSA (2013)
- Fast Nonlinear Analysis (FNA) method is used for nonlinear dynamic evaluation of the structural system because it is well suited for time history analysis and recommended over direct integration applications (https://goo.gl/ruOcih).

3.2 Structural and material model

For the purpose of this investigation, a ten storey moment resistant building was used as shown in Figure 3-1. The model was built using a commercially available multi-purpose finite element program, SAP 2000. The frame consists of five spans along the y-axis of 6m in length and four spans along the x-axis of 4.5m in length. A constant storey height of 3.5m was adopted. The structure was designed based on the provision of Eurocode 3, 2005 using SAP 2000.

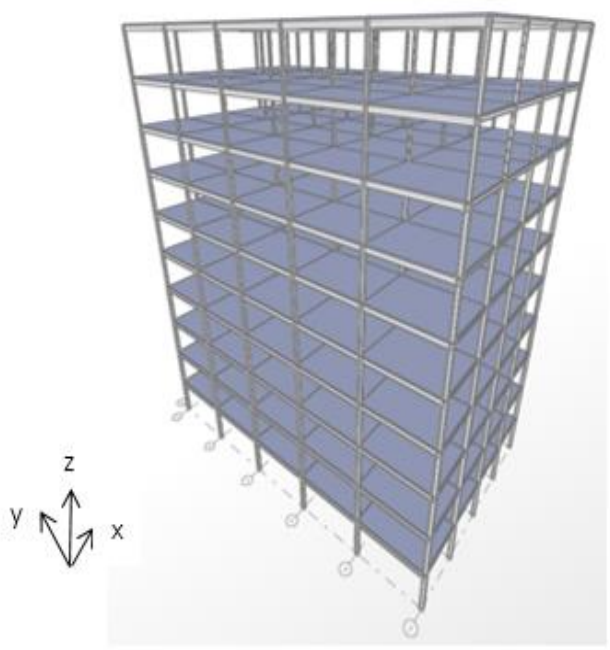

Figure 3-1 3D model of steel building

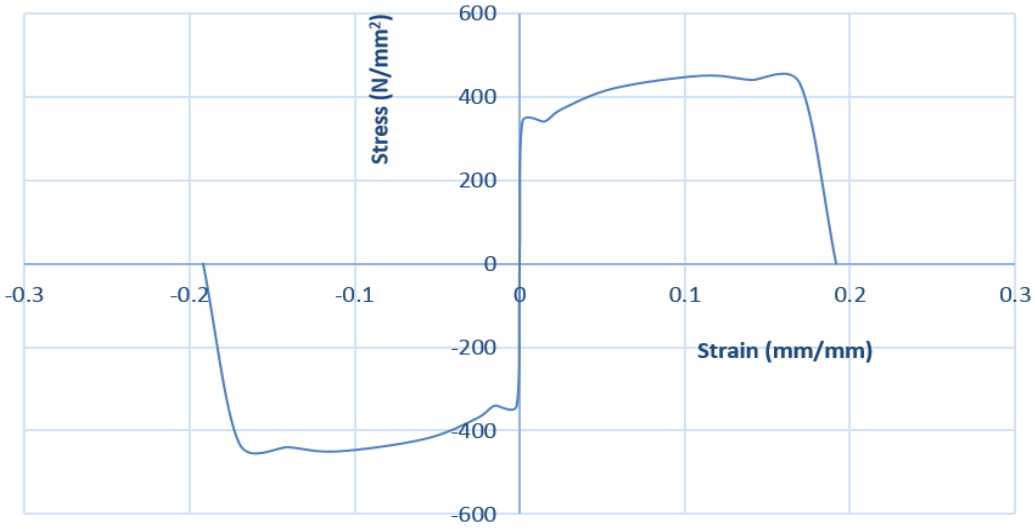

a) Stress vs strain (Steel)

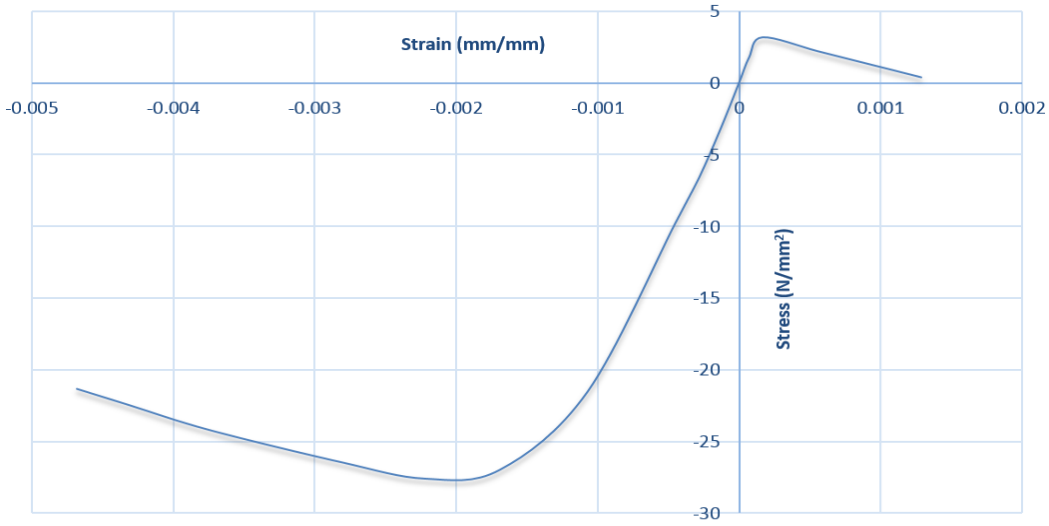

b) Stress vs strain (Concrete)

Figure 3-2 Stress strain curve for steel and concrete (SAP 2000)

The structure was designed based on the provision of Eurocode 3, 2005 using SAP 2000. The beam section along the y-axis is 406 × 140 × 39UB while 254 × 102 × 22 UB is used along the x-axis. The column section from the ground floor to the fourth floor is 305 × 305 × 198UC, from the fifth to the seventh floor it is; 254 × 254 × 167 UC and 203× 203 × 60UC from the eighth to the tenth floor. The slab is modelled using shell elements with a thickness of 130mm. The modulus of elasticity of steel and concrete is 200 x 10^3N/mm^2 and 24.86 x 10^3N/mm^2 respectively. Stress-strain properties of the material is presented in Figure 3-2.

3.2.1 Study locations on the model

These locations are the edge column removal scenario (ECRS), corner column removal scenario (CCRS) and the interior column removal scenario (ICRS). These locations are shown on the floor plan of the building in Figure 3-3. The edge column located on grid A-4 and the interior column located on grid 3-c are the study positions. At each of these positions, the four modelling technique groups described in the subsequent section of this chapter were evaluated. The first stage is to assess the extent at which the time lapse defined by (R_t) significantly affects the response of the structure. The second stage is to use the time lapse from the first analysis to compare structural responses based on different modelling techniques.

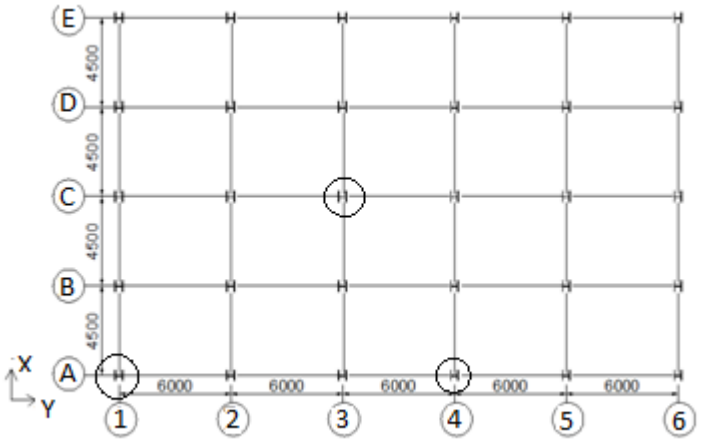

Figure 3-3 Floor plan study locations

3.2.2 Load application (GSA 2003)

The dynamic loading condition was based on the provision of GSA 2003 as shown in Equation 3-1 and Equation 3-2 for static and dynamic analysis respectively. A factor of 2.0 as shown in Equation 3-1 accounts for the dynamic amplification factor and the acceptance criteria is based on the demand capacity ratio defined in Equation 3-3 for static analysis. GSA 2003 limits the number of storey building to ten floors for linear static analysis.

$$N_s = 2 \times (DL + 0.25LL) \quad \textbf{3-1}$$

$$N_d = (DL + 0.25LL) \quad \textbf{3-2}$$

$$DCR = {}^{AF}/_{CE} \qquad \textbf{3-3}$$

Where the demand capacity ratio (DCR) is the acceptance criteria, AF is the acting or applied force on component or connection which could either be moment, axial force, or shear. N_s is the static load combination, N_d is the dynamic load combination, CE is the ultimate un-factored capacity of the component or connection which could be moment, axial force and shear. For the purpose of this investigation, the slab thickness is assumed to be 130mm, the unit weight of concrete to be 23.6kN/m^3, perimeter wall loading of 15kN/m excluding the roof level. The assumed dead and live load on the floors is 4.2kN/m^2 and 3.0kN/m^2 respectively.

The column internal forces and the gravity loading are defined by the time history function path of PVM and N which are discussed under the "Description of modelling technique". The gravity load (N) and the internal forces (PVM) representing the removed column is hypothetically assumed to follow the time history paths while the loading is shown in Equation 3-2.

3.2.3 Removal of Load bearing elements

The removal of load bearing member must ensure a beam to beam continuity across the removed column. The principle is shown in

Figure **3-4**

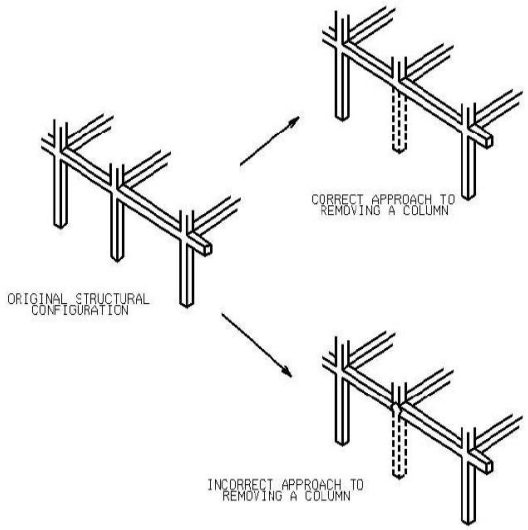

Figure 3-4 Alternative Path Method (DoD 2009)

3.3 Concept of sudden column removal

This section briefly describes the various modelling techniques for progressive collapse assessment. The four techniques are described in subsequent subsections.

3.3.1 Technique one: Sudden removal of internal forces

Figure 3-5 is a two-dimensional portal frame used in illustrating the concept of modelling sudden column loss using this approach. The first step is to determine the internal forces in the column using static analysis. Figure 3-5 (a) below is the initial state of the structure with the proposed column to be removed under gravity loading condition. The column to be removed suddenly is replaced with the internal forces determined from Figure 3-5(a) while Figure 3-5(b) represents the state of the structure with the internal forces. The principle of modelling sudden column loss based on this technique is to ramp the internal forces to zero over a short duration. It is also possible to consider the stability period at which internal forces of the column balances the gravity loading before it is ramped to zero. Hypothetically, this idea captures the sudden removal of a column under gravity loading condition.

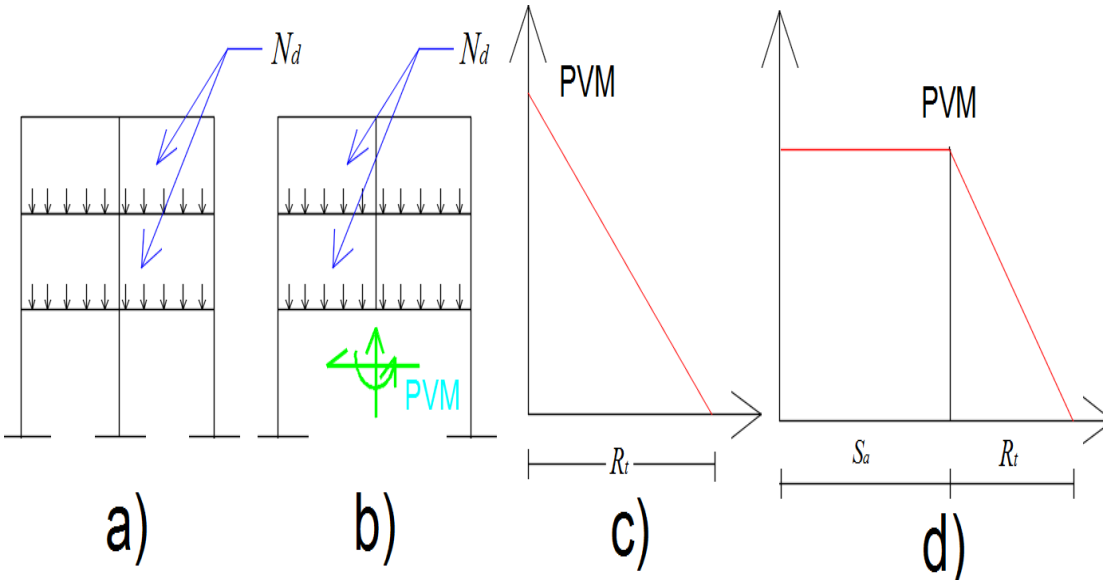

Figure 3-5 Removal of internal forces suddenly

Figure 3-5 (c) is a time history function for modelling the removed column without considering the equilibhrium duration (S_a) of reacting internal forces and gravity loads. In this case, the magnitude of the internal forces from the column is applied at the node of the

removed column and ramped to zero over a time lapse (R_t). The application of Function 1A can be found in Kokot et al. (2012).

The maximum joint displacement and rotation response are the criteria adopted for these investigation. Similar procedure is also considered for Figure 3-5(d) except that a constant equilibrium duration (S_a) of 3s was assumed because within this time lapse, sudden column loss is not activated. It is chosen to ensure that an equilibrium is reached interacting the gravity loading to the reactive internal column forces.

3.3.2 Technique two: Sudden application of gravity loading

This method is a conservative approach to modelling sudden column loss due to unforeseen circumstance. This approach is conservative because sudden application of gravity loading is not the same as sudden removal of column. Sudden removal of column from analytical perspective requires diminishing of the internal forces of the structural member to be investigated over a very short duration.

One of the key assumptions of this approach is that sudden application of gravity load without the "removed column" captures the response of the structure to progressive collapse. Some researchers (Vlassis et al. 2009; Vlassis et al. 2008; Tsai 2010) adopt this conservative approach because it does not consider the column removal time and its ease of application. However, this approach could be modelled to consider the time lapse at which the maximum gravity load is been applied to the structure. In addition, it can be argued that some unforeseen events affect the structure over a fraction of a second while others take longer time.

A typical 2D portal frame as shown in Figure 3-6 is used to illustrate the concept. Figure 3-6 (a) is the initial state of the structure under gravity loading conditions. The model is replicated without the *'missing column'* as shown in Figure 3-6 (b).

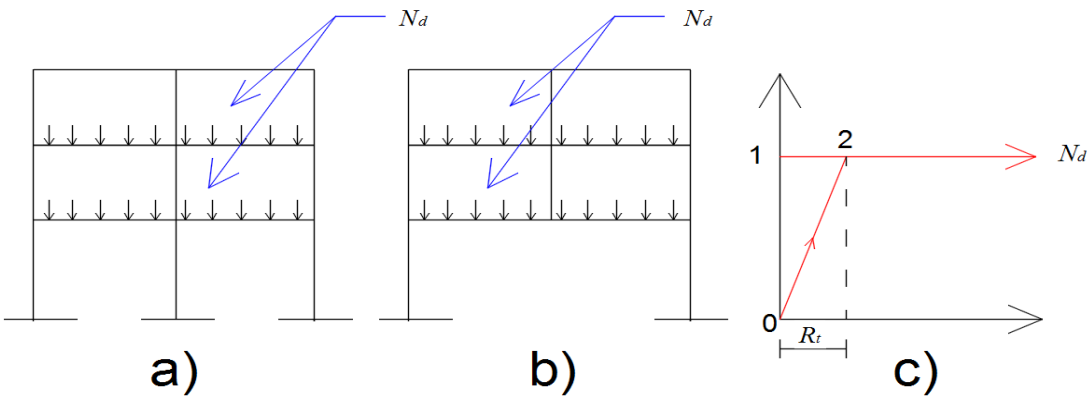

Figure 3-6 Sudden application of gravity loads

Figure 3-6 (c) is the time history function that is used in modelling the gravity load (N_d) to conservatively capture the instantaneous loss of the interior column as illustrated in Figure 3-6(a) and Figure 3-6(b). Figure 3.6(a) is the state of the structure in its original state while Figure 3-6(b) is the second stage when the column is deleted or the structure modelled without it. It is important to note the two paths defined in Figure 3-6(c). There are two similar ways to address this form of loading application, either using the UNIFTH default function path defined by 1-2- N_d or using a customised path defined by 0-2-N_d. For the default function path, the column removal time is zero while the customised function path enables the time history function to be defined. Since one of the objectives is to compare the response of all these functions, the path defined by 0-2-N_d is used in these study. The region defined 0-2, is the linear path at which the gravity load is applied to the structure as shown from the origin of the plot (Figure 3-6(c)). This region defines the column removal time R_t.

The application of the approximate method is the concept used in Imperial College London using the software (ADAPTIC). This method is applied because of it is computationally efficient. For this approach, there is no need to model the sudden column loss using the internal reactive forces because the sudden application of gravity load approximately replicates the dynamic response of instantaneous column loss.

The load path defined by (0) to (2) of Figure 3-6(c) has been used by some researchers Malla et al. (2011) to simulate the inelastic and postbuckling behaviour of a two - dimensional truss system. The time lapse at which the load was applied to the structure was four times the natural period of the structure which is 0.024s.The value used for the time rise was 0.096s. This is possible because the natural period of the structure was very small, this assumption

may not hold if a 3D structure is investigated because it may likely not capture the inherent dynamic response of the structure.

The initial investigation is to study the behaviour of the time history function for the range $0.001 \leq R_t \leq 5s$ using the path defined from origin (0) through (2) and kept constant.

3.3.3 Technique three: Balancing of gravity to reactive forces

This method is the most widely used approach by researchers and is illustrated in Liu (2013). The concept of sudden column removal using this technique requires a balancing technique between the gravity load and the internal forces. The concept is illustrated using a 2D portal frame show in Figure 3-7.

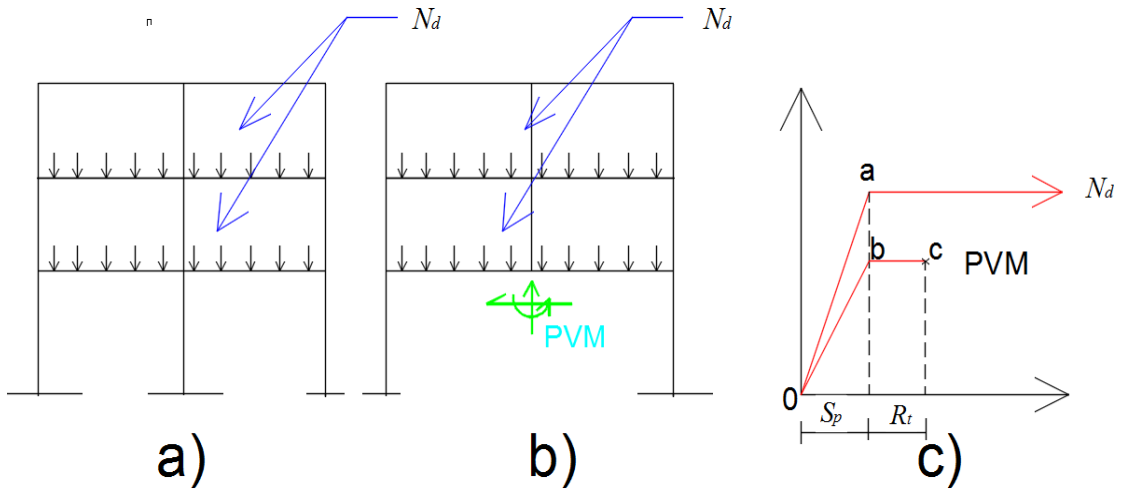

Figure 3-7 Balancing of gravity to internal forces

Part (a) denotes the equilibrium state of the structure at initial condition under loadings. Part (b) shows the application of the stress resultants (PVM) to represent the missing column. Finally, part (c) is the time history functions which show the path of the internal forces and the gravity load increasing linearly up to the maximum time period called stability period (S_a). This is then kept constant over a period (R_t) before diminishing the internal forces to zero to simulate the sudden column loss while keeping the gravity load constant.

The gravity load and the internal forces are increased linearly from zero, the origin of the time history function curve to their respective maximum values as defined by (oa) and (ob) respectively. The points (b) and (c) on the internal forces path defines the time lapse at which the internal forces is diminished to zero. Although, some researchers could use this time period to ensure static equilibrium state of the structure before it diminishes to zero which

still gives rise to the same result. The value of R_t determines the how '*sudden*' a column is removed and this affects the way the structure response.

3.3.4 Technique four: Opposite applied column forces

This method is not a common, it is a proposed technique for modelling sudden column loss using the time history function. The 2D portal frame structure is used to illustrate the principle that surrounds this method. The structure is originally analysed for static forces and the internal forces for the proposed column to be removed is determined. The initial state of the structure is shown in Figure 3-8(a).

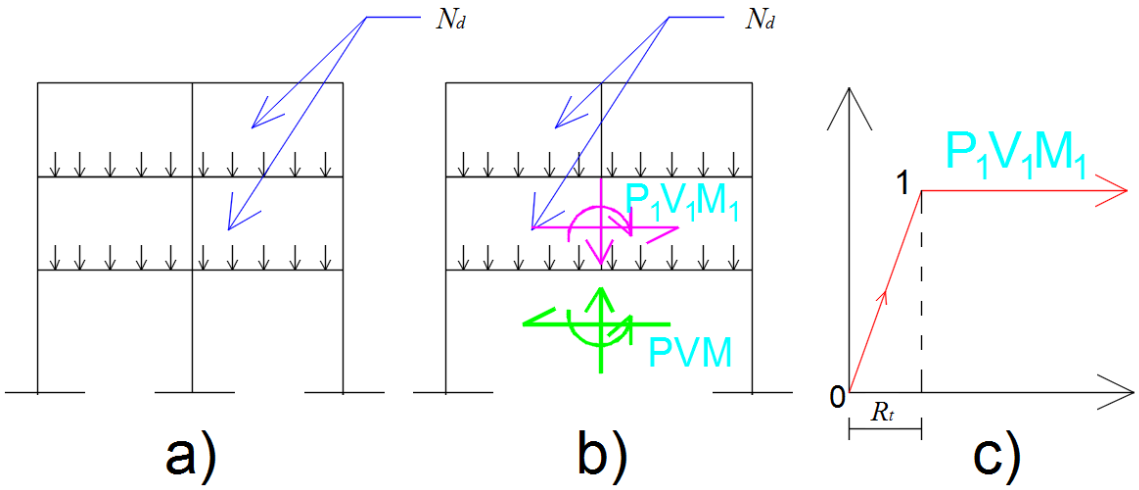

Figure 3-8 Balancing gravity to internal forces suddenly

Figure 3-8(b) is a proposed modelling technique in which the internal reactive forces representing the column is equally applied in the opposite direction as action forces. Part (a) represents the state of the structure under gravity loading defined by GSA 2003. The model is analysed statistically, the stress resultants from the column to be removed are recorded and applied at the nodal point from the top and bottom of the node having the same magnitude but opposite in direction as shown in part (b). The internal force applied at the top are modelled as a time history function as shown in part (c). At t=0, the structure in part (a) and (b) is the same. After a time (R_t), the stress resultant (P1V1M1) at the top cancels the effect of the stress resultants representing the column (PVM) to simulate sudden column loss. Different values for R_t could be adopted, therefore the next section is aimed at assessing the effect of R_t on structural response within the range $0.001 \leq R_t \leq 5s$. This approach can be found in the progressive collapse studies carried out on a single degree freedom system by Buscemi and Marjanishvili (2005).

3.4 Results of column removal time (R_t) on structural response

This section presents the results obtained in investigating the effect of (R_t) on structural response within the range $0.001 \leq R_t \leq 5s$. The four groups of modelling technique are assessed to study the extent at which the column removal time affects structural response. The results for the three column removal locations are presented in the following order: edge, corner then the interior. A brief description of each study location is given before the presentation of the results.Figure 3-9 shows the location of the column removal. The removed column has a label of 31 and is connected to Beam 561 and Beam 571 at the first floor.

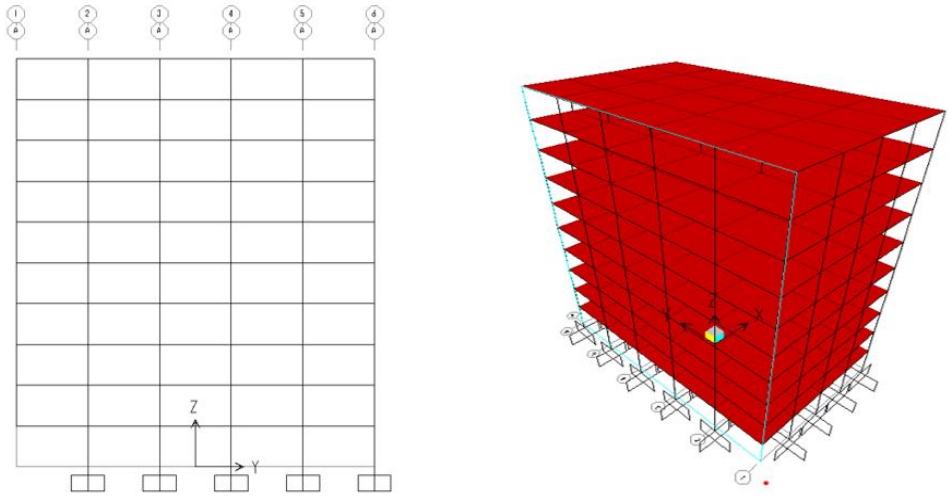

Figure 3-9 Corner column removal location (CCRS)

The scope of this study is within the range $0.001 \leq R_t \leq 5s$ as described previously, Preliminary investigations shows that for column removal less than 0.001 s, the response remains the same. For column removal time greater than 2s, the variation of structural response is less than 1%. Consequently, the study is defined with the scope 0.001s up to 5s. Within this time range, selective time points were used and the dynamic response of the structure with time is plotted at each column removal time.

3.4.1 Corner Column Removal Scenario (CCRS)

Technique one results

This technique has been described in section 3.3.1. The result of the investigation is presented in Figure 3-10 and Figure 3-11 for displacement response of the structure. The

maximum displacement is 120.17mm for Function 1A. A linear response is observed from 0.001s to 0.111s at which the dynamic response gradually begins to diminish to static response. The maximum rotation of the joint is 0.0097 rads (Figure 3-11) which occurs after 2s. At 0.111s up to 2.31s, the rotation stabilises from 0.0058rads to 0.0097rads and remains stable thereafter. Beyond 2s, the displacement and rotational response of the structure remains constant up to 5s. Using this time loading function to model sudden column loss requires a careful assessment of the column removal time.

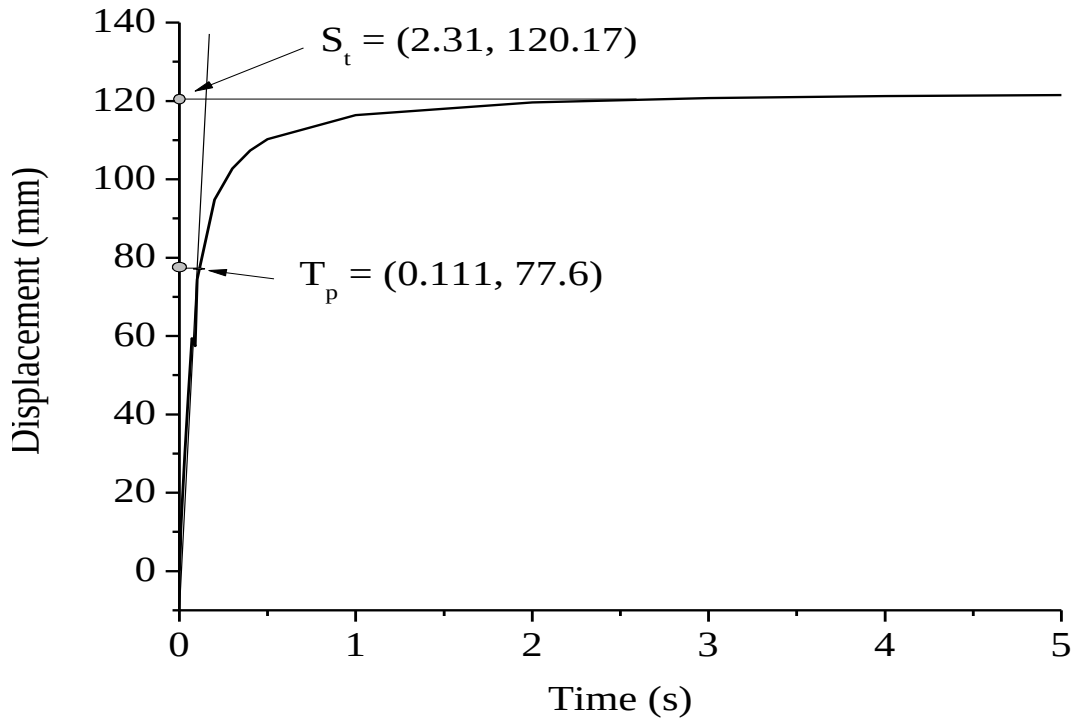

Figure 3-10 Displacement vs time (Function 1A)

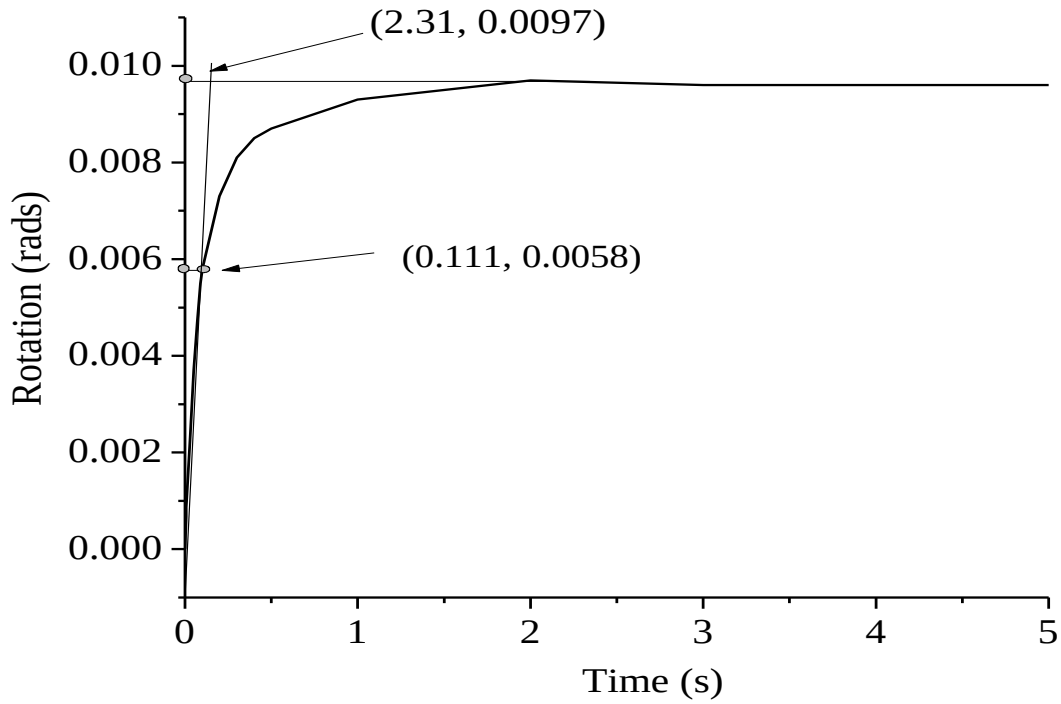

Figure 3-11 Rotation vs time (Function 1A)

A horizontal tangent drawn up to the y axis, shows that at 2s, the maximum response of the structure is obtained. Figure 3-12 and Figure **3-13** shows the displacement and rotation of the beam-column connection under varying column removal time (Function 1B).

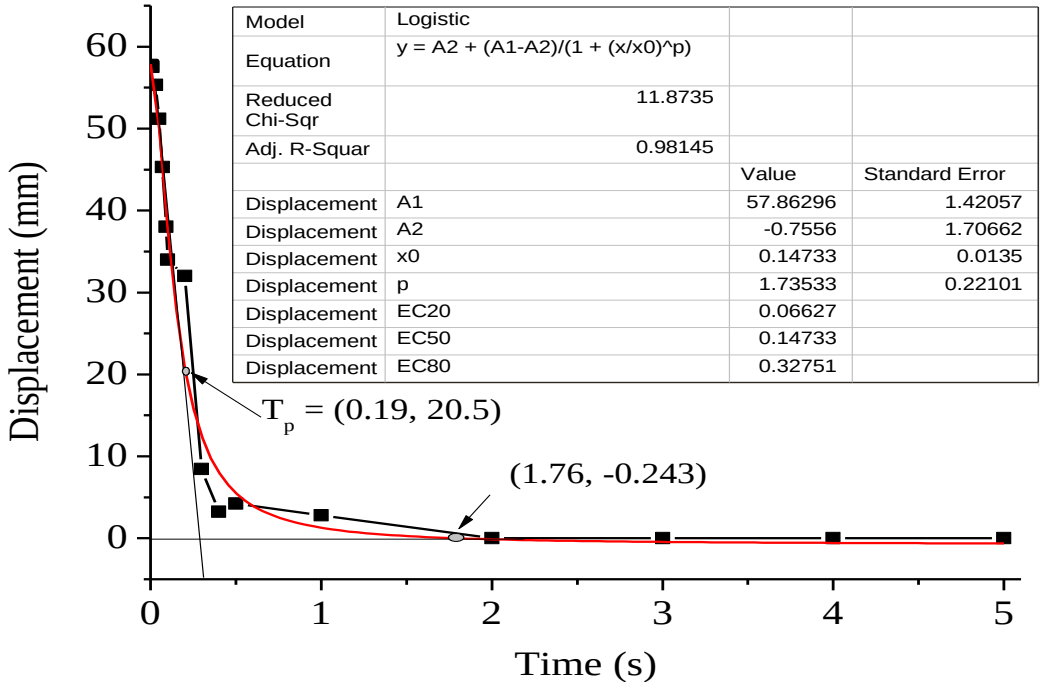

Figure 3-12 Displacement vs time (Function 1B)

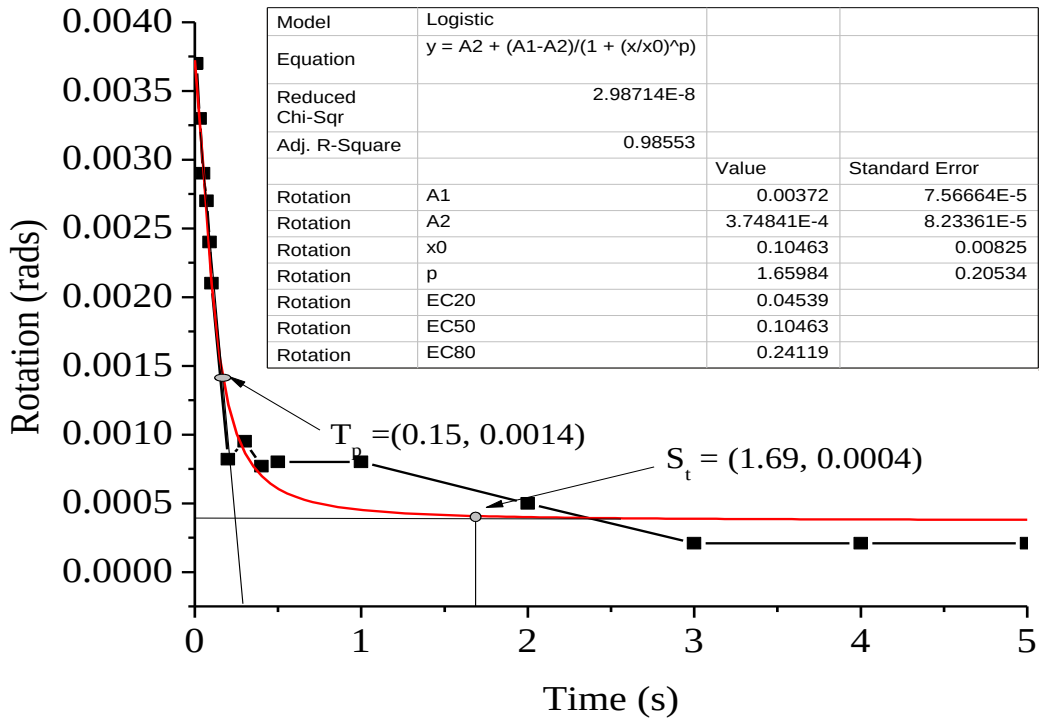

Figure 3-13 Rotation vs time (Function 1B)

The response pattern is different from that of Function 1A. As described earlier, Function 1B considers the stability period of 3s before the column removal time while Function 1A does not consider that.

From the displacement response of Function 1B (Figure **3-13**) within the time range $0.001 \leq R_t \leq 5$s it is observed that for $0.001 \leq R_t \leq 0.01$s, the variation in structural response is less than 1%. Therefore, column removal time from 0.001s up to 0.01s, replicates approximate structural response for structural analysis and subsequent design output. Drawing a tangent from the maximum displacement and rotational response, it is observed that the turning point (T_p) at which the structure begins to stabilise from dynamic state to static state occurs approximately at 0.19s corresponding to 20.4mm and 0.0014 rads.

Beyond the turning point (T_p) up to 1.76s, the structure stabilises to a static state. It is observed that the displacement and rotational response of the structure are not affected by an increase in column removal time beyond 1.76s. Using a column removal time from 0.001s to 0.01s gives the maximum response of the structure which could adequately capture the worst scenario such as bomb explosions. The correlation of displacement to time is shown by Equation 3-4 while Equation 3-5 relates rotation to time.

$$D_y = -0.756 + \frac{58.62}{(1 + \left(\frac{R_t}{0.147}\right)^{1.74})} \quad \textbf{3-4}$$

$$R_y = 0.00038 + \frac{0.0033}{(1 + \left(\frac{R_t}{0.105}\right)^{1.66})} \quad \textbf{3-5}$$

Equation 3-4 and Equation 3-5 are the derived correlation between the column removal time and the dynamic and rotational response of the structure. Where D_y is the dynamic structural response, R_y is the rotational response of the structure and R_t is the column removal time. These equations were derived from the curve fitting data which was obtained by carrying out several iterations to ensure it approximately fits the data points. Knowing the value of R_t, the dynamic displacement and the corresponding rotation can be obtained. The next results is the outcome of using technique two.

Analysis and discussion of results for technique two

This section presents the analytical results obtained in investigating the response of structures under sudden application of gravity load based on the time history function described in Section 3.3.2.

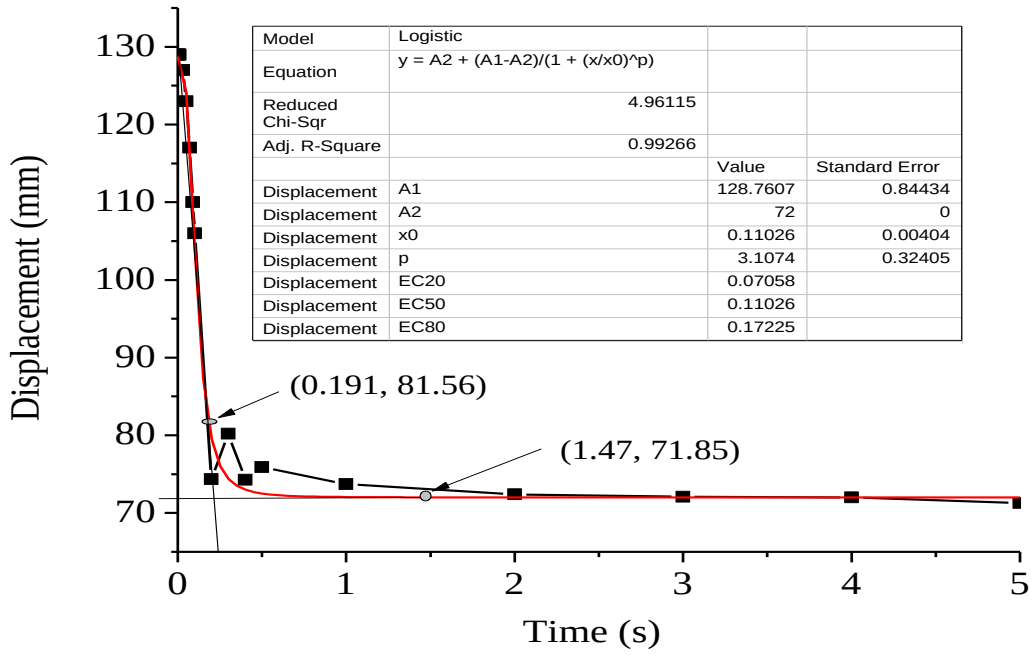

Figure 3-14 Displacement vs time (Function two)

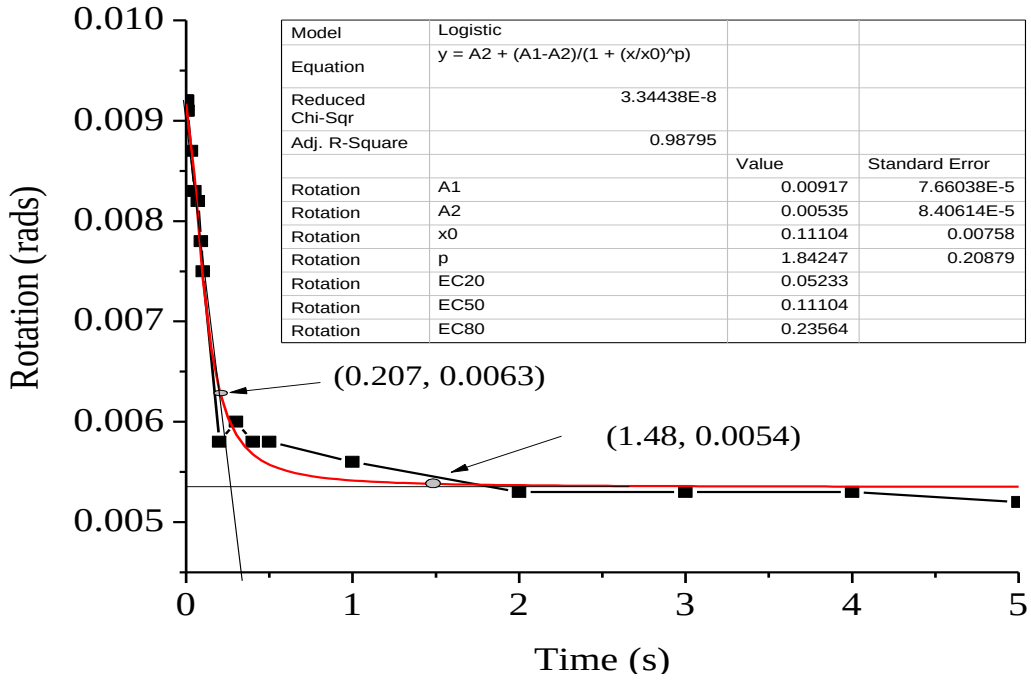

Figure 3-15 Rotation vs time (Function two)

The equation describing the variation of displacement and rotation to time is shown in Equation 3-6 and Equation 3-7 for Figure 3-14 and Figure 3-15 respectively.

$$D_y = 72 + \frac{56.76}{\left(1 + \left(\frac{R_t}{0.110}\right)^{3.1}\right)} \quad \textbf{3-6}$$

$$R_y = 0.00535 + \frac{0.0038}{\left(1 + \left(\frac{R_t}{0.111}\right)^{1.84}\right)} \quad \textbf{3-7}$$

Mathematically,

$$\text{Taking } \lim_{Rt \to 0} \left(1 + \frac{R_t}{0.110}\right)^{3.1} = 0, \ [D_y = 128.76\text{mm}] \quad \textbf{3-8}$$

$$\text{Taking } \lim_{Rt \to 0} \left(1 + \frac{R_t}{0.110}\right)^{3.1} = 0, \ R_y = 0.0092\text{rads} \quad \textbf{3-9}$$

The expression of Equation 3-8 and Equation 3-9 are the limits of the functions as $R_t \to 0$, the maximum dynamic displacement and rotational response is 128.8mm and 0.0092 rads respectively. From the displacement time response of technique two, the maximum displacement is 128.8mm which occurs at 0.001s. Taking a tangent through the data points on the vertical part of the curve of the displacement response shows that the turning point of the curve occurs at 0.19s. There is no significance change in the displacement for column

removal time from 0.001s up to 0.01s. At 0.19s as shown on the displacement time curve, structural stabilisation occurs, and the graphs begins to drift to a static state. From 0.19s up to approximately 1.5s, the dynamic effect of sudden column removal diminishes to a static state. Beyond 1.5s up to 5s considered for the studies, it is observed that increase in column removal time does not affect the response of the structure. The dynamic response of the structure for this time loading function occurs when the column removal time is less than 1.5s while the critical column removal ranges from $0.001s \leq R_t \leq 0.01s$.

Analysis and discussion of results for technique three

This section investigates the response of the structure based on technique three described in Section 3.3.3 of this chapter. The equilibrium period (S_a) of 3s was assumed throughout the analysis while the column removal time, R_t was varied from 0.001s to 5s. The displacement and rotational response of the structure is presented in Figure 3-16 and Figure 3-17 respectively.

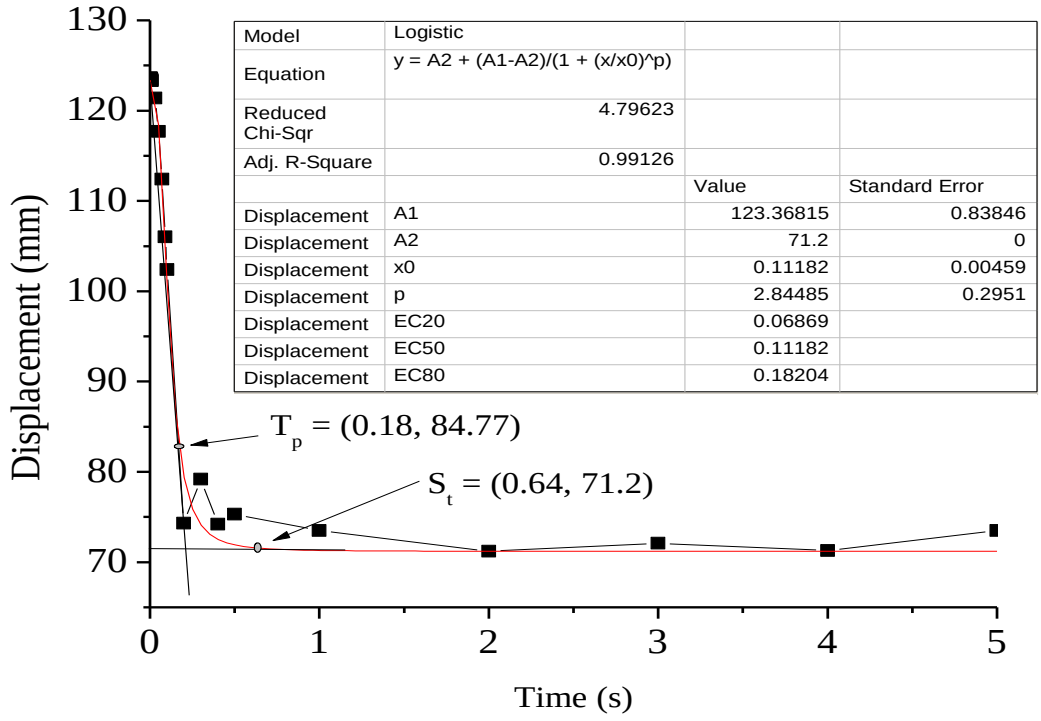

Model	Logistic		
Equation	y = A2 + (A1-A2)/(1 + (x/x0)^p)		
Reduced Chi-Sqr	4.79623		
Adj. R-Square	0.99126		
		Value	Standard Error
Displacement	A1	123.36815	0.83846
Displacement	A2	71.2	0
Displacement	x0	0.11182	0.00459
Displacement	p	2.84485	0.2951
Displacement	EC20	0.06869	
Displacement	EC50	0.11182	
Displacement	EC80	0.18204	

Figure 3-16 Displacement vs time (Function 3)

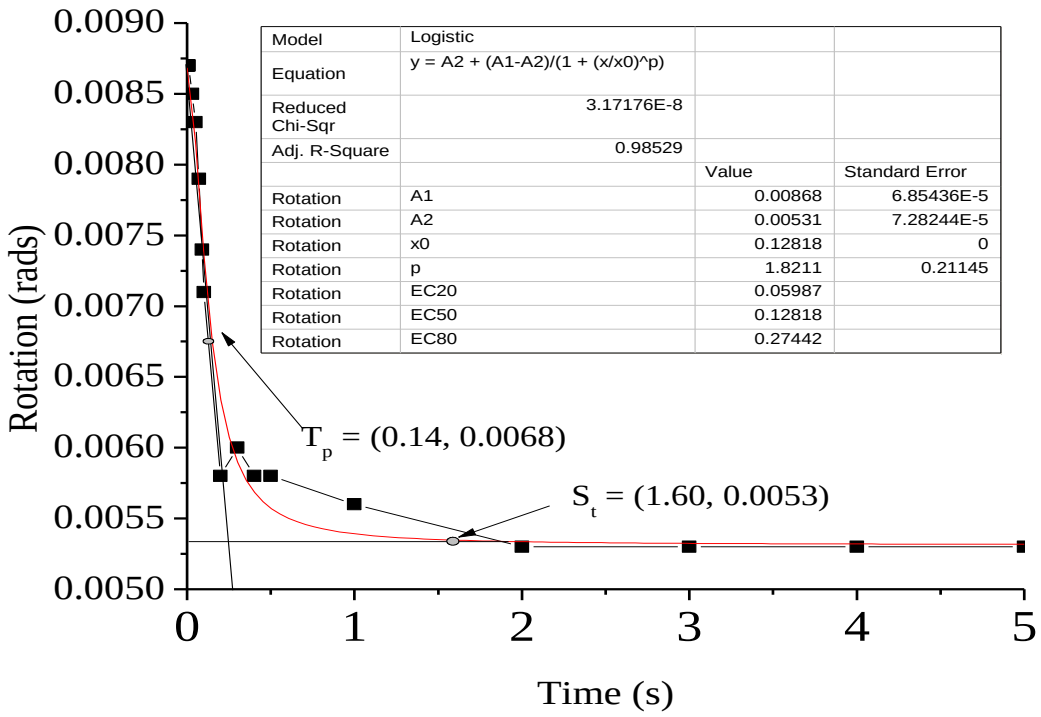

Figure 3-17 Rotation vs time at CCRS (Function3)

The maximum displacement is 123.4mm and it occurs at 0.001s. A tangent from the maximum displacement through the data point's shows that the turning point (T_p) occurs at 0.18s corresponding to a displacement of 84.7mm. From the dynamic displacement response, it is observed that a tangent drawn through the vertical points, at 0.18s the structure begins to change state from dynamic to static state. From 0.18s to 0.64s, it could be viewed as the transitory phase where the structural dynamic response diminishes to a static state. A horizontal line is drawn through some of the data points and, a tangent on the curve indicates that at 0.64s up to 5s, column removal time has no effect on the column removal time. The static response remains approximately constant at 71.2mm corresponding to a time range of $0.64s \leq R_t \leq 5s$.

The maximum rotational responses of the structure is .0087rads (Figure 3-17). The rotational response shows a similar trend in the rotational response of the structure. A tangent through the vertical data points shows that the turning point is at 0.14s. From 0.14s to 1.6s, the behaviour of the structure begins to diminish from a dynamic state to a static state. Beyond 1.6s, the column removal time has no significant effect on the rotational response of the structure.

$$D_y = 71.2 + \frac{52.17}{\left(1 + \left(\frac{R_t}{0.111}\right)^{2.84}\right)} \quad \textbf{3-10}$$

$$R_y = 0.00531 + \frac{0.0034}{\left(1 + \left(\frac{R_t}{0.128}\right)^{1.82}\right)} \quad \textbf{3-11}$$

Equations 3-10 and 3-11 are derived from the curve fitting data of Figure 3-16 and Figure 3-17. This equation correlates the dynamic displacement response with time, and the rotational response with time. This correlation can approximately predict the displacement and rotational response at any given column removal time. The peak or maximum response of a structure occurs when the column removal time tends to zero. At this point, the maximum rotation and dynamic displacement is expected to occur. Mathematically, this can be expressed as:

Taking $\lim_{Rt \to 0} \left(1 + \frac{R_t}{0.111}\right)^{2.84} = 0$, $D_y = 71.2 + 52.17 = 123.37$mm **3-12**

Taking $\lim_{Rt \to 0} \left(1 + \frac{R_t}{0.128}\right)^{1.82} = 0$, $R_y = 0.00531 + 0.0034 = 0.0087$rads **3-13**

Analysis and discussion of results for technique four

The next plots show the response of the structure to varying column removal time based on technique four (Section 3.3.4). The result for this time history function is presented for displacement and rotational response in Figure 3-18 and Figure 3-19. A curve fitting plot of the data points correlate the column removal time with the structural response. For this technique, the maximum displacement and rotational response of the structure is 137.7mm and 0.0103rads.

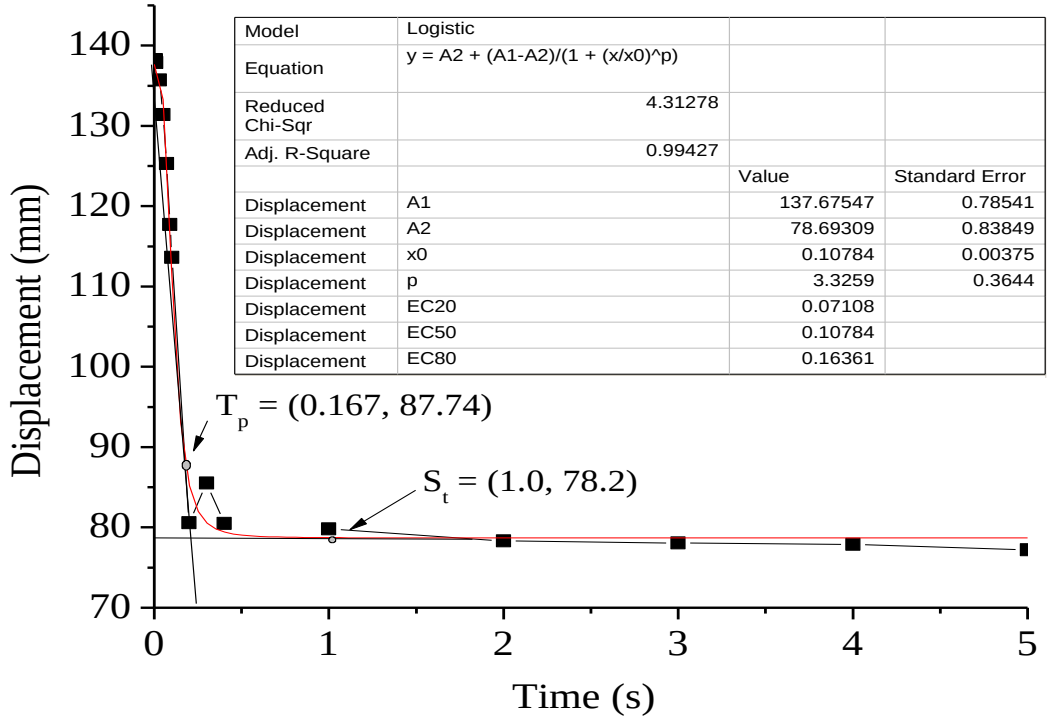

Figure 3-18 Displacement vs time (Technique four)

From the graph of displacement against time, the turning point on the curve is 0.167s on the vertical axis. At this point, the dynamic response of the structure begins to diminish to a static state which starts at 1s. Beyond 1s up to 5 s, the increase in column removal time does not affect the response of the structure. The transition phase from a dynamic state to a static state occurs between 0.167s to 1s. The rotational and displacement response exhibits a similar pattern. The turning points for a tangent through the data point for the rotation occurs at 0.18s.

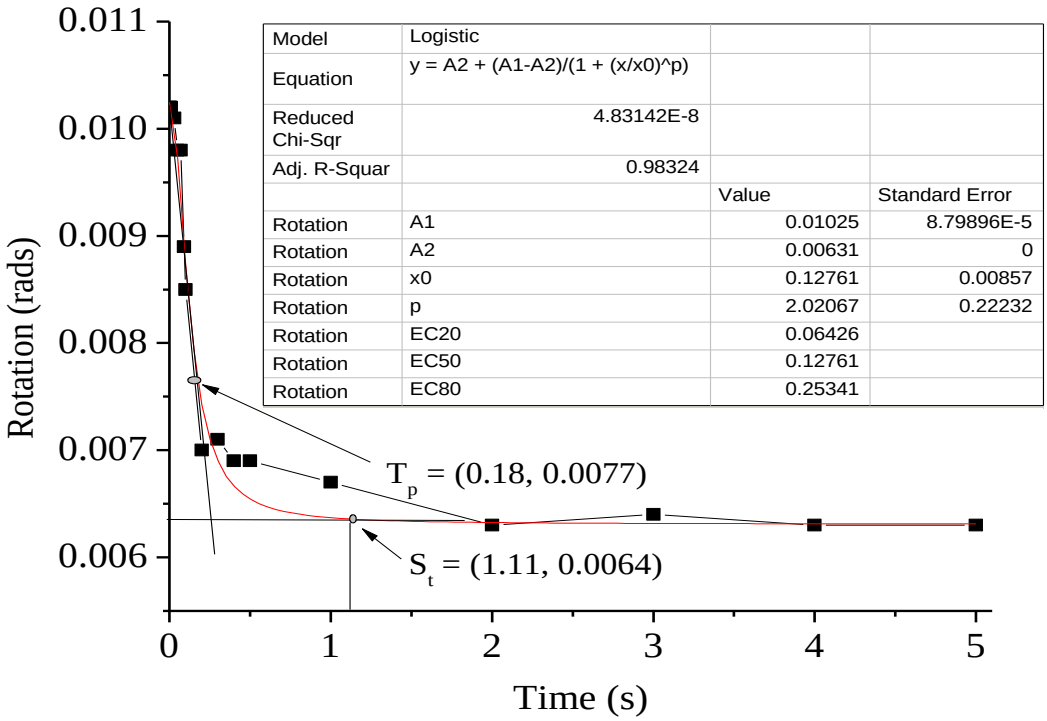

Figure 3-19 Rotation vs time (Technique four)

Beyond 1.11s up to 5s column removal time does not impact on the response of the structure significantly.

$$D_y = 78.69 + \frac{59}{(1+\left(\frac{R_t}{0.108}\right)^{3.33})} \quad \textbf{3-14}$$

$$R_y = 0.00631 + \frac{0.004}{(1+\left(\frac{R_t}{0.128}\right)^{2.02})} \quad \textbf{3-15}$$

The correlations between the dynamic displacement and column removal time is derived from the curve fitting curve as shown in Equation 3-14 while the rotational response relate to column removal time is shown in Equation 3-15. Mathematically, taking the limits of D_y and R_y for the worst scenario of column removal time, the maximum displacement and rotation of Equation 3-16 and Equation 3-17 are obtained.

$$\text{Taking } \lim_{Rt\to 0}\left(1+\frac{R_t}{0.108}\right)^{3.33} = 0,\ D_y = 78.69 + 59 = 137.7\text{mm} \quad \textbf{3-16}$$

$$\text{Taking } \lim_{Rt\to 0}\left(1+\frac{R_t}{0.128}\right)^{2.02} = 0,\ R_y = 0.00631 + 0.0034 = 0.0097\text{rads} \quad \textbf{3-17}$$

3.4.2 Results of Edge Column Removal Scenario (ECRS)

A similar analytical process as carried out for the corner column removal scenario was repeated for the edge column removal scenario. Figure 3-20 shows the location of the edge column removal scenario at which all the techniques are assessed.

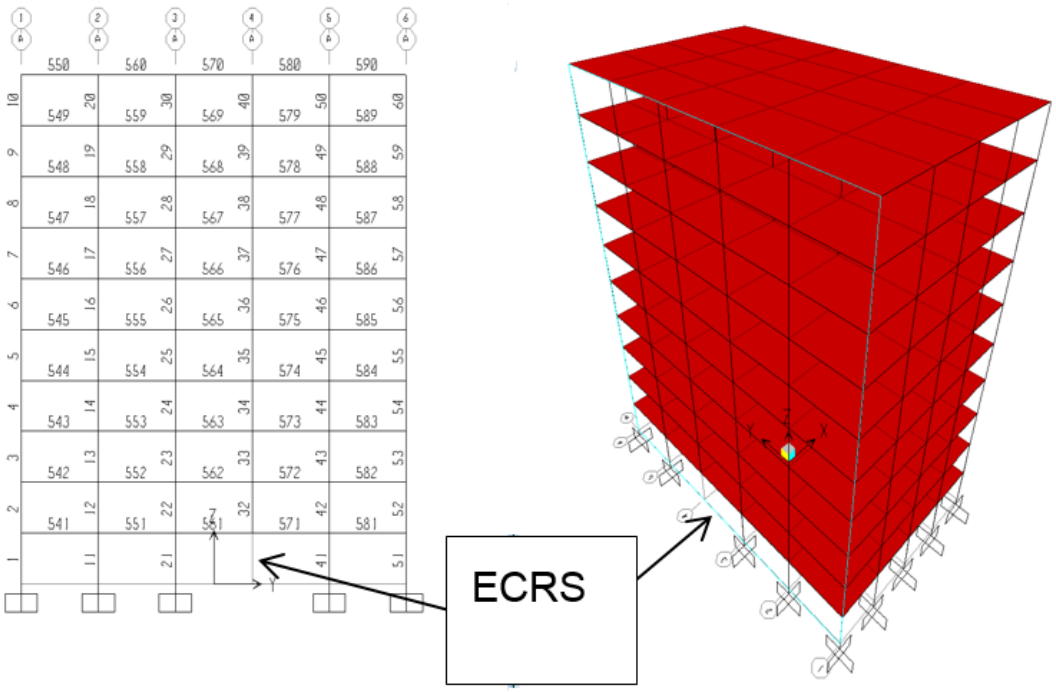

Figure 3-20 Edge column removal scenario (ECRS)

This section presents the results obtained using edge column removal scenario (ECRS) for technique one (Section 3.3.1). The results due to Function 1 is presented for displacement and rotational response in Figure 3-21 through Figure 3-24.

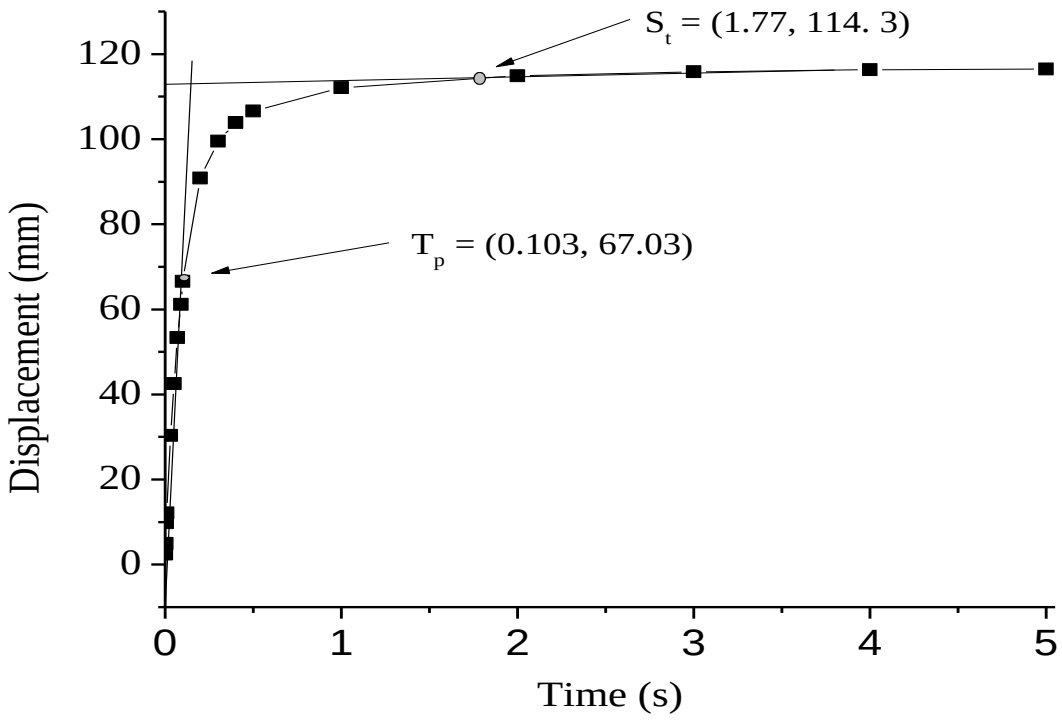

Figure 3-21 Displacement vs time at ECRS (Function 1A)

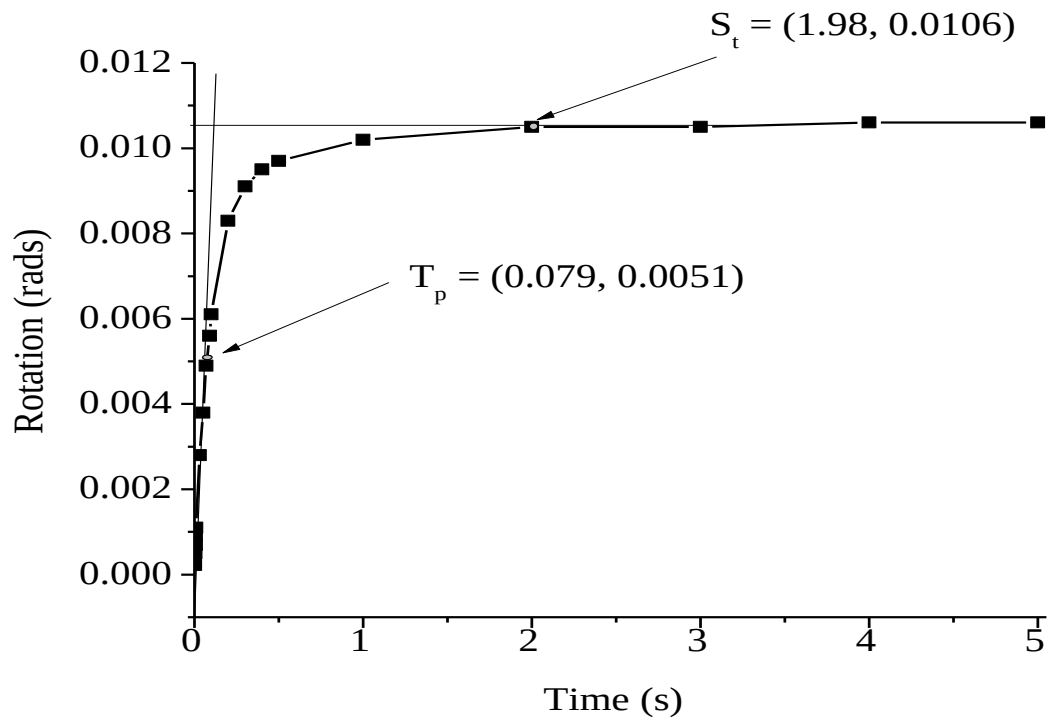

Figure 3-22 Rotation vs time at ECRS (Function 1A)

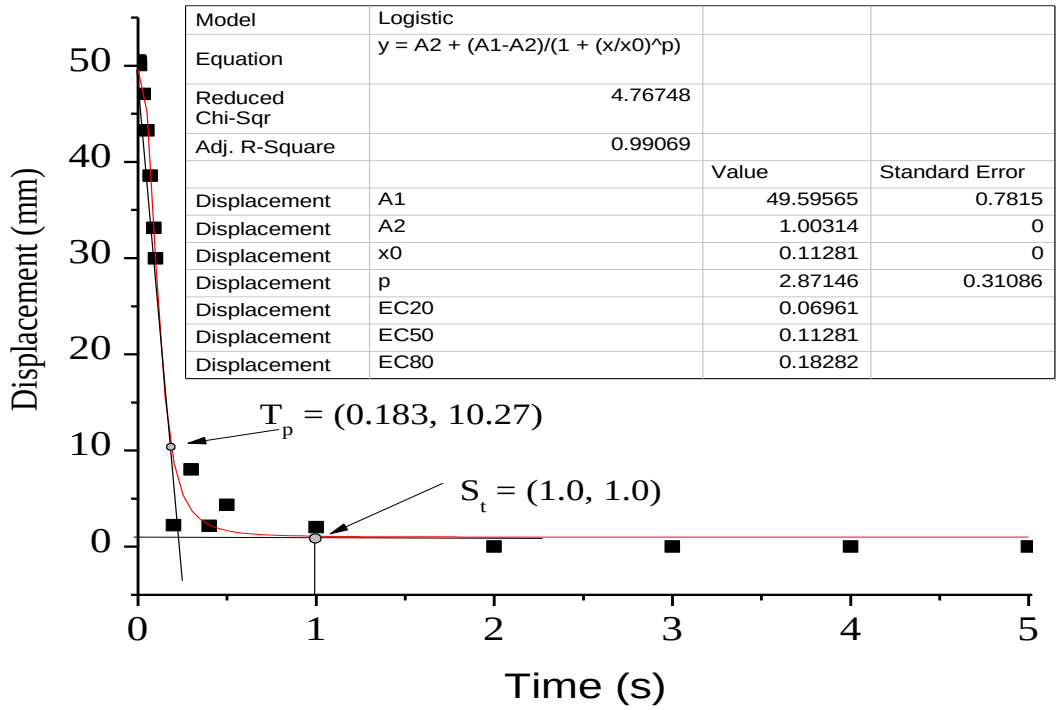

Figure 3-23 Displacement vs time at ECRS (Function 1B)

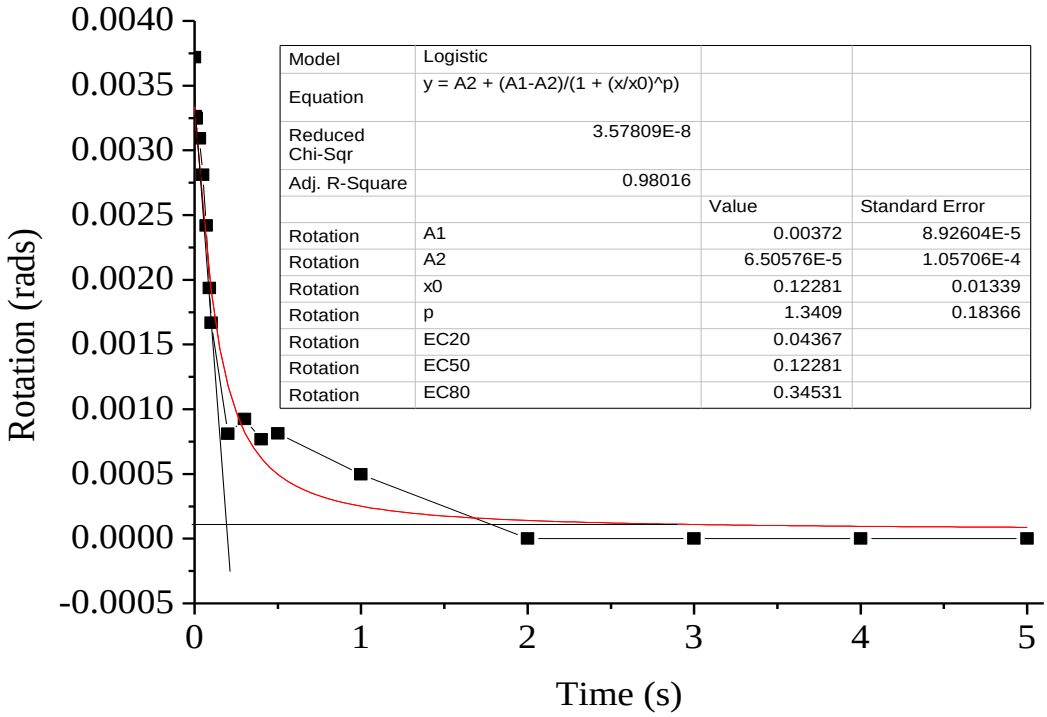

Figure 3-24 Rotation vs time (Function 1B)

The maximum displacement and rotational response using Function 1A are 114.3mm and 0.0106 rads respectively while Function 1B responses are 49.6mm and 0.00372rads. For Function 1A, the turning point began at 0.103s, and the structure stabilises at 1.77s. For the rotation, the turning point (T_p) began at 0.079s while it stabilises at 1.98s. Comparing the response of Figure 1A and Figure 1B show that the response paths are different. The equations describing the displacement and rotational response of the structure for Function 1B is shown in Equation 3-18 and Equation 3-19.

$$D_y = 49.60 + \frac{1.003}{(1 + \left(\frac{R_t}{0.113}\right)^{2.87})} \quad \textbf{3-18}$$

$$R_y = 0.000065 + \frac{0.0037}{(1 + \left(\frac{R_t}{0.123}\right)^{1.34})} \quad \textbf{3-19}$$

Where D_y is the dynamic displacement, R_y is the rotational response (radians), R_t is the column removal time.

Technique two results.

Function 2 is a modelling approach for technique two. This technique has been discussed in section 3.3.2. This approach is an approximate method at which the removed column is modelled as sudden application of gravity load.

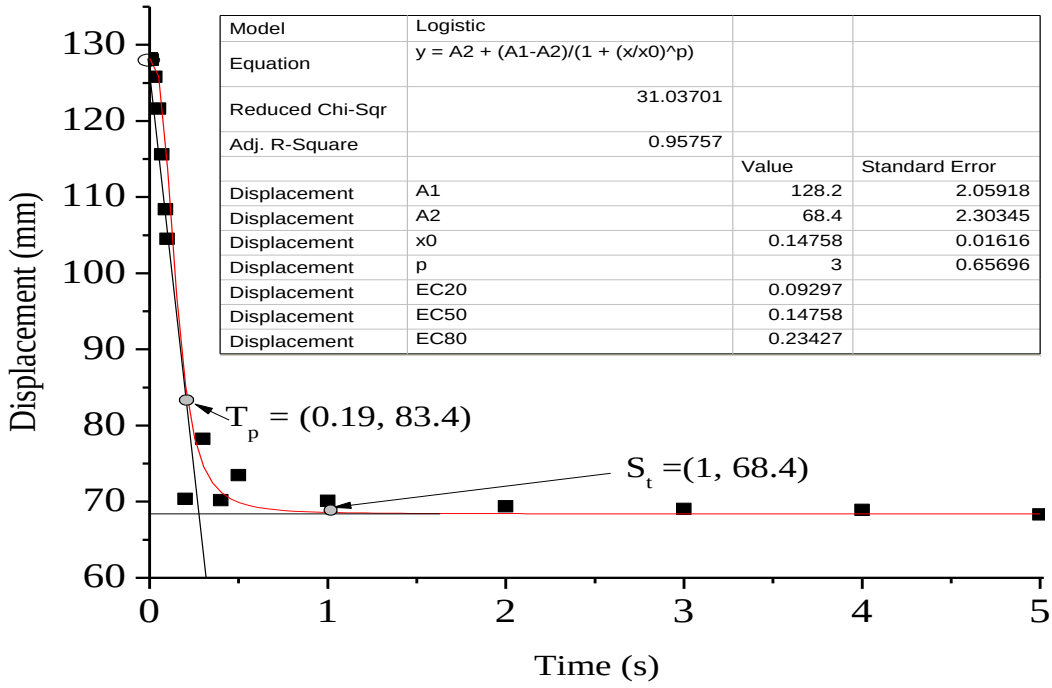

Figure 3-25 Displacement vs time at ECRS (Function 2)

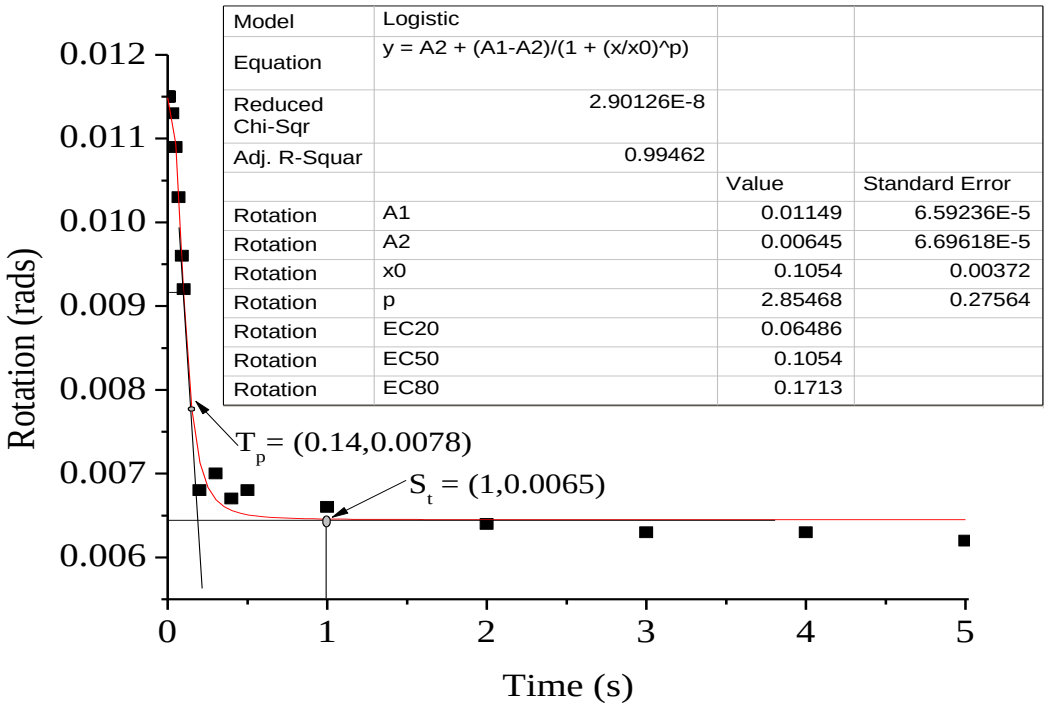

Figure 3-26 Rotation vs time at ECRS (Function 2)

The displacement of the joint due to Function 2 is shown

Figure **3-25**. The turning point for Function 2 using the displacement response is approximately 0.19s, stabilising at 1s. Beyond 1s, it is observed that the structure stabilises to a static response. For the rotational response of the structure, the turning point began at 0.14s and also stabilises after 1s.

The maximum displacement and rotational response of the structure using technique two is 128.2mm and 0.0115rads respectively. Equation 3-20 and Equation 3-21 describe the displacement and rotational response of the technique two with respect to column removal time.

$$\mathbf{D_y = 68.40 + \frac{59.8}{1+\left(\frac{R_t}{0.148}\right)^3}} \qquad \textbf{3-20}$$

$$R_y = 0.0065 + \frac{0.0051}{1+\left(\frac{R_t}{0.105}\right)^3} \qquad \textbf{3-21}$$

Where D_y is the dynamic displacement response, R_t is the column removal time while R_y is the rotational response of the structure.

Technique three

This technique is based on the principle of stabilising the gravity load and the column internal forces to achieve equilibrium over a length of time before simulating the column removal. Details of this technique has been described in Section 3.3.3. The result of the study is shown in Figure 3-27 and Figure 3-28

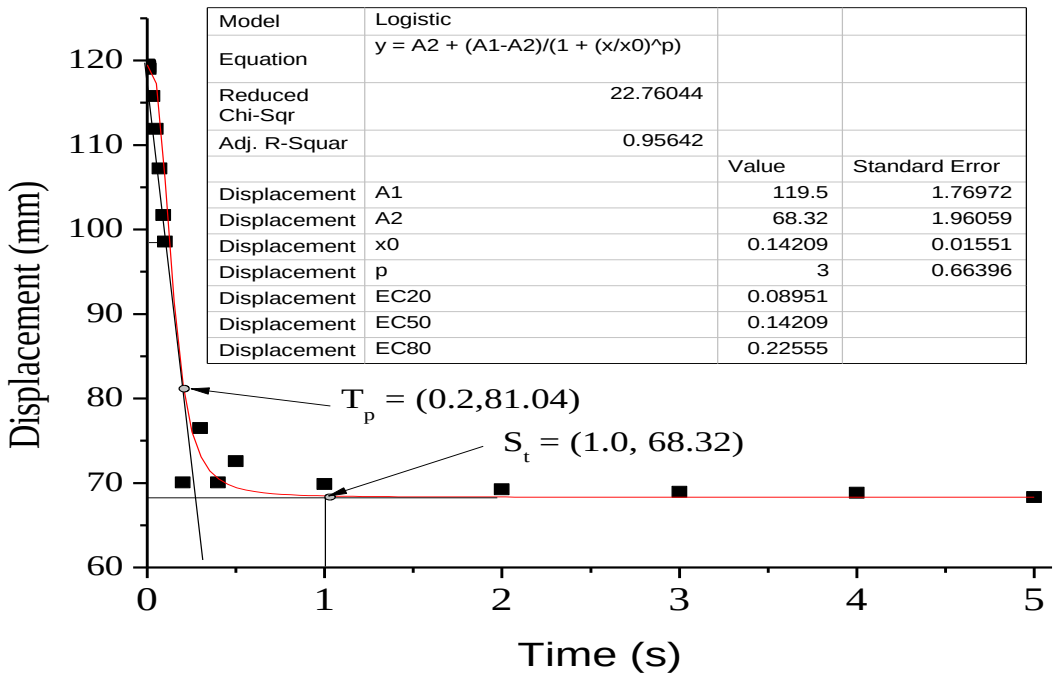

Figure 3-27 Displacement vs time at ECRS (Function 3)

It was observed that the maximum displacement and rotational response of the structure is 119.5mm and 0.0106rads respectively. From the graph of displacement against response time, the turning point range is $0.2 \leq R_t \leq 1$s. Beyond 1s, increase in column removal time does not affect the dynamic response of the structure initiated by instantaneous column loss. Similar trend was observed for the rotational response of the structure for technique three. The turning point has a range $0.2 \leq R_t \leq 1$s which is the same as the displacement response of the structure. Mathematically, expressions can be derived that describes the path of the curve for displacement and rotational response of the structure as a function of time is shown in Equation 3-22 and Equation 3-23

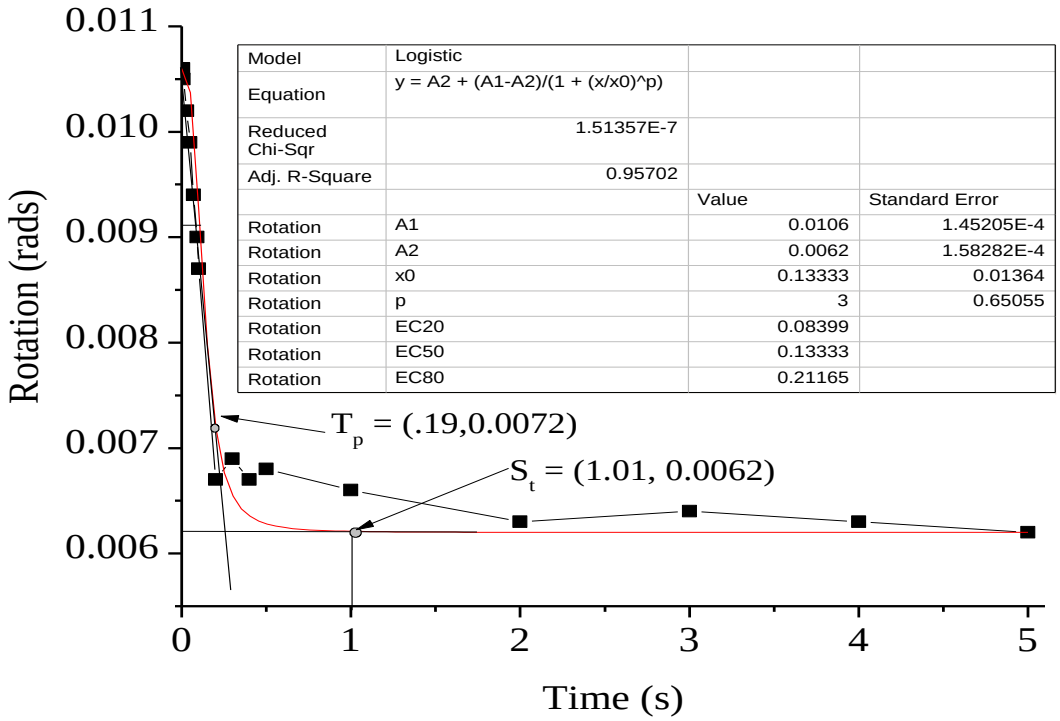

Model	Logistic		
Equation	y = A2 + (A1-A2)/(1 + (x/x0)^p)		
Reduced Chi-Sqr	1.51357E-7		
Adj. R-Square	0.95702		
		Value	Standard Error
Rotation	A1	0.0106	1.45205E-4
Rotation	A2	0.0062	1.58282E-4
Rotation	x0	0.13333	0.01364
Rotation	p	3	0.65055
Rotation	EC20	0.08399	
Rotation	EC50	0.13333	
Rotation	EC80	0.21165	

Figure 3-28 Rotation vs time at ECRS (Function 3)

$$D_y = 68.320 + \frac{59.8}{1+\left(\frac{R_t}{0.148}\right)^3} \quad \textbf{3-22}$$

$$R_y = 0.0065 + \frac{0.0051}{1+\left(\frac{R_t}{0.105}\right)^3} \quad \textbf{3-23}$$

Equation 3-22 and Equation 3-23 describe the curves for technique three. The variables:D_y, R_y and R_t are the displacement (mm), rotation (rads) and the column removal time (s) respectively.

Technique four (Function four)

This method is described in Section 3.3.4. The results obtained for the investigation are presented in Figure 3-29 and Figure 3-30 for displacement and rotational response of the structure.

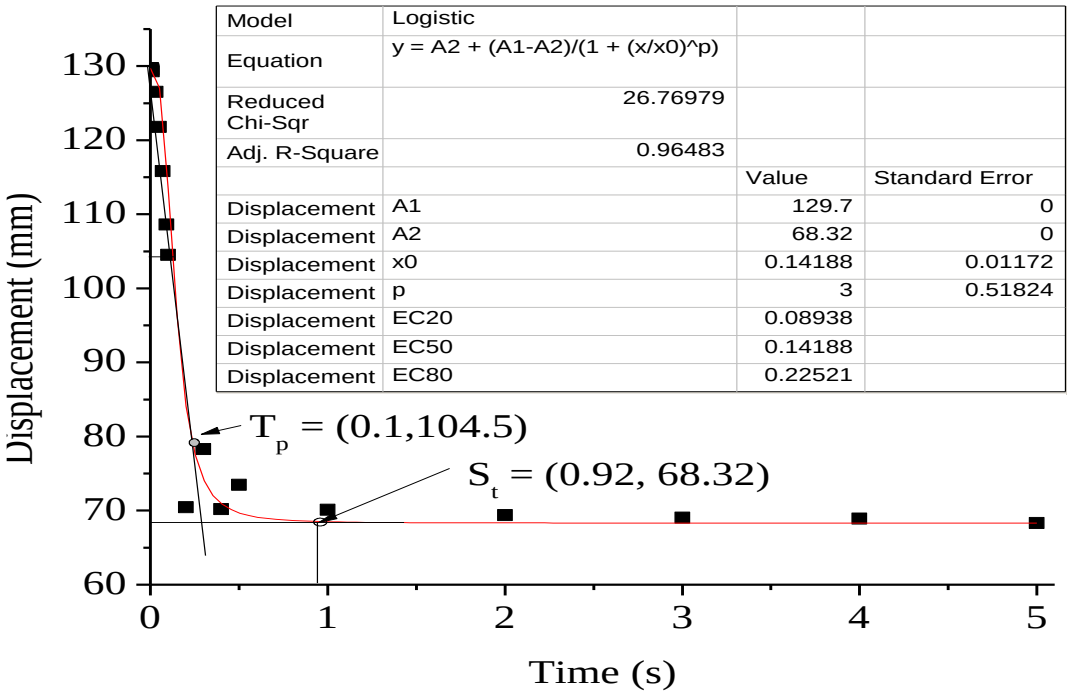

Figure 3-29 Displacement vs time at ECRS (Function 4)

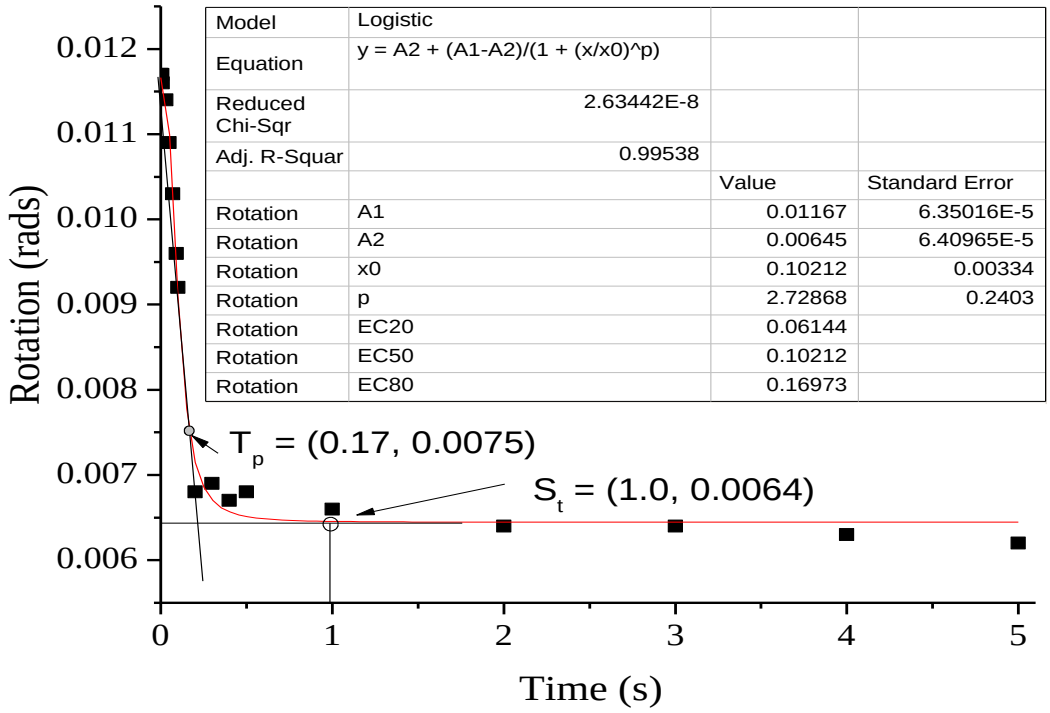

Figure 3-30 Rotation vs time at ECRS (Function 4)

At equilibrium of vertical and downward forces, column removal scenario is simulated which sets the structure to a dynamic state. The range of the column removal time (R_t) is $0.0001 \leq R_t \leq 5s$. The maximum displacement and rotational response of technique four are

129.7mm and 0.01167rads. The displacement curve and the rotational curve has a similar pattern. The turning point using the displacement curve begins at 0.1s to 0.92s at which the structural response due to instantaneous column removal changes from dynamic equilibrium state to a static state. Beyond, 0.92s column removal time does not affect the response of the structure as shown on the displacement response time plots. Similar response is observed in the rotation verse time curve plots. At 0.17s, the dynamic phase diminishes to static equilibrium state at 1s. When column removal time exceeds 1s, the condition is considered as a simple static case. A tangent drawn on the horizontal curve of the graph gives the approximate rotation which is no longer a function of the column removal time.

3.4.3 Results of Interior Column Removal Scenario (ICRS)

This subsection presents the results obtained at the interior column location of the building to investigate column removal time. The displacement response of the structure is used for the evaluation, the rotation is not considered because of the compressive arching of the slab which significantly limits the joint rotation due to column removal. That is, the rotation at the column removal location is negligible, therefore it is neglected.

Technique one results

The result of the study for the functions described in Section 3.3.1 for ICRS is presented in Figure 3-31 and Figure 3-32 for technique one. For Function 1A, it was observed that the pattern and response to column removal time differ from other functions. The maximum displacement for Function 1 is 87mm, which occurred at 5s. The maximum displacement for Function 1B is 40mm which occurs at 0.001s. The notion that the lower the column removal time, the higher the dynamic structural response of the structure does not hold for Function 1A but it is valid for Function 1B. For both functions, the equilibrium of the structure to a static state begins at approximately 1s. For Function 1B, beyond 1s, the increase in column removal time does not affect the response of the structure significantly.

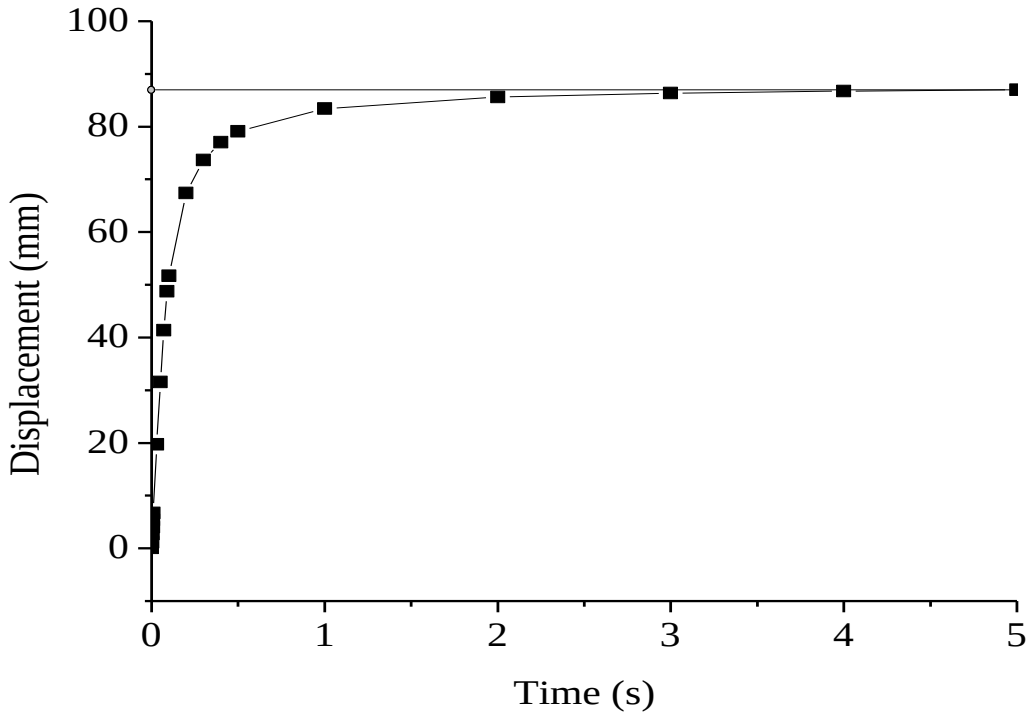

Figure 3-31 Displacement vs. time at ICRS (Function 1A)

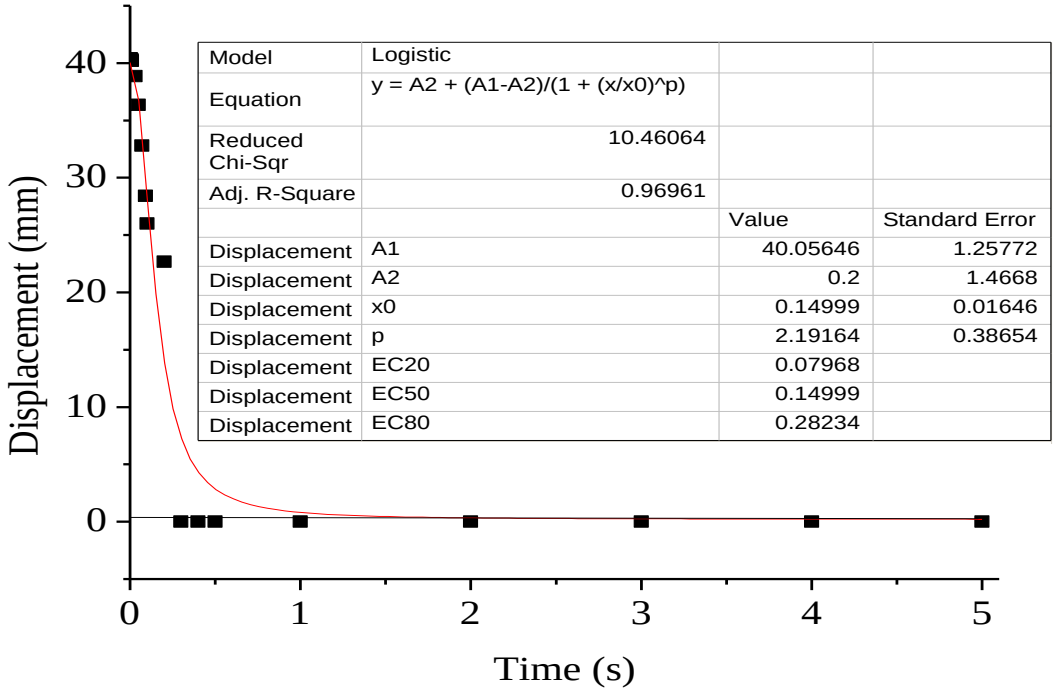

Model	Logistic		
Equation	y = A2 + (A1-A2)/(1 + (x/x0)^p)		
Reduced Chi-Sqr	10.46064		
Adj. R-Square	0.96961		
		Value	Standard Error
Displacement	A1	40.05646	1.25772
Displacement	A2	0.2	1.4668
Displacement	x0	0.14999	0.01646
Displacement	p	2.19164	0.38654
Displacement	EC20	0.07968	
Displacement	EC50	0.14999	
Displacement	EC80	0.28234	

Figure 3-32 Displacement of Function 1B vs. time (Technique one)

Technique two results (Function 2)

Figure **3-33** and Figure 3-34 is the detailed result for the technique described in Section 3.3.2 for displacement and rotational response respectively.

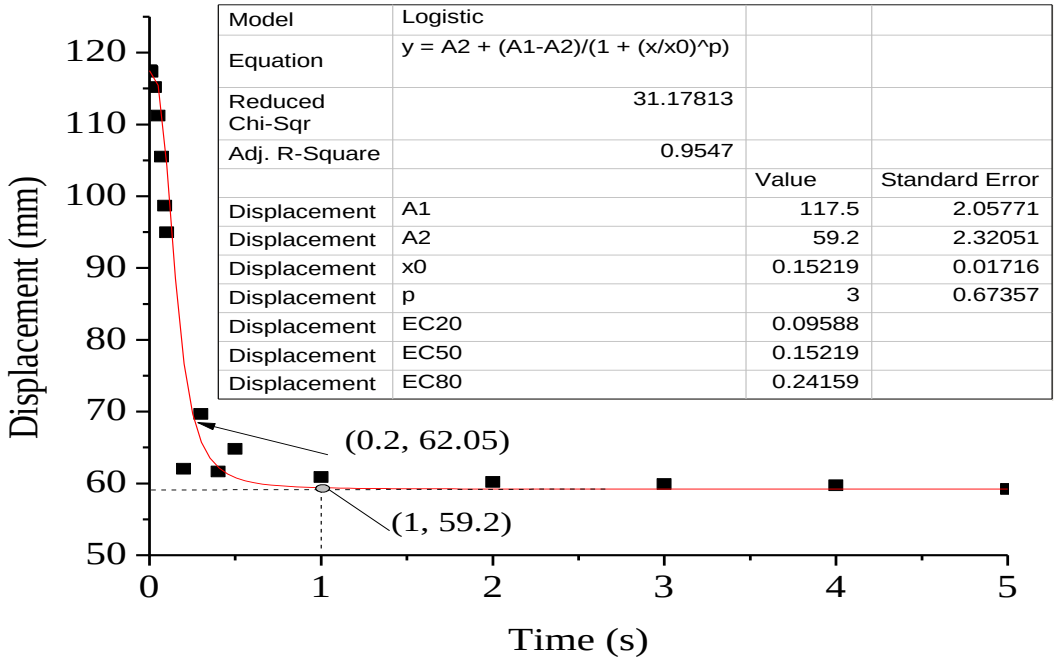

Figure 3-33 Displacement vs time at ICRS (Function 2)

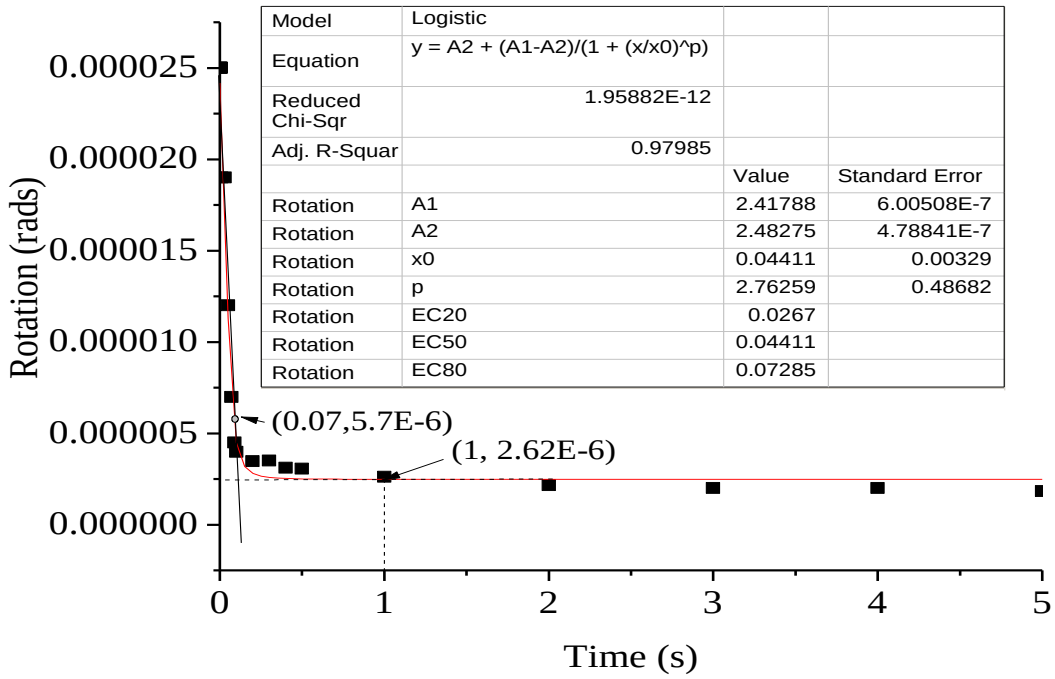

Figure 3-34 Rotation vs time at ICRS (Function 2)

Within the range $0 \leq R_t \leq 5$s, the maximum displacement and rotation are 117.5mm and 0.000025rads respectively, and this occurs at 0.001s. Taking a tangent through the curve fitting path of the plots, it is observed that the turning point for the displacement and rotational response occurs at 0.2s and 0.07s respectively. Within the range of $1 \leq R_t \leq 5$s, column removal time does not have any significant effect on the displacement and rotational response of the structure.

Technique three results

This technique has been described in Section 3.3.3, it involves the gravity load (N) interacting with the column internal reaction forces (PVM) at the joint to simulate column removal. The displacement response of the structure is shown in Figure **3-35**.

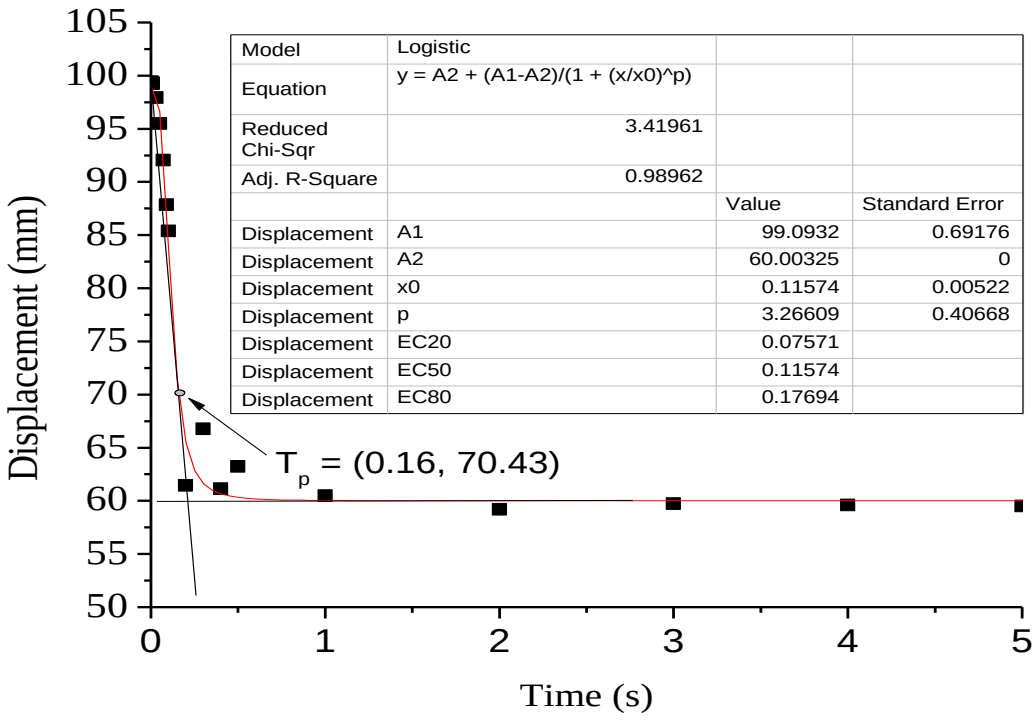

Figure 3-35 Displacement vs time at ICRS (Function 3)

The maximum displacement response due to this technique is 99mm and this occurs at 0.001s. Taking a tangent through the curve fitting curve, it is observed that the turning point from the dynamics state began at approximately 0.16s. Beyond 1s up to 5s, there is no significant increase in the dynamic response of the structure. Within the range $1 \leq R_t \leq 5$, column removal times do not affect the response of the structure significantly, therefore the analysis approximately represents a static response. Figure 3-36 is the rotation of the joint

using Function 3. The maximum rotation is negligible, though the turning point is approximately the same as the displacement response.

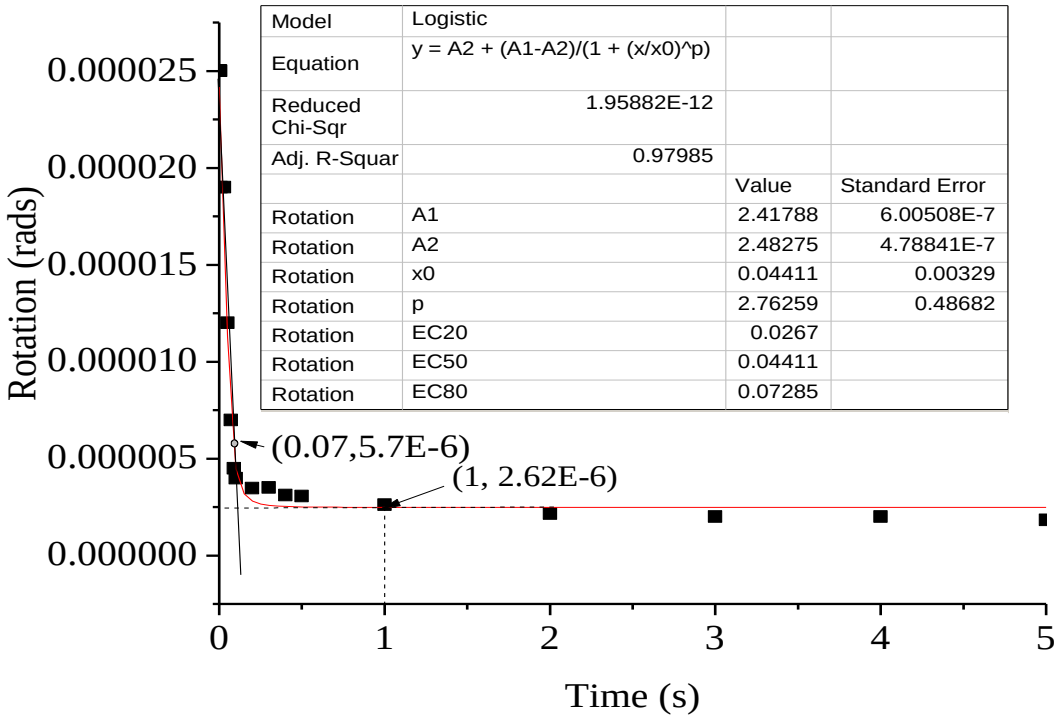

Figure 3-36 Rotation vs time at ICRS (Function 3)

Technique four results

This technique as described previously (Section 3.3.4) requires the balancing of column reaction forces (PVM) at the column removal node with the same magnitude of action forces which are in the opposite direction. This is not a common technique because of the perceived time required for the modelling. Figure 3-37 and Figure 3-38 shows the rotation and displacement response based on technique four. The maximum joint displacement response is 87.88mm which occurs at 0.001s. This corresponds to a maximum joint rotation of 0.0000024rads. The turning points for displacement and rotational plots occur at approximately 0.2s and 0.13s respectively. This corresponds to a displacement of 62.9mm and a rotation of 0.000012rads respectively. Based on this technique, the stability of the structural system is after 2s.

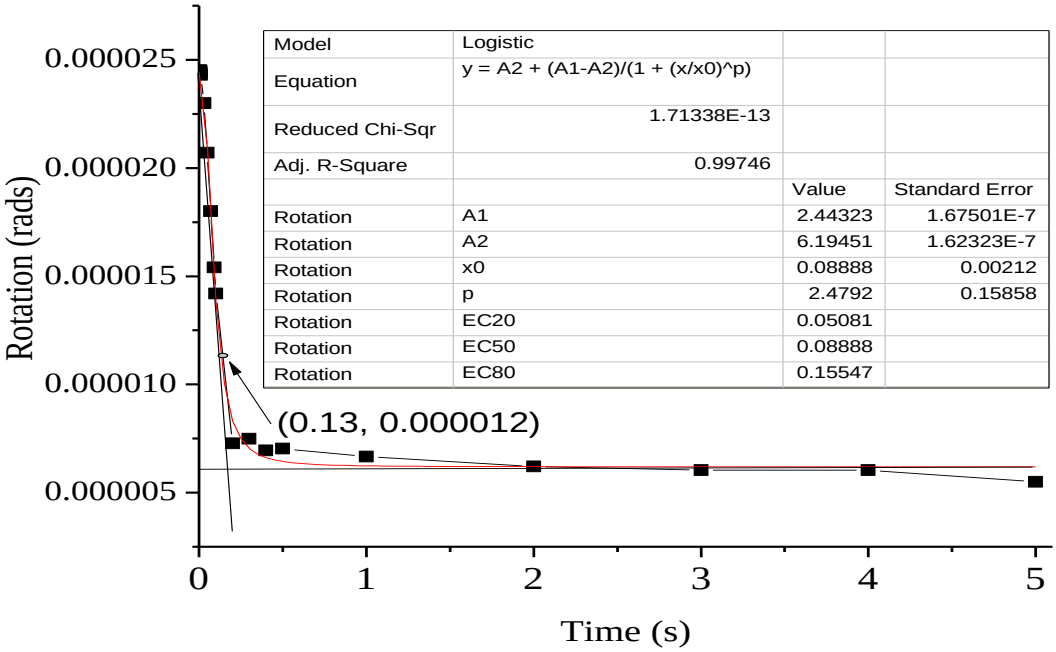

Figure 3-37 Rotation vs time at ICRS (Function 4)

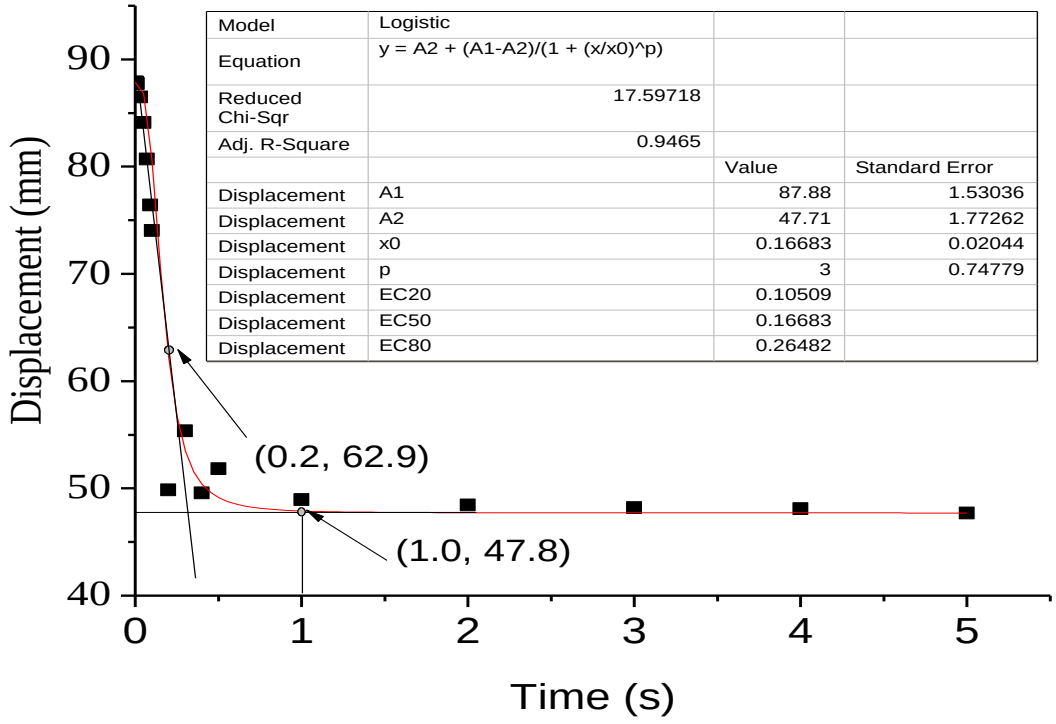

Figure 3-38 Displacement vs time at ICRS (Function 4)

3.4.4 Summary of investigation

The assessment presented in Section 3.4 addresses one of the objectives of the thesis: to determine the effect of column removal time on progressive collapse assessment of high-rise steel structures. All the techniques described in Section 3.3 as a function of $\mathrm{R_t}$ were evaluated at three different locations within the structural system.

The column removal time (R_t) was investigated at the edge or perimeter of the building (ECRS), corner column removal scenario (CCRS) and the interior column removal (ICRS) locations. The column removal time (R_t), was treated as a random variable which depicts different scenarios of the impact of an unforeseen event on structures. Within the range of $0.001 \leq R_t \leq 5$s of column removal time, it was observed that the critical response of the structure occurs within the range $0.001 \leq R_t < 0.01$s. Irrespective of the location of the column removal, the structural stability from the dynamic equilibrium state to a static state is within the range $0.1 \leq R_t < 2$s. This phase could be viewed as transitory phase of the structure. The sway mode of the structure has a period of approximately 2s.

Generally, five unknown parameters are required to correlate the displacement (D_y) and rotational response (R_y) to column removal time. These parameters depend on the time loading paths. Regression analysis was used to derive a correlation between the displacement and the rotational response as shown in Equation 3-24 and Equation 3-25 respectively.

$$D_y = A_2 + \frac{A_1 - A_2}{1 + (x/x_0)^p} \qquad \textbf{3-24}$$

$$R_y = B_2 + \frac{B_1 - B_2}{1 + (r/r_0)^n} \qquad \textbf{3-25}$$

In conclusion, *critical* response is within the range $0 \leq R_t \leq 0.01$s which corresponds to $\frac{T}{1000} s$; where T is the period of the structure in seconds. However, for $R_t \geq 2$s, it was observed that column removal time does not have a significant impact on the response of the structure. The response of the structure is approximately a static response and not recommended for progressive collapse assessment.

3.5 Relative evaluation of modelling techniques

This section addresses one of the critical decisions to be made before carrying out progressive collapse assessment. The choice of the modelling technique to be adopted is one of the most important factor to be considered as it affects the response of the structure. The time loading function considered in modelling sudden column loss affects the response of the structure. It is important to note that all the time history functions observed in existing literature is a function of column removal time.

3.5.1 Evaluation of modelling techniques at (ECRS) scenario

The results obtained comparing the four techniques described under the same condition of 0.002s column removal time is shown in Figure 3-39 and Figure 3-40. Technique one has two functions, which are assigned Function 1A (DT1A) and Function 1B (DT1B). The former does not consider the stability period of the reacting forces between the gravity loading and the internal reactive forces.

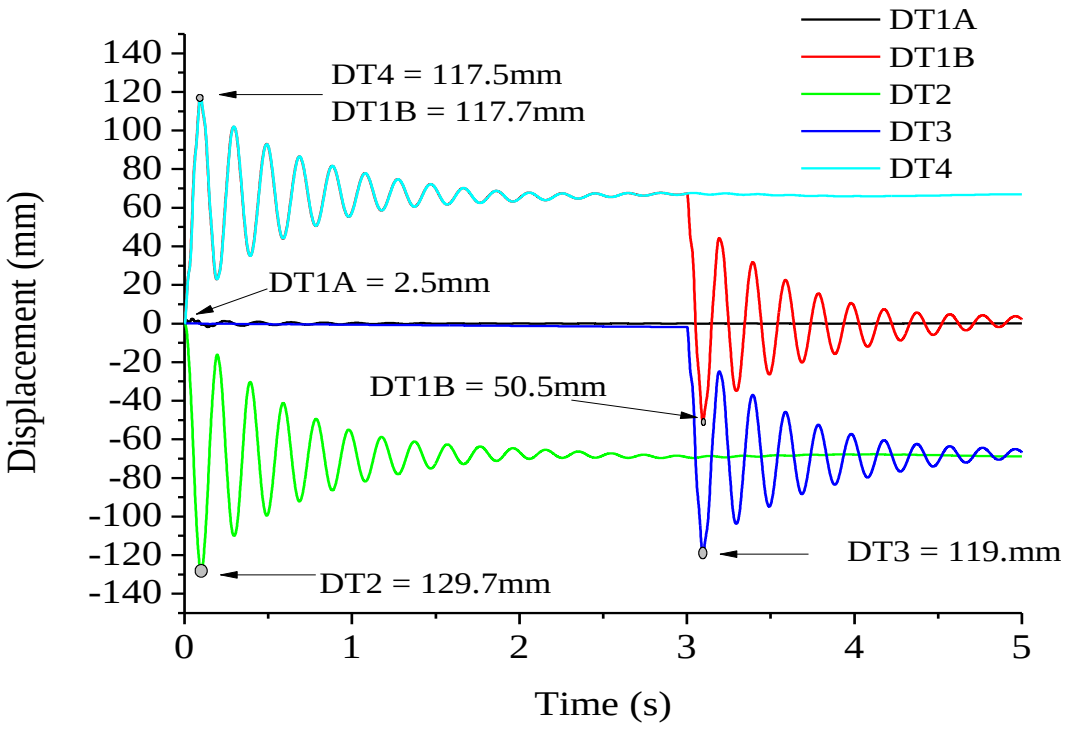

Figure 3-39 Displacement responses for the four techniques

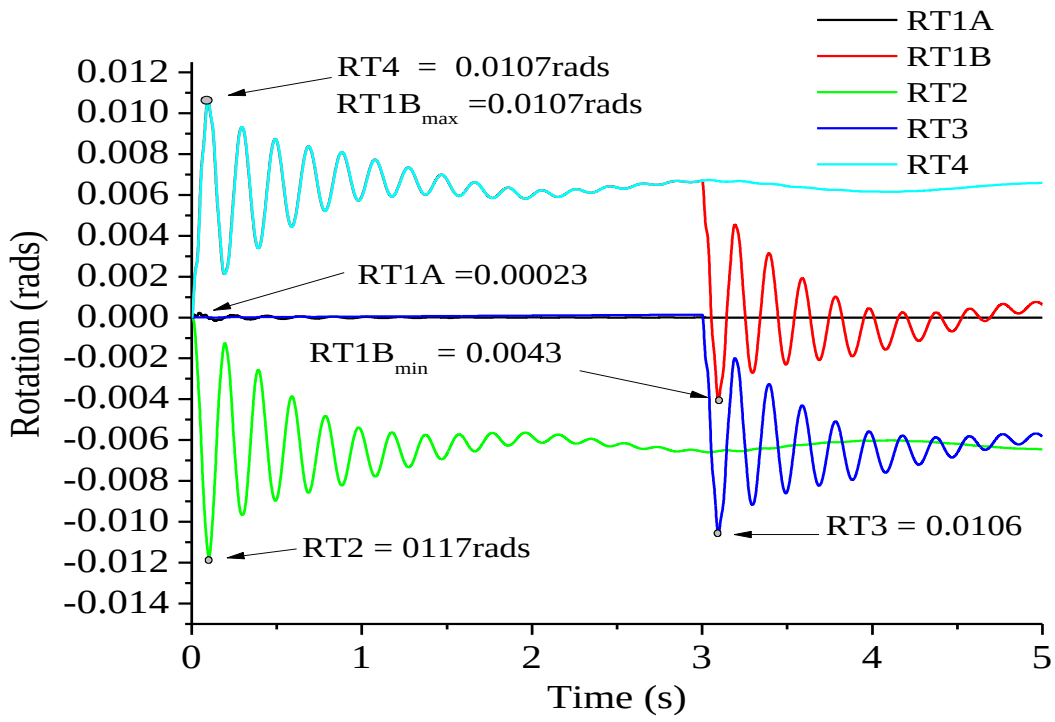

Figure 3-40 Relative rotational responses of four techniques

It is observed that the maximum displacement and rotational response for Function 1A (DT 1A) is 2.5mm and 0.00023rads respectively. Function 1B (DT 1B) considers the stability period of the reacting gravity load and the internal column force has a maximum displacement and rotational response of 50.5mm and 0.0043rads respectively at the column removal region.

However, within the stability period of 3s, the maximum displacement and rotational response are 117.7mm and 0.0107rads. Function 1A and Function 1B are grouped into technique one, using this technique to model sudden column loss requires the consideration for stability of gravity and reactive force equilibrium. Otherwise, the response from the structure could be misleading in making a coherent structural judgement. Technique two which is the approximate method shows a maximum displacement and rotational response of 129.7mm and 0.0117radians as shown in the green colour code of the plots. The maximum displacement and rotational response for technique three are 119mm and 0.0106radians. This technique is the most common technique used in existing literature for progressive collapse assessment. The maximum displacement and rotational response for this technique are 117.7mm corresponding to a rotation of 0.0107rads respectively. It was observed that the response from this technique is approximately the same with technique four within the stability period.

The maximum dynamic displacement and rotational response of the structure are 117.5mm and 0.0107rads. Using the edge column removal scenario (ECRS) for this investigation, three functions (Technique two, three, and four) are recommended for progressive collapse evaluation. However, it is important to note that Technique one using Function 1B, shows a maximum response of 117.7mm within the stability period. Technique two which is the sudden application of gravity load has a displacement of 129.7mm which exceeds technique three and four by 9% and 10.2% respectively. Comparing technique three and four, it was observed that technique three exceeds technique four by 1.1% which is negligible. Similar observation was observed for the rotational response of the structure. The rotational response of technique two, three, and four are, and 0.0117: 0.0106: and 0.0107 respectively. Technique 2 exceeds technique three and four by 10.4% and 9.3% respectively, and the rotational response of technique three and four, differs by just 0.9%.

By using the edge column removal scenario to analyse the four techniques identified, it can be concluded that technique two or technique three will be a better option for progressive collapse assessment. The advantage of technique two over technique three is the ease of modelling and it does not require for the reactive internal forces in the column to be determined. Technique three has been the favourable approach in existing literature because it considers the stability of the gravity load and the reacting force in ensuring the equilibrium of the forces.

3.5.2 Evaluation of modelling techniques at (CCRS) scenario

This subsection is to evaluate the response and behaviour of the structure using the corner column removal scenario (CCRS). Relative structural responses of the four techniques are compared to evaluate the extent at which the modelling techniques differ. The results for the investigation of the four techniques for CCRS are presented in Figure 3-41. It was observed that Function 1A of technique one gives the minimum dynamic response (2.39mm) and corresponds to the stable state of function 3 approximately at the column removal phase. Technique 1B has a two-phase response, the process of stabilising the gravity loading and the column removal phase. The behaviour of this function is unique, the maximum dynamic response (DT1B = 122.8mm) for this function occurs at the process of stabilising the gravity load with the reactive force. The second phase which actually defines the sudden column removal phase has a maximum displacement response of 51.6mm.

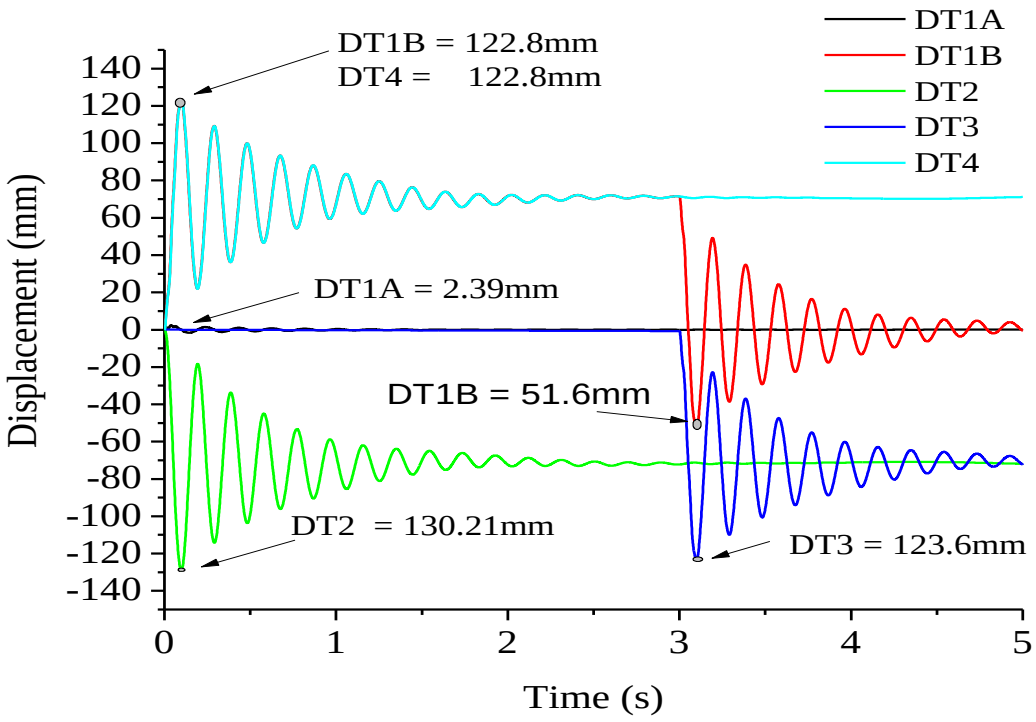

Figure 3-41 Displacement responses of techniques (CCRS)

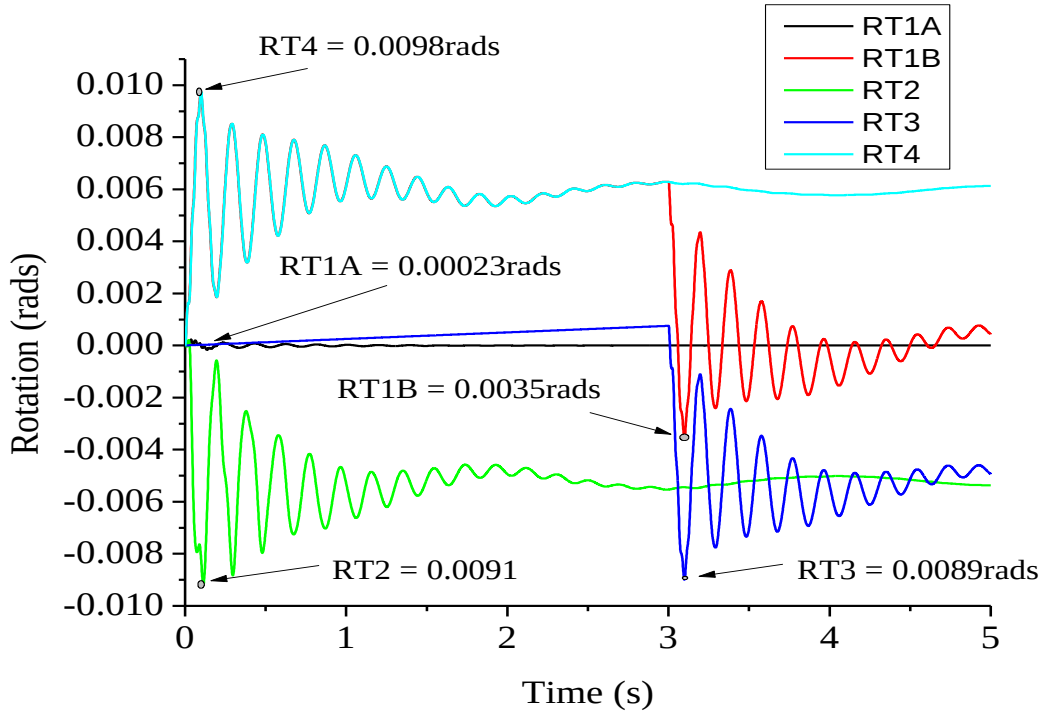

Figure 3-42 Joint rotation of different techniques (CCRS)

Technique two, three, and four has a maximum displacement of 130.21mm: 123.6mm and 122.8mm respectively. This implies that the approximate method (Technique two) exceeds technique three and four by 5.3% and 6% respectively.

Technique three and four differ by just 0.7%. There is no significant variation between technique three and four from the displacement response of the structure. Relative joint rotations of the structure is shown in Figure 3-28. The rotational response of the structure increases in the order Function 1A (RT1A), Function 1B (RT1B), Function 3 (RT3), Function 2 (RT2), and Function 4 (RT4) and these corresponds to .00023rads, 0.0035rads, 0.0089rads, 0.0091rads, and 0.0098rads respectively. It is important to note that Technique *one* using Function 1B has two-phase response, the phase of stabilising the gravity load to the reactive internal column force and the phase of column removal scenario. It is observed that the maximum rotational response for this function normally takes place at the stabilising phase of gravity loads and reactive forces. This phase coincides with the response of technique four as shown in Figure 3-42. Maximum joint rotation occurs in Technique four (RT 4) and the stabilising phase of Technique one (RT 1B) with a magnitude of 0.0098rads.

3.5.3 Relative evaluation of modelling techniques (ICRS)

The displacement response using the interior column removal location scenario (ICRS) for Technique one, two, three and four are presented in Figure 3-29. The maximum response due to Function 1A of Technique one is 1.79mm, the maximum response due to Function 1B on the stabilizing phase is 98.70mm and on the column removal phase is 42.6mm, the maximum response due to technique three is 101.6mm and for technique four is 123.2mm. The displacement respond of the structure was used for the relative comparison alone because the rotational response is negligible due to the compressive arching of the slab. The response of the structure differs from the edge and corner column removal scenario. In this case, Technique two and Technique four have similar behavioural response with a maximum displacement of 123.2mm. Technique three (DT3) has a maximum displacement of 101.6mm, Technique one using Function 1B (DT1B) has maximum displacement of 98.7mm and 42.5mm for the stabilising phase and column removal phase respectively.

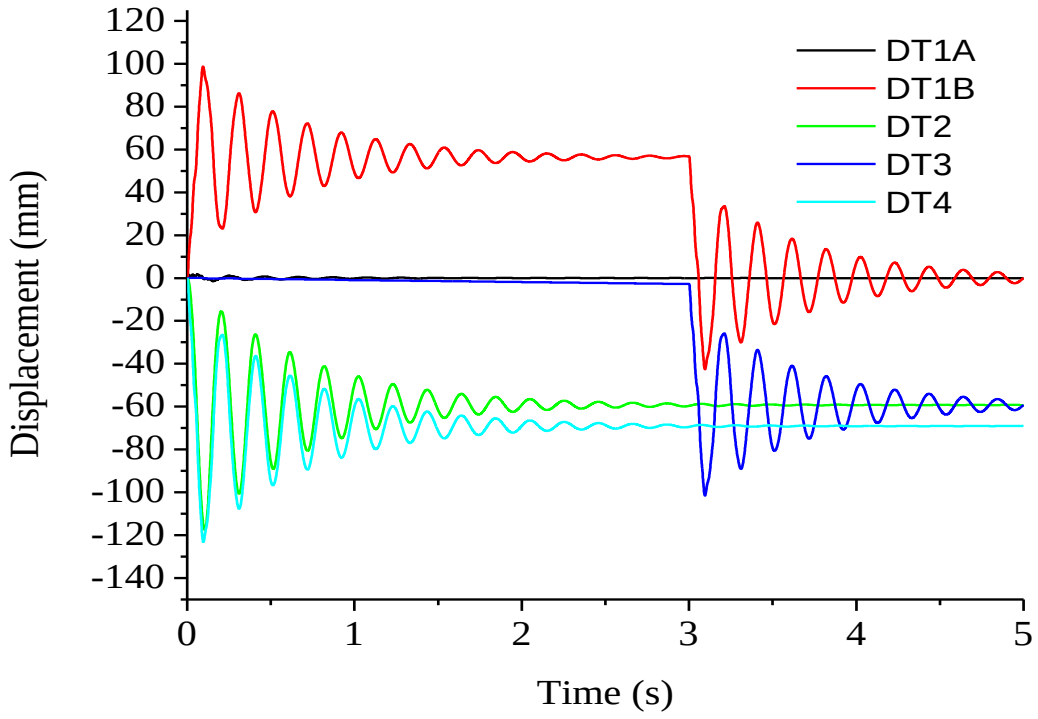

Figure 3-43 Comparing modelling techniques at ICRC

Technique two, which is the approximate method shown by the green colour plot (DT2) and Technique four have the maximum displacement response of 123.2mm which exceeds Technique three by 21%.

3.6 Chapter summary

As discussed previously, the objective of this investigation was to assess the effect of column removal time on structural response and to compare modelling techniques. This section summarises the main conclusions of the investigation carried out in this chapter.

The GSA 2003 design guideline, proposes the duration of instantaneous column removal time(R_t) to be less than one-tenth of the period(T) of the structural response mode for the vertical motion of the bays above the removed column. The standard states that the duration of the analysis shall continue until the maximum displacement is reached. Different standards estimate the natural period of the structure with a particular focus on the sway mode of the structure with little or no consideration for the vertical mode. For instance, NEHRP (1994) provisions recommend that the natural period (T) of the structure should be estimated as a tenth of the Number of storeys with a restriction to 12 stories having a storey height of 3m. In Eurocode 8, the natural period expression is given as:

$$T_1 = C_t(H)^{0.75}$$

Where H (m) is the height of the building, C_t is 0.085 for moment resistant steel frame and 0.075 for moment resisting concrete frame. A value of 0.050 was recommended for all other structures. On the other hand, NEHRP (1994) suggests a coefficient of 0.030 and 0.035 for reinforced concrete and moment resisting frame structure. Other proposals for the period of the structure can be found in the literature Goel (1997) and Salama (2015). Modal analysis of the structure using Ritz vectors was carried out to determine the period of the structure under vertical vibration mode as proposed by GSA 2003. In this study, it was observed that the period of the structure in the vertical vibration mode is approximately a tenth of the sway mode under column removal scenario.

The natural period of the structure before the column removal was 2.02s approximately, and 2.04s under column removal scenario. This corresponds to the sway mode. The natural period of the structure under vertical motion before and after column removal is approximately 0.11s and 0.19s respectively. Therefore, using GSA 2003 clause 3.2.13.4.2 design recommendations, the column removal time should be less than a tenth of 0.19s which is 0.019s ($R_t < 0.019$s).

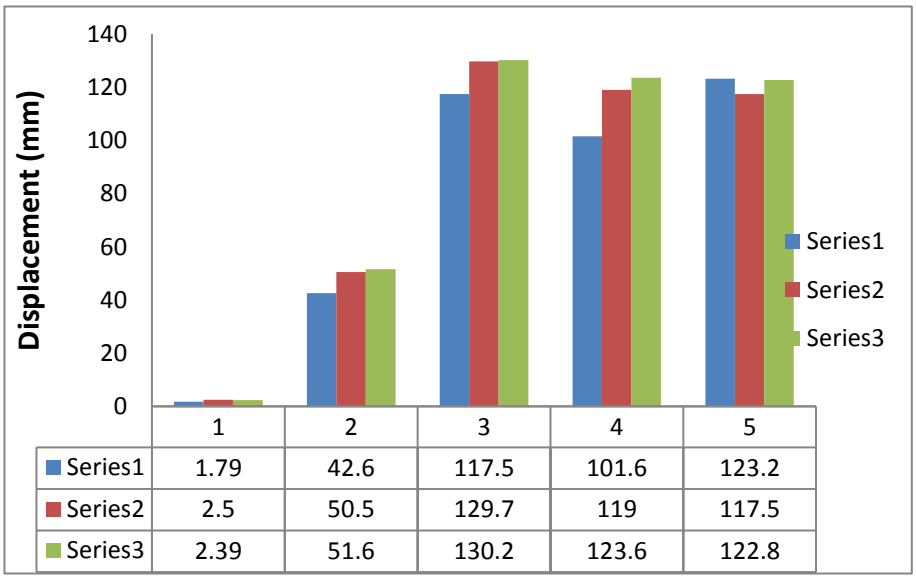

	1	2	3	4	5
Series1	1.79	42.6	117.5	101.6	123.2
Series2	2.5	50.5	129.7	119	117.5
Series3	2.39	51.6	130.2	123.6	122.8

Figure 3-44 Displacement responses of different techniques

This study shows that the column removal time affects the response of the structure within defined ranges. For this study, it is proposed that the critical column removal time for progressive collapse assessment should be a hundredth of the period of the structure in the vertical direction under column removal.

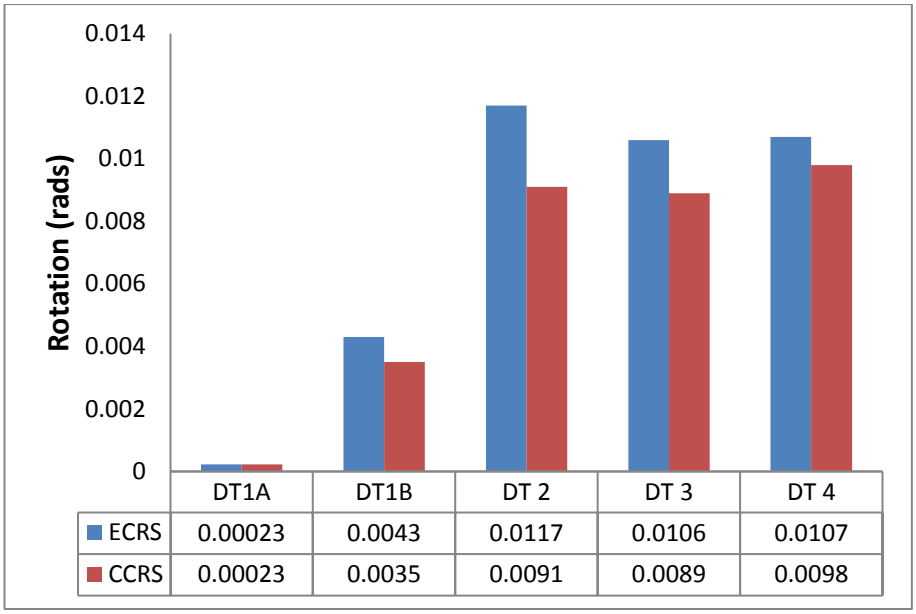

Figure 3-45 Rotational responses of different techniques

The summary of the relative evaluation of the modelling techniques are presented in Figure 3-44 and Figure 3-45 respectively. The approximate method (DT2) gives the highest response compared to other time loading functions. This approach is computationally more efficient relative to other methods because it does not require the modelling of the reactive forces. Technique one which has two functions defined as DT1A and DT1B is not recommended for progressive collapse assessment without having a sound knowledge of how the column removal time affects the response. Figure 1A gives a maximum dynamic response when the column removal time falls within the range $1<R_t\leq 3s$.

Technique three (DT3) which requires the balancing of reactive forces to gravity load considers the equilibrium of reactive forces and gravity loading before the instantaneous column loss. The approximate method (DT 2) exceeds Technique three with 15.7%, 10% and 5.3% at ICRS: ECRS and CCRS respectively based on the displacement response. Using the rotational response criteria, it was observed that DT 2 exceeds DT 3 by 10.37% (ECRS) while DT 4 is approximately the same with DT 3. For CCRS, DT2 exceeds DT 3 by 2.2% while DT 4 exceeds DT 3 by 10.1 %. The study shows that the maximum displacement and rotational response of the structure occurs using Technique two (DT2). This approach is computationally efficient compared to the other techniques considered.

Hence, this study provides evidence that sudden application of gravity loads is more critical to structural response under progressive collapse as compared to the other methods studied.

Therefore, the author recommends application of gravity loading for progressive collapse assessment of structures.

In conclusion, for building structures having a period of T (s) in the vertical motion, the critical instantaneous column removal recommended is $1/100^{th}$ of the period of the structure.

Chapter 4 Assessment of moment resisting frame (MRF)

4.1 Introduction

This chapter addresses one of the key objectives of the thesis: to determine the internal force redistribution and the dynamic effect of sudden column loss on moment resisting frame structures. If a structural member is damaged or lost instantaneously, the structural system seeks a new equilibrium state in redistributing its internal forces through alternative paths. A brief background of the study is presented in subsequent paragraphs. Part of this study was published in a conference proceeding (Stephen et al. 2012), and the feedback and observations have been integrated into this thesis.

In recent times, structures that have high economic and political importance are potential targets for terrorist resulting in the perimeter of such buildings being susceptible to greater energy impact from unforeseen events such as blast. The perimeter of a structure has a higher tendency of been subjected to progressive collapse relative to the interior of the building.

Understanding the load redistribution mechanisms of building structures during a progressive collapse is important for proposing a design factor for simplifying the nonlinear dynamic analysis approach. The change in magnitude and redistribution of internal forces in structures may likely exceed the one estimated during the traditional design stage of the structure. Such changes can then be accounted for in the design of connections linking critical vertical load bearing members. Since abnormal loads on structures often results to reduction in the strength capacity over time, this section seeks to investigate the changes in the internal forces in the structures over time. Events like blast loads on structures affects the stress redistribution over a short period of time while events like high temperature affects the stress redistribution over a longer period of time.

In conclusion, a proposal for the dynamic amplification factor is made relative to the provision of GSA 2003. In addition, the provision of Eurocode 3 which requires that connections should be capable of withstanding a tensile force of 75kN would be assessed if such recommendations hold under progressive collapse scenario.

4.2 Model description

The model assumed for the investigation is a 10 storey moment resisting frame structure. The structure has 5 bays along the Y-axis with an equal span of 6m. There are 4 bays along the X-axis having an equal span of 4.5m. The building has a typical storey height of 3.5m with a slab thickness of 130mm. The section sizes are shown in Table 4-1 while the elevation and plan view showing the location where the case studies were carried out is shown in Figure 4-1.

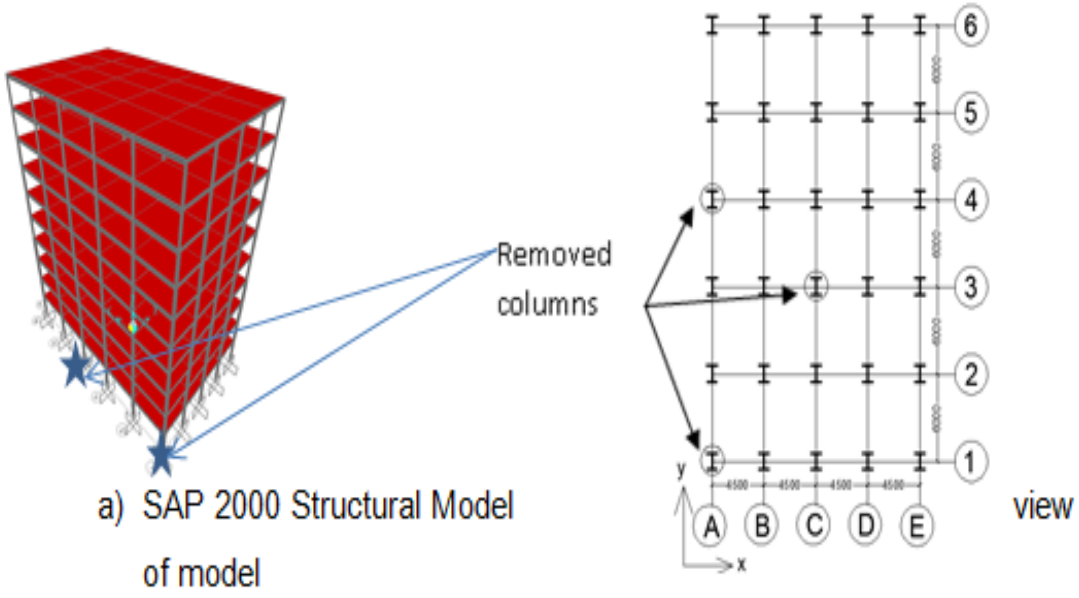

Figure 4-1 3D elevation and plan view of the model

The model for this investigation was designed based on the provision of Eurocode 3, 2005 with a target capacity ratio of 0.7 to 0.85 using the governing equation 6.2.1 of the code. The load combination is based on the ultimate load capacity; 1.35 factor for the dead load and 1.5 for the imposed load as recommended in Table NA.A1.2 (B), NA to BS EN 1990:2002+Al: 2005.

4.2.1 Material description

The nonlinear material behaviour remains the same as presented in previous chapter (Section 3.2).

Table 4-1 Section sizes for the investigation

Section sizes	Number of storeys
254×102×22UB	1-10 (x-axis)
406×140×39UB	1-10 (y-axis)
203×203×60UC	7-10
254×254×167UC	4-6
305×305×198UC	1-3

4.2.2 Progressive collapse load combination

The combination of applied loads used for the investigation has been described in the previous chapter as recommended in GSA 2003 for static and dynamic loading. The guideline recommends 2.0 simplifying the perceived complexity of nonlinear dynamic analyses for progressive collapse evaluations.

4.3 Time loading function

The methodology used for the assessment was based on the instantaneous application of gravity loading as shown in Figure 4-2

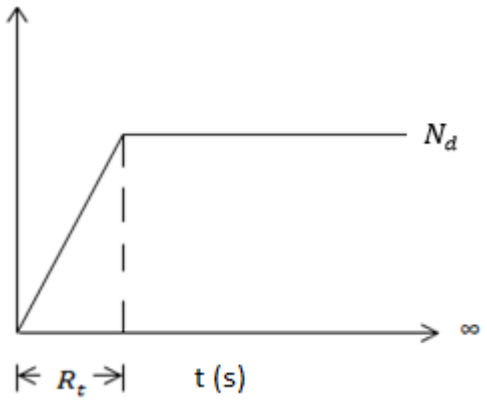

Figure 4-2 The step force function (Tsai and Lin 2009)

Where N_d is the GSA gravity load combination and R_t is the column removal time in seconds (s). Further information on the time step size can be found in Gerasimidis and Baniotopoulos (2011).

4.4 Scope of investigation

The assessment presented in this study is limited to only a ten storey moment resisting frame structure. Assessment of the building is carried out at four column removal locations (Edge, interior, corner, eight); however, only the perimeter of the building was considered for multiple column loss. The study covers member structural responses, joint displacements and rotational responses under linear, nonlinear static and nonlinear dynamic analyses. Evaluation of the dynamic amplification factor and the relative responses in single to multiple column loss scenarios are presented in this chapter.

In addition, the development of catenary force in beams has been a subject of interest in recent times, though important, however it's not often considered in conventional structural design. This chapter will assess the behaviour catenary effects in beams as well as the redistribution of forces that takes place due to column loss. The columns within the boundary of the removed columns will be assessed to evaluate the extent to which the internal forces are been affected as a result of single and multiple column loss.

At the end of the investigation, a proposed dynamic amplification factor for displacement and joint rotational responses, axial forces, shear forces and moments in beams and columns will be recommended. Furthermore, conclusions will be drawn on the extent at which column removal locations affects the joint conditions used in evaluating a joint model.

4.4.1 Position one: Corner column removal scenario

Figure 4-3 is the elevation of the model showing the position of the column removal (Col1). The corner column is connected to Beam 541 on the YZ plane and Beam 301 on the XZ plane and bounded to Col 11 and Col 61 at the long and short span respectively. Investigating the structure without column 1 as shown in Figure 4-3 is deem to significantly affect the connecting beams and the adjacent columns too.

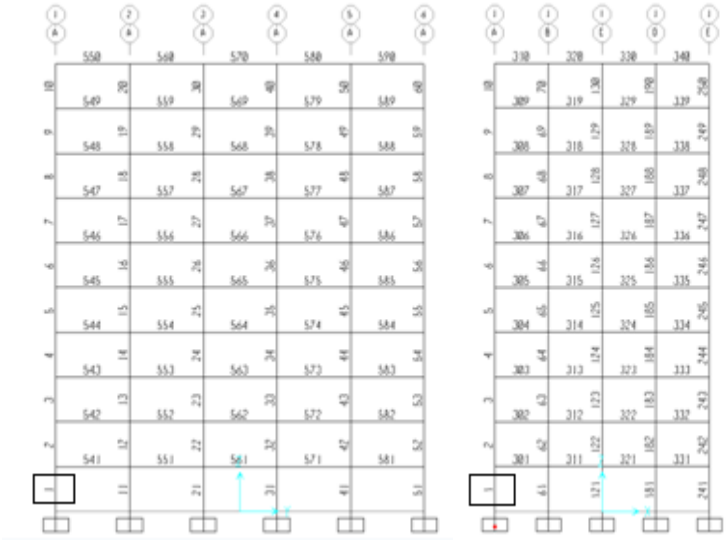

Figure 4-3 YZ and XZ elevation of model

The initial forces in these members were recorded, and the model was built without column one. The analysis was re-run to assess the percentage increase in the connecting members (Beam 541, Beam 301, Column 11 and Column 61). Table 4-2 shows the initial forces in all the members and the maximum connection response due to the removed column.

The change in the force distribution due to static analysis of the structure results in 33.5% of axial force (P) of Col 11 while Col 61 experiences a change of 38.8% in axial force. Relatively, Col 11 experience significant changes in shear and moment response due to the loss of the corner column as compared to Col 61. The maximum joint displacement and rotation was 71.4mm and .0052 rads respectively. The maximum shear force occurs in Beam 541 having a magnitude of 157.60kN. The beam axial forces are within a safe limit since Eurocode 3 recommends a minimum of 75kN tensile force for connection design. The maximum rotation of 0.0052 rads exceeds 0.0035rads recommended for simple connections.

Table 4-2 Redistribution of forces due to CCRS

Conditions	P (kN)	P' (kN)	V (kN)	V' (kN)	M (kNm)	M' (kNm)
Col 11	3068.02	4011.43	0.531	48.45	1.16	124.14
COL 61	2815.44	3907.93	11.28	34.59	34.59	86.00
BM 301	4.08	40.76	34.75	71.63	25.78	112.21
BM 541	9.94	33.36	80.39	157.60	79.57	315.84
Jt2 = 71.4mm, Jr = 0.0052						

The change in the axial force due to static analysis of the structure results to 33.5% for Col 11 while Col 61 experience a change of 38.8%.

Relatively, Col 11 experience significant changes in shear and moment response due to the loss of as compared to Col 61. The maximum joint displacement and rotation were 71.4mm and 0.0052 rads respectively.

4.4.2 Position two: Linear static analysis (ECRS)

Figure 4-4 shows the XY and XZ plane elevation of the building at the edge column removal scenario (ECRS). The removed member is Column 31. On the short span; it is bounded by Beam 421 and Column 91. On the long span, the removed column is bounded by Beam 561, Beam 571, Column 21 and Column 41.

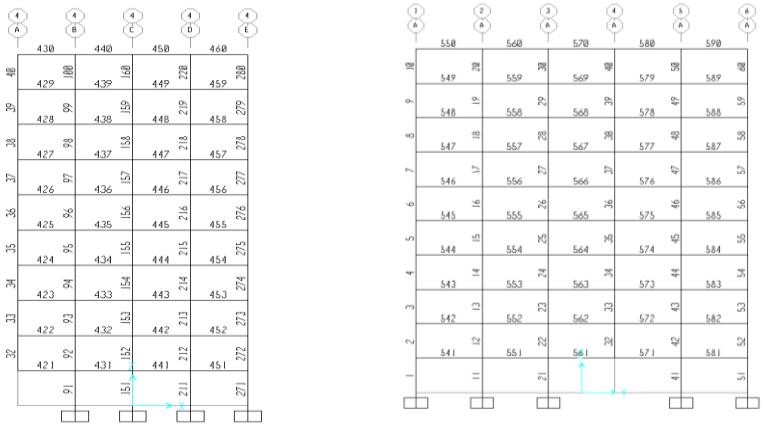

Figure 4-4 XZ and YZ elevation of model at CCRS location

The joint about the removed column is labelled as Joint 35. The forces in the connecting members before and after the loss of the edge column are shown in Table 4.3. Comparing the three columns (Column 91, Column 21 and Column 41), it is observed that the increase in axial force of the columns is 27.3%, 31.16% and 31.8% respectively. The increment in load redistributed to column 41 exceeds that of column 21 because of increase in span to the left of column 21. The most important phenomenon is the change in shear force in the beams from 80.17kN to 163.47kN, which is a 103.9% increment and the change in the beam end moment from 80.17kNm to 325.02kNm which is a 305% increment.

Table 4-3 Removal of edge column (Column 31)

Conditions	P (kN)	P' (kN)	V (kN)	V' (kN)	M (kNm)	M'(kNm)
Col 21	3098.02	4063.34	0.07	49.14	0.14	118.21
COL 41	3068.02	4046.55	0.53	48.15	1.16	120.78
COL 91	4208.46	5358.24	0.07	0.41	0.14	1.67
BM 561	0.85	35.57	80.17	163.47	80.17	325.02
BM 571	1.26	35.90	80.17	162.25	80.15	321.49
BM 421	0.02	55.55	0.97	0.97	1.08	1.08
Jt 35 = 68.4mm, Jr = 0.0063						

As a result of the loss in column, there is a significant development of catenary forces in Beam 421, which is transversely connected to the removed column. The initial axial tension was negligible (0.02kN); however, the removal of the perimeter column resulted in a maximum axial force of 55.55 kN in the transverse beam (Beam 421), as shown in Table 4-3. The maximum joint displacement due to the perimeter column removal is 68.4mm at J_t 35, corresponding to a joint rotation (J_r35) of 0.0063 rads. The perimeter columns connecting the removed columns 41 and column 91 exhibit significant changes in the end shear force and moments. Conventional design of column 21 and 41 at the design stage may not consider shear and moment as principal forces since the magnitude is negligible.

4.4.3 Position three: Static analysis response due to ICRS

Figure 4-5 is a two planes (XY and YZ) defining the position of the interior column removal scenario (ICRS).

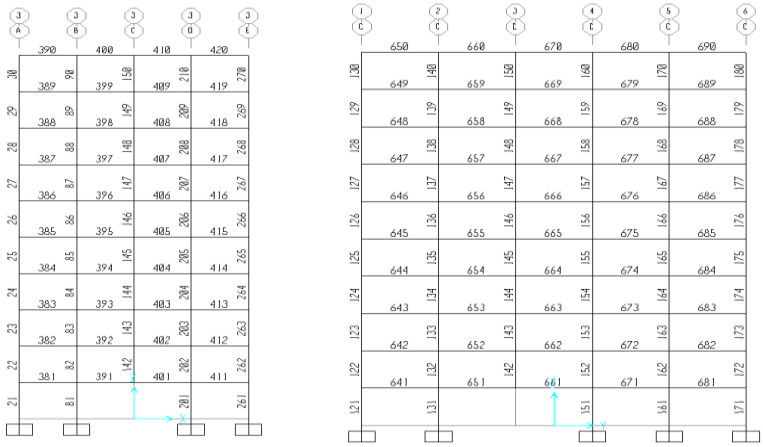

Figure 4-5 Elevation of XZ and YZ at ICRS

The beams and columns connecting the removed columns are Beam 391 and Beam 401 along the short span, and Beam 651 and Beam 671 at the long span. The columns adjacent to the removed interior column at the short span is column 81 and column 201, while the columns bounding the removed interior column along the long span are column 131 and column 151. The joint about the column removal point is labelled as joint 156 and, the displacement and rotational response of the joint after the column removal is shown in Table 4-4

Table 4-4 Interior column removal scenario (COL 141)

Conditions	P (kN)	P' (kN)	V (kN)	V' (kN)	M (kNm)	M' (kNm)
Col 81	4208.46	5317.39	0.64	39.18	0.14	92.02
COL 201	4208.46	5317.39	0.64	39.18	0.14	92.02
COL 131	4252.89	5003.43	0.71	49.90	1.62	122.18
Col 151	4367.12	5057.29	0.08	49.19	0.15	120.56
BM 391	0.65	39.44	0.97	0.97	1.08	1.08
BM 401	0.65	39.44	0.97	0.97	1.08	1.08
BM 651	1.21	39.21	68.04	137.56	68.04	271.66
BM 661	0.79	39.59	68.04	137.56	68.04	271.75
Jt 156 = 59.20mm Jt 156 = 0.000002						

The maximum joint displacement (JT 156) due to the removal of the interior column is 59.2mm, with a corresponding rotation of 0.000002 rads. From the results obtained, the axial force of column 81 and column 201 along the transverse direction (short span) increased by 26.4%, while the shear and moment are negligible. Along the longitudinal direction (long span), the axial force increase by 17.6% in column 131 (Col 131) and 15.8 % in Column 151 (Col 151). The shear force in columns 81 and 201 on the short span is negligible as it changes from 0.07 to 0.095kN. The change in moment is also negligible as it only increases from 0.14 to 0.177kNm. A significant change in the shear force response of column 131 and 151. This is still within the joint design consideration at the conventional design stage. However, significant changes in moment occur in columns 131 and 151, increasing from 1.62 kNm to 122.18 kNm and from 0.15 to 120.56 kNm respectively. It is obvious that the most significant change in the internal forces of the columns is the moment change.

Significant changes in beam axial forces occur in all the beams (391, 401, 651, 661), although these differences are considered negligible since they are lower than the minimum considered in the conventional design stage provision of Eurocode 3 for beam tensile force (75kN). Similarly, the change in shear forces and moment in Beam 391 and 401 are negligible. This implies that the most important change that takes place is the axial force developed in the tie beams. The behaviour in shear and moment is different for Beams 651 and 661 in

the long span. As for the axial force of the beams in the long span, the response is similar to that of the short span, although significant changes occur in the shear force and moment. The shear force and moment for these beams (Beam 651 and Beam 661) increase by 101% and 299% respectively. This change is significant and will affect the behaviour of the beam-column connections originally designed to resist a shear force of 68.04kN and a moment of 68.04kNm. The rotational response of joint 156 connecting the removed column at the first floor is 0.000002 rads. This is not significant. Based on static analysis, the maximum joint displacement due to the removal of the column is 59.20 mm.

4.4.4 Position four: Static analysis at EFCRS

Table 4-6 shows the YZ and XZ elevation of the building and the eighth-floor position where the column is removed. The eighth-floor column has a biaxial connection to Beam 548 on the YZ plane and Beam 308 on the XZ plane, as shown by the square section. The model is built without the missing column and the analysis re-run to assess the load distribution due to static analysis of the structure.

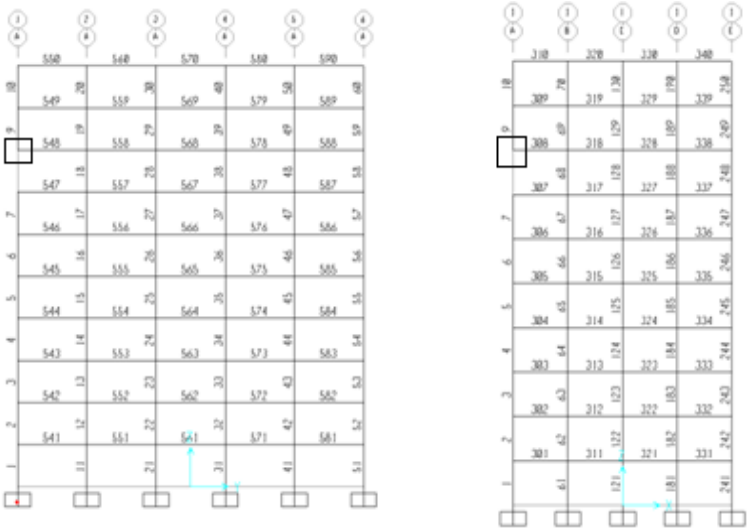

Figure 4-6 Eight floor column removal scenario (EFCRS)

The removed column is connected to beam 548 along the long span and Beam 308 along the short span. The columns connecting these beams are Column 18 and Column 68 which is adjacent to the removed column as shown in Figure 4-6

The static response of the structure before and after the removal of the eight floor column is shown in Table 4.5. The initial axial force of column 18 is 848.1kN which increases by 37.2% while the initial force in Column 68 is 777.7kN with an increase of 41.9% due to the

removed column. A significant increase in the shear force occurs from 5.56kN to 52.77kN in Column 18 corresponding to 849% increase in the shear force. There is an insignificant change in the shear force of Column 68.

Table 4-5 Static response due to EFCRS

Conditions	P (kN)	P' (kN)	V (kN)	V' (kN)	M (kNm)	M' (kNm)
Col 18	848.1	1163.30	5.56	52.77	10.56	31.80
COL 68	777.7	1103.50	30.13	28.80	58.35	51.79
BM 308	8.82	133.20	35.51	59.98	27.07	94.03
BM 548	16.95	126.0	82.26	141.00	83.68	279.96
Jt 9 =89.30mm, Jr = 0.0138						

A decrease in moment in Column 68 was observed. This is not the case in Column 18 which experiences an increase from 10.56kNm to 31.80kNm, corresponding to 201% increment. Given these changes, it can be concluded that the most important change in adjacent columns connecting the removed column at the eighth floor is the axial force.

4.5 Nonlinear static analysis (GSA 2003)

This section presents a nonlinear static analysis of the moment resisting frame structure under monotonic loading conditions. The procedure used for the investigation is based on Marjanishvili (2004). The structural deformation and hinge formation at maximum GSA loading combination for nonlinear static analysis are presented in Figure 4-7. Nonlinear modelling parameters for this study is based on Table 5-6 of FEMA 356 FEMA 356 (2000).

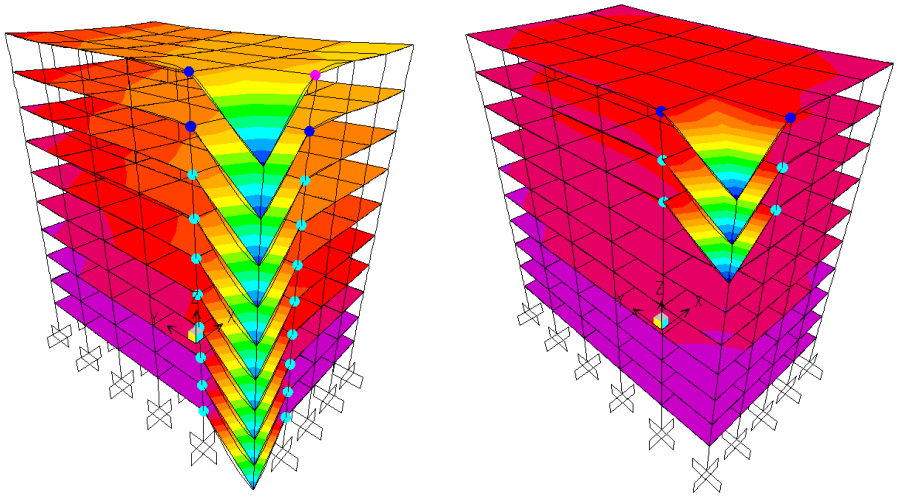

a) NLS at CCRS b) NLS at EFCRS

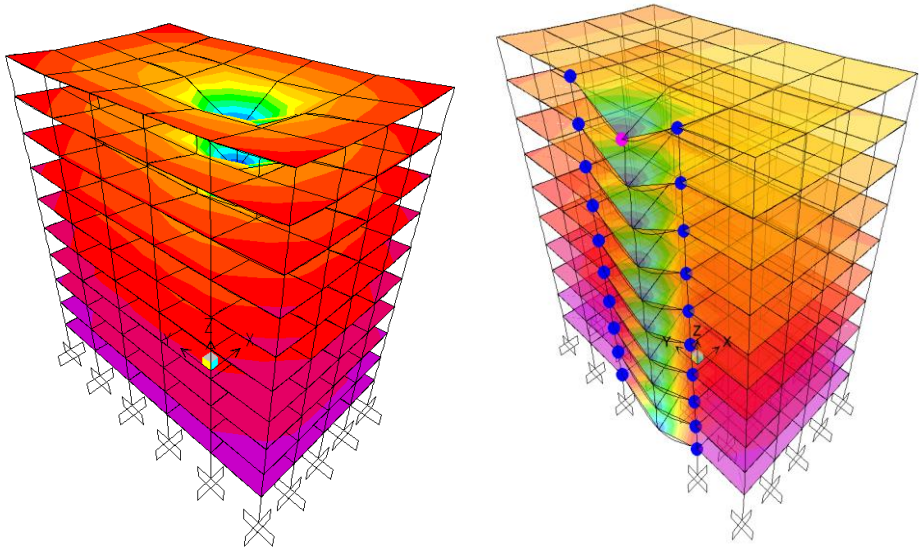

c) NLS at ICRS d) NLS at ECRS

Figure 4-7 Nonlinear hinge formation at maximum loads

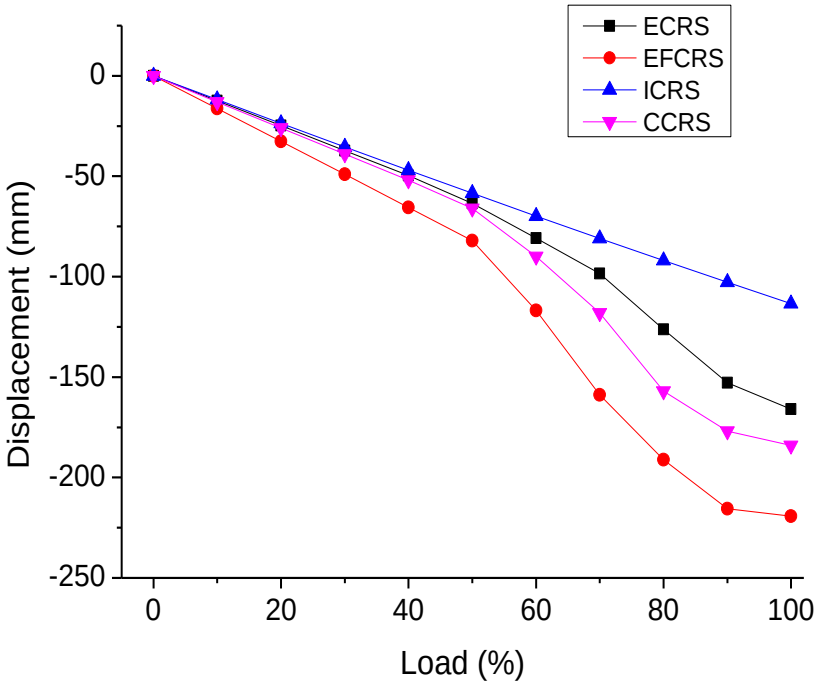

Figure 4-8 Displacement response under load increment

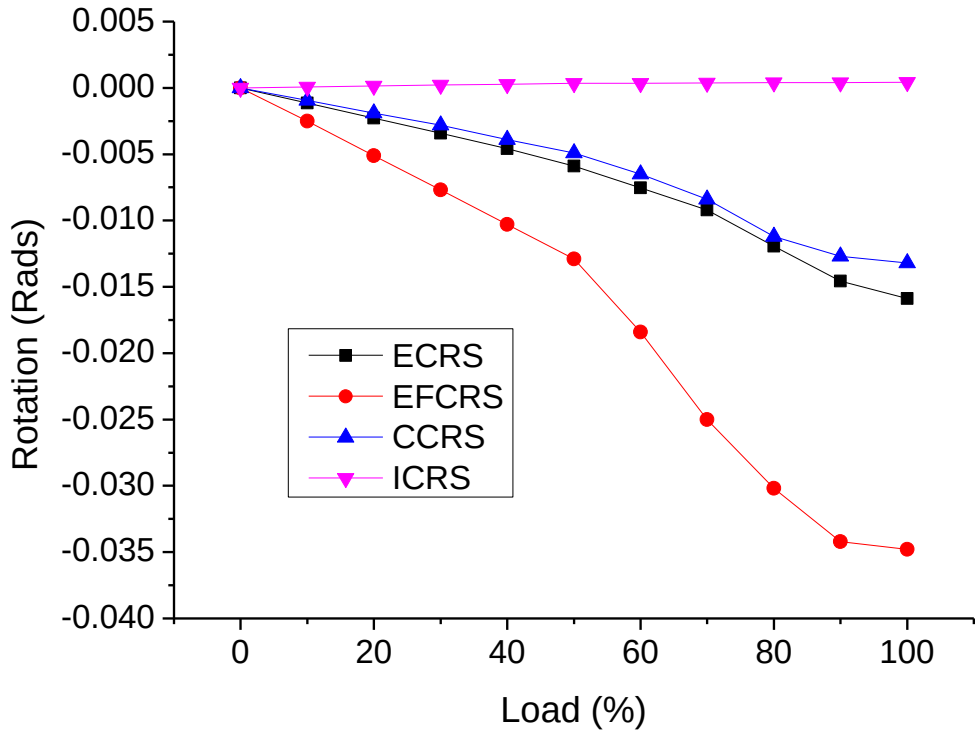

Figure 4-9 Rotational response under load increment

Figure 4-8 and Figure 4-9 present the nonlinear static response of the structure under factored monotonic loading condition recommended in GSA 2003 as shown in Equation 2-1. As the load increases, interior column removal scenario (ICRS) exhibit a linear response up to its full load combination (DL+0.25LL) having a displacement response of 113mm at step 10 and a rotational response of 0.00042 radians. For the same loading condition, the maximum displacement responses due to ECRS, EFCRS and CCRS are 166mm, 219mm and 184mm respectively. The corresponding rotational responses are 0.0159, 0.0348, and 0.0132rads.

With the exception of the ICRS, a linear response was observed for all column removal scenarios up to step 5, at 50% loading combination. Beyond this point, a nonlinear static response occurs up to the full loading at 100%. It was observed that at 50% loading corresponding to DL+0.25LL, the displacement response due to ECRS is 70.1mm with a rotation of 0.0062radians. The response for the CCRS, ICRS and EFCRS is 74mm, 52.7mm, 90.7mm respectively while the maximum joint rotational responses are 0.0052rads, 0.0000022rads and 0.0138rads respectively. These responses are used for the computation of the DAF in the preceding chapters.

4.6 Dynamic analysis investigation

The nonlinear dynamic analysis has been deemed to accurately represent the behaviour of structures under abnormal loading conditions. This form of analysis captures the dynamic effects as a result of the sudden application of gravity load or sudden column removal of critical structural elements. It is practically impossible to predict the exact behaviour and response of a structure with absolute certainty under abnormal conditions; however, nonlinear dynamic analysis is a preferred reliable method relative to the static method. This method is perceived to be more complex relative to the static analysis method since series of assumptions are made to simplify the analysis. The procedure for this investigation is based on the work by Marjanishvili and Agnew (2006) using SAP 2000 finite element code for progressive collapse assessment.

4.6.1 Position one: NLD assessment at CCRS

Figure 4-10 shows the elevation of the ZY plane and ZX plane about the removed column. The corner column as described previously, is bounded by two adjacent columns (Col 11 and Col 61) and connected to Beam 301 and Beam 541.

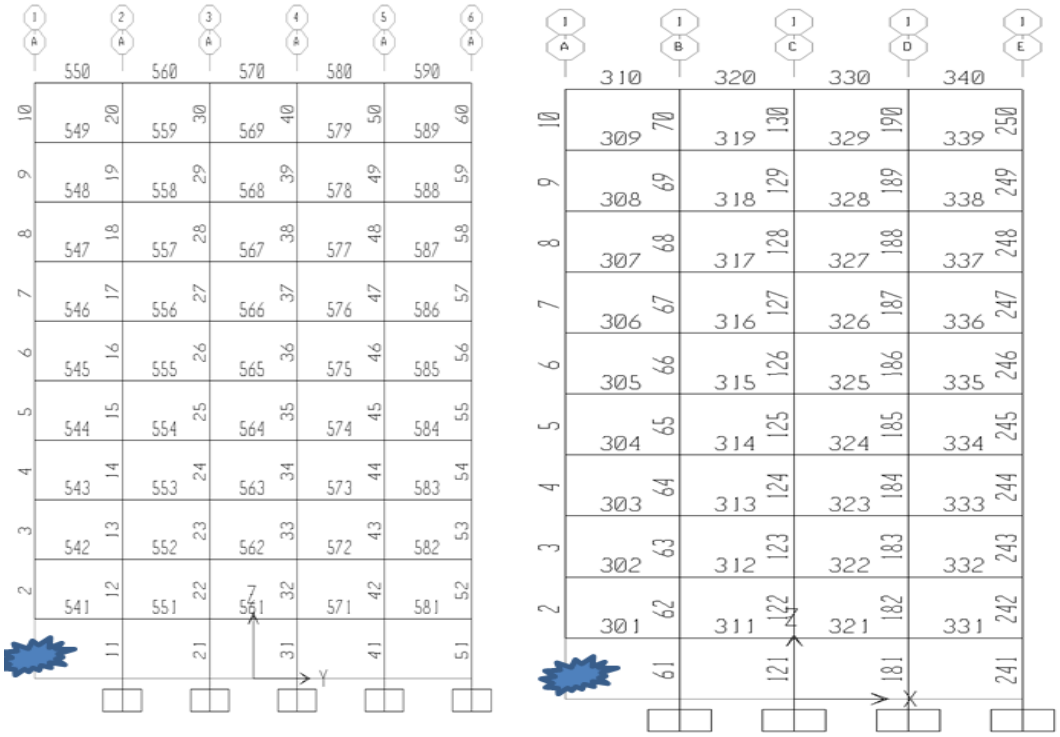

Figure 4-10 Corner column removal scenario (CCRS)

The elevations shown in Figure 4-10 show the positions of the beams and columns investigated after the removal of the corner column.

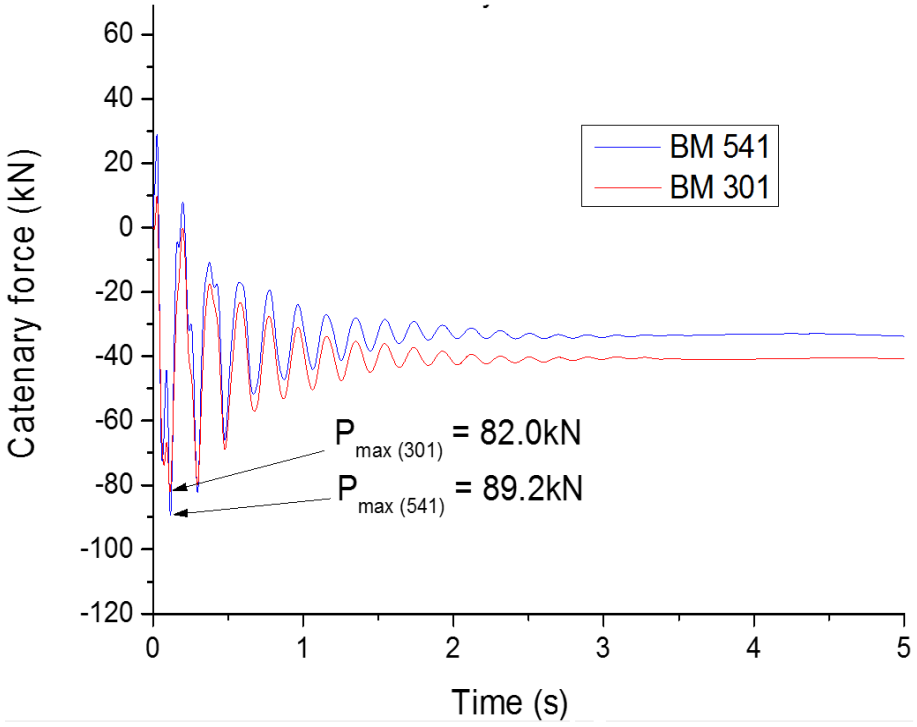

a) Catenary force vs time

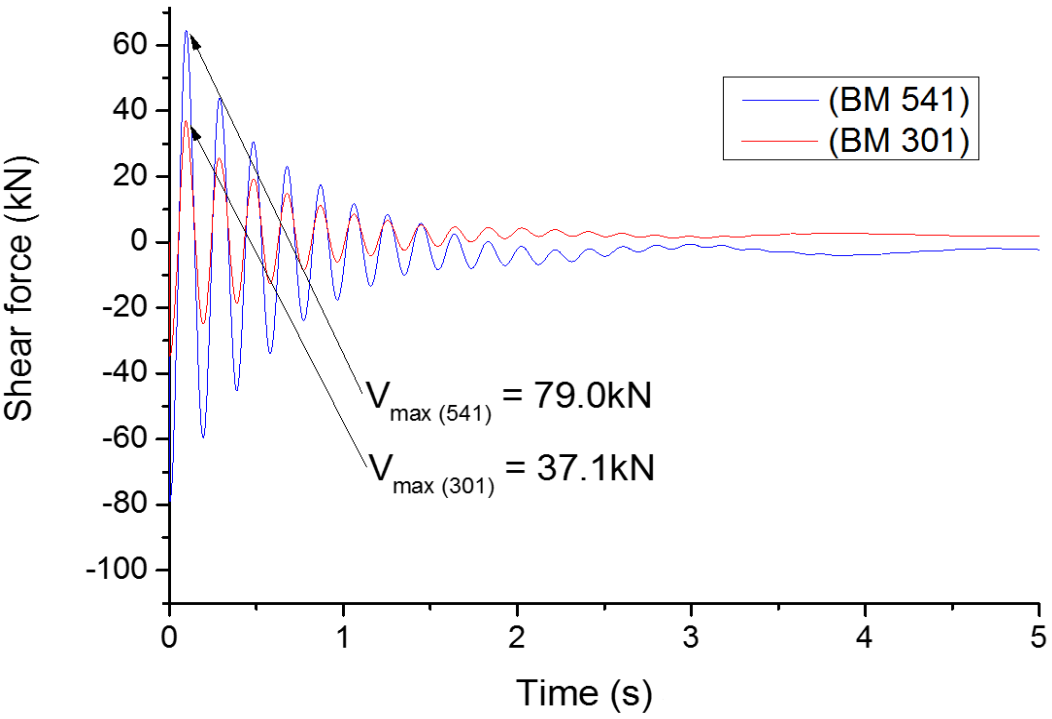

b) Shear force vs time

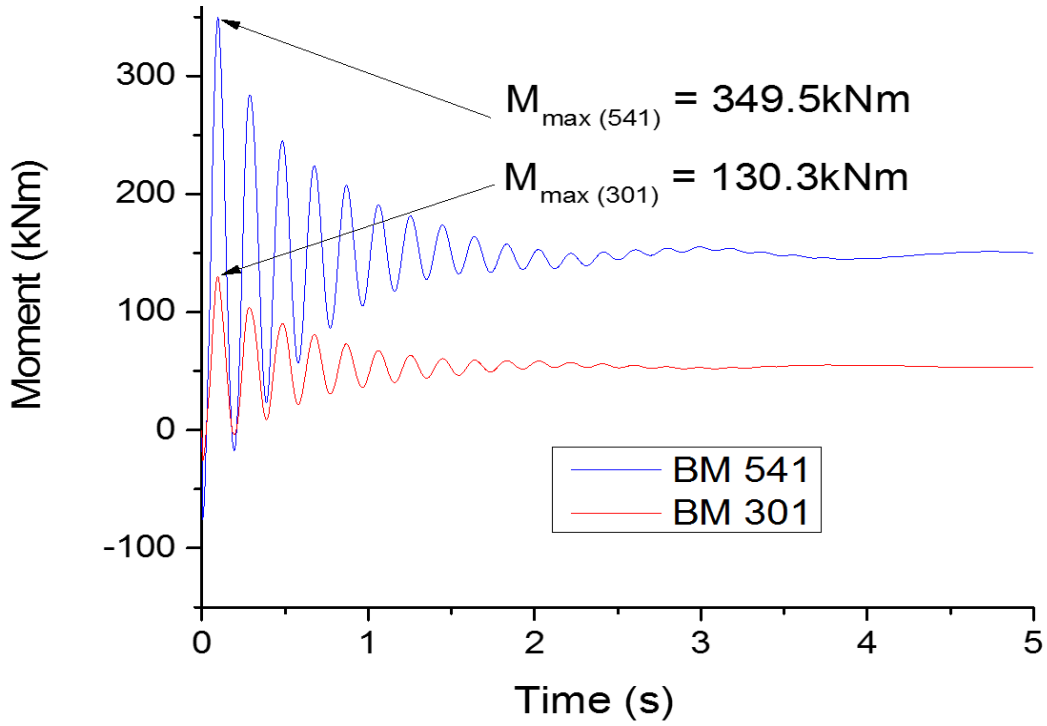

c) Moment vs time

Figure 4-11 Beam responses due to CCRS

As shown in Figure 4-11, the maximum axial force in Beam 301 along the short span is approximately 82kN with a shear force of 37.1kN and a moment of 130.3kNm. The response of Beam 541 for axial force, shear force and moment is 89.2kN, 79.0kN and 349.5kNm respectively. When this is compared with the response from Beam 301, it was observed that the axial force response in Beam 541 exceeds that of Beam 301 by 8.8%. However, for the shear force and moment, Beam 541 exceeds Beam 301 with 113.3% and 168.2% respectively.

The columns bounded to the removed corner column are Column 11 (Col11) and Column 61 (Col 61) at the long span and short span respectively. These columns behave dynamically with varying internal forces due to the removal of the corner column. The response of Column 11 and Column 61 for axial force, shear force and moment is presented in Figure 4-12.

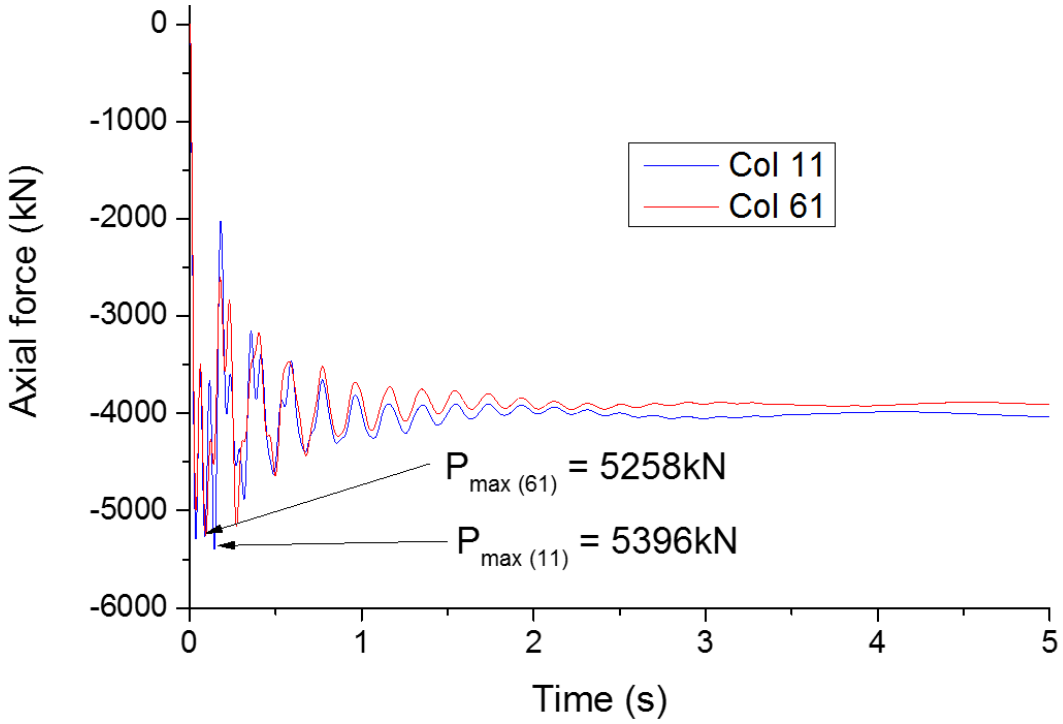

a) Axial force vs time

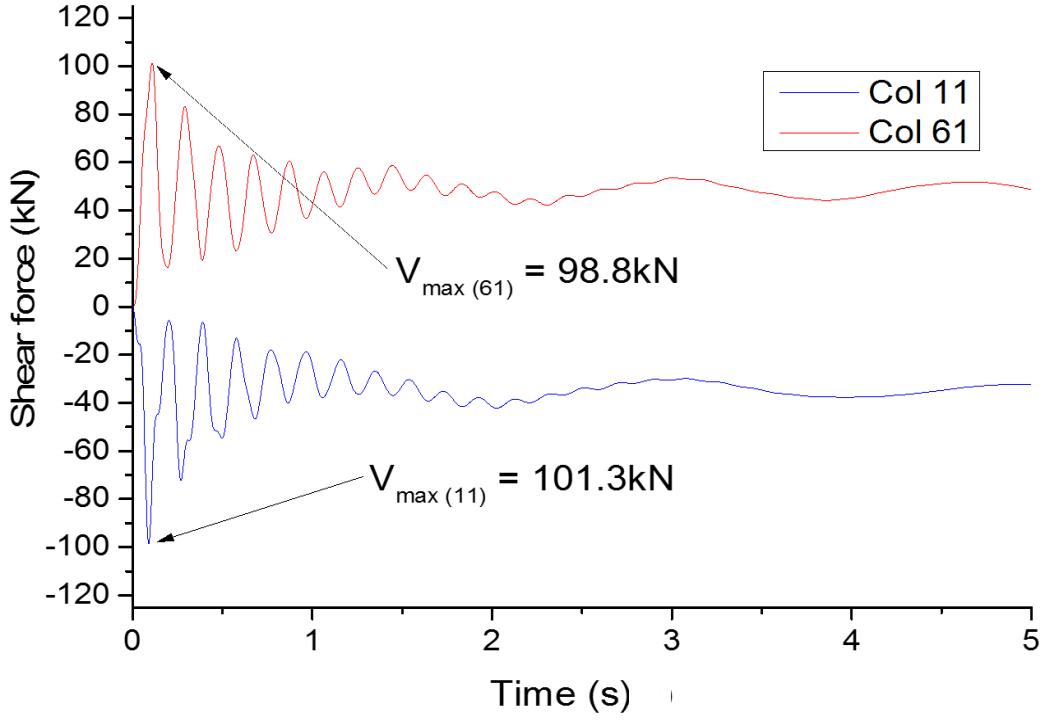

b) Shear force vs time

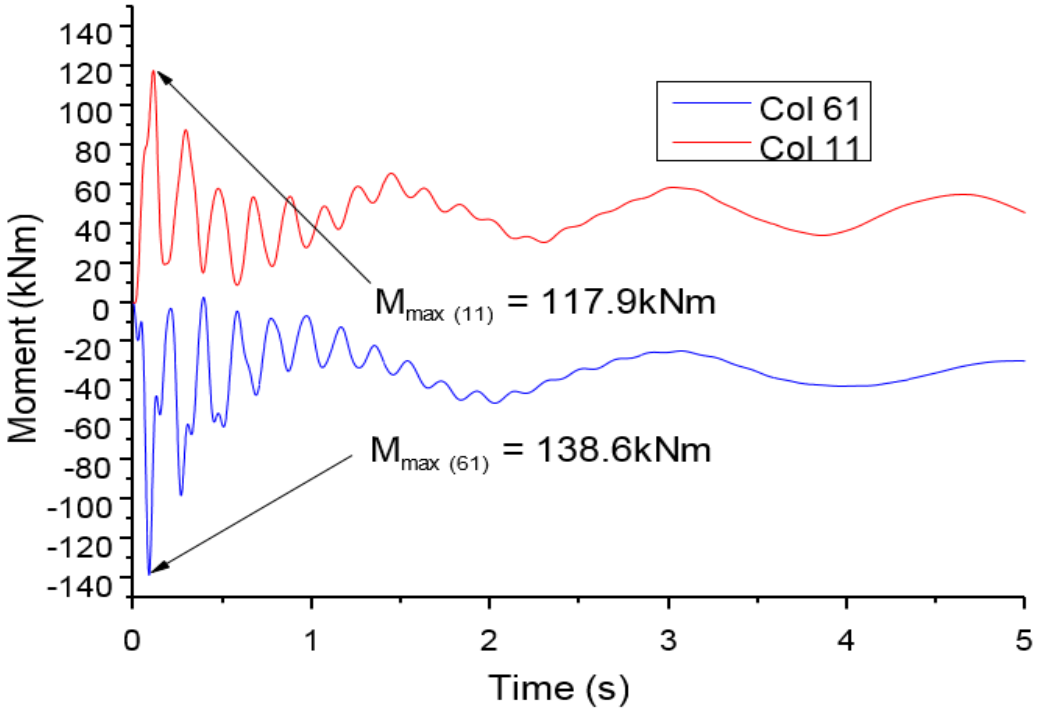

c) Moment vs time

Figure 4-12 Column responses with time due to CCRS

From Figure 4-12, the maximum axial force, shear force and moment in Column 61 is 5258kN, 98.8kN and 138.6kNm respectively. The maximum responses in the internal forces of Column 11 are 5393kN for the axial force and 101.3kN for the shear force. The maximum moment is 117.9kNm. Comparing the responses, it was observed that the axial force in Colum 11 exceeds that in Column 61 by 2.5%, the shear force is exceeded by 2.5% and the moment decreases by 14.9%. There is no significant variation in the axial and shear force response due to the corner column removal scenario relative to the variation in moment response of the two columns. Figure 4-13 joint rotation and displacement response about the node of the removed column connecting the Beam 301 and Beam 541.

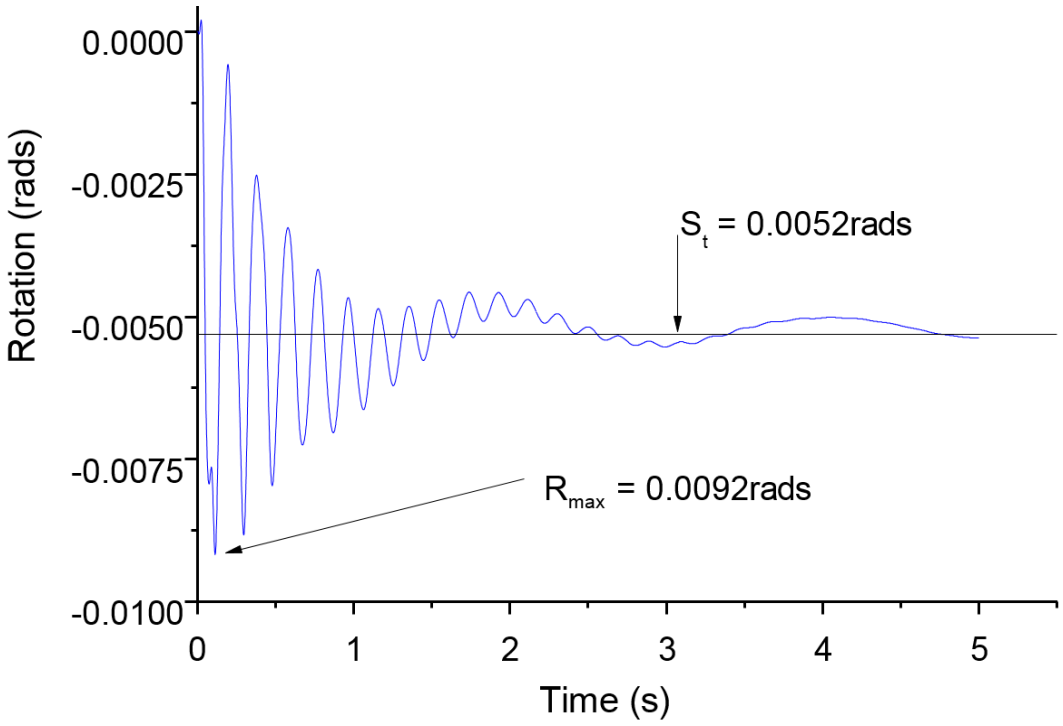

a) Rotation vs time

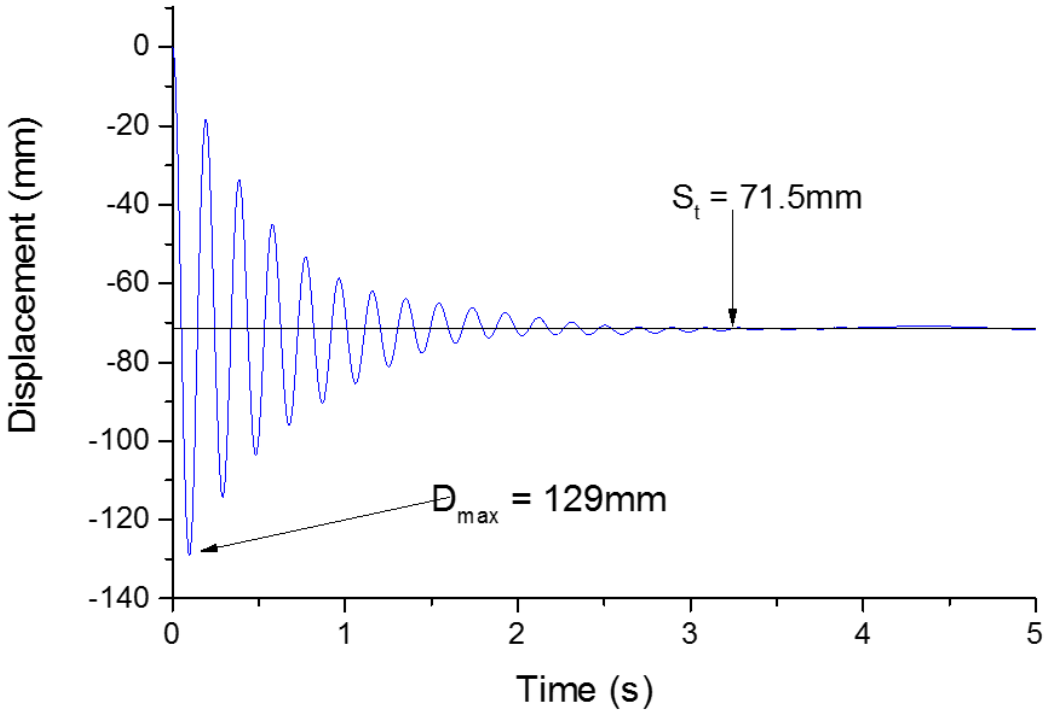

b) Displacement vs time

Figure 4-13 Joint response due to CCRS

The maximum displacement and rotation response due to a corner column removal scenario is 129mm and 0.0092 rads respectively. As the structures seeks a new stable state without

dynamic effect, the displacement and rotational responses is 71.5mm and 0.0052rads respectively.

4.6.2 Position two: NLD assessment at ECRS

This subsection presents the study at the perimeter of the building due to column loss. The location of the column removal point is shown in Figure **4-14** for the long span and the short span respectively.

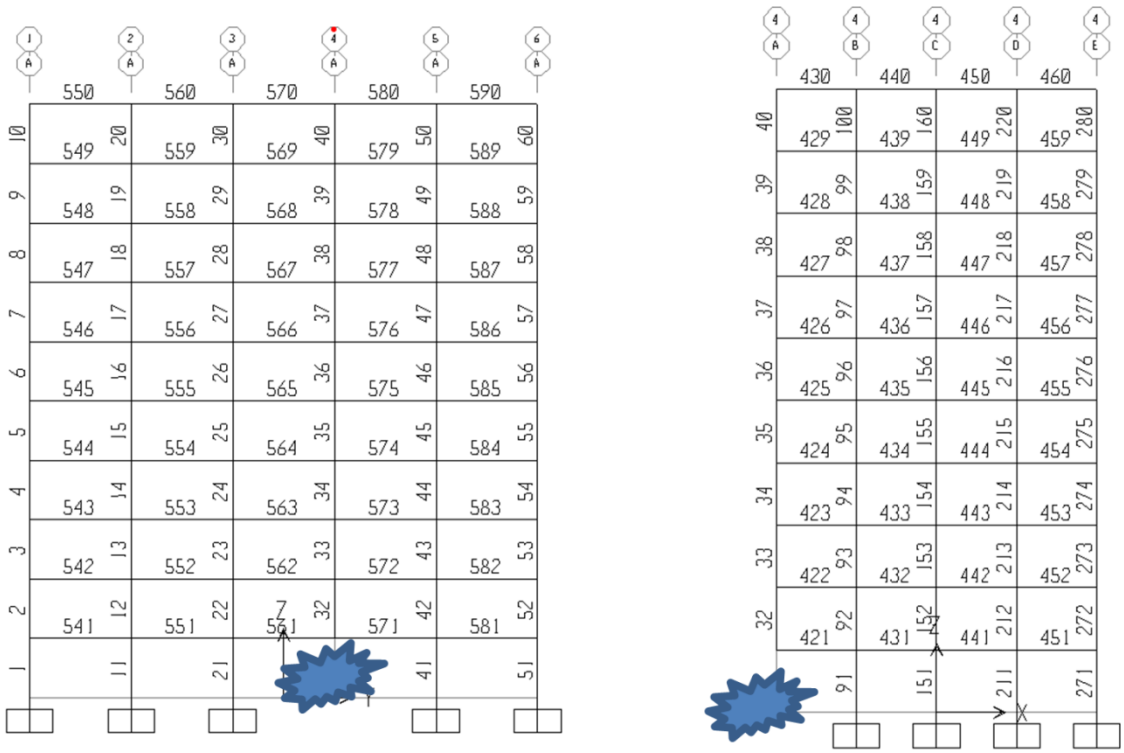

Figure 4-14 Location of perimeter column removal location

The removed column is bounded by column 21 and column 41 along the main span while along the short span is column 91. The beams connecting the removed column along the long span is Beam 561 and Beam 571 along the long span while along the short span is Beam 421. In this case, the internal forces in all these members will be assessed to check the redistribution of forces about the column removal node. The maximum displacement and rotation of this joint is equally assessed to evaluate the response of the structure over time.

Response of columns 21, 41 and column 9

The labels of these columns are shown in Figure **4-14**. The internal forces (PVM) of these columns are assessed due to the instantaneous removal of the edge column (Col 31).

The maximum response occurs in Column 91 (Col 91) for axial force response, shear and moment as shown in subsequent plots.

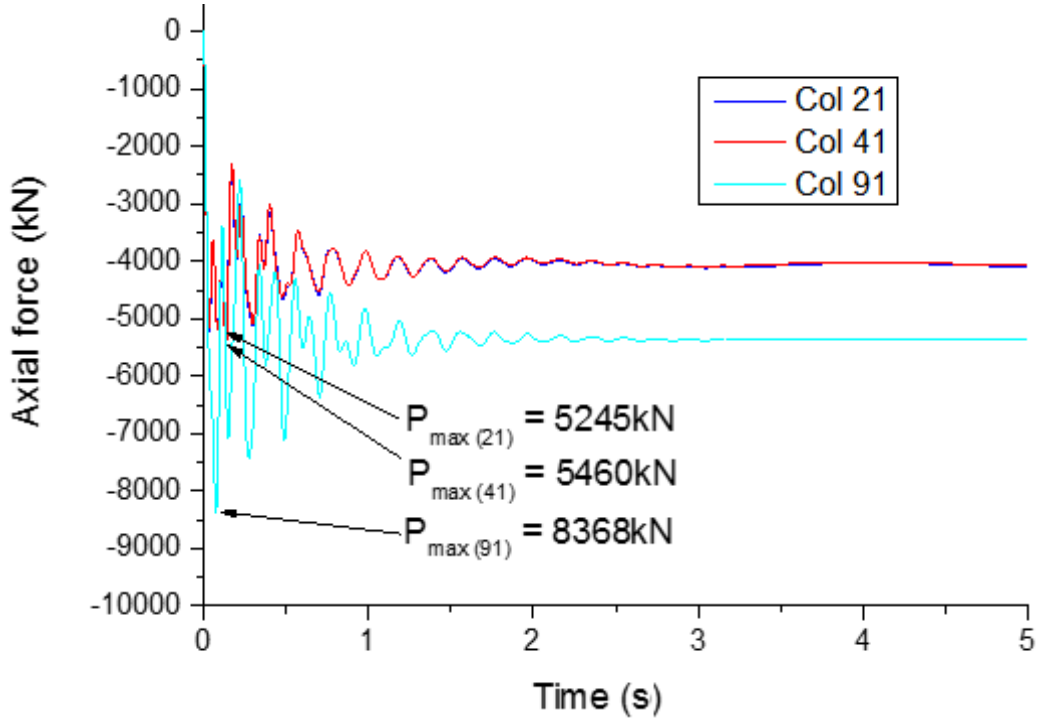

a) Axial force vs time

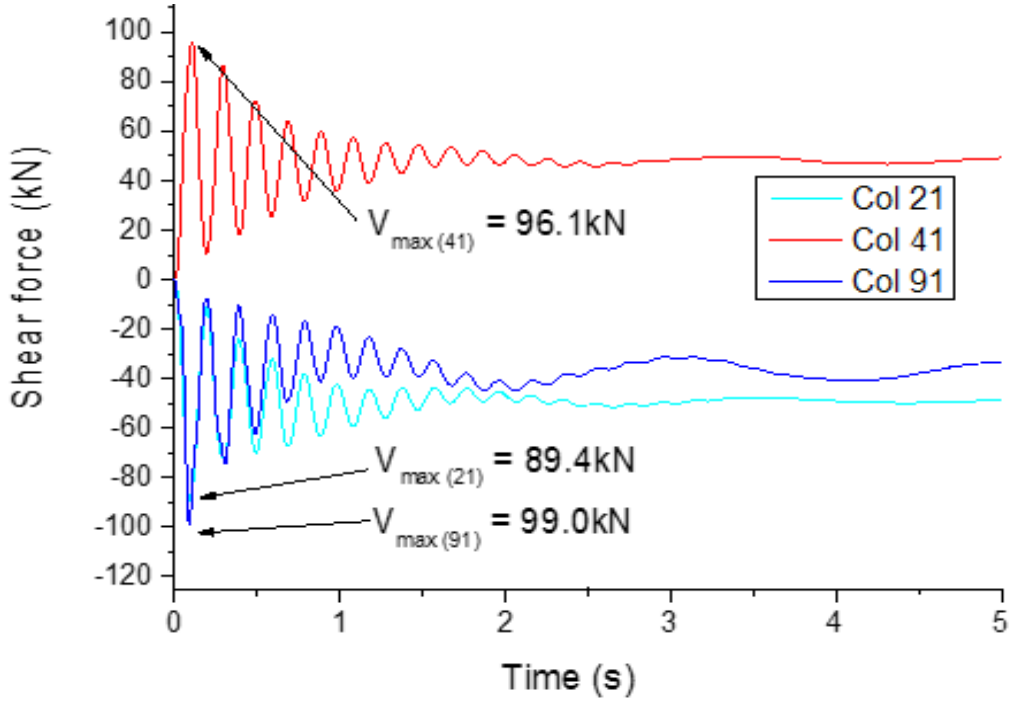

b) Shear force vs time

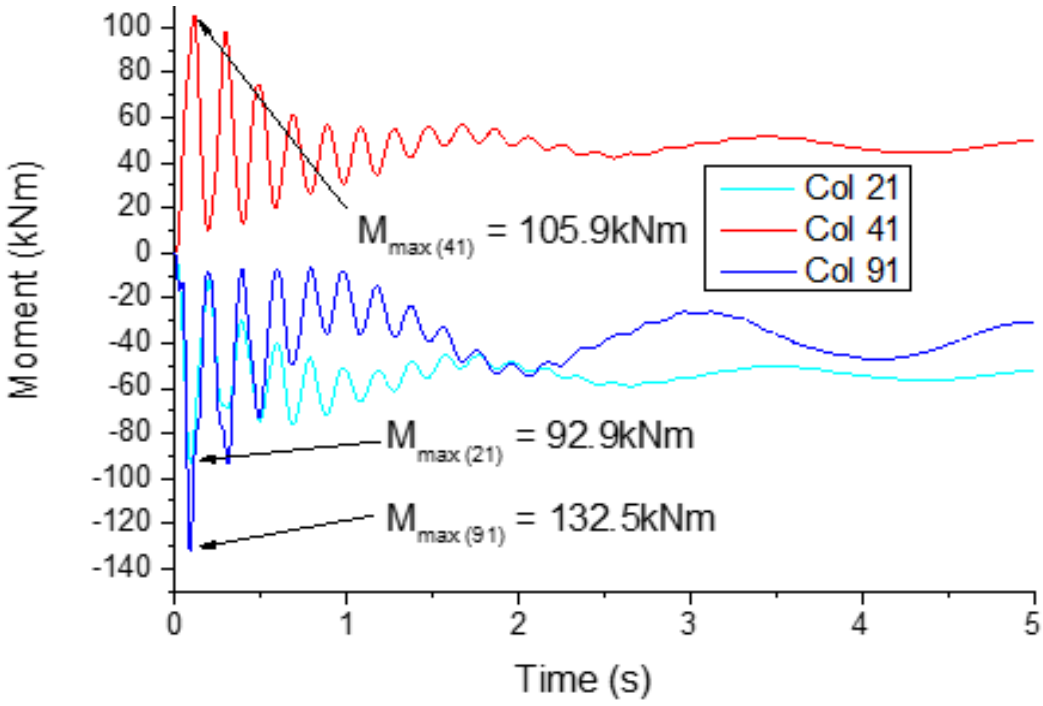

c) Moment vs time

Figure 4-15 Column responses vs time

The maximum internal forces in axial, shear and moment are shown in the plots of Figure 4-15. The next plot shows the variation of internal forces (PVM) of the Beams 421, Beam 561 Beams 571 with time are shown in Figure 4-16.

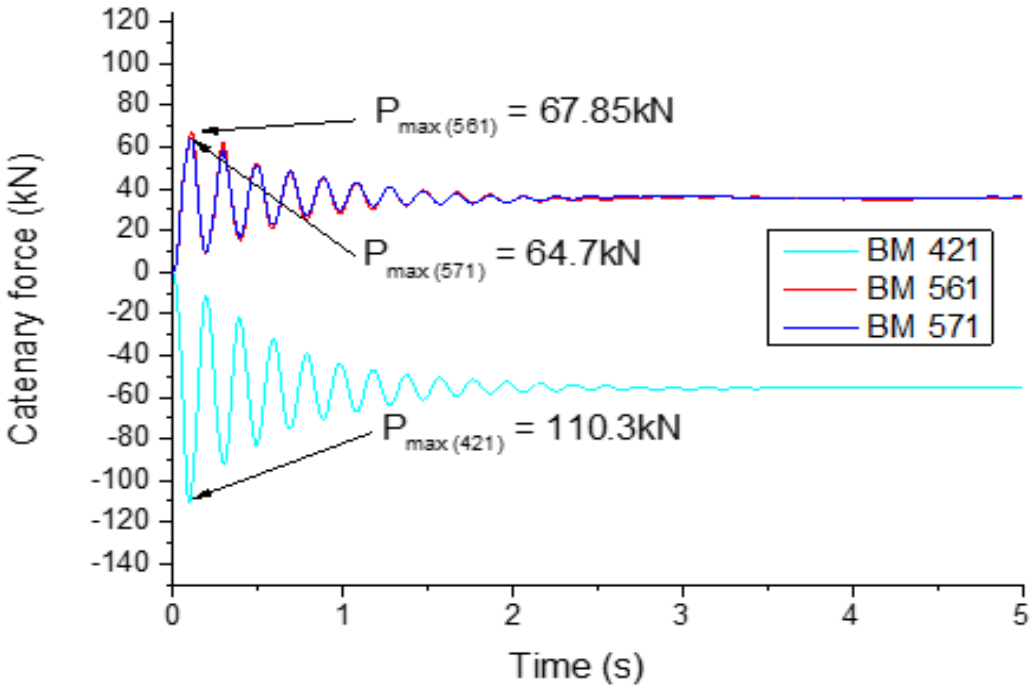

Catenary force vs time

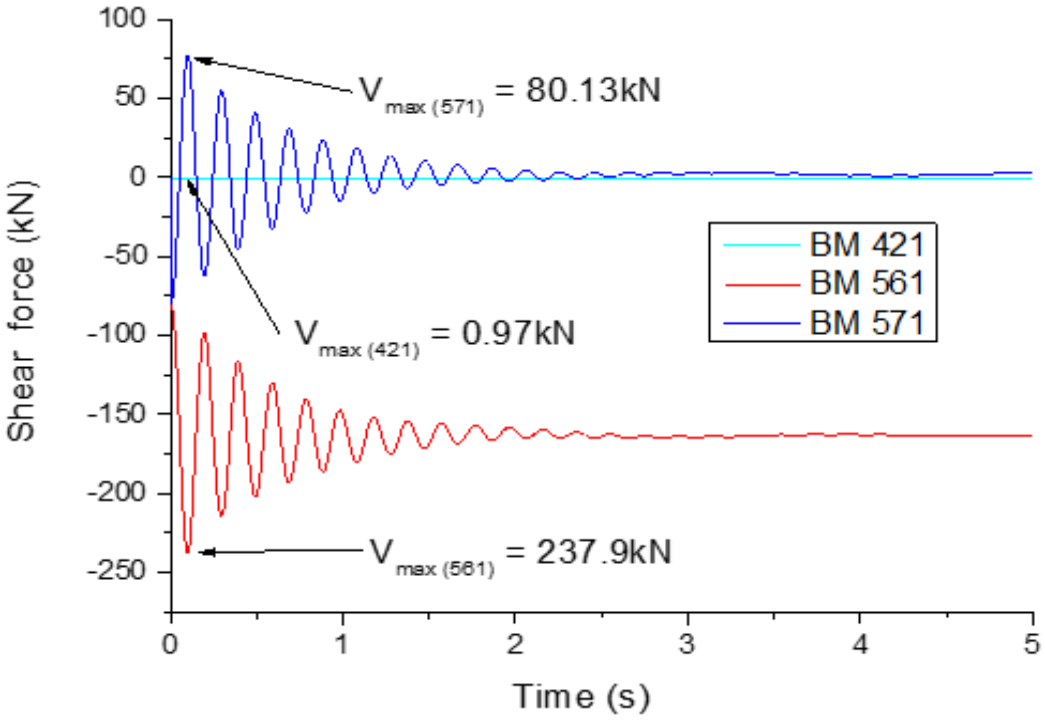

a) Shear force vs time

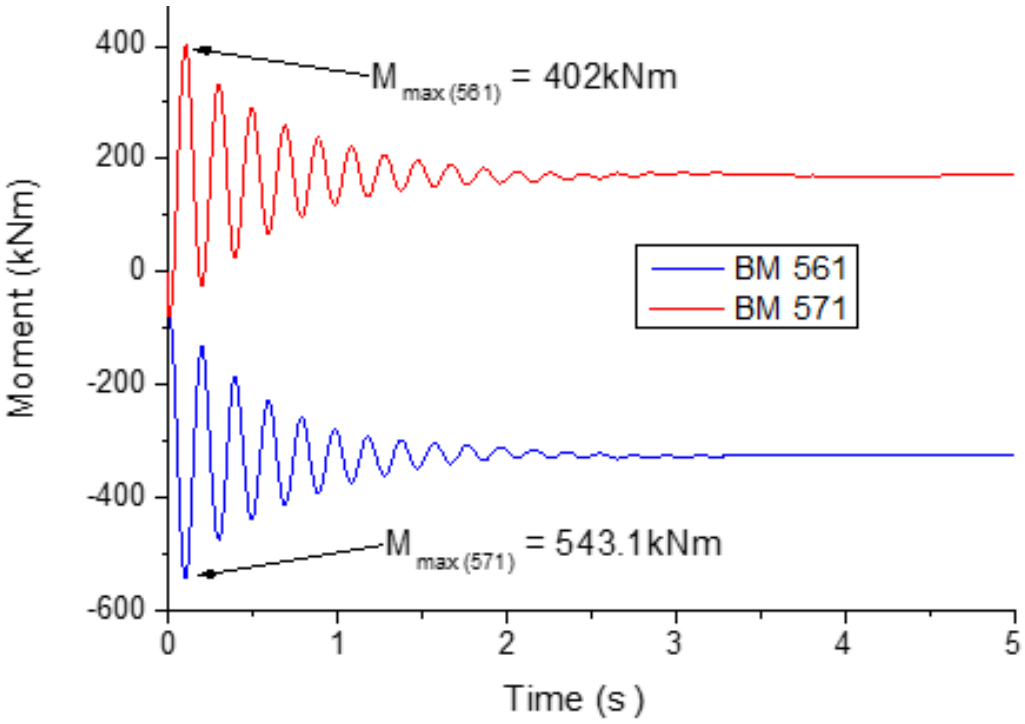

b) Moment vs time

Figure 4-16 Beam responses vs time (ECRS)

The maximum catenary force in Beam 421 is 110.3kN while the maximum shear force in the beam is 0.97kN. The connection is expected to resist this internal member forces safely. According to Eurocode 3 for connection design, the joint is expected to safely resist a tensile force of 75kN inclusive of other internal forces. This implies that the connection would be subjected to 47.1% increase in tensile force if it was considered for tensile force of 75kN at the conventional design stage.

The maximum axial force response in the Beam 561 is 67.85kN, the maximum shear force response in the beam is 237.9kN while the maximum moment response in the beam is 402.2kNm. On the other hand, the response obtained from Beam 571 for the maximum axial force 64.7kN, 80.13kN for the maximum shear force and 543.1kNm for the maximum moment response. There is no significant variation between the axial force response in Beam 561 and Beam 571 since it differs by only 4.9%.

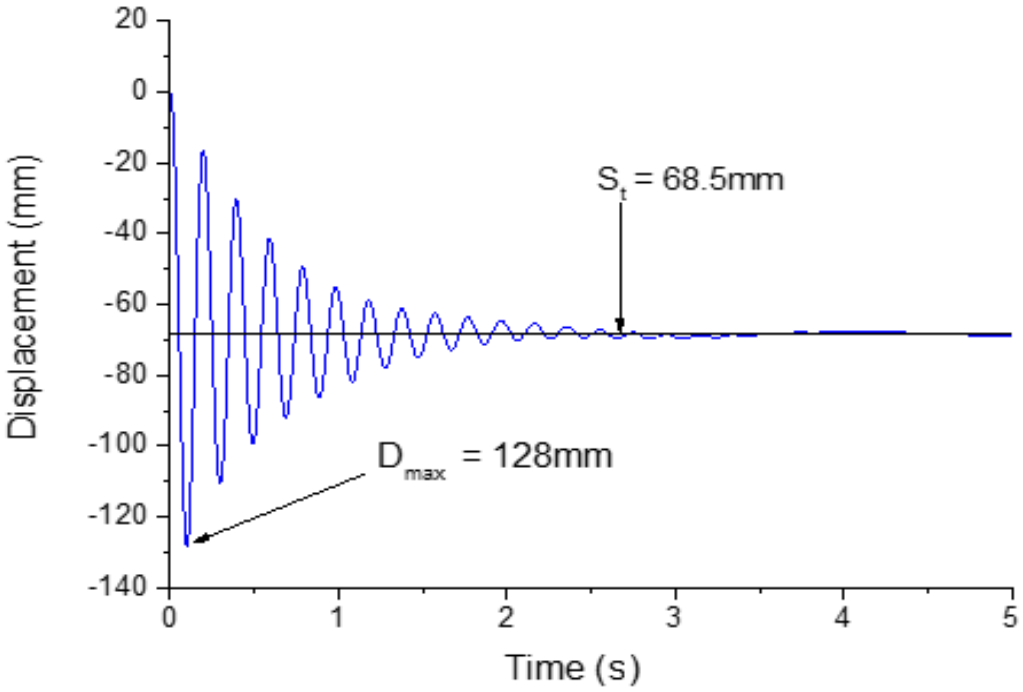

a) Displacement vs time

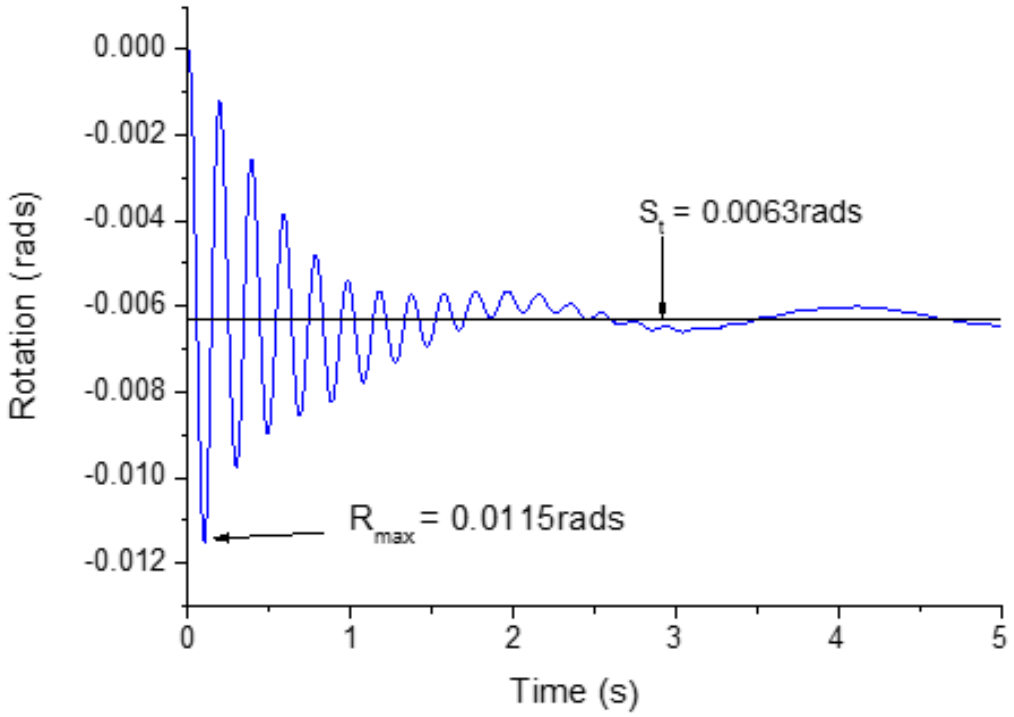

b) Rotation vs time

Figure 4-17 Joint response vs time (ECRS)

The maximum displacement at the column removal node is 128mm while the maximum rotation is 0.0115rads (Figure 4-17). The horizontal line drawn at the midpoint of nodal vibration corresponds to the static response of the structure. The maximum static response of the structure for displacement and rotational response are 68.4mm and 0.0063rads (Figure 4-17).

4.6.3 Position three: NLD assessment at ICRS

The internal column removed is connected to Beam 651 and Beam 661 along the longitudinal direction and Beam 391 and Beam 401 along the transverse direction (Figure 4-18). The node connecting the removed column is JT 156.

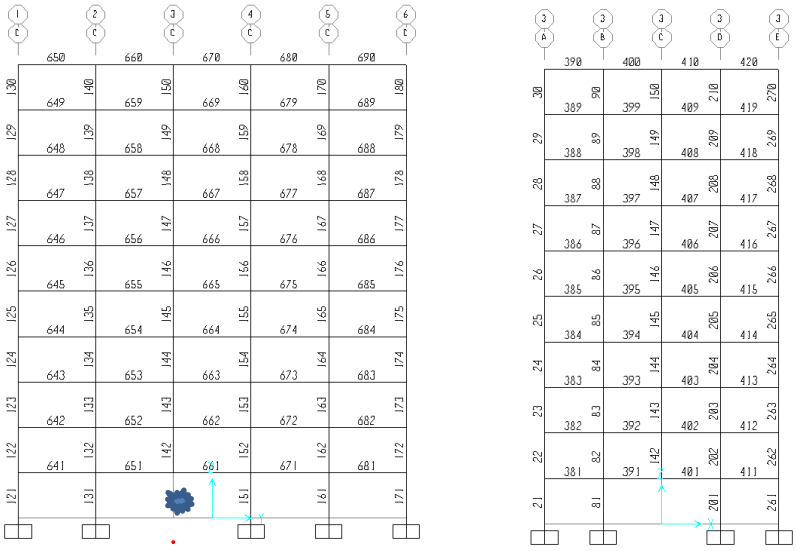

Figure 4-18 Descriptive labels of structural members

The internal force response of structural members within location of column removal is presented below.

Column response:

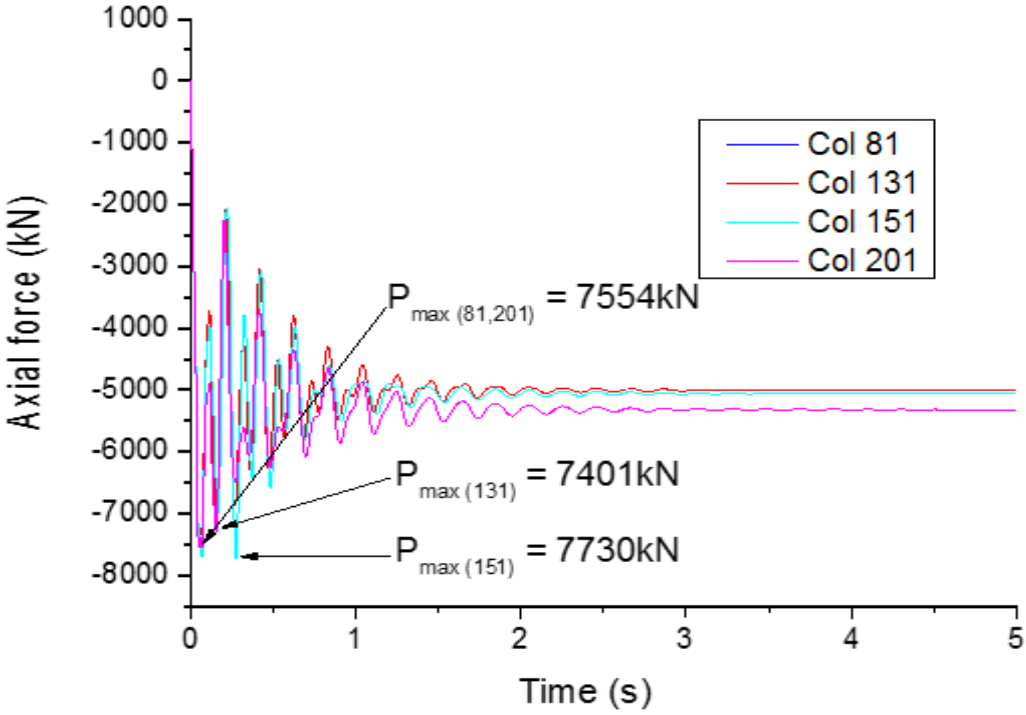

a) Axial force vs time

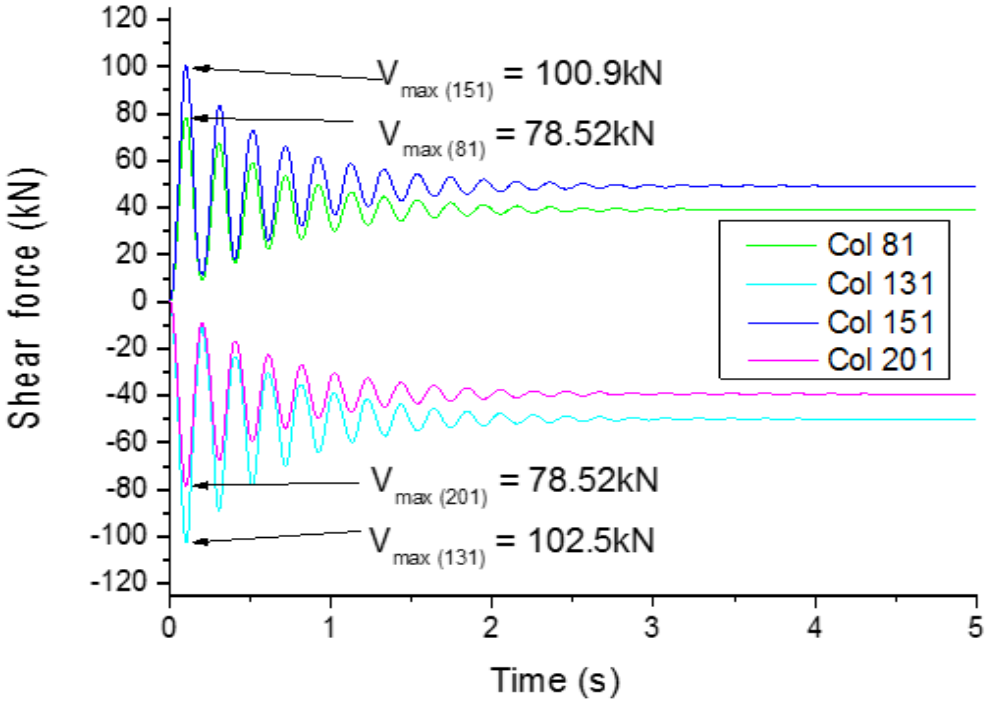

b) Shear force vs time

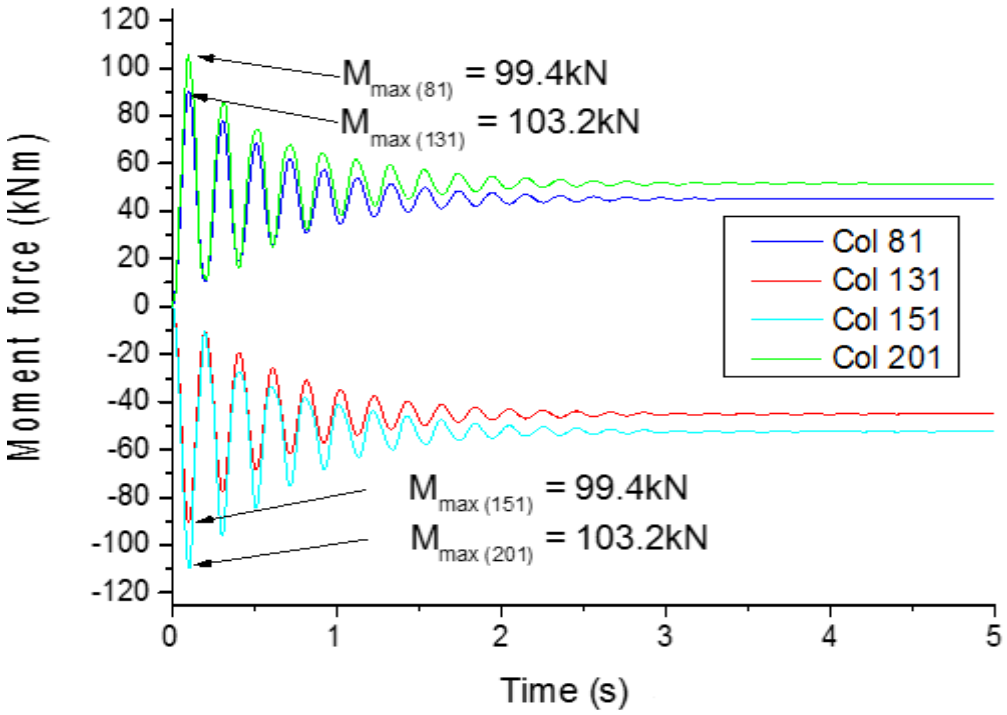

c) Moment vs time

Figure 4-19 Column response vs time

The response of Column 131 and 151 in the longitudinal direction and column 81 and 201 in the transverse direction is shown in Figure 4-19. The maximum dynamic axial force response in Column 81 and Column 201 is 7554kN. A horizontal line drawn through the mid axis of the dynamic response corresponds to the static response of 5317.17kN. The ratio between the maximum dynamic response and the stable static response is 1.42. Column 131 has a maximum axial force response of 7401kN. There are two spans to the left of the removed column and three spans to the right of the removed column. This resulted in Column 151 having a 4.4% increment in axial force relative to Column 131. Using the shear force criteria, the maximum shear force response in Column 151 is 100.9kN, while Column 131 exceeds Column 151 by 1.6%. The difference in response could be attributed to unequal spans about the node of the removed column. Using the moment response criteria, Column 151 and Column 131 has a moment response of 99.4kNm and 103.2kNm respectively, although there is a reduction in the moment response of Column 151 relative to Column 131.

Beam responses

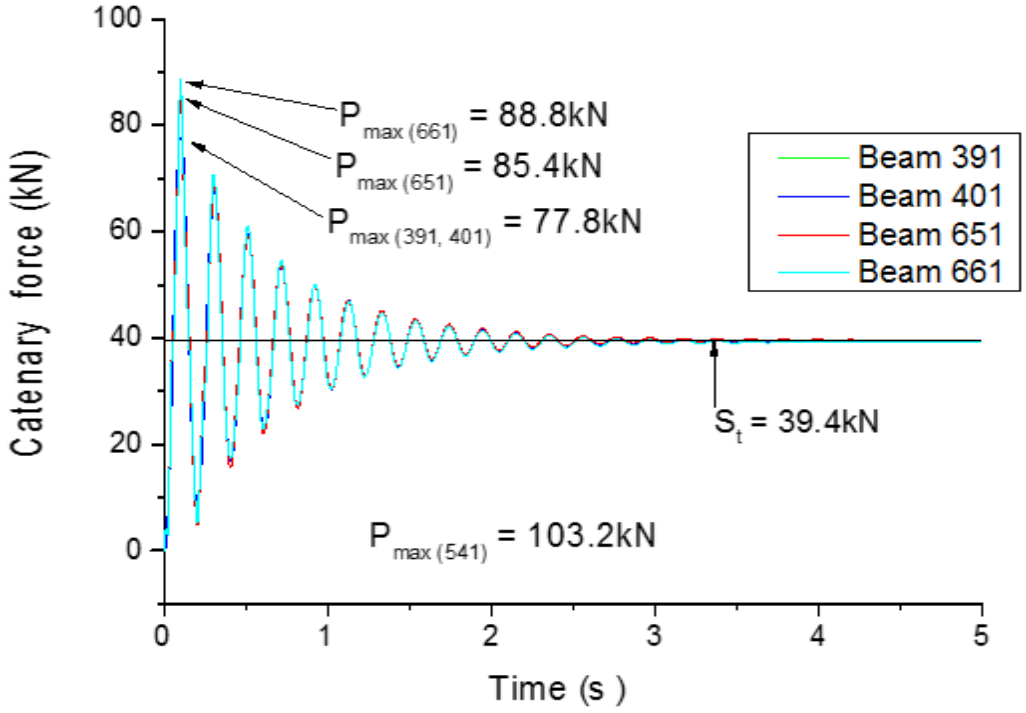

Figure 4-20 Catenary force response in beams vs time

The most important internal force considered for beams is the catenary force response. As shown in Figure 4-20, the maximum catenary force action is 88.8kN, which occurs in Beam 661. The stabilised state of the structure after 3s corresponds to an approximate static response of 39.4kN. This response exceeds the recommended tying force of BS EN 1991-1-7 by 18.4%.

Connection response

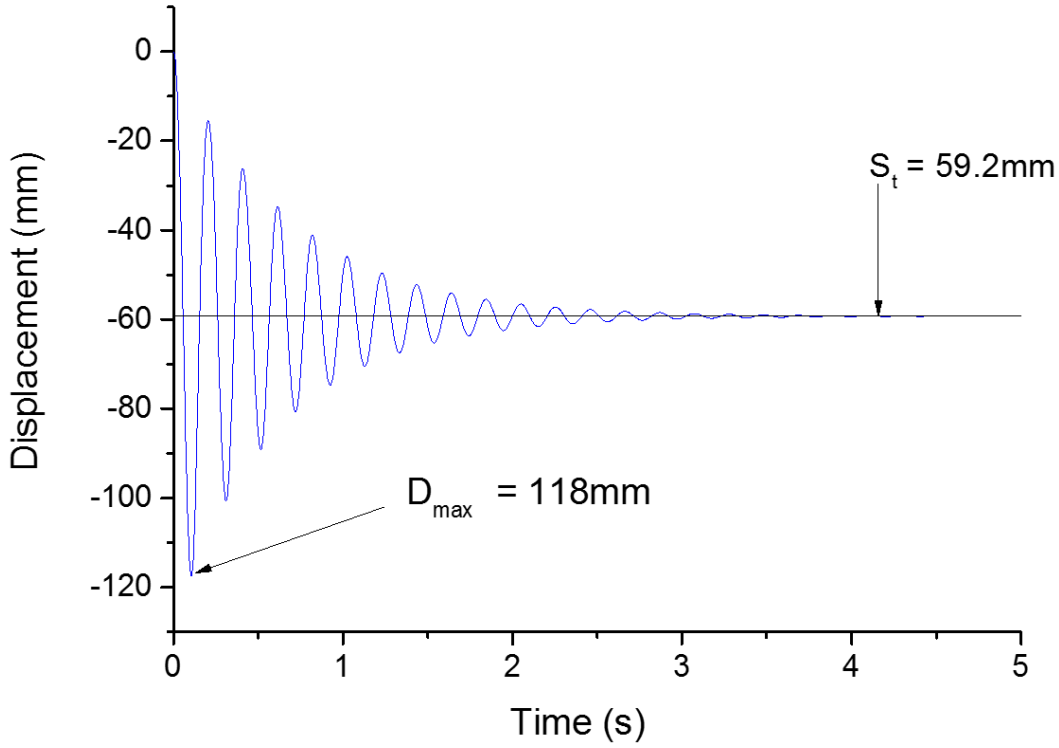

Figure 4-21 Joint Displacement response versus time

Figure 4-21 shows a maximum dynamic joint displacement response of 99.4mm due to the interior column removal scenario (ICRS). As shown on the plots, a horizontal line midway of the dynamic response corresponds to a stabilised static respond of 59.20mm after 3s. The next subsection presents an investigation at the eight floor column removal scenario.

4.6.4 Position four: NLD assessment at EFCRS

The eight-floor column was removed instantaneously to simulate the response of the connecting structural members and to determine the connection behaviour with respect to time.

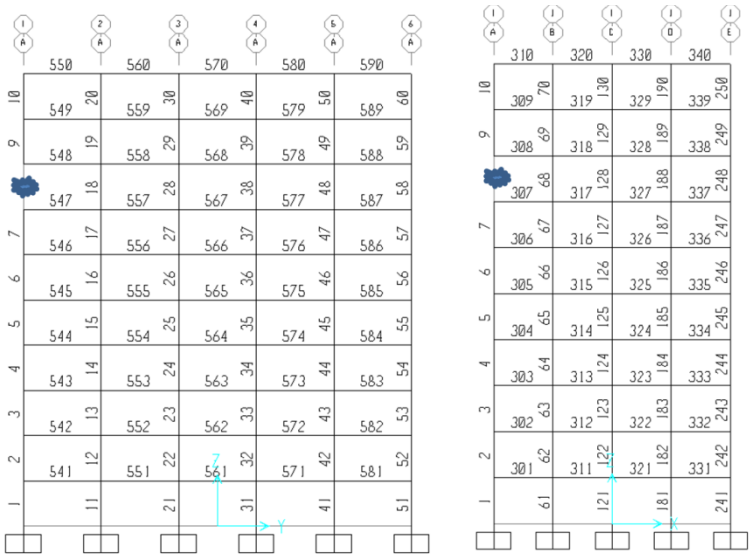

Figure 4-22 Eight floor column removal scenario (EFCRS)

The column removal location at the eight floors is shown at the two elevations (Figure 4-22) along the long span and the short span. The beam column joint at the column removal node is connected to Beam 548 and Beam 308 while the columns adjacent to the removed column along the long and short span is Column 18 and Column 68. An Assessment was made at this location involving the members connecting the node of the removed column. The maximum internal forces due to the eight floor column removal scenario (EFCRS) are presented in Figure 4-23.

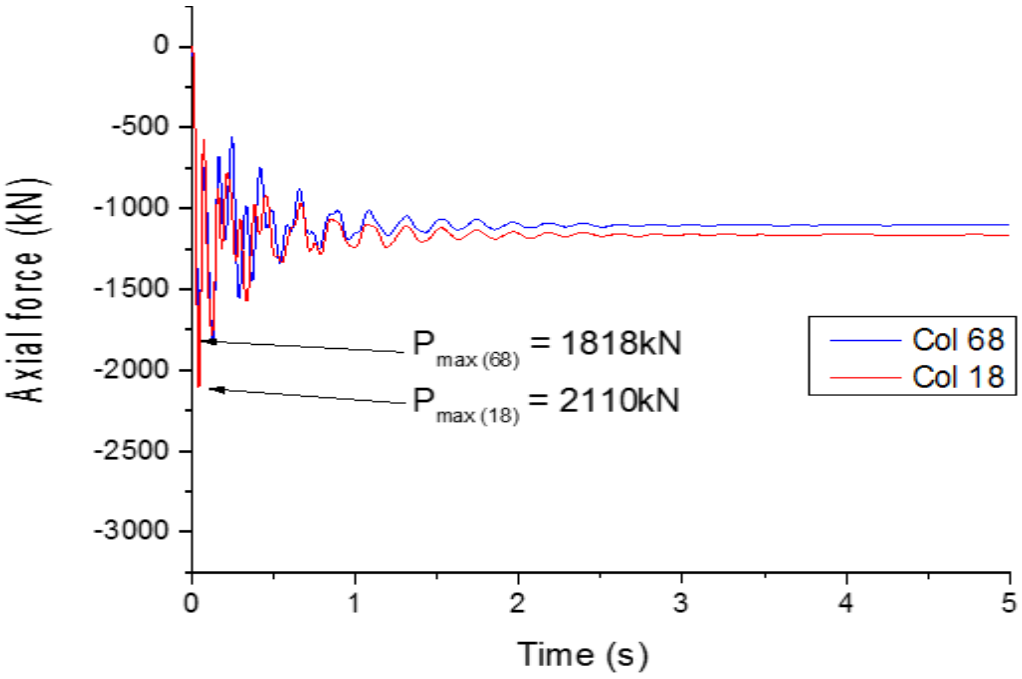

a) Axial force vs time

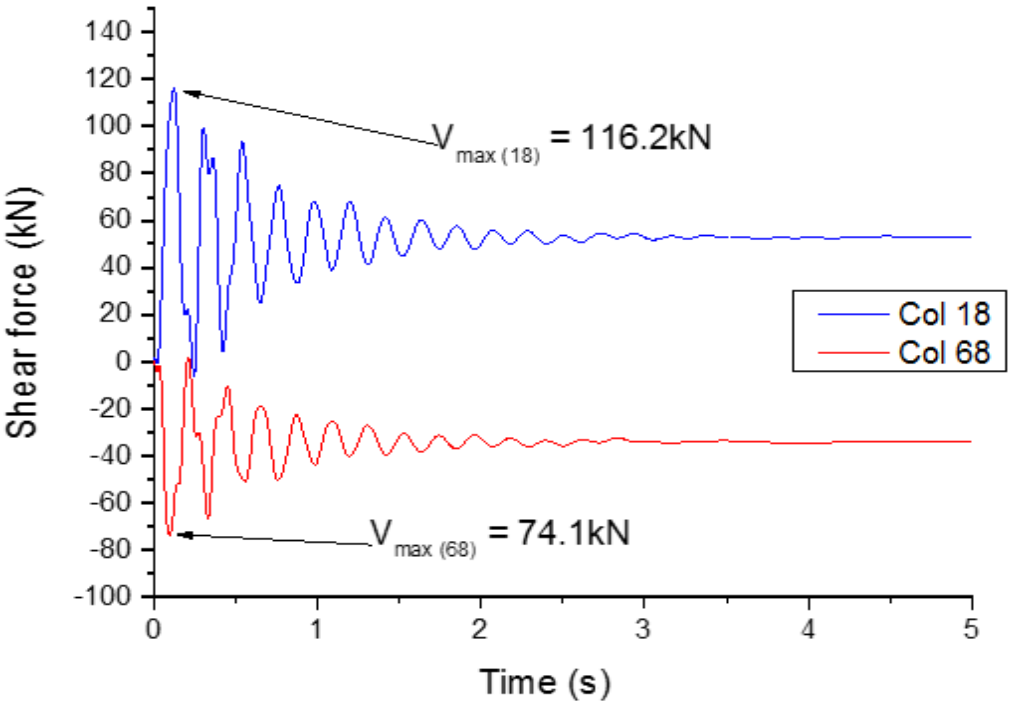

b) Shear force vs time

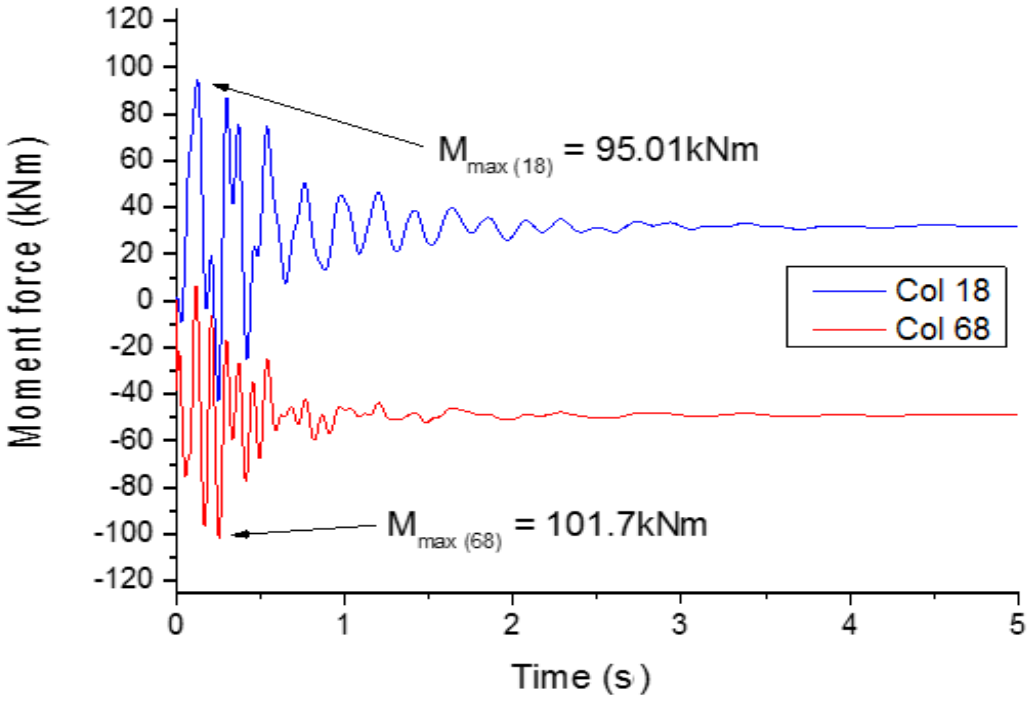

c) Moment vs time

Figure 4-23 Column response due to EFCRS

The axial force response in Column 18 (Col 18) exceeds Column 68 by 16.1%, while the shear force response of Column 18 exceeds that of Column 68 by 55.8%. However, the moment response of Column 68 exceeds that of Column 18 by 7.04%.

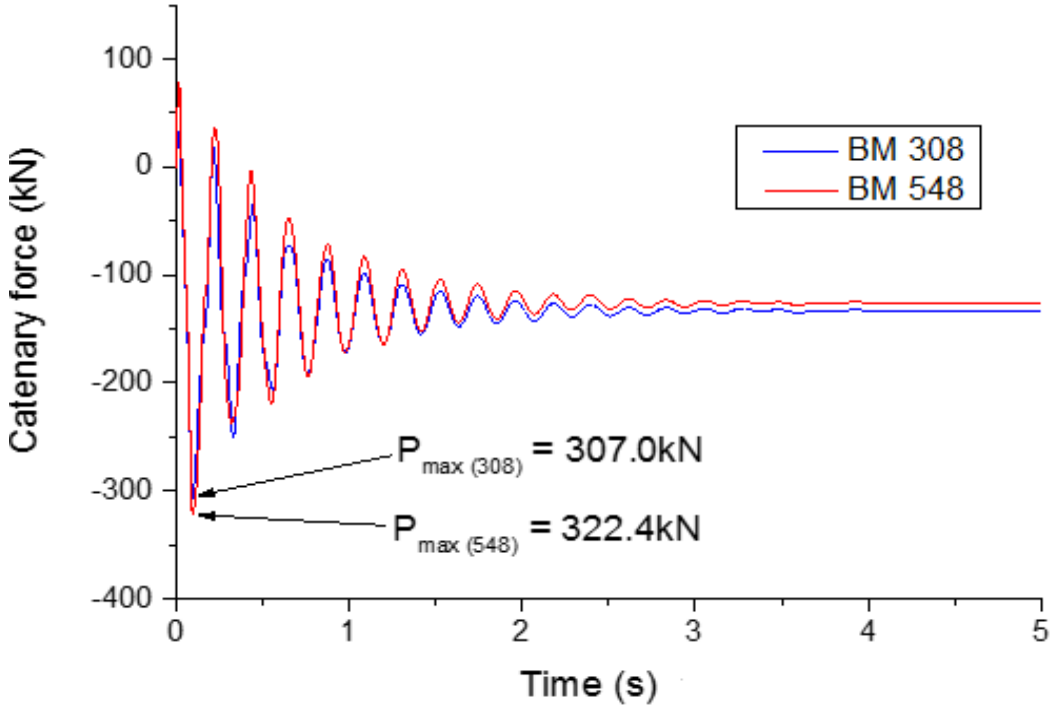

a) Catenary force vs time

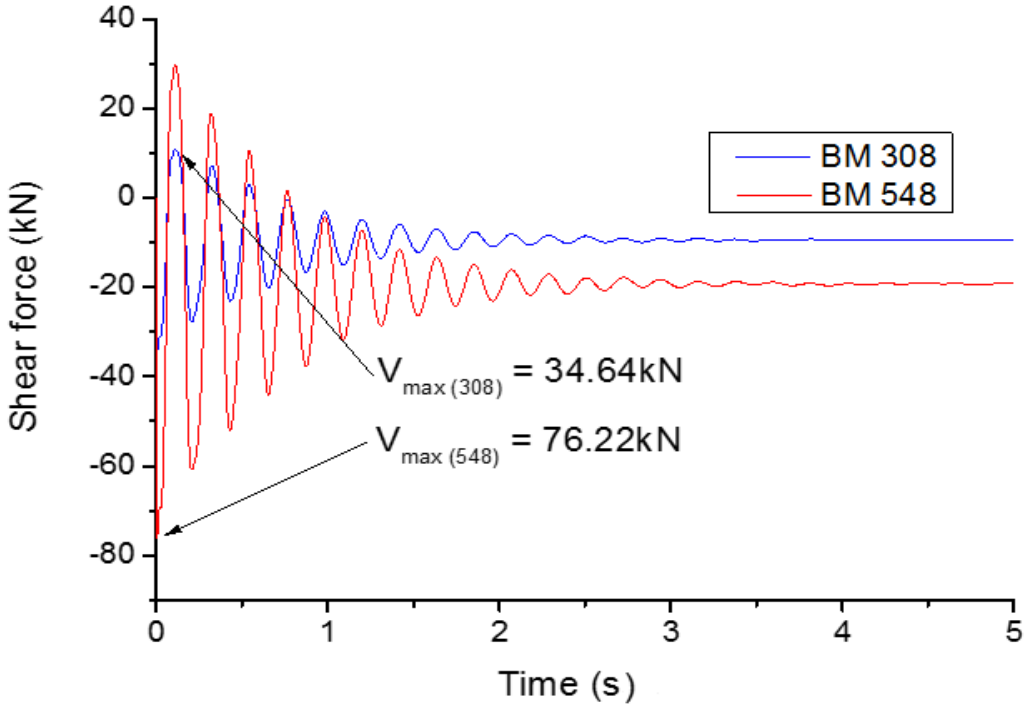

b) Shear force vs time

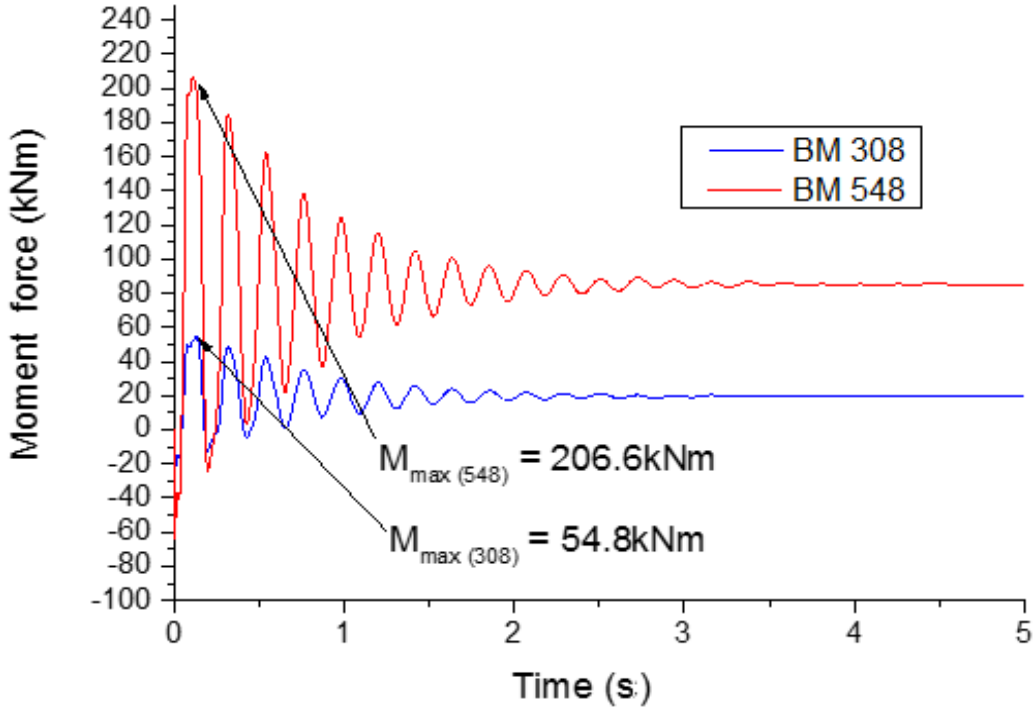

c) Moment vs time

Figure 4-24 Beam response due to EFCRS

The maximum response in axial force, shear force and moment of Beam 548 are 322.4kN, 76.22kN and 206.6kNm respectively. The axial force response of 322.4kN is 329.9% greater than the recommended value for simple connection design in Eurocode 3. The maximum axial force, shear force and moment in beam 308 are 307kN, 34.63kN and 54.8kNm respectively. The axial force response is the dominant internal force resulting from the removal of eighth floor column.

As shown in the joint response (Figure 4-25), the maximum dynamic displacement response is 163mm. A horizontal line through the mid axis of the displacement response corresponds to an approximate static analytical response of 89.3mm. The maximum dynamic rotation is 0.026rads. A horizontal line through the middle of the vibration of the structure, corresponds to a response of 0.0138rads after 3 s.

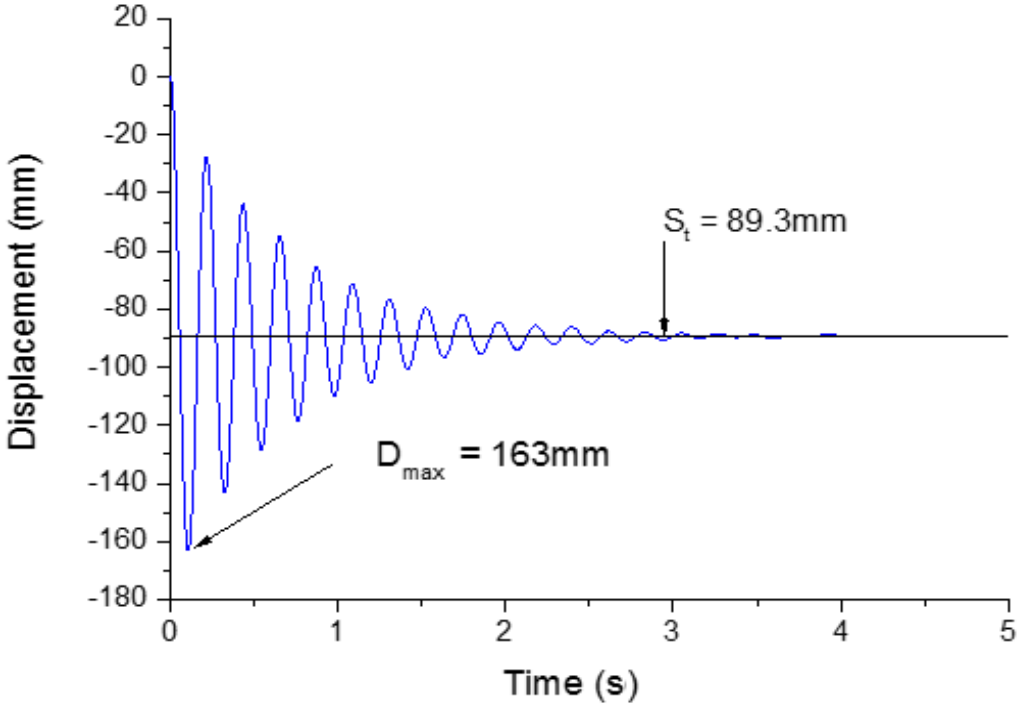

a) Displacement vs time

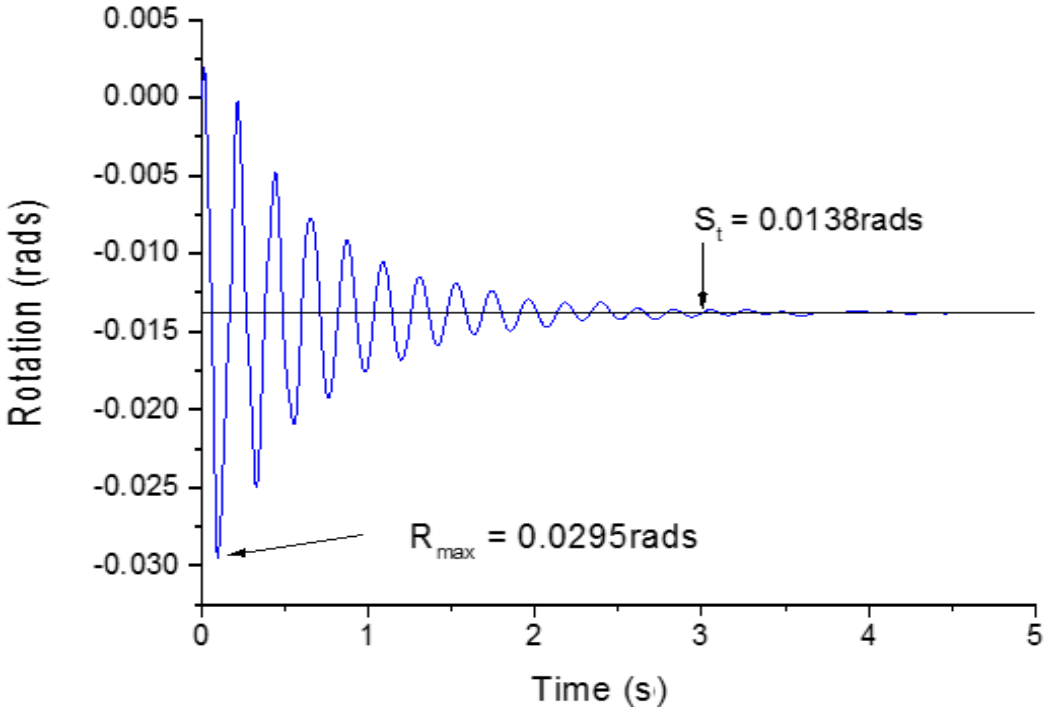

b) Rotation vs time

Figure 4-25 Joint responses vs time (EFCRS)

4.7 Multiple column loss scenario (MCRS)

Introduction: The scope of GSA 2003 for progressive collapse scenario is defined within the context of a single column removal scenario. However, unforeseen events like blast or airplane impact could result in multiple column losses. In view of that, this section seeks to investigate the response of structures to multiple column loss events using the edge and interior column removal locations. In this section, the primary objective of this investigation is to assess the redistribution of forces in high rise structures under double column loss scenario. The deformed shape under double column loss is shown in Figure 4-26.

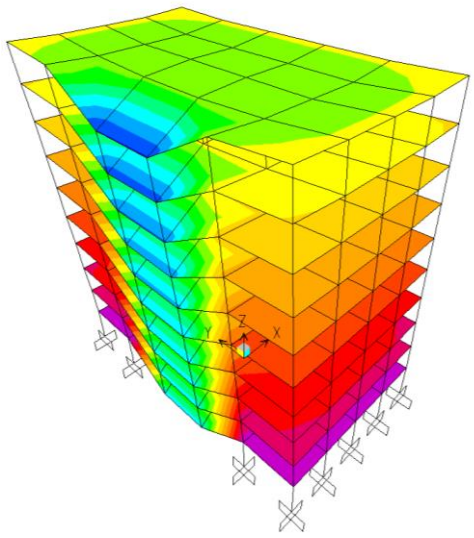

Figure 4-26 Deformed shape due to double column loss

4.7.1 Scope of investigation

As shown in Figure 4-27, two columns were removed instantaneously to assess the stress redistribution of the structure within the connecting structural members and at higher elevations. The beams at the first, fifth and eighth floors were investigated to see if the storey height affects the stress redistribution of the structure. In the longitudinal direction of the building, the first floor beams have a label of 551 and 561, the fifth floor beams have label of 555 and 556 while the eight floor beams have a label of 558 and 559. Along the transverse direction the beam at the first, fifth and eighth floor is labels 381, 385 and 388 respectively. Details of the labels about the column removal members are shown in Figure 4-27.

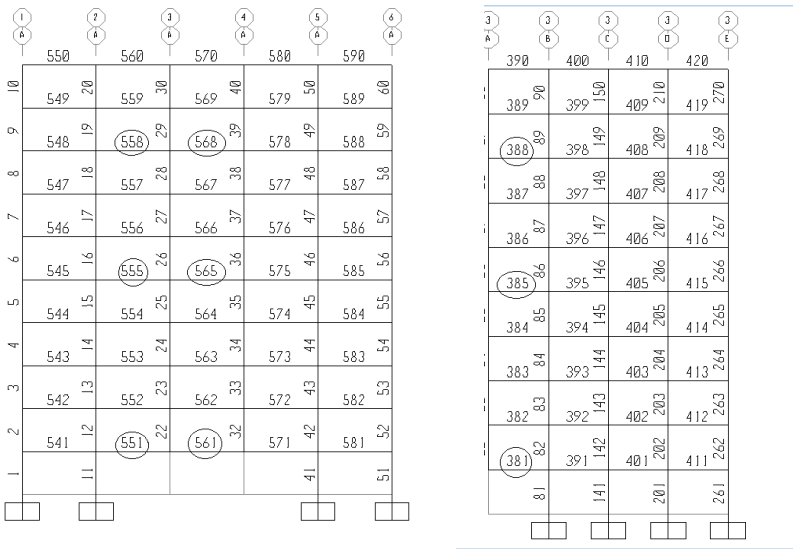

Figure 4-27 Study locations for MCRS

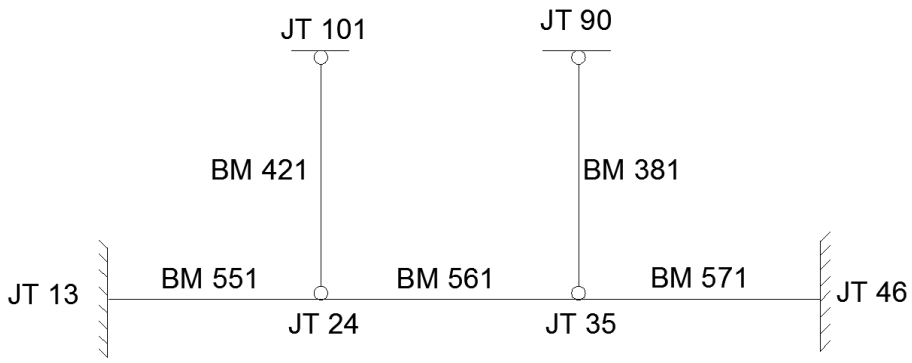

Figure 4-28 Labels on multiple column removal scenario (MCRS)

The internal forces assessed in the longitudinal direction are the axial force (P), shear force (V) and moment (M). Along the short span, only the axial force is assessed. During modelling it is assumed that only the perimeter frame structure is rigid while the interior frame structure is pinned. The tie beams are not expected to transmit moment but axial forces only. The sudden loss of the edge columns would result in a dynamic response of the structure with the development of catenary forces in beams. The beams with label 551, 555 and 568 within the same elevation will be compared on one plot while 561, 565 and 568 on a separate plot. The tie beams with labels 381, 385 and 388 will be compared on a different plot. Finally, the joint displacement responses at the column removal node and the neighbouring beam-column joint will be assessed.

4.7.2 Main beam responses along the long span

Figure 4-29 compare the catenary, moment and shear force developed by beams 551, 555 and 558 at the first, fifth and eighth floor respectively

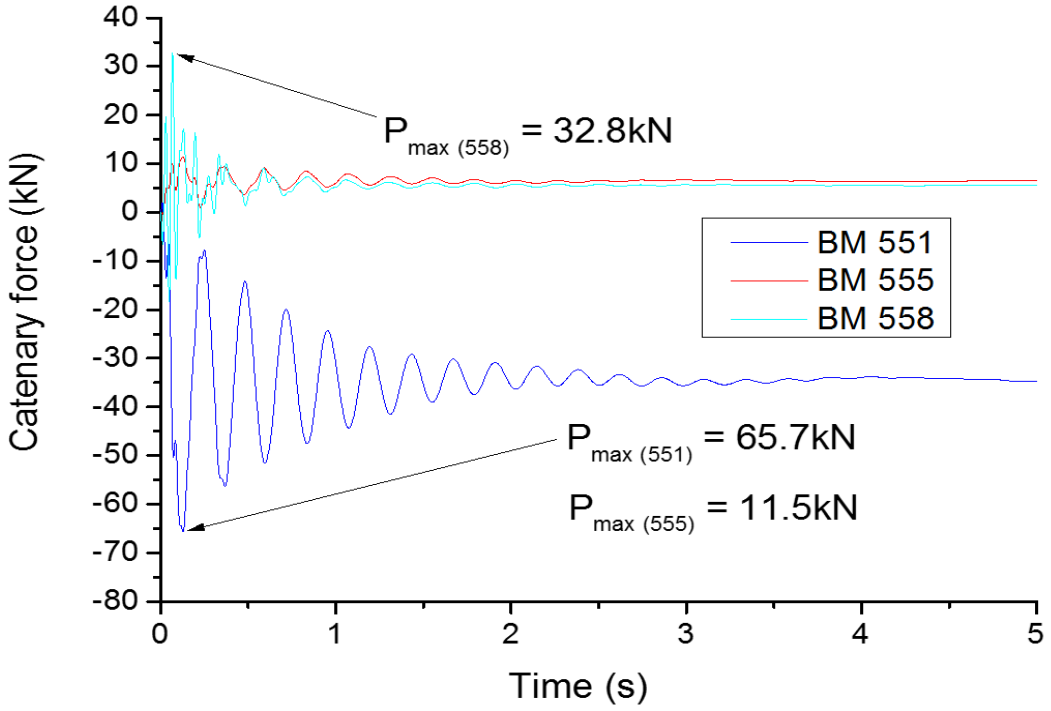

a) Catenary force vs time

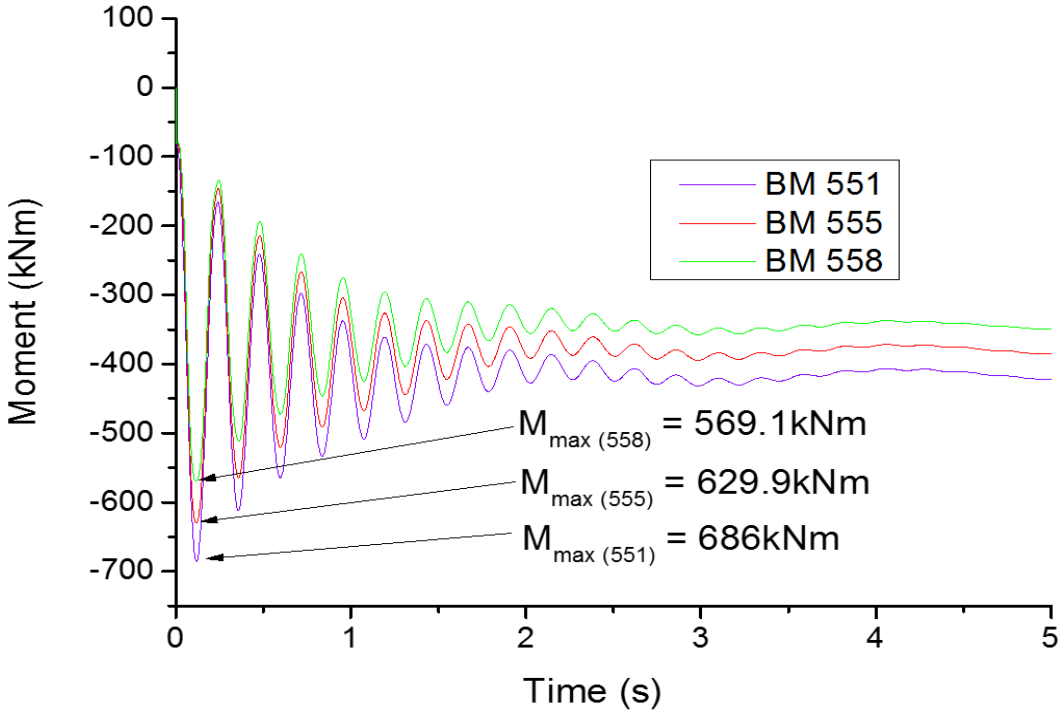

b) Moment vs time

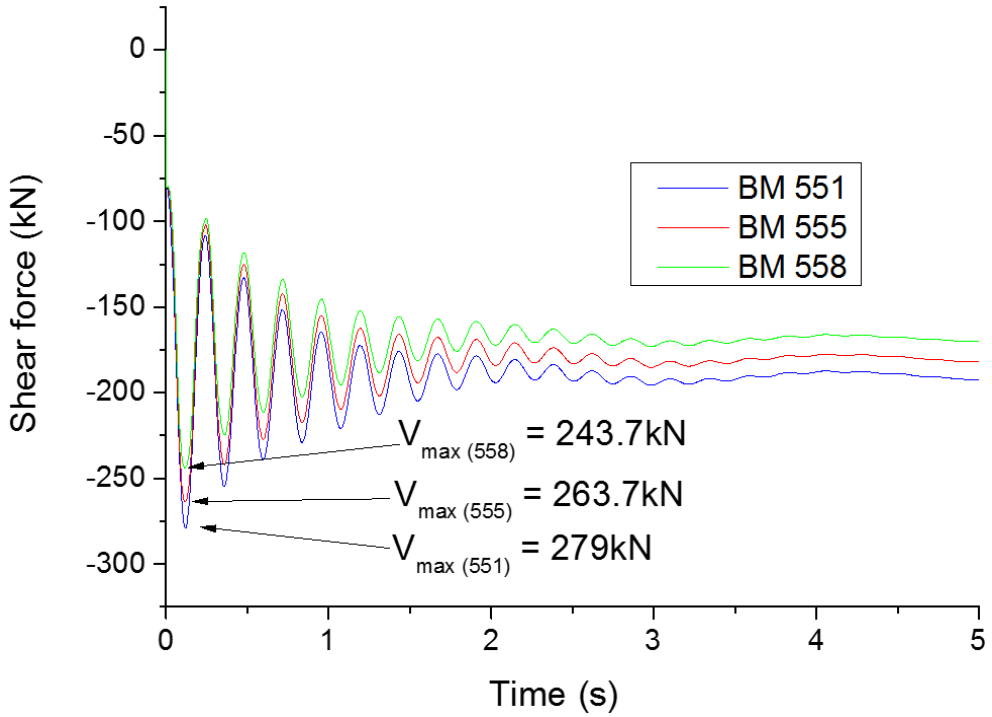

c) Shear force vs time

Figure 4-29 Beam response to double column loss

Beams 561 between the nodes of the removed columns act in compression while the beams connecting the removed columns with the adjacent columns act in tension. The magnitude of catenary force developed in the beam depends on the horizontal restraint at the beam ends.

From the plot of Figure 4-29 it was observed that the maximum axial force response in Beam 551, Beam 555 and Beam 558 are 65.7kN, 11.5kN and 32.8kN respectively. This response shows that the maximum catenary force occurs on the first floor in Beam 551. For design purpose, it can be concluded that catenary checks should be carried out on the beams connecting the node of the removed column. The maximum moment response in Beam 551, Beam 555 and Beam 558 are 686kNm, 629.9kNm and 569.1kNm respectively. The first-floor beam (Beam 551) is more critical than Beam 555 and Beam 558. In view of these responses, design checks in beams can be limited to first-floor beams under multiple column removal scenarios. The maximum shear force response occurs on the first floor with a value of 279kN while the shear force in Beam 555 and Beam 558 is 263.7kN and 243.7kN respectively. The response at the first floor differs from the fifth and eighth floor by 5.8% and 14.5% respectively. The response of Beam 561, Beam 565 and Beam 568 are shown in Figure 4-30.

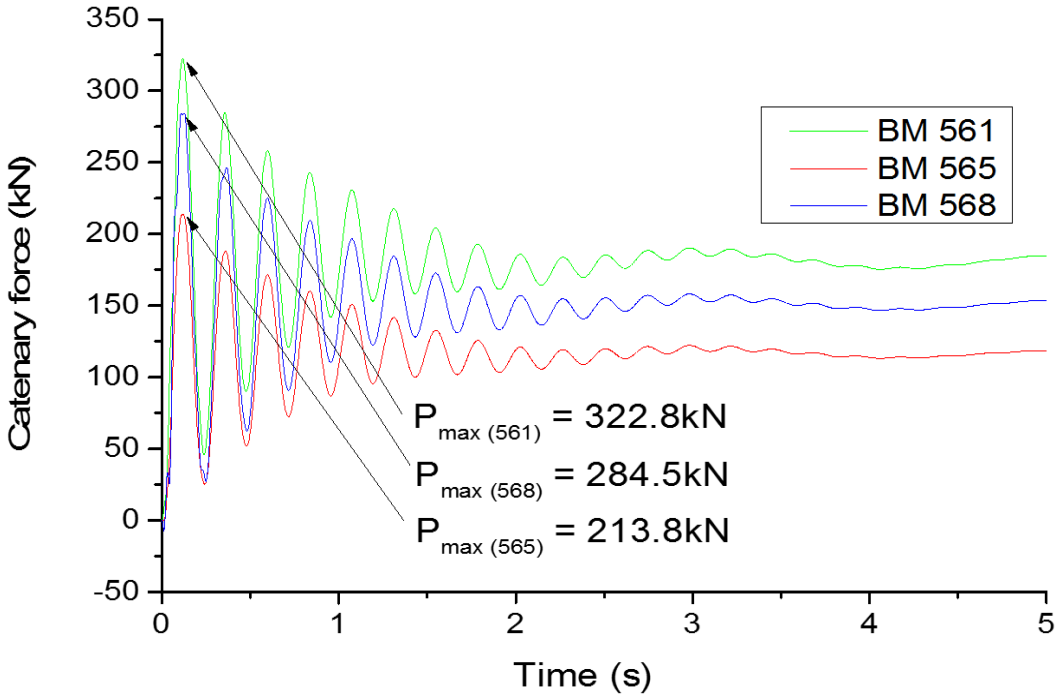

a) Catenary force vs time

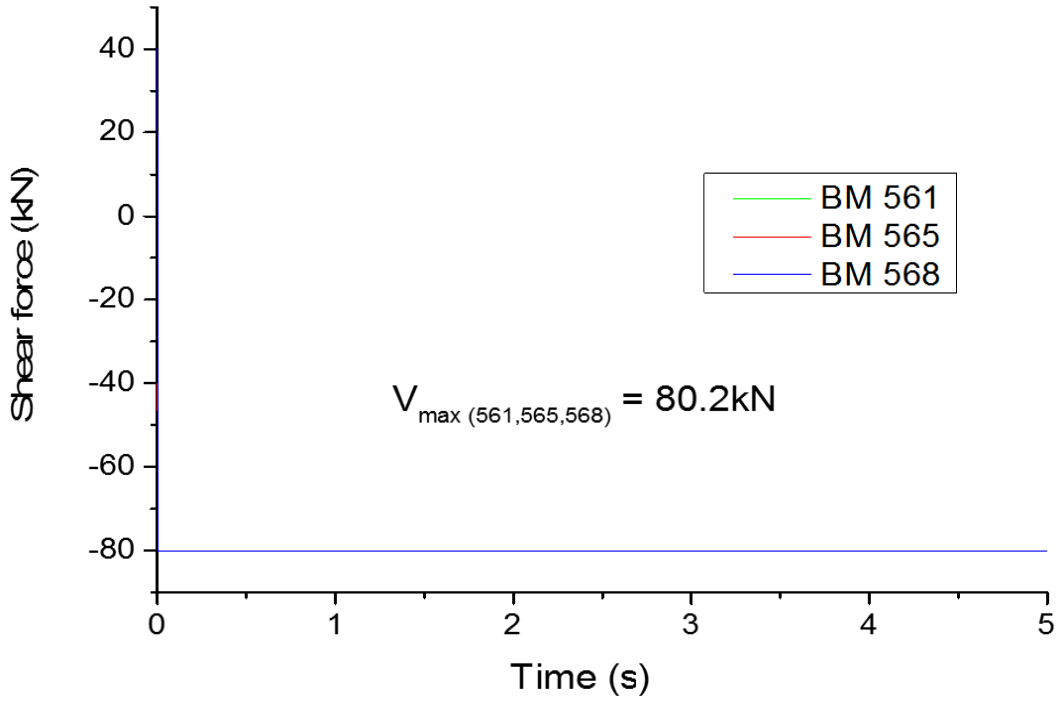

b) Shear force vs time

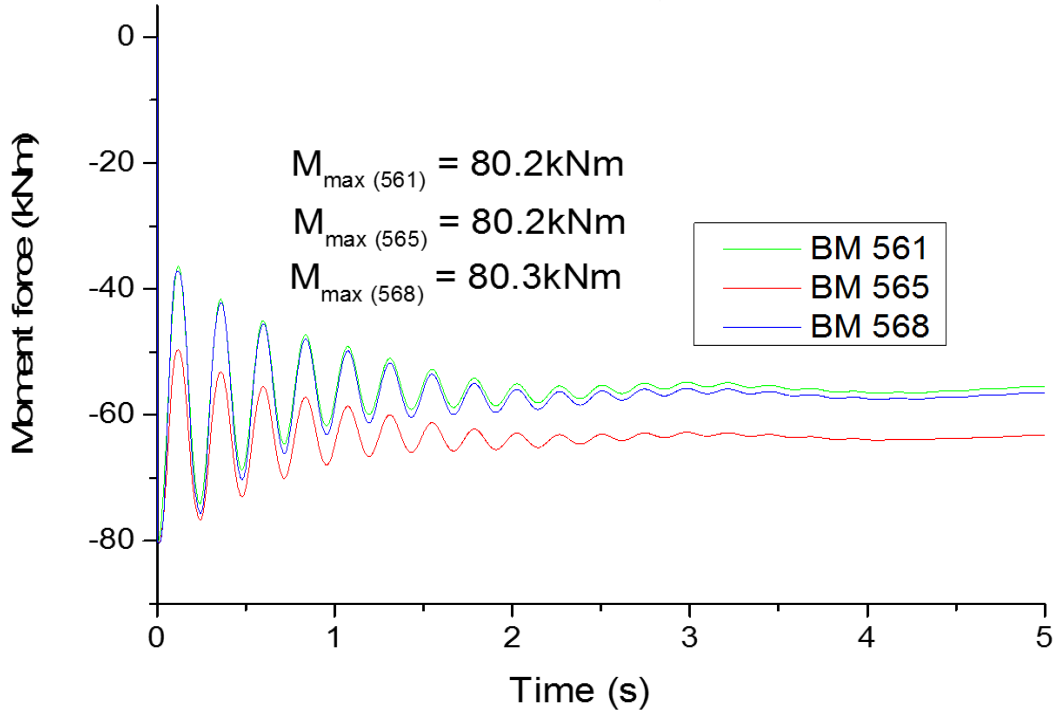

c) Moment vs time

Figure 4-30 Main beam responses due to DCRS

From Figure 4-30, the tensile force response with time in beam 561, 565 and 568 has a similar phase of vibration; however the magnitude is not the same. The axial force of beam 561, 565 and 568 are 322.8kN, 213.8kN and 284.5kN respectively. This implies that the beams at the first floor connecting the nodes of the removed column is more critical relative to other beams on higher elevation about the same alignment. Relative to the first floor response, maximum tensile force decreased by 33.8% at the fifth floor and 11.9% at the eighth floor. This implies that the critical response to catenary force occurs at the beams connecting the node of the removed columns and the response decrease as the storey height increases. The shear forces in Beam 561, Beam 565 and Beam 568 is 80.2kN. There is no change in the shear force relative to other beams on the same vertical alignment. The maximum moment response of the beams at the first floor (Beam 561), fifth floor (Beam 565) and eight floor (Beam 568) are 80.2kNm, 80.2kNm and 80.3kNm respectively. The next phase is to investigate the response of the tie beams connecting the nodes of the removed column along the short span.

4.7.3 Tie beam responses due to double column loss (DCRS)

Figure 4-31 is the axial force, shear force and the moment of Beam 381 (BM 381), Beam 385 (BM 385) and Beam 388 (BM 388).

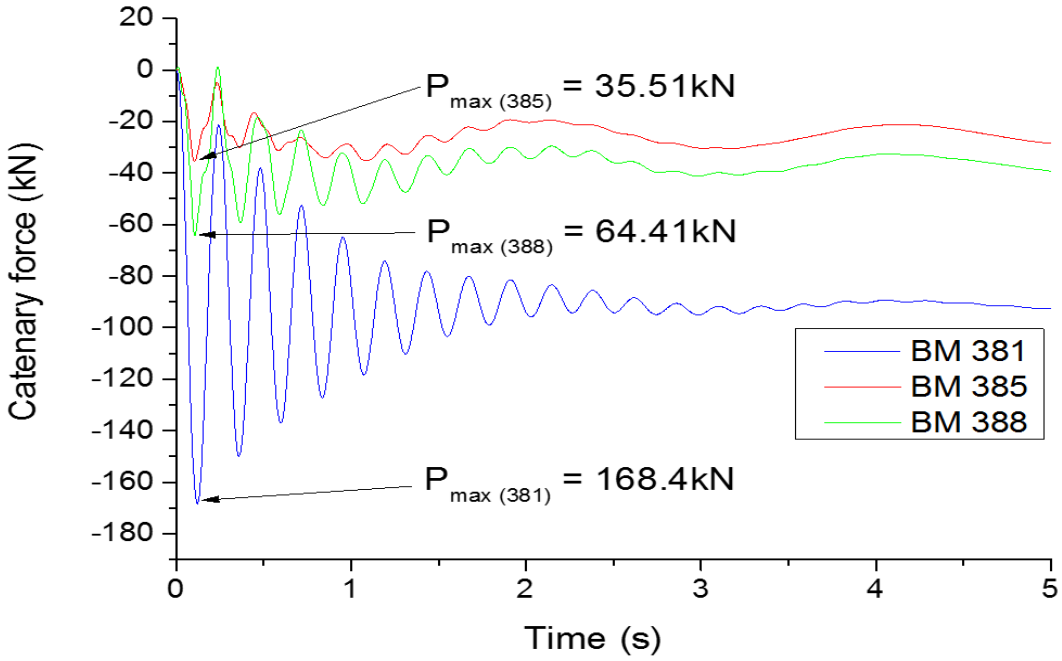

a) Catenary force vs time

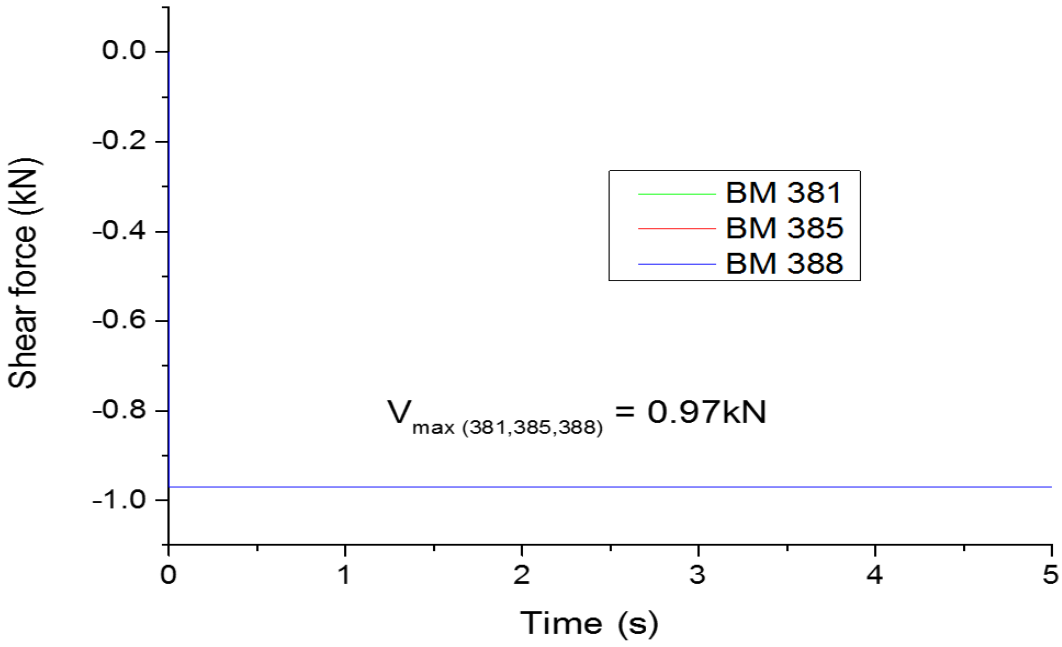

b) Shear force vs time

Figure 4-31 Tie beam response

The maximum axial force in Beam 381, Beam 385 and Beam 388 are 168.4kN, 35.5kN and 64.41kN respectively, while the maximum shears force response with time is approximately 0.97kN in the tie beams which is negligible. From this investigation, the most important consideration during progressive collapse for tie beams is the axial force response of the beams which occurs at the first floor. The first floor beam (Beam 381) connecting the node of the removed column is the critical beam relative to the beams on the same plane at higher elevations. The maximum catenary force response in the tie beams occurs in Beam 381 with a maximum axial force response of 168.4kN. Comparing the maximum catenary responses at main beams with the tie beams, it was observed that that the catenary response of the main beams exceeds the response at the tie beam by 91.6%. The next subsection presents the responses of the columns within the vicinity of the removed column.

4.7.4 Joint response due to multiple column loss

Joint 24 (JT 24) and Joint (JT35) are the nodes of the removed double columns. Since JT 90 and JT 101 are symmetrical in terms of loads and position, only JT 101 is considered for displacement response. JT 24 and JT 35 are equally symmetrical, in view of this only JT 35 is considered. Furthermore, joint 13 and joint 46 are symmetrical within the structure model, therefore, only joint 46 is considered for the investigation.

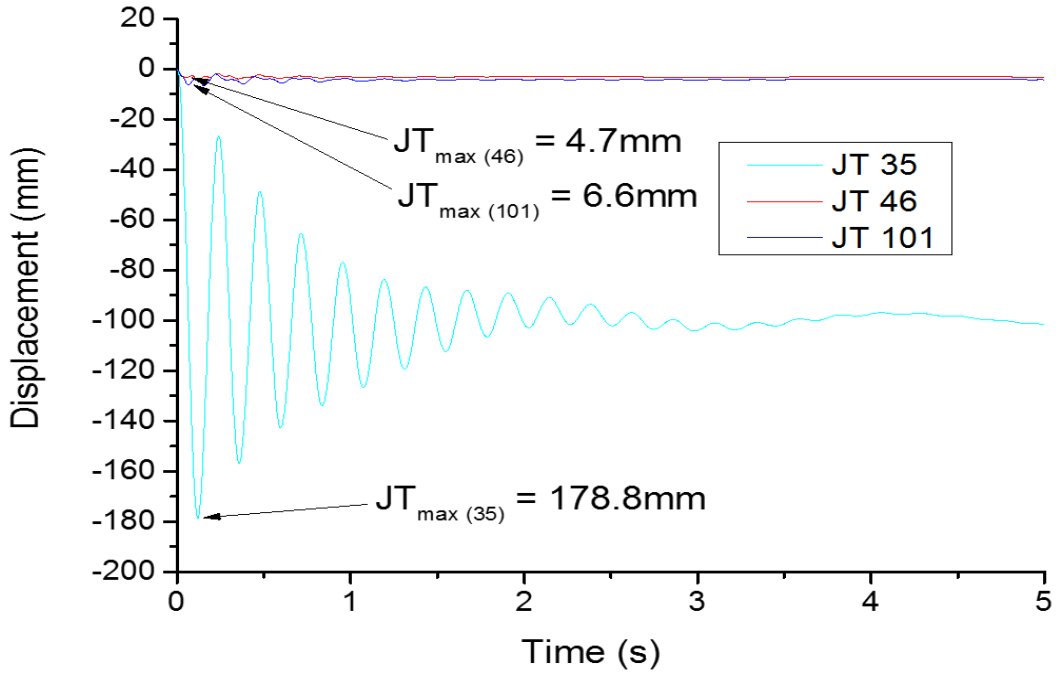

a) Displacement vs time

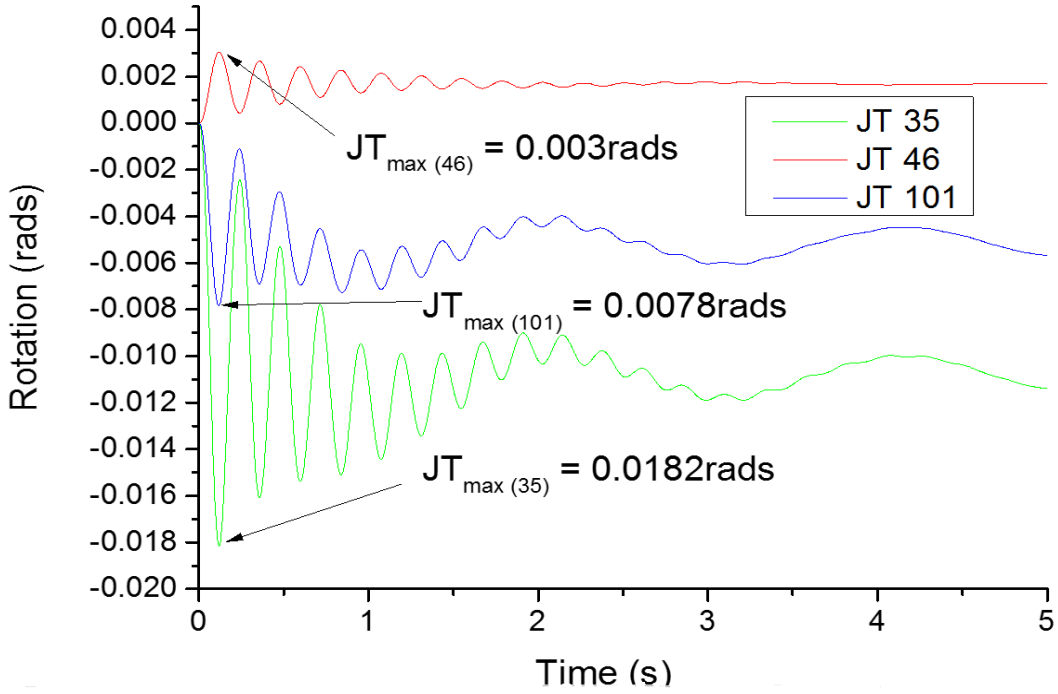

b) Rotation vs time

Figure 4-32 Joint response for double column loss (DCRS)

The vertical displacement of these joints and their rotational response is shown in Figure 4-32. The maximum vertical displacement at Joint 35 is 178.8mm, the displacement response at joint 46 (JT 46) is 4.7mm and for Joint 101 (JT 101) is 6.6mm. From the joint displacement response, it was observed that Joint 35, (JT 35), Joint 46 (JT46) and Joint 101 (JT 101) has a rotational value of 0.0182rads, 0.0030rads and 0.0078rads respectively.

4.7.5 Adjacent column responses due to multiple column loss

When multiple columns are damaged and rendered incapacitated in resisting vertical load, complex stress redistribution take places within a period of time which may result to partial or total collapse of the structure. This subsection is aimed at assessing the response of the adjacent columns mostly affected by the instantaneous loss of multiple vertical load bearing members. The sub-frame model used for the purpose of illustration is shown below in Figure 4.36. The removed columns are labelled 21 and 31 respectively. Along the longitudinal direction, the columns mostly affected are Column 11 and Column 41. Along the minor axis, the columns critically affected are Column 81 and Column 91. These affected columns are

loaded symmetrical and in view of that, checks were made to see if the responses are the same.

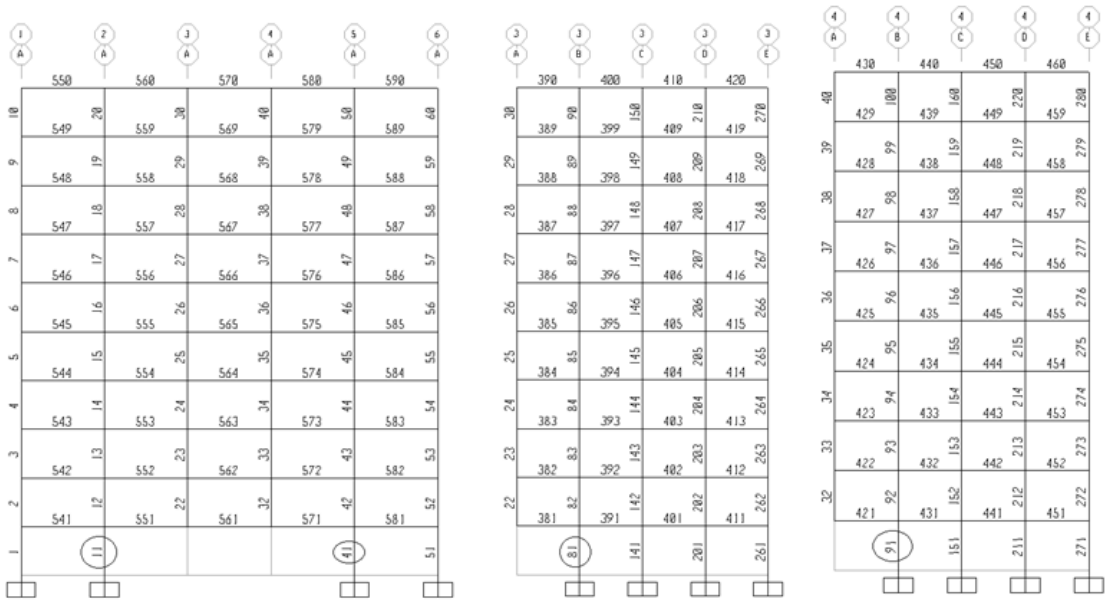

Figure 4-33 Elevation showing double column removal locations

The elevation shown in Figure **4-33** illustrates the location at which the double columns were assessed. The adjacent columns affected by the removal of the double columns are labelled as 11, 41, 81 and 91. The responses of these columns are compared to assess the redistribution of the internal forces over a period of time. Considering the symmetry due to the double column loss, it can be observed that Column 11 and Column 41 have the same response while Column 81 and Column 91 on the short span have equal response. The static responses of the structure are shown in Table 4-6 below. It is observed that Column 81 and Column 91 exceed the response of Column 11 and Column 41 by 37.5% in axial force, however column 11, 41 exceeds Column 81 and 91 by 16.1% in shear and 11.7% in moment.

Table 4-6 Static response under multiple column loss

Member	Ps (kN)	Vs (kN)	Ms (kNm)
Col 11,41	4509.75	70.36	172.32
Col 81,91	6200.80	60.58	154.33

The dynamic response of the structure was carried out to assess the redistribution of forces under double column removal scenario. The maximum axial force response in Column 11 and Column 41 is 6757kN while the maximum response of Column 81 and Column 91 is 9549kN. This indicates that Column 81 and Column 91 exceeds Column 11 and Column 41

by 41.3%. Comparing the percentage increase in static response in the axial force (37.5%) to the dynamic response (41.3%), it is obvious that there is no constant proportionality in the consistency between the static and dynamic response.

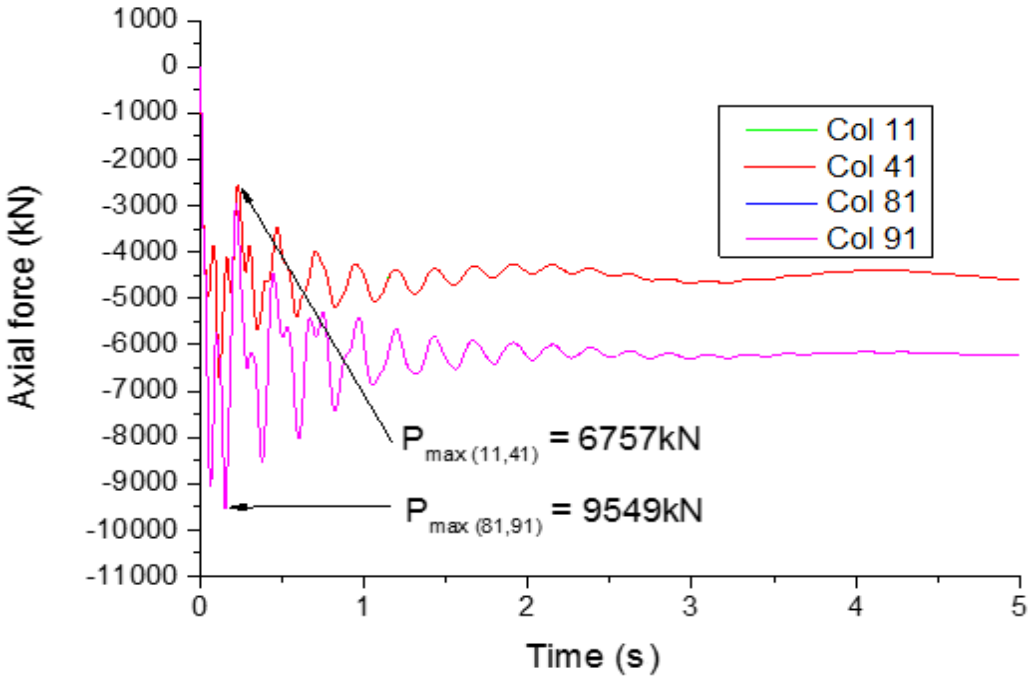

a) Axial force vs time

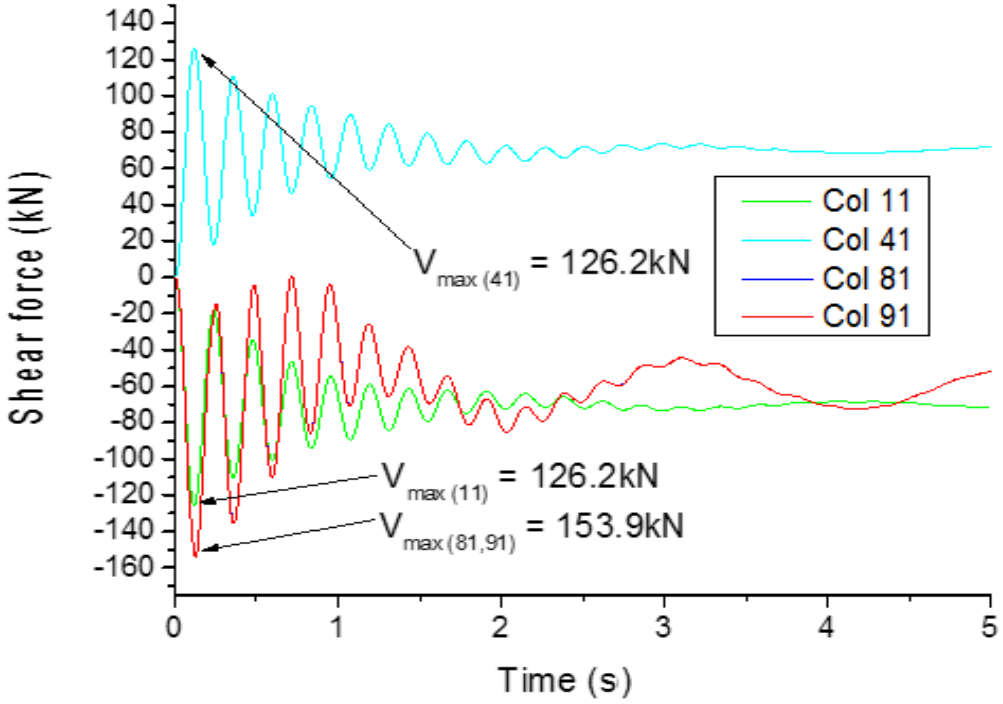

b) Shear force vs time

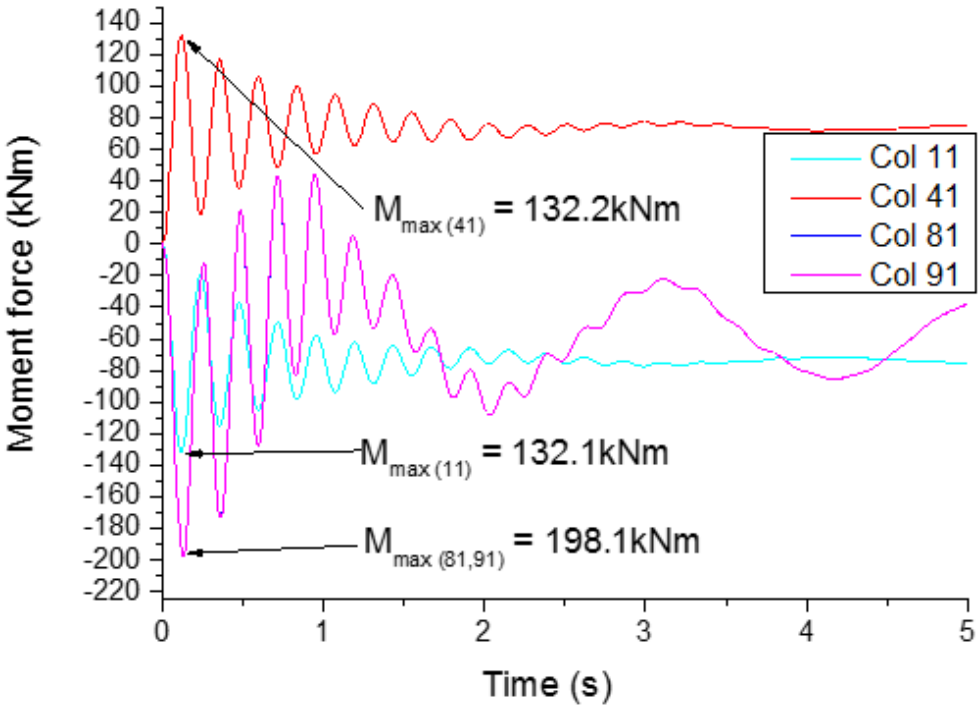

c) Moment vs time

Figure 4-34 Moment response of adjacent columns verse time

As shown in Figure 4-34, the maximum shear force response of Column 11 and 41 is 126.2 and 126.2kN respectively while that of Column 81 and Column 91 are 153.9kN. The maximum moment in Column 11, Column 41, Column 81 and Column 91 are 132.1kNm, 132.2kNm, 198.1kNm and 198.1kNm respectively. The maximum moment responses occur at the columns along the short span relative to the columns along the long span.

4.8 Dynamic amplification factor

The dynamic amplification factor of 2.0 (GSA 2003) is a subject of debate among researchers whether it is conservative or not. It is a dimensionless number defined as a ratio of the nonlinear dynamic action effect to the corresponding nonlinear static response effect. A previous investigation carried out by the author shows that the column removal time, modelling technique and assessment criteria significantly affects the decision on which side of the argument. In addition, if the response is based on the nodal displacement at column removal joint, two important factors has to be considered: rotational response and displacement response. This section critically evaluates the dynamic amplification factor

based on the beam- column connection response in addition to the internal force response in the key structural members. (Columns and Beams).

4.8.1 Structural member response criteria

The internal forces in the beam or column can be used for the computation of the dynamic amplification factor (DAF).

Summary of column response criteria

When sudden column loss occurs, the axial and shear force responses are the dominant internal forces affected with the shear force being the most important consideration. As shown in the summary plots of Figure 4-35 and Figure 4-37, if the axial force response is used in evaluating the dynamic amplification factor, the value ranges from 1.3 to 1.5.

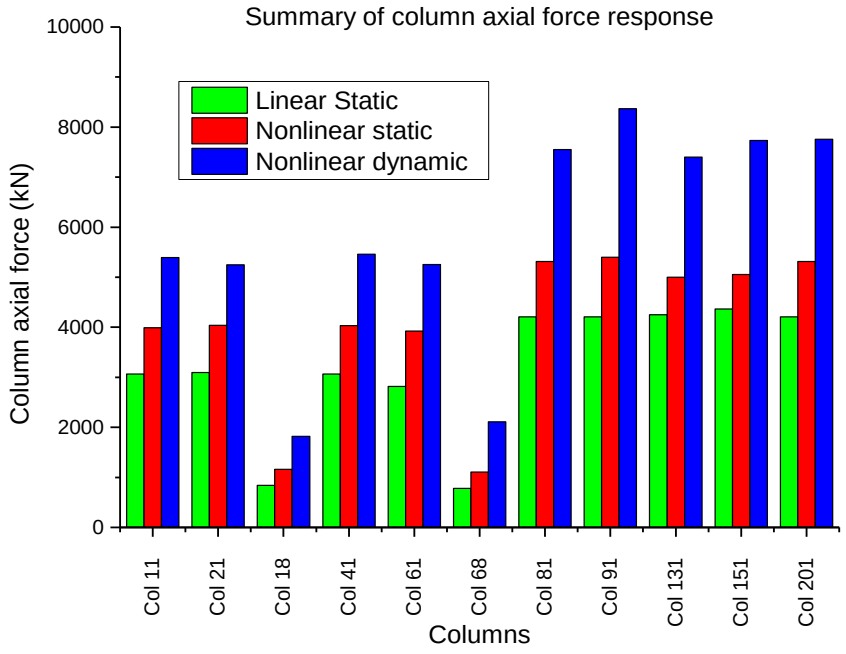

Figure 4-35 Comparison of axial force response

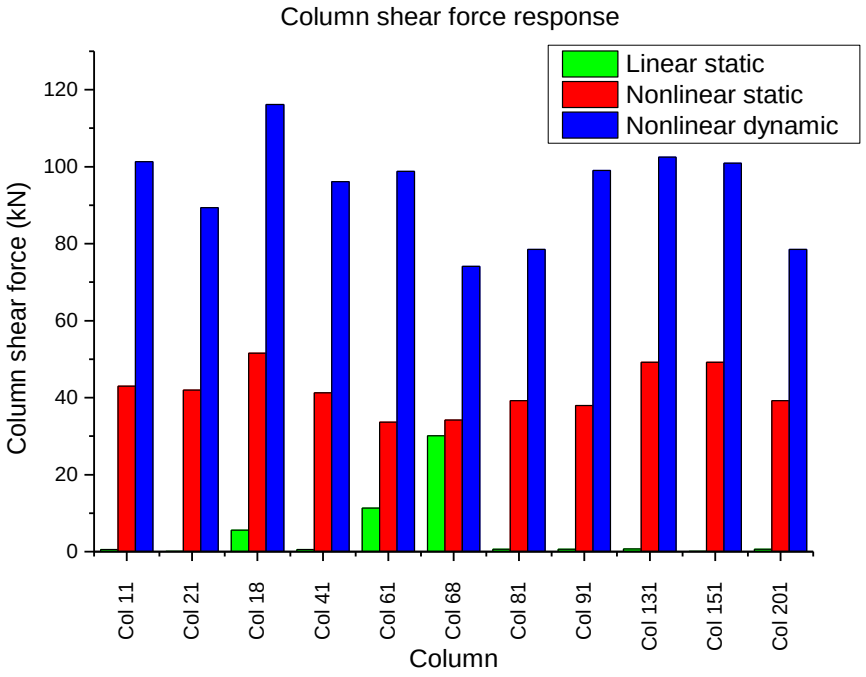

Figure 4-36 Comparison of shear force response

The DAF ranges 1.66 to 2.17 using the shear force response criteria, the maximum occurring in Column 91. Figure **4-36** shows the summary of the shear force response in columns based on a single column loss at different locations for linear static, nonlinear static and nonlinear dynamic response. The shear force response is the most critical internal force in column affected by dynamic effects.

Summary of beam response criteria

Beam response to column removal scenario is an important consideration for assessing the performance of high-rise structures during progressive collapse; although beam response criteria are not often considered in assessing the dynamic amplification factor response as compared to the connection response. In this subsection, a summary assessment is presented for the initial, static, and dynamic response of the structure. Consequently, a proposal is made for the dynamic effect of sudden column loss on beam response based on the developed catenary force.

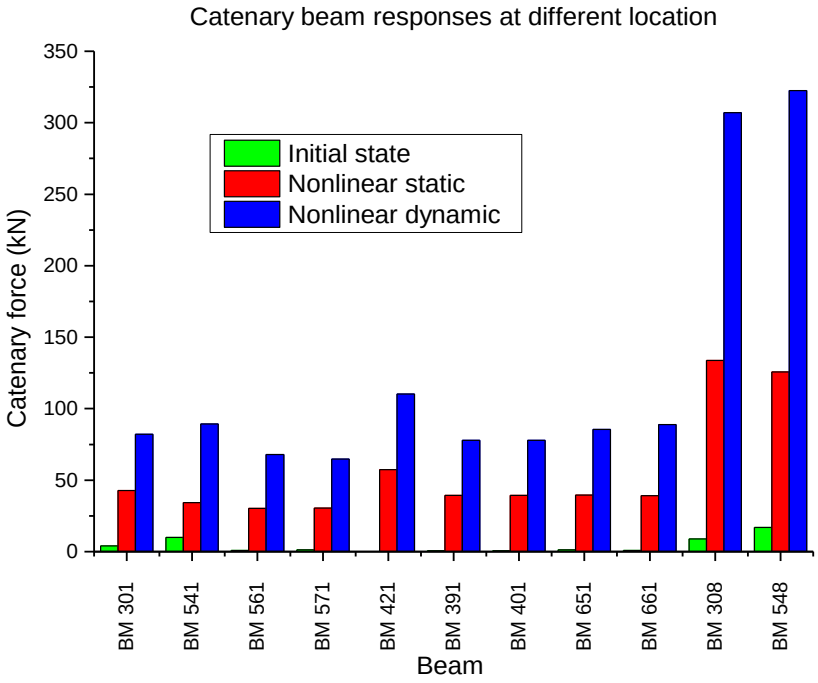

Figure 4-37 Comparison of catenary forces in beams

The summary of the beam response to a single column removal scenario at different locations is presented in Figure 4-37. The ratios of the dynamic response to the nonlinear static response for all the cases considered ranges from 1.70 to 2.2 while the mean response was 1.84 with a standard deviation of 0.19. The maximum dynamic response is observed in Beam 308 and 548 which occurs under eight-floor column removal scenario. In all the responses obtained, catenary force response at the eight floor is more critical than the catenary force response at the corner, interior and the edge.

4.8.2 Beam - column connection response criteria

Figure 4-38 is the summary of the displacement and rotational responses for nonlinear statics and the nonlinear dynamic response at different building locations. The eight floor column removal scenario (EFCRS) corresponds to JT 9, the edge column removal scenario (ECRS) corresponds to JT 35, the corner column removal scenario corresponds (CCRS) to JT 2 and the interior column removal scenario corresponds to JT 156. The joint responses are presented in Figure 4-38 for the GSA load combination.

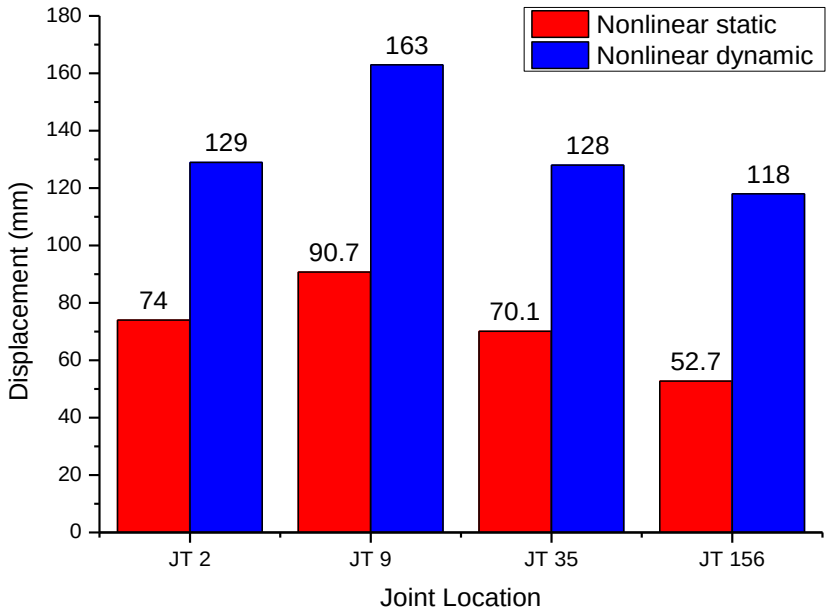

a) Summary of displacement response (NLS and NLD)

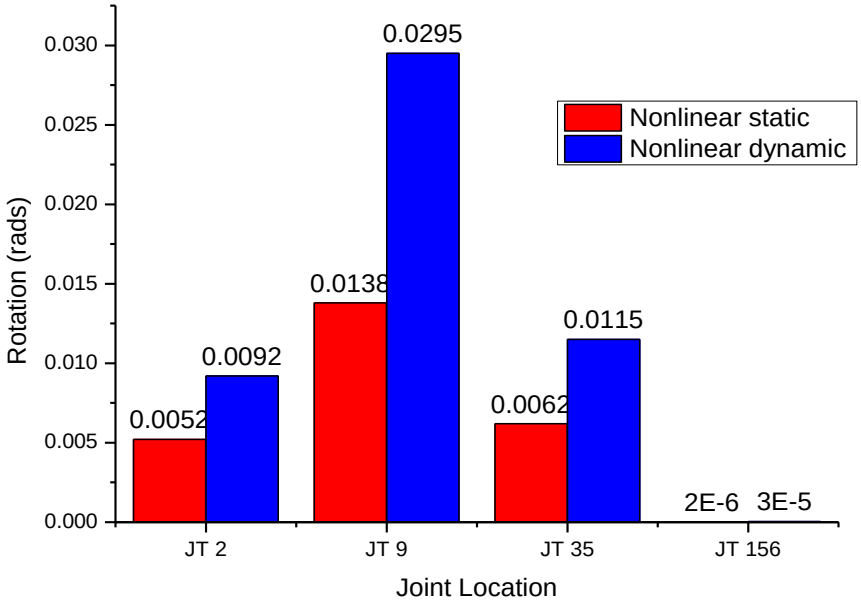

a) Summary of rotation response (NLS and NLD)

Figure 4-38 Summary responses due to NLS and NLD.

Using the rotational displacement response at all these locations as shown in Figure 4-38, it was observed that the maximum rotational response occurs at joint 9 while the minimum occurs at joint 156 (interior joint). The DAF is defined in Equation 4-1

$$DAF = \left(\frac{(DL+0.25LL)_{N_d}}{(DL+0.25LL)_{N_s}}\right) \quad \textbf{4-1}$$

The dynamic amplification factor using the displacement responds ranges from 1.7 to 1.88, with maximum occurring at the eighth floor.

4.9 Chapter summary

In this chapter, an assessment of a moment resisting frame structure is presented by determining the redistribution of internal forces under column loss scenario. The various analyses carried out in this chapter resulted in the following conclusions:

- Susceptibility to progressive collapse depends on the location of the column removal. This is equally observed by Mark Adom-Asamoah and Ankamah (2016).

- From the nonlinear static and nonlinear dynamic analysis carried out in this study, the dynamic amplification factor ranges from 1.6 to 1.88 based on connection response.

- Based on this study, the eighth-floor column removal scenario is more critical as compared to the corner, perimeter and the interior column removal scenario.

- The dynamic amplification factor depends on the internal force of the connection component considered, study location, joint displacement and rotational responses, damping ratio and the modelling technique (Kaewkulchai and Williamson 2004). A similar observation made by Tsai 2007, Tsai and Lin; 2009).

- Assessment carried out on the columns adjacent to the removed columns shows that the shear force response criteria are the most important criteria for progressive collapse evaluation relative to the axial force and moment.

- A maximum DAF response of 2.2 occurs at the eight-floor column removal scenario using the shear force response in the column. A similar response was observed for beam catenary action. Hence, catenary force in beams and shear force in a column are two critical forces impacted most by the dynamic effect.

In conclusion, as clearly observed by Kim et al. (2009), the dynamic amplification factor can exceed the conservative factor of 2.0 recommended in guidelines. Therefore, the DAF of 2.0 recommended by GSA 2003 is to account for all variabilities in assessing the structure for dynamic effects.

Chapter 5 Assessment of brace frame system (BFS)

5.1 Introduction:

This chapter investigates the behaviour of braced frame system under a progressive collapse scenario. This segment of the study addresses one of the key objectives of the thesis: to determine the internal force redistribution of braced frame systems under a progressive collapse scenario.

Concentric brace systems (CBS) and eccentric brace systems (EBS) are two commonly used types of bracing systems in the construction industry. In current practice, different types of bracing configurations are utilised in the construction industry and the choice of a braced system is at times dictated by the architectural provisions. These brace systems are designed primarily to resist wind forces and to contribute to the lateral stability of the structure. In seismic regions, brace systems are designed to limit cyclic excitations induced by earthquake vibrations causing structural instability. In conventional design of high-rise structures, brace systems aim to provide adequate strength and stiffness within the elastic range in order to resist lateral loads induced by wind pressure or seismic loads.

Under the sudden loss of critical structural members, a significant amount of stored energy is dissipated as the structure seeks a new equilibrium state. Consequently, the brace systems buckles in compression and yields in tension or fractures in the worst scenario as the structure stabilises to a new equilibrium state.

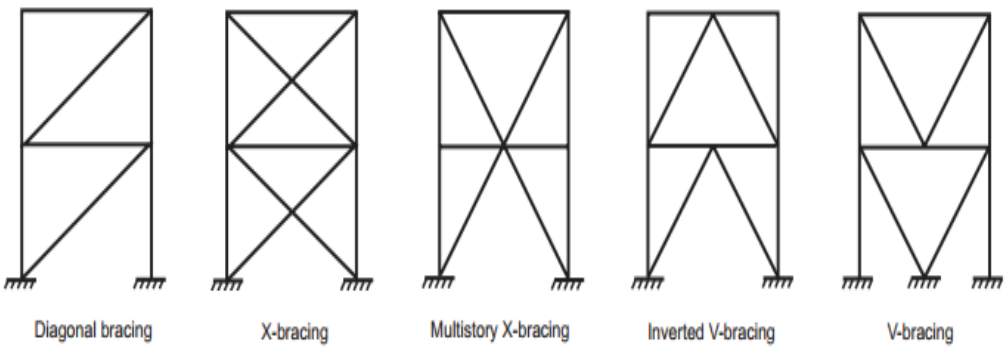

Figure 5-1 Different type of bracing systems

The configuration of the brace system significantly affects its performance under abnormal conditions. Generally, for design considerations, a bracing system must be balanced to ensure

that the lateral resistance in tension and compression is comparable in both directions. Different types of bracing system used in practice are shown in Figure 5-1. Detailed experimental and numerical analysis carried out by Türker and Bayraktar (2011) show that cross bracing significantly contributes to the overall stiffness of the connection relative to other bracing systems. Consequently, a cross bracing system is adopted for this study.

The ability of the structure to distribute the internal forces under sudden column loss was investigated at the perimeter of the structure, interior and the eight-floor location. The beams connecting the node of the removed column at one end and the columns connecting the other end of the beams are equally assessed. Since the structure deforms under sudden column loss, the two most important parameters are investigated: joint displacement and rotational response that determine the strength, stiffness, and joint rotational capacity.

5.2 Model description and scope of investigation

The same geometry used in previous sections is adopted for this investigation; however, for the brace frame system, moment releases were assigned to the ends of the beams to simulate the assumption of a pin connection. The assessment is limited to the four locations within the structural system as described previously. The load combination (GSA 2003) for progressive collapse assessment and material behaviour is the same as previously described.

5.3 Linear static analysis

The static analysis was carried out by building up the model without the member to be removed and the analysis re-run to assess the response of the structure. The initial forces in the members are recorded before and after the column removal scenario for each case considered. The primary objective of this investigation is to determine the percentage increase or decrease in the internal forces of the structural components connecting the removed column. Furthermore, the assessment is to check the most important internal force to be accounted for in designs that consider progressive collapse.

5.3.1 Position one: Static assessment due to CCRS

The elevations shown in Figure 5-2 are the transverse elevation, longitudinal elevation and the 3D elevation of the model under the corner column removal scenario (CCRS). From the transverse elevation, the removed corner column connects beam 301 at one end and Column 61 (Col 61) at the other end.

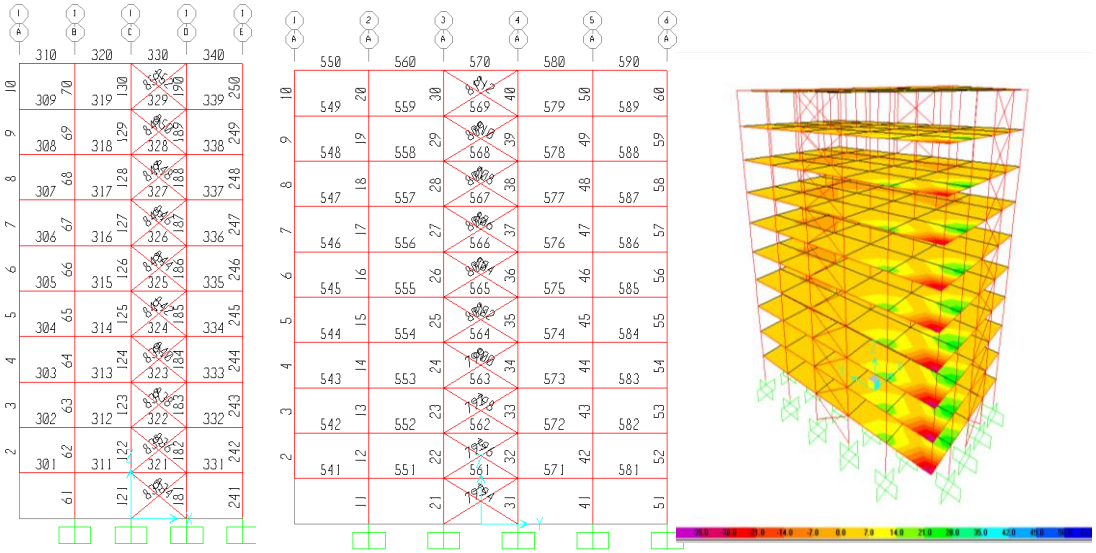

A) Short span elevation **B) Long span elevation** **c) 3D Elevation**

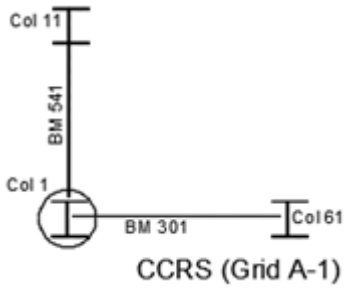

D) Members assessed

Figure 5-2 Description of corner CCRS

On the other hand, at the longitudinal direction, the removed column connects Beam 541 (BM 541) at one end and column 11 at the other end of the beam. The initial forces in these members were recorded during the linear static analysis of the structure and the analysis re-run without the corner column. The changes in the internal forces of these members are presented in Table 5-1.

Table 5-1 Member response under CCRS

Conditions	P (kN)	P' (kN)	V (kN)	V' (kN)	M (kNm)	M' (kNm)
Col 11	3077.95	3521	0.90	23.61	1.92	58.70
COL 61	2810.26	4201.85	0.863	45.06	1.65	107.98
BM 301	1.07	64.15	34.72	34.15	38.58	38.58
BM 541	2.64	29.41	80.17	80.17	120.25	120.25
Jt2 = 12.51mm						

From the response presented in Table 5-1, there is a significant change in the axial force, shear force, and moment of the structure relative to its initial static condition before the column removal. Column 11 has an initial axial force of 3077.95kN before the column removal; after column removal the axial force in Column 11 increases by 14.4%, corresponding to 3521kN. The shear force response of the column increases from 0.90kN to 23.61kN while the moment increases from 1.92kNm to 58.70kNm. The shear and moment increases by 2523.3% and 2957.3% respectively. On the other hand, the axial force response of Column 61 increases by 49.5% while the shear force and moment increases by 5121.13% and 6444.24% respectively. For this, the actual magnitude of shear force and moment after column removal is 45.06kN and 107.98kNm respectively. The shear force and moments in the beams remain constant while the axial force increases by 5895.3% and 1014% for beams 301 and 541 respectively.

In this preliminary assessment, the moment and shear force responses in columns is a dominant consideration for assessment. The beam responses show that the catenary force criterion is most critical in beams since it may not be considered during the conventional design stage of the structure. The next assessment presents a similar investigation using the edge column removal scenario (ECRS).

5.3.2 Position two: Assessment due to ECRS

Figure 5-3 shows the 3D elevation of the model and the label description shows the region where the column is removed. The edge column removed is Column 31 (Col 31). Beam 561 connects the node of the deleted column at one end and to Column 21. In the transverse direction, Beam 421 (BM 421) is connected to the node of the removed column and connected to Column 91 (Col 91). The bracing at the column removal node is Bracing 793

and Bracing 794. For the column removal location at the edge, the node of the removed column is labelled as 35.

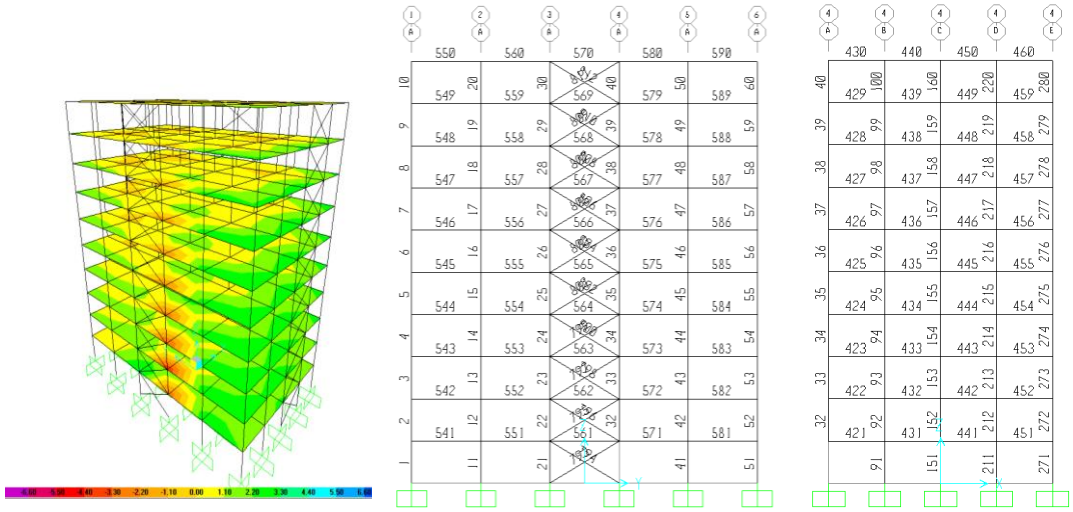

Figure 5-3 Description of ECRS

The static response of the structure after the column is removed is presented in Table 5-2 and shows the initial forces in the members before and after column removal.

Table 5-2 Member response due to ECRS

Conditions	P (kN)	P' (kN)	V (kN)	V' (kN)	M (kNm)	M' (kNm)
Col 21	3066.31	4643.38	0.919	6.34	1.97	44.86
COL 41	3077.95	3104.84	0.91	21.01	1.92	70.92
COL 91	4202.59	4484.40	0.869	16.2	1.86	57.08
BR 794	232.63	860.24	3.72	3.72	6.62	6.62
BR 793	232.63	1670.57	3.72	3.72	6.62	6.62
BM 561	34.93	128.23	80.17	80.17	120.25	120.3
BM 571	14.10	22.40	80.17	80.17	120.25	120.25
BM 421	0.11	13.46	0.97	0.97	1.08	1.08
Jt 35 = 19.3						

From Table 5-2 the maximum changes in the axial force response in columns 21, 41 and 91 are 51.4%, 0.87% and 6.7% respectively. Column 41, which is located at the short span experiences a significant change in axial force relative to Column 21 and Column 91 along the longer span. The maximum response in shear and moment in the columns occurs in Column 41, with an increase in shear and moment of 2233.3% and 3593.8% respectively. The bracing which is assumed to resist only lateral loads significantly acts as an alternative path in load redistribution, as evident in the increase in axial compression force. The bracing connected to the node of the removed edge column (BR 793) has a change of 6181.2% increase in axial force while the axial force in the crossed braced (BR 794) increases by

269.79%. The most important changes in the beams are the axial tension when the model is built without the edge column. The maximum change in axial force in beams occurs at BM 561.

5.3.3 Position three: Linear static assessment (ICRS)

The model description of the interior column removal scenario (ICRS) is shown in Figure 5-4, which shows the location of the ICRS, the connecting structural members and their labels. The node of the removed column is connected to Beam 651 on one end and Column 131 on the other end. Beam 661 is connected to the node of the removed column on one end and Column 151 at the other end of the longitudinal direction. Along the short span of the structure, the node of the deleted column is connected to Beam 391 and Beam 401, while these beams connect to Columns 81 and Column 201 on the other end.

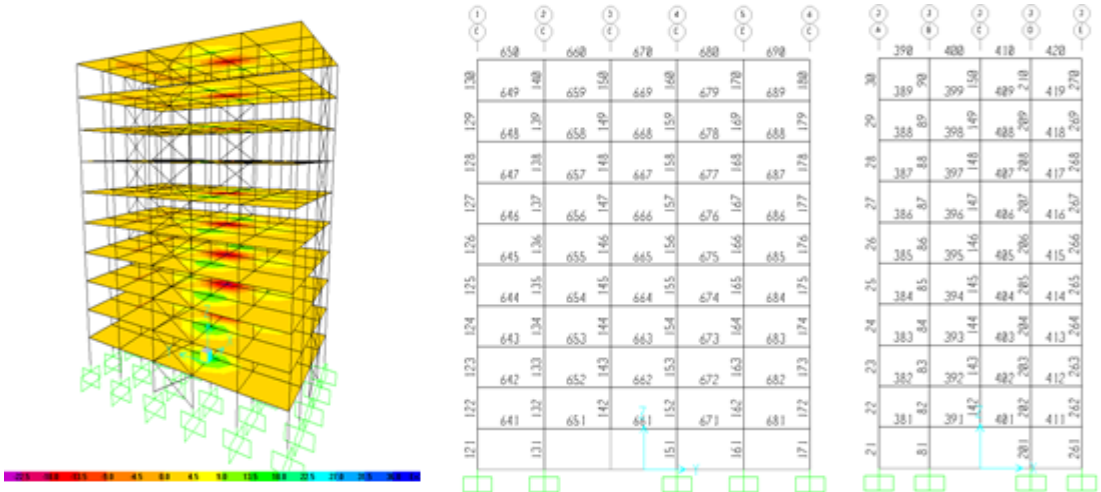

a) 3D Elevation b) Interior elevations

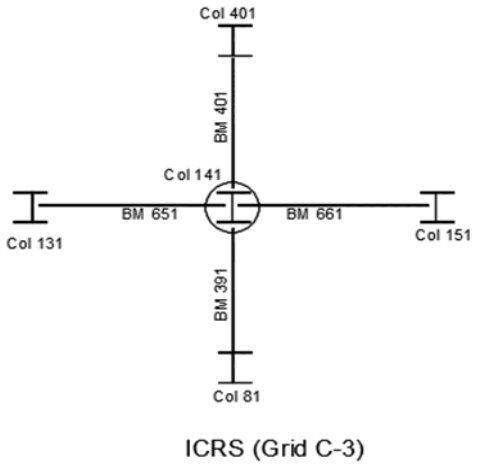

Figure 5-4 Description of ICRS

Static analysis of the structure without the interior column affects the behaviour of these members as shown in Table 5-3

Table 5-3 Member response due ICRC

Conditions	P (kN)	P' (kN)	V (kN)	V' (kN)	M (kNm)	M' (kNm)
Col 81	4202.59	5689.86	0.869	49.95	1.86	117.13
COL 201	4203.03	5690.33	0.48	49.56	1.23	116.49
COL 131	4255.12	4589.96	1.13	27.28	2.12	66.32
Col 151	4303.54	4638.26	0.23	26.39	0.44	64.37
BM 391	1.15	50.36	0.97	0.97	1.08	1.08
BM 401	2.05	51.38	0.97	0.97	1.08	1.08
BM 651	4.63	25.06	68.04	68.04	102.06	102.06
BM 661	3.99	24.58	68.04	68.04	102.06	102.06
Jt 156 = 74.87mm						

The columns (81, 201 and 131) were compared and, it was observed that the shear and moment after the removal of the interior column is approximately the same. The most important change that took place after column removal was the change axial force; Col 81 experiences an increase of 35.4%, Col 201 an increment of 35.4%, while Col 131 and 151 experience an increment of 7.9% and 7.8% respectively. In conventional design of structures, the interior columns are conservatively designed as pure axially loaded columns since the initial shear forces and moments are negligible as shown in Table 5-3. However, under column removal scenario, the moment and shear forces become significant with the columns in the short span (Col 81 and Col 201) of the removed column becoming more stressed relative to the columns on the longer span (Col 131 and Col 151) of the removed column.

The maximum moment and shear forces in the columns (Col 81 and Col 201) are 117.13kNm and 49.95kN respectively, which occur as a result of the removed column.

The beams along the short span are designed as tie beams. These beams have negligible initial stress resultants (PVM). However, under column removal scenario, it was observed that the beams along the short span (BM 391 and BM 401) significantly develop a maximum catenary force of 51. 4kN in trying to resist the effect of the removed column while the shear force and moment remain relatively stable after the column removal. On the other hand, the beams along the long span (BM 651 and BM 661) connecting the removed interior column experience a maximum increase in the catenary force of 20.59kN. The initial mid-span moment and shear force remain stable and the most significant contribution in resisting the effect of interior column removal is the catenary force response of the beams along the short span. The next plot shows the static response of the structure under eighth-floor column removal scenarios

5.3.4 Position four: Static assessment due to EFCRS

Figure 5-5 shows the position of the eighth floor column removal scenario (EFCRS) and the labels of the connecting structural members. The node of the removed is labelled as 9. This joint is connected to Beam 548 on the longitudinal direction and Beam 308 on the transverse direction. These beams are connected to Column 18 and Column 68 at the longitudinal and transverse direction respectively.

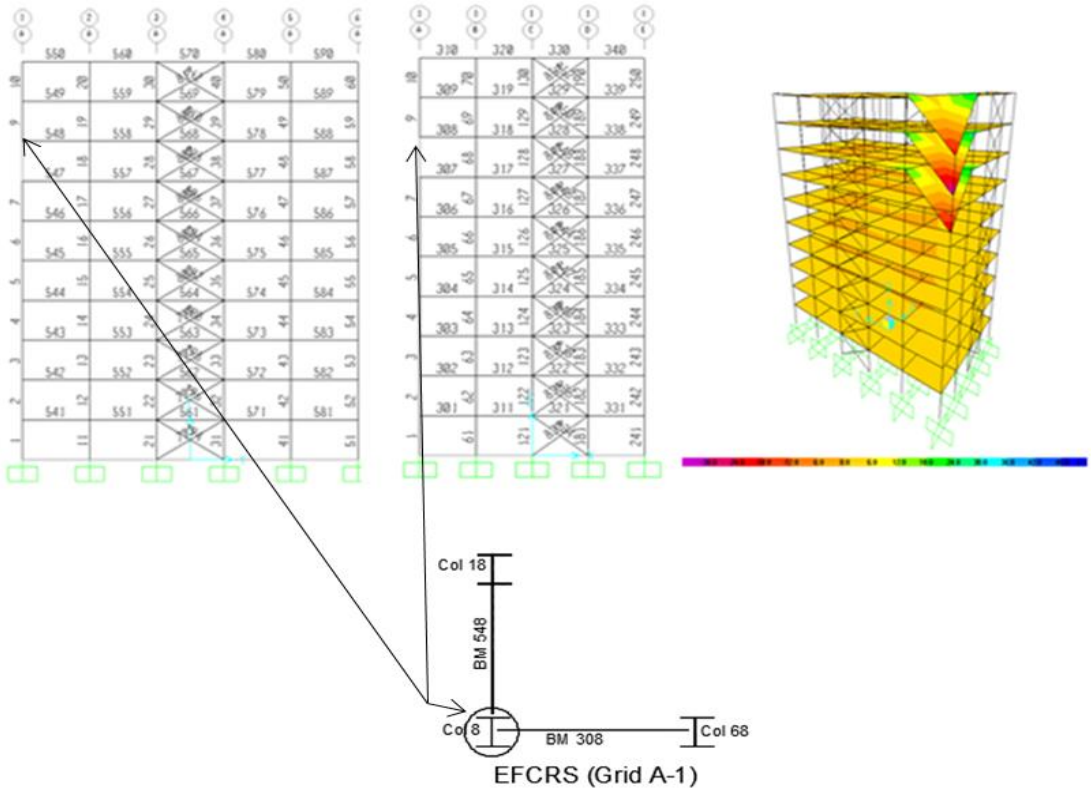

Figure 5-5 3D elevation and labels of the structure

The linear static analysis of the structure with and without the removed column is presented in Table 5-4. It compares the forces in the structural members before and after the eighth-floor column removal. Comparing the column responses, it was observed that the maximum column response occurs at Column 68 with an increment of 50.5%. The shear force increases from 5.57kN to 45.78kN, corresponding to an increment of 721.9%, while the moment changes from 10.99kNm to 123.45kNm, corresponding to a increment of 1023.3%.

Table 5-4 Member responses due to EFCRS

Conditions	P (kN)	P' (kN)	V (kN)	V' (kN)	M (kNm)	M' (kNm)
Col 18	846.84	1036.17	7.58	33.34	14.33	95.75
COL 68	782.92	1177.97	5.57	45.78	10.99	123.45
BM 308	0.55	228.26	34.72	34.72	38.58	38.58
BM 548	1.06	133.94	80.17	80.17	120.25	120.25
Jt 9 =143mm, 0.0217rads						

The condition is not the same for the beams connecting the removed column at the eighth floors. The response of the beams shows that the most important changes is the catenary force in the connecting beams. Comparing Beams 308 and Beam 548, the maximum

increment in the catenary force response occurs in Beam 308 with an increment of 227.71kN. The most important internal force in the beam is the catenary force response of the beams. Under the eight floor column removal scenario, the ratio of the catenary force response for the beam along the short span to the response along the long span is 1.7.

5.4 Nonlinear static analysis

The nonlinear static response of the structure was carried out under full application of gravity load saved at multiple steps.

5.4.1 Nonlinear static analysis at CCRS

This section presents the investigation of the nonlinear static response of the brace system under the corner column removal scenario. The maximum catenary force in Beam 301 is 224.9kN, while that of Beam 541 is 258.7kN. The corresponding shear force response for the beams are 69.4kN and 160.3kN respectively as shown in Figure 5-6. The maximum axial force response of Column 11 and Column 61 is 7090kN and 8361kN respectively. The shear forces in the columns are 82.98kN and 36.72kN respectively. Moment responses for the columns are 38.6kNm and 93.09kNm as shown in Figure 5-7.

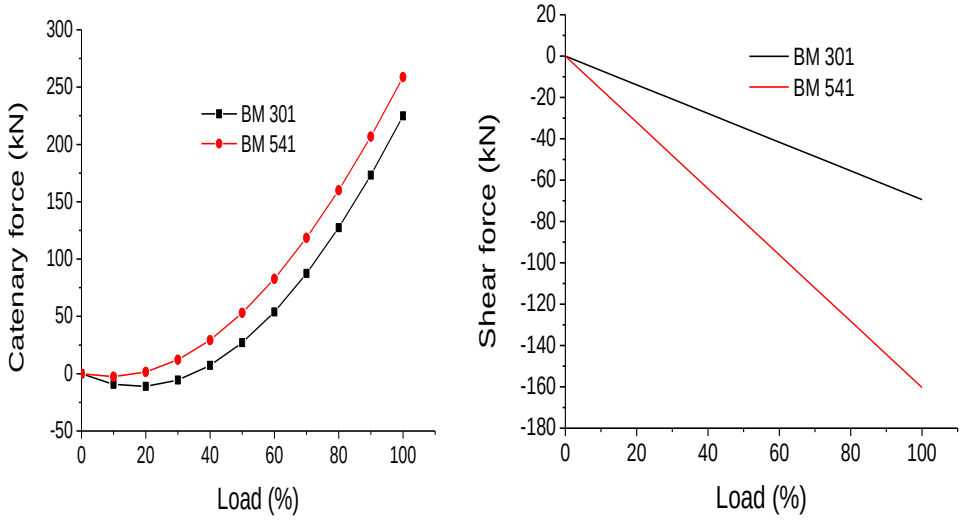

a) Catenary force vs time b) Shear force vs time

Figure 5-6 Beam responses at incremental loading (CCRS)

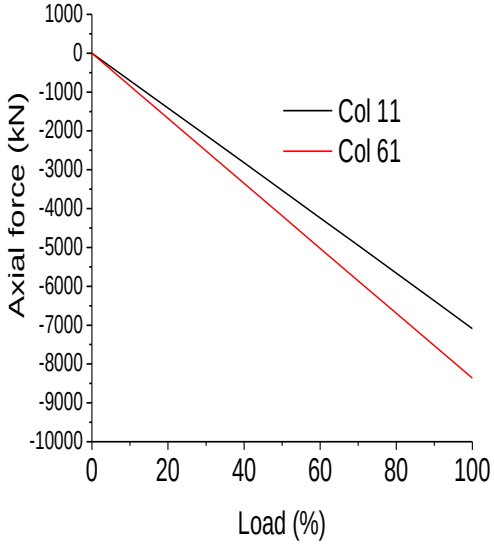

a) Axial force vs time

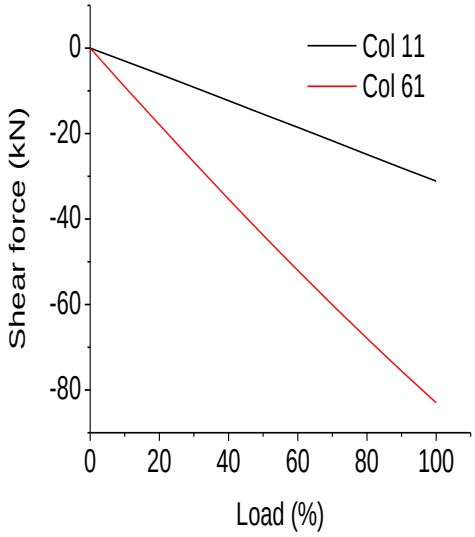

b) Shear force vs time

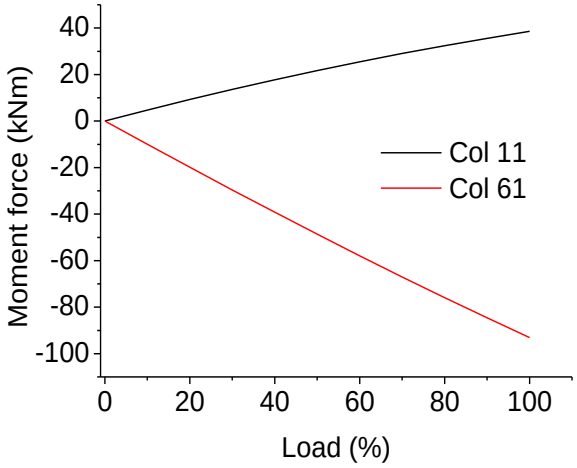

c) Moment force vs time

Figure 5-7 Column responses at incremental loads (CCRS)

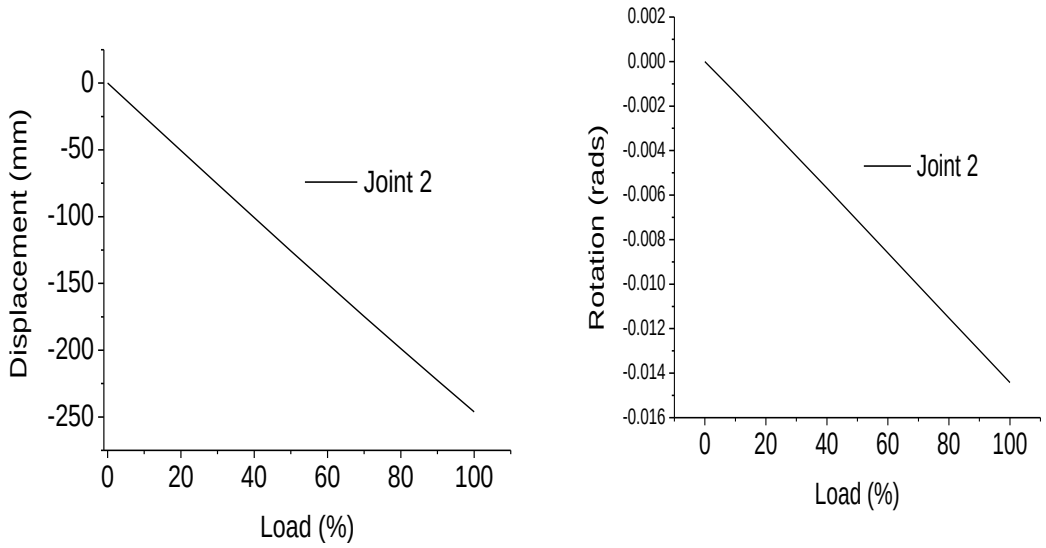

a) displacement response vs load

b) Rotation response vs load

Figure 5-8 Joint response due to CCRS

The displacement and rotational responses of the beam-column connection is presented in Figure 5-8. The maximum displacement response is 246.1mm while the rotation is 0.0144rads. However at 50% load combination, (DL+0.25LL), the maximum displacement is 125.6mm, corresponding to a maximum joint rotation of 0.00714rads.

5.4.2 Nonlinear static analysis at ECRS

The nonlinear static response at the ECRS is presented in Figure 5-9 for the beams and columns connecting the removed column.

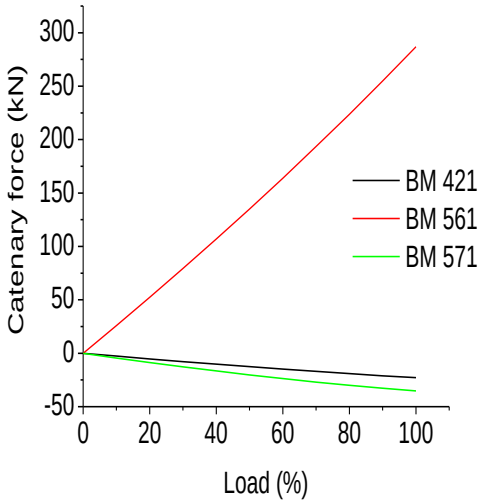

a) Catenary force vs Load

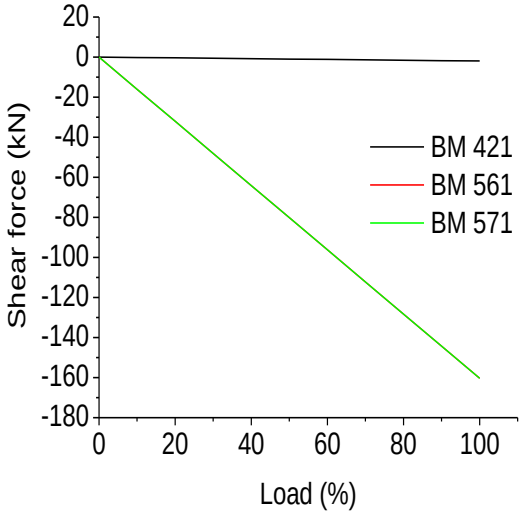

b) Shear force vs Load

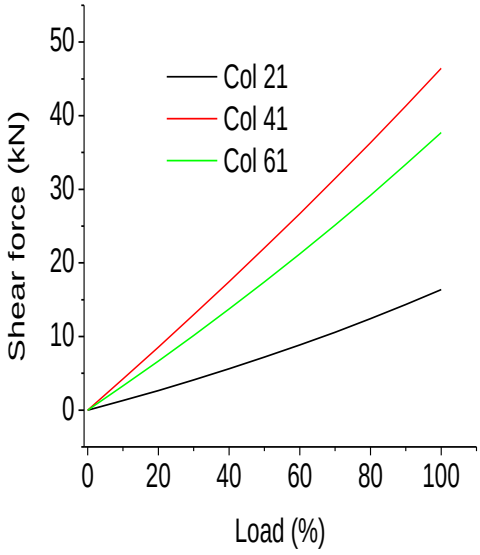

c) Shear force vs Load

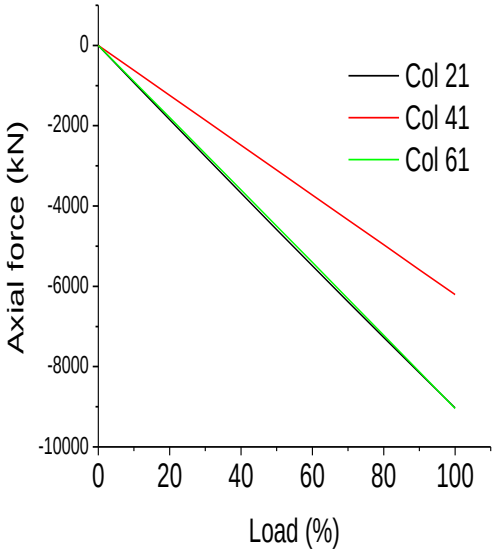

d) Axial force vs load

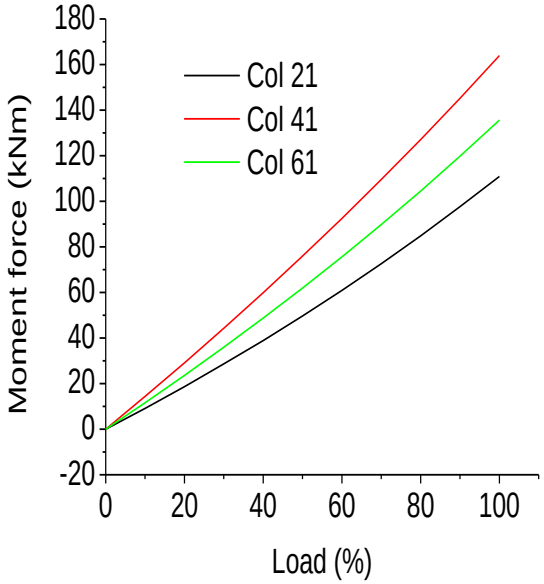

e) Moment vs Load

Figure 5-9 Nonlinear static column response under (ECRS)

The maximum displacement and joint responses under ECRS is 42.4mm and 0.0038rads respectively. The catenary forces in BM 571, BM 561 and BM 421 are 35.21kN, 286.8kN and 22.9kN respectively. The shear forces in the beams are 160.3kN, 160.3kN, 1.94kN respectively. The maximum axial forces in columns 21, 41 and 91 are 9029kN, 6208kN respectively.

5.4.3 Nonlinear static analysis at EFCRS

Figure 5-10 shows the response of the structure under Eighth Floor Column Removal Scenario (EFCRS). The maximum axial force in BM 308 is 138.2kN with a shear force response of 69.4kN along the short span. At the long span, BM 548 develops a catenary force of 57.5kN while the shear force is 160.3kN. The axial forces, shear and moment in Columns 18 (COL. 18) are 2082kN, 52.5kN and 31.5kNm respectively.

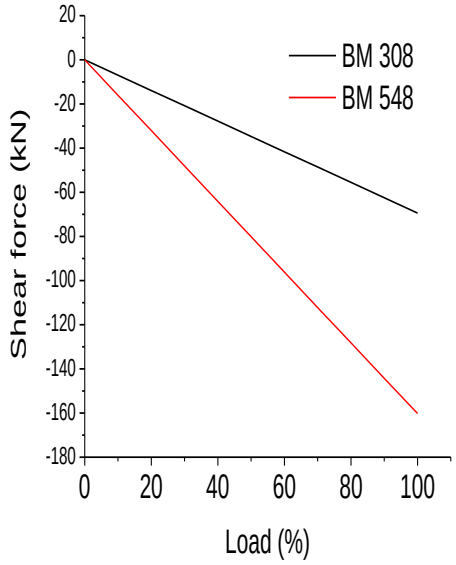

a) Shear force vs time

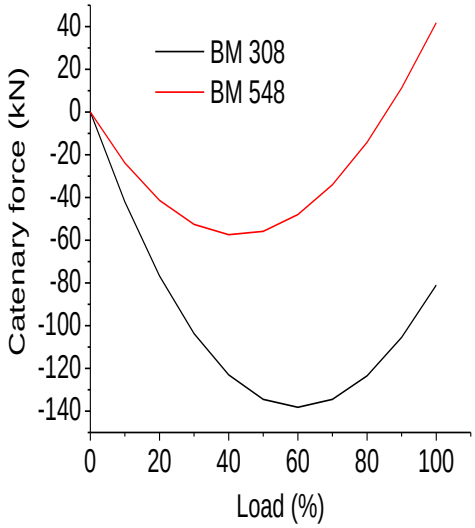

b) Catenary force vs time

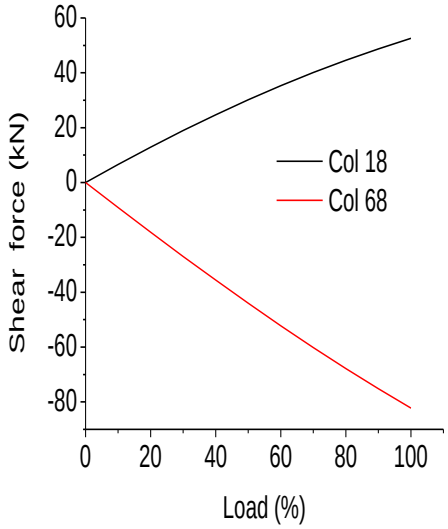

c) Shear force vs time

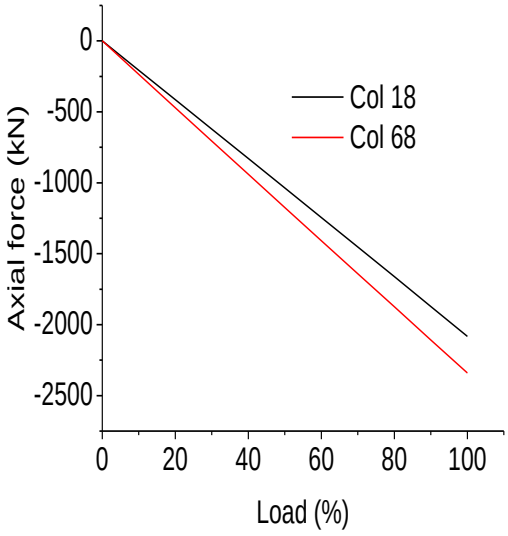

d) Axial force vs time

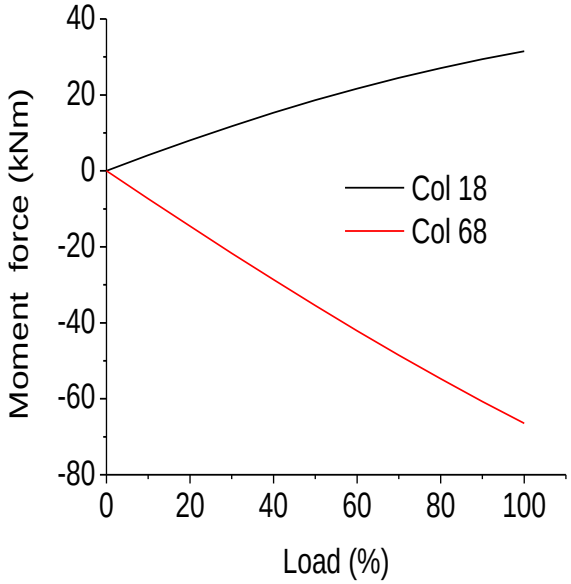

e) Moment vs time

Figure 5-10 Nonlinear static column response due to EFCRS

At the long span, axial force, shear and moment in the Column 68 (Col 68) are 2340kN, 82.3kN and 66.5kNm. The maximum displacement and rotational joint responses are 284.5mm and 0.0467rads. At 50% loading, (DL+.25LL), the maximum displacement and rotational responses are 144.1mm and 0.0229rads respectively.

5.5 Nonlinear Dynamic analysis investigation

This section investigates the dynamic response of the structure at four different locations: the corner, edge, interior, and eight-floor locations. The internal forces of the members connecting the removed columns and the displacement responses are assessed. Each subsection presents the results of the investigation at each location within the structural system. The joint displacement and rotational responses at these areas are shown.

5.5.1 Position one: NLD assessment due to CCRS

This subsection focuses on the corner column removal scenario (CCRS). As described previously, the structural members connecting the removed columns are investigated in order to assess the dynamic effect of the member response relative to the static response. The beams connecting the node of the removed column are Beam 301 and Beam 541, while the ends of these beams are connected to Column 61 and Column 11. Under the nonlinear

dynamic analysis, the response of these structural members are evaluated and presented under different subheadings.

Internal force response in Beams

The beams connecting the removed column at the corner point location as described previously in the static assessment were investigated for dynamic responses as shown in Figure 5-11. Beam 301 at the short span of the beam has a maximum dynamic catenary response of 118.2kN, which later stabilises to a static state of 64.15kN after four seconds. The maximum catenary force action of Beam 541 is 50.2kN under dynamic analysis and it stabilises to a static response of 29.4kN after four seconds.

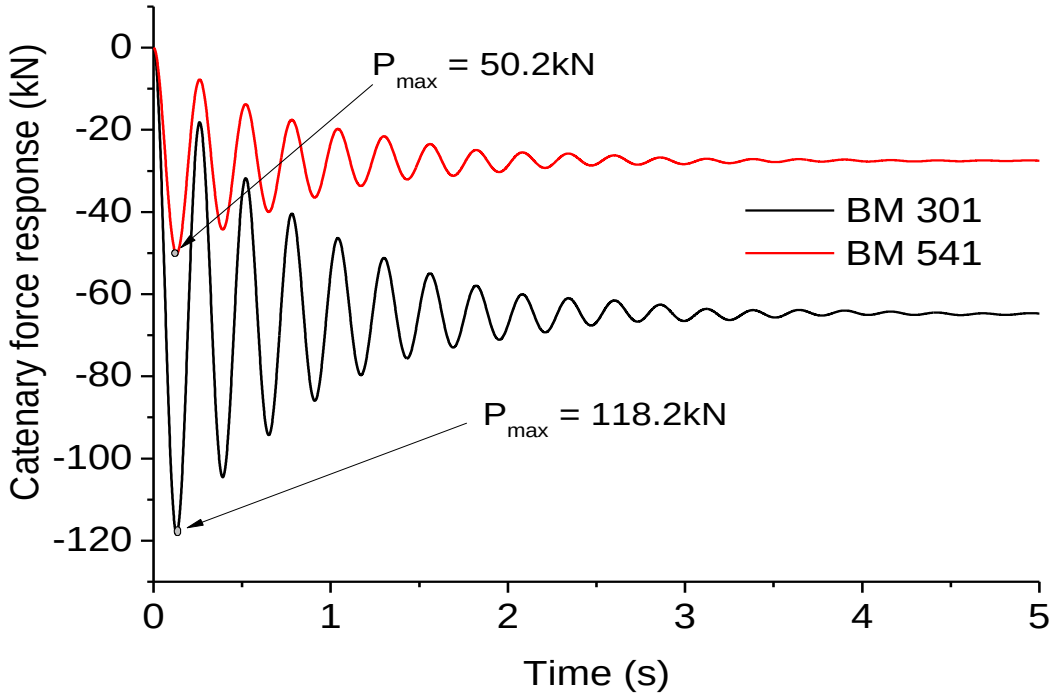

Figure 5-11 BM catenary force response due to CCRS

The ratio of the dynamic response to the static response is 1.84 compared to 2.0 recommended in GSA 2003 design guidelines. The next plot presents the moment response of the columns (Col 11 and 61) as shown in Figure 5-12. This shows that Column 61 (Col 61) has a definite pattern with a stable frequency as compared to Column 11 (Col 11). The moment response of the Columns 11 and Column 61 under dynamic analysis is 59.71kNm and 110.2kNm respectively. The members stabilise to a static equilibrium state after four seconds.

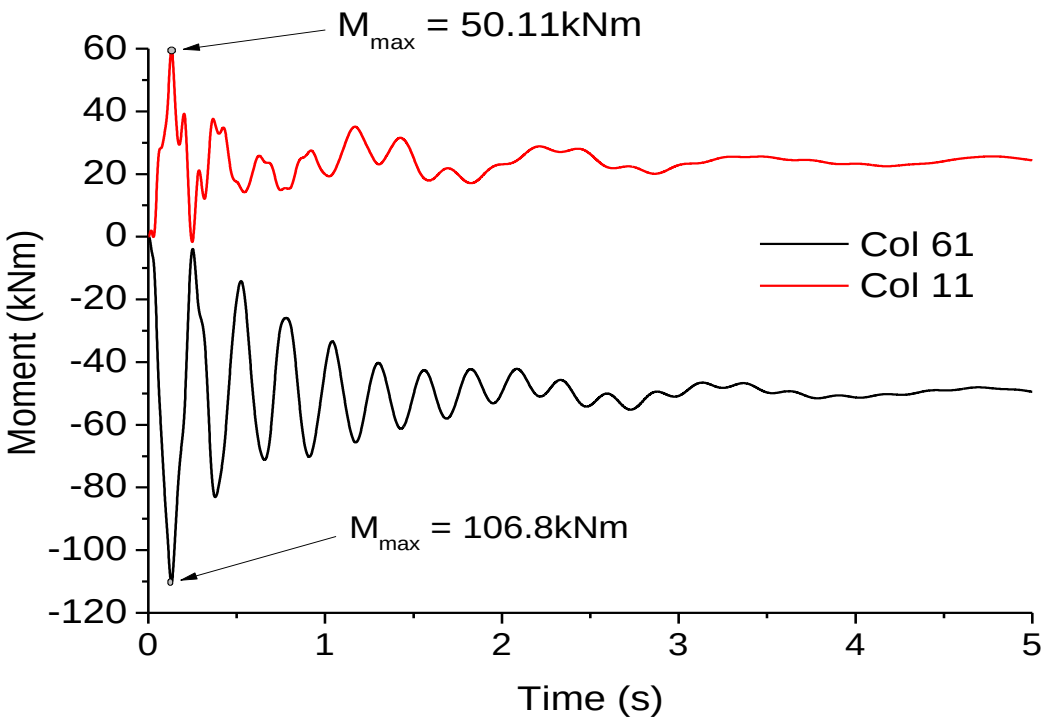

Figure 5-12 Force responses in columns due to CCRS

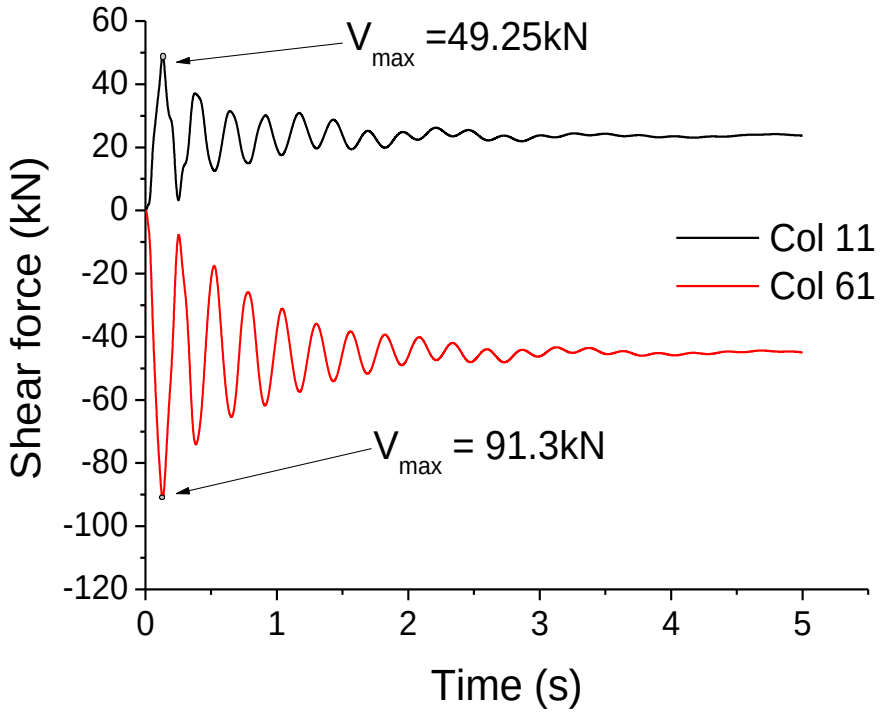

Figure 5-13 Shear force vs time in columns (CCRS)

The maximum shear force response occurs in Column 61 (Figure 5-13) with a value of 91.3kN while Column 11 has a shear force response of 49.25kN. This response later stabilises to a static response of 45.06kN and 23.61kN after four seconds for Columns 61 and Column 11 respectively. The shape of the dynamic responses for axial force has an irregular pattern and inconsistent up to 1.5s, thereafter a definite pattern is observed.

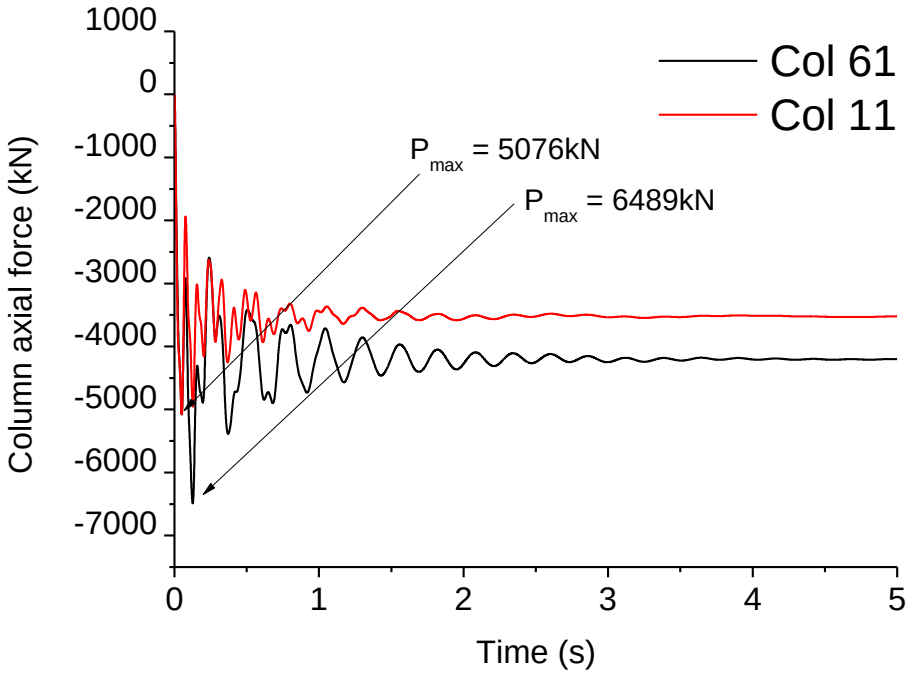

Figure 5-14 Axial force responses in columns due to CCRS

Figure 5-14 presents the axial force responses of Column 61 and Column 11 under dynamic loading condition. The maximum axial force response of the columns is 6489kN and 5076kN respectively. These forces stabilises to 4201.85kN and 3521kN respectively. The dynamic amplification factor for Column 61 and Column 11 is 1.55 and 1.44 respectively. The assessment for the CCRS shows that the most important changes in the internal force response in beams is the catenary action which results in a dynamic amplification factor (DAF) of 1.85. The dynamic effect on the moment responses of the columns bounding the removed column is insignificant. Using the axial force criterion, the DAF is 1.54. The shear force criterion in the column is the most important because the maximum DAF is 2.09, which occurs on the column (Col 11) at the short span. Based on this assessment, catenary force in beams and shear force in columns are the most important internal forces for progressive collapse. The next assessment determines the response of the connecting beam elements to the removed edge column and the brace response under sudden column loss.

5.5.2 Position two: NLD assessment due to ECRS

Edge beam responses

This subsection investigates the nonlinear dynamic assessment (NLD) of the structure under edge column removal scenario (ECRS). The structural members closely affected by the sudden removal of the perimeter column are BM 561, and BM 571 in the longitudinal direction and BM 421 in the transverse direction. The node of the removed column connects these beams at one end and Columns 21, Column 41 and Column 91 at the other end. The braces at the region of the removed columns are BR 793 and BR 794; these braces were assumed to resist lateral loads only at the conventional design stage. The responses of these elements mentioned are presented in subsequent plots below

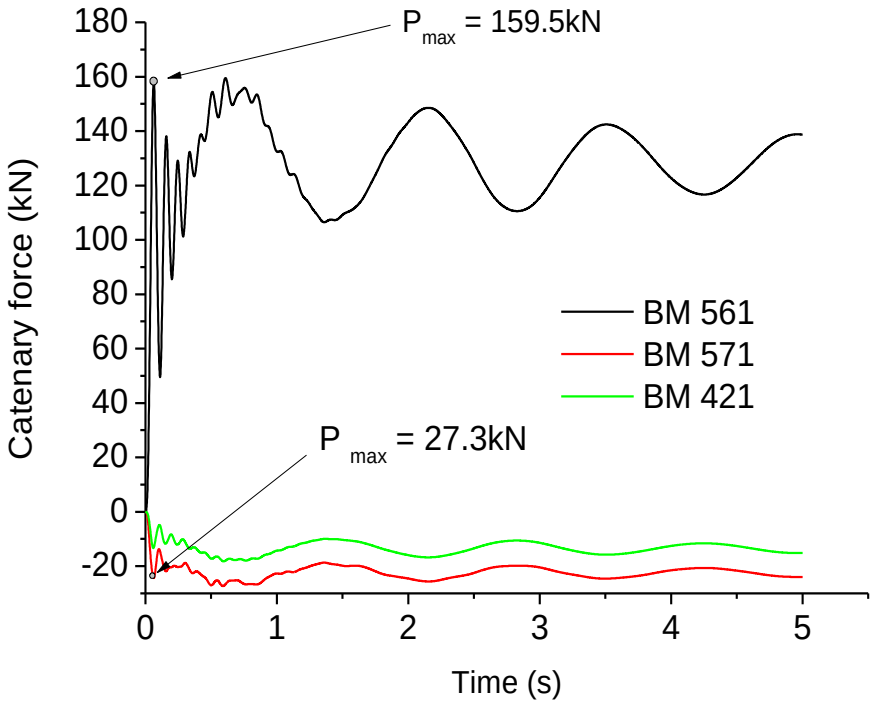

Figure 5-15 Catenary force response in beams

Figure 5-15 shows the catenary force response of the beams investigated under edge column removal scenario (ECRS). The maximum beam catenary force response occurs in Beam 561 (BM 561) with a maximum response of 159.5kN. This response is significant when compared to the recommended maximum tie force adopted in conventional design.

Brace frame responses

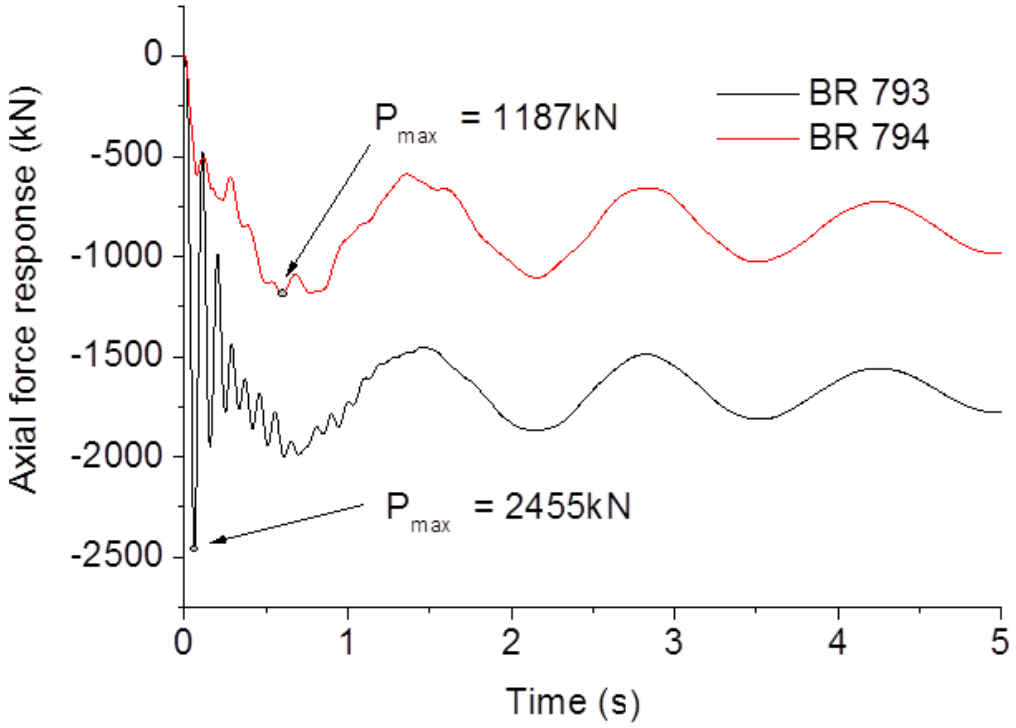

Figure 5-16 Axial force response of the brace members

Figure 5-16 presents the axial force response under sudden column removal scenario. The maximum axial force response in the cross bracing occurs in brace 793 (BR 793) with a value of 2455kN relative to Brace 793 having a response of 1187kN. Bracing provides an alternative path for load distribution under progressive collapse scenario. It was observed that Brace 793 (BR 793) increases by 955.3%, with a dynamic amplification factor of 1.47 and Brace 794 (BR 794) increases by 510.3% with a corresponding DAF of 1.38.

The dynamic effect of sudden column loss on brace response depends on the location of the bracing relative to the position of the removed column. Figure 5-17 presents the axial force responses in the columns bounding the removed column of the brace frame system (BFS). Maximum axial force response occurs in column 21 with an axial force of 8651kN which gradually stabilises to a static response of 4643.38kN after 2s. On the other hand, column 91 and column 41 has a maximum response of 7394kN and 4316kN respectively which stabilises after 2s to a static response of 4484.4kN and 3104.84kN respectively.

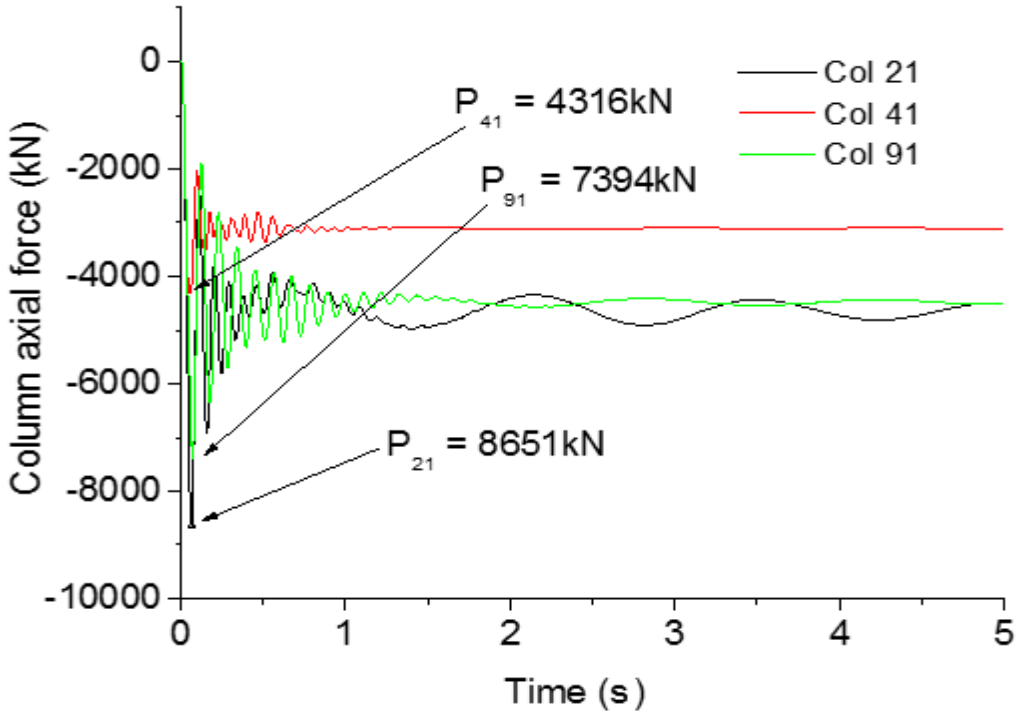

Figure 5-17 Axial force responses of columns due to ECRS

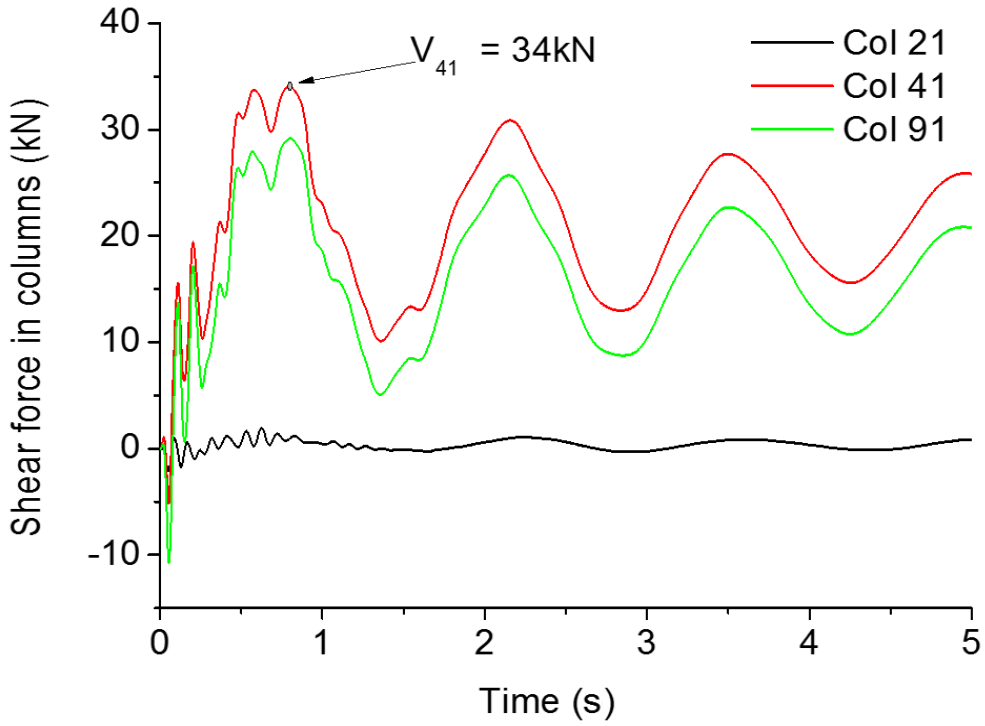

Figure 5-18 Column shear force response of BFS

Figure 5-18 shows that the maximum dynamic shear force response of the columns occurs at column 41 with a value of 34kN relative to its static response of 21.01kN. This implies an

increase of 38.2% which is a consequent of the dynamic response as a result of the sudden column loss. The shear force at these columns is significantly reduced due to the effect of the bracing system.

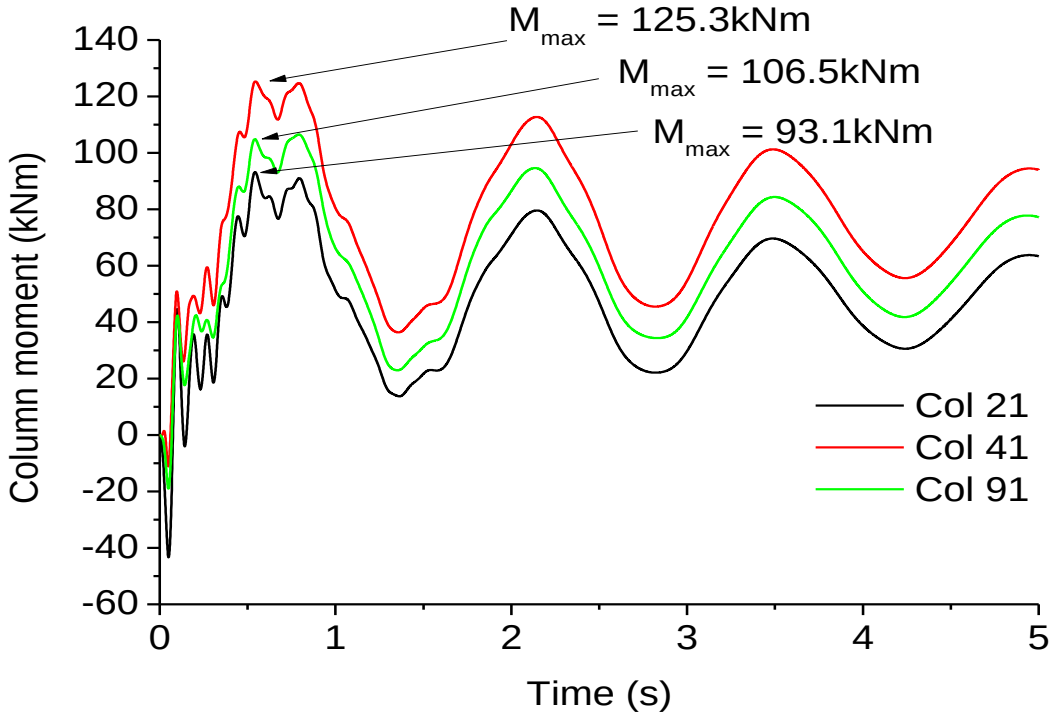

Figure 5-19 Moment response in columns due to ECRS

Figure 5-19 presents the dynamic moment response of the columns connecting the edge column removal scenario (ECRS). The columns connecting the ends of beams 561 and 571 along the long span are Columns 21 and Column 41. The removed column is located between these columns is labelled as 31. The maximum response of Column 41 is 125.3kNm which occurs at 0.5s relative to the static response of the columns which is 70.92kNm. Using the maximum moment response in the columns, the dynamic amplification response for Column 41 is 1.8 as compared to the 2.0 recommended in the design guideline.

In conclusion of the assessment of ECRS, bracing provides an alternative path for load redistribution under progressive collapse scenario. The location of the bracing significantly influences catenary force development in beams, thereby limiting the tensile force response of the beam-column connection. The dynamic amplification factor (DAF) response based on the change in catenary force is approximately 1.25, which is attributed to the bracing effect. On the other hand, the DAF based on the shear force criterion in the columns is 1.62 and that for the moment criterion is approximately 2.07. For these studies, the moment

response criterion in columns is the dominant assessment criterion for the DAF while the catenary force is the dominant factor for the beams.

5.5.3 Position three: NLD assessment due to ICRS

This subsection investigates the behaviour of the structure under interior column removal scenario. A tiled view of the model showing the response of the structure and the structural labels in the transverse and longitudinal planes is shown in Figure 5-20.

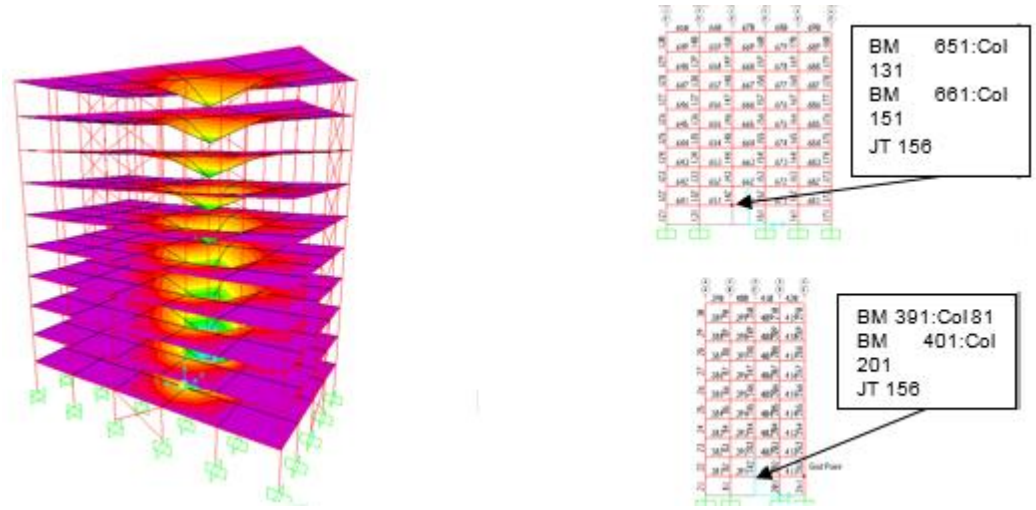

Figure 5-20 Deformed shape and elevation planes due to ICRS

From Figure 5-20, the interior joint is labelled as 156 (JT 156). Along the longitudinal direction (Long span), as shown in the top right corner of Figure 5-20, the joint of the removed column is connected to Beam 651 and Beam 661. These beams at one end are connected to Columns 131 and Columns 151 respectively. Along the transverse direction, the joint of the removed column (Jt 156) as shown in Figure 5-20 is connected to beam 391 and beam 401. These beams are connected to column 81 and column 201 respectively. The 3D elevation at the left hand corner shows the stresses developed due to the interior column removal scenario (ICRS).

The objective of this investigation is to assess the redistribution of forces in these members due to the sudden loss of the interior column (Col 41). The assessment order at which the investigation was carried out is as follows: slab, beams, columns and joints. Before the assessment of the slab, a brief description of the stresses in the shell is presented and the sign convention briefly described. The assessment of the slab is focused on the maximum principal stresses developed at the top and bottom face of the slab, which is modelled as a

shell and its redistribution along the storey height. In addition, the assessment of the slab includes an evaluation of the dynamic amplification factor using the maximum principal stress at the top and bottom surface of the slab and the maximum shear stress developed.

Since catenary effects is the most important consideration in evaluating joint and beam responses under progressive collapse, the catenary force developed in all the beams connecting the node of the removed column will be compared and assessed. Nonetheless, the columns would be evaluated for the axial force response, shear force response and moment response. All the columns (Col 81, Col 201, Col 131, and Col 151) bounded to the removed column via the beams will be compared for axial force response and maximum shear force response. Finally, since GSA 2003 recommends a dynamic amplification factor of 2.0., the assessment will check the dynamic amplification factor using the axial force response criterion, the shear force response criterion, and the moment response criterion with a view of proposing a dynamic amplification factor for each type of structural member under progressive collapse scenario. The next subsection presents a brief description of the slab stresses and the response of the panels at each floor along the storey height of the slab.

Slab Response under Progressive Collapse Scenario

As shown in Figure 5-21 the numbers 1, 2 and 3 describe the local axis of the shell in a direction perpendicular to the positive face.

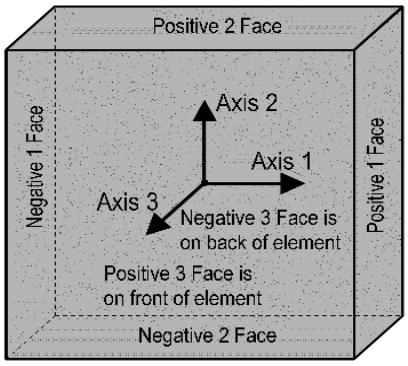

Figure 5-21 Shell element stress convention SAP 2000)

The shell stresses as defined in the user manual (SAP 2000) are S11, S22, S12, S13 and S23. S12 and S21 are expected to have the same value as stated in SAP 2000 user manual. Stress S11 acts normal to the positive face 1 and acting along the direction of the local axis 1.

Similarly, S22 acts normal to face 2 of the shell element and along the direction of the local axis 2. The shell stresses based on SAP 2000 is presented in Figure 5-22.

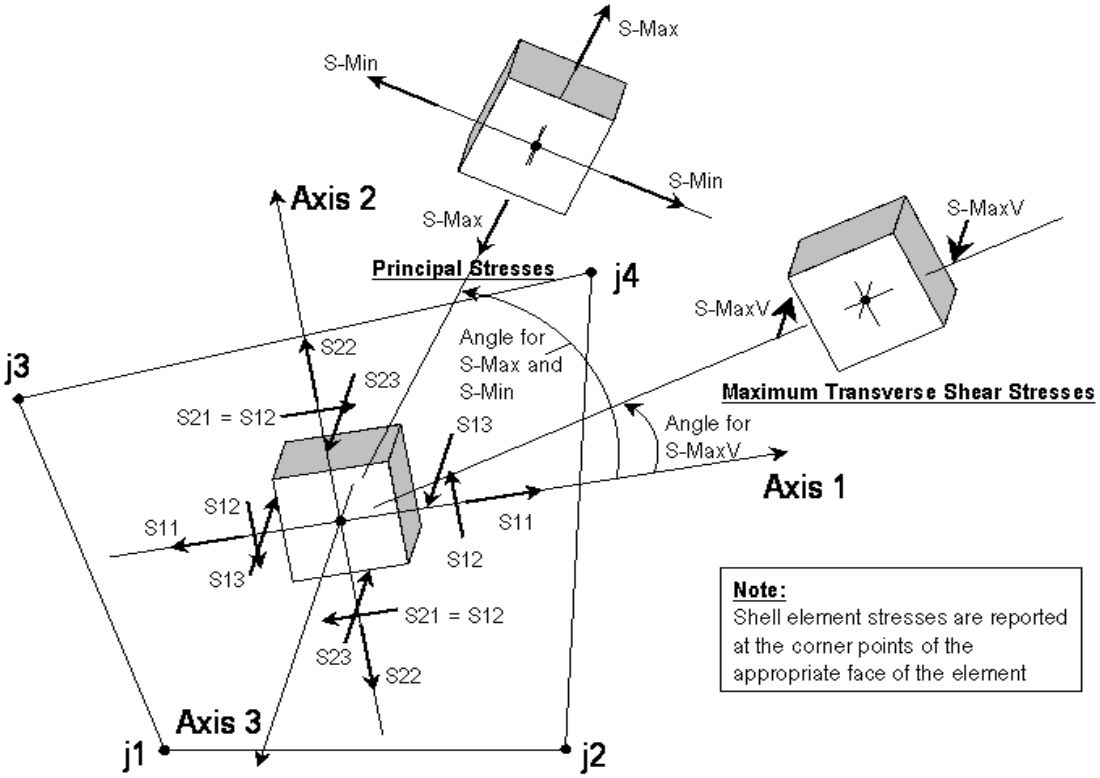

Figure 5-22 SAP 2000 stress definition along a shell (SAP 2000)

Table 5-5 is the stress redistribution at different storey height. The studies shows that the stress at the bottom of the shell is more critical as compared to the stress developed at the top of the shell. From the left, the first column is the storey height of the building, the next two columns represent the shell principal stresses at the top and bottom (S-Max(t), S-Max(b)) while the fourth column represents the maximum shear stress (S-MaxV).

Table 5-5 Stress redistribution and DAF for shell assessment

H (m)	S-Max (t) N/mm²	S-Max(b) N/mm²	S-MaxV N/mm²	DT N/mm²	DB N/mm²	DS-MaxV N/mm²	DAF-v	DAF-t	DAF-b
0	0	0	0	0	0	0	0	0	0
3.5	25.32	37.98	0.365	49.8	74.3	0.720	1.97	1.97	1.96
7	24.4	36.45	0.353	49.32	73.12	0.709	2.01	2.02	2.01
10.5	23.47	34.85	0.337	48.62	71.51	0.683	2.03	2.07	2.05
14	22.55	33.05	0.318	47.83	69.37	0.671	2.11	2.12	2.10
17.5	21.55	31.22	0.299	46.95	67.26	0.647	2.16	2.18	2.15
21	20.95	30.17	0.289	46.68	66.48	0.640	2.21	2.23	2.20
24.5	20.05	29.47	0.282	46.57	66.17	0.638	2.26	2.32	2.25
28	19.72	27.64	0.262	45.57	63.23	0.604	2.31	2.31	2.29
31.5	18.17	24.87	0.229	43.62	58.91	0.549	2.40	2.40	2.37
35	17.35	23.32	0.211	42.46	56.38	0.519	2.46	2.45	2.42

The fifth, sixth and seventh columns (DT, DB, DS-MaxV) represents the shell dynamic response at the top and bottom and the shear respectively. The last three columns are the dynamic amplification factor using the shear force criterion, the shell stresses at the top and bottom respectively. Increase in the number of storey height reduces the magnitude of the stress developed in the shells at that storey level. In Figure 5-23, an approximate linear correlation between the dynamic amplification factor and the principal shell stresses in slabs is presented. The derived regression equation, $Y = 1.913 + 0.054X$, where Y is the dynamic amplification factor and X is the number of storeys approximately predicts the dynamic amplification factor at any given floor.

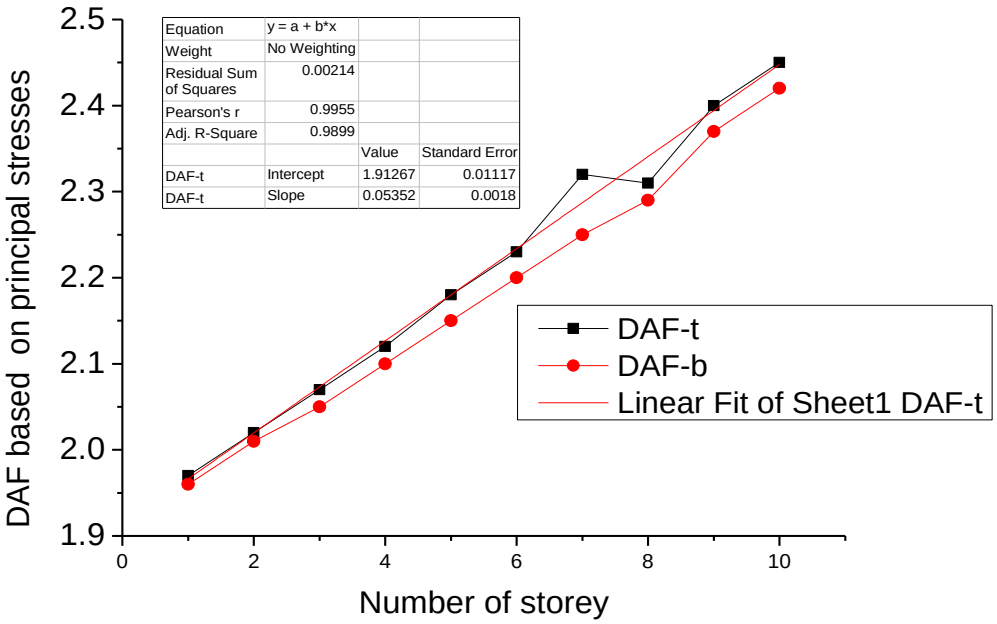

Figure 5-23 DAF vs number of storey using shell stresses

The loss of an interior column (Frame 141) located on grid 3-C on the floor plan affects the connecting beams (651 and 661) along the long span as well as Beam 391 and Beam 401 along the short span. These beams are connected to Column 131 and Column 151 along the long span, and Column 81 and Column 201 along the short span. Due to sudden loss of Frame 141, the changes in the internal forces of these elements are assessed as presented in subsequent subsections.

Beam response due to ICRS

Two response criteria are considered for the beams under interior column removal scenario (ICRS): catenary force response and shear force response. As shown in Figure 5-24, the maximum catenary force response is 98.33kN which occurs in Beam 401 along the short span. Along the long span, the maximum catenary force response is 46.23kN in Beams 651 and Beam 661.

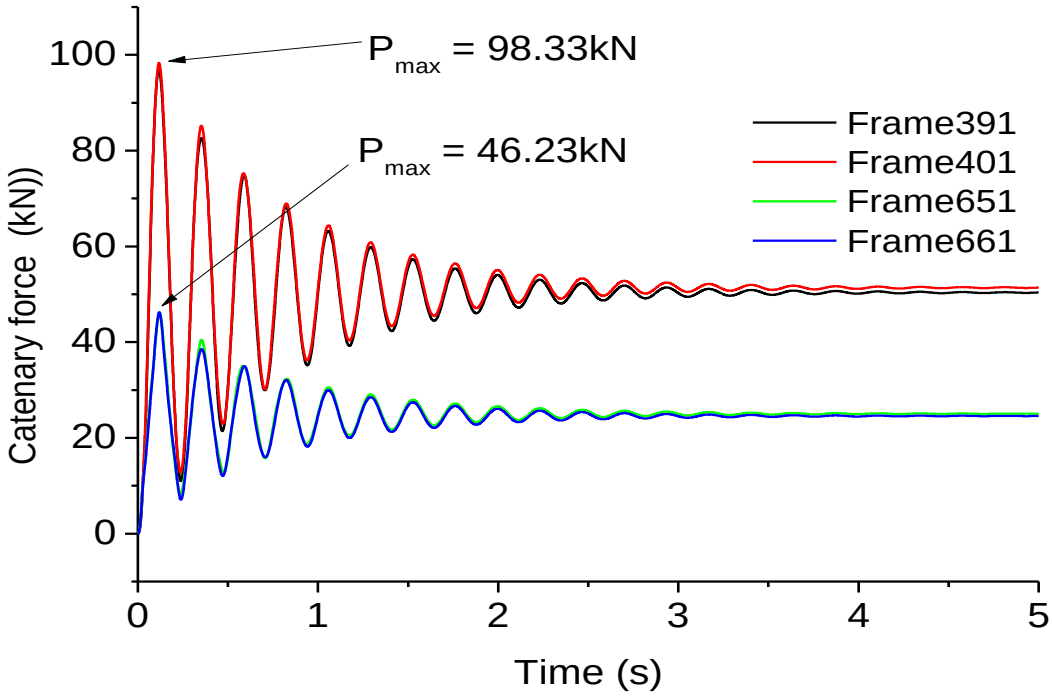

Figure 5-24 Catenary force response due to ICRS

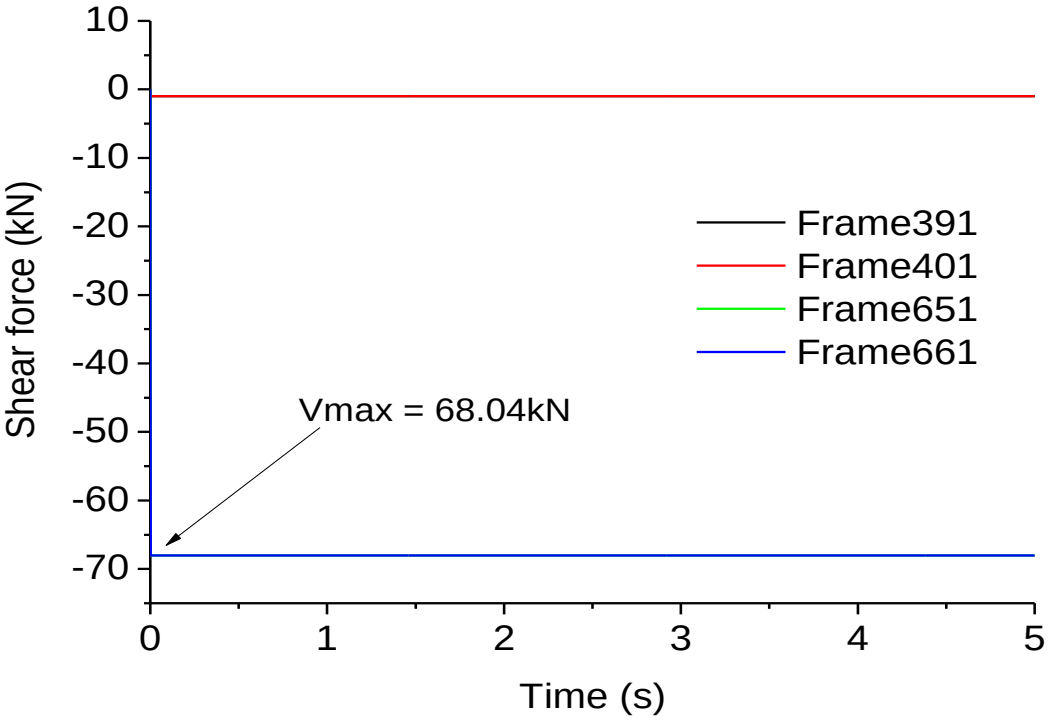

Figure 5-25 Shear force response due to ICRS

The catenary force response can be compared with the internal ties provision in Eurocode 1 EN1991-1-7 as shown in Equation 5-1

$$T_i = 0.8(g_k + \varphi q_k)sL \; or \; 75kN \qquad 5\text{-}1$$

Where T_i is the internal tie force, g_k is the gravity load and q_k is the imposed load, s is the spacing of the ties and L is the span of the ties. Using this expression and comparing it with the minimum accidental tensile load of 75kN, the design tensile accidental force is 123.12kN while the catenary force developed in the beams is 98.33kN. The design tie force of 123.12kN exceeds the catenary force in the interior beam responses by a maximum of 20.13%.

The maximum shear force response occurs in beams 651 and 661 along the long span, with a maximum response of 68.04kN at 0.002s corresponding to the column removal time. However, there is negligible shear response in the tie beams (Beam 391 and Beam 401) along the short span of the removed column.

To summarise the internal beam response under progressive collapse scenario, the most important internal force response in beams is the catenary force response. Using this response criterion, relative comparison of the nonlinear static response to the nonlinear dynamic response is 1.91. This is 4.5% less than the recommendation in GSA 2003. The maximum catenary force response of the beams connecting the removed interior column is 98.33kN. The following section presents column responses under interior column removal scenario. Changes in the internal force response (axial, shear and moment) of the columns around the interior removed column are presented.

Column response due to ICRS

Figure 5-26 is the axial force response of the column members adjacent to the node of the ICRS. The maximum axial force response in columns occurs in Column 201 which has an axial force response of 8539kN and Column 81 which is the column along the short span of the removed column. The axial force response stabilises to a static condition after 2.5s. Comparing the static and dynamic responses in Column 81 and Column 201. It was observed that the dynamic amplification factor is 1.5. For Columns 131 and Column 151, a dynamic amplification factor of 1.56 and 1.59 is observed respectively.

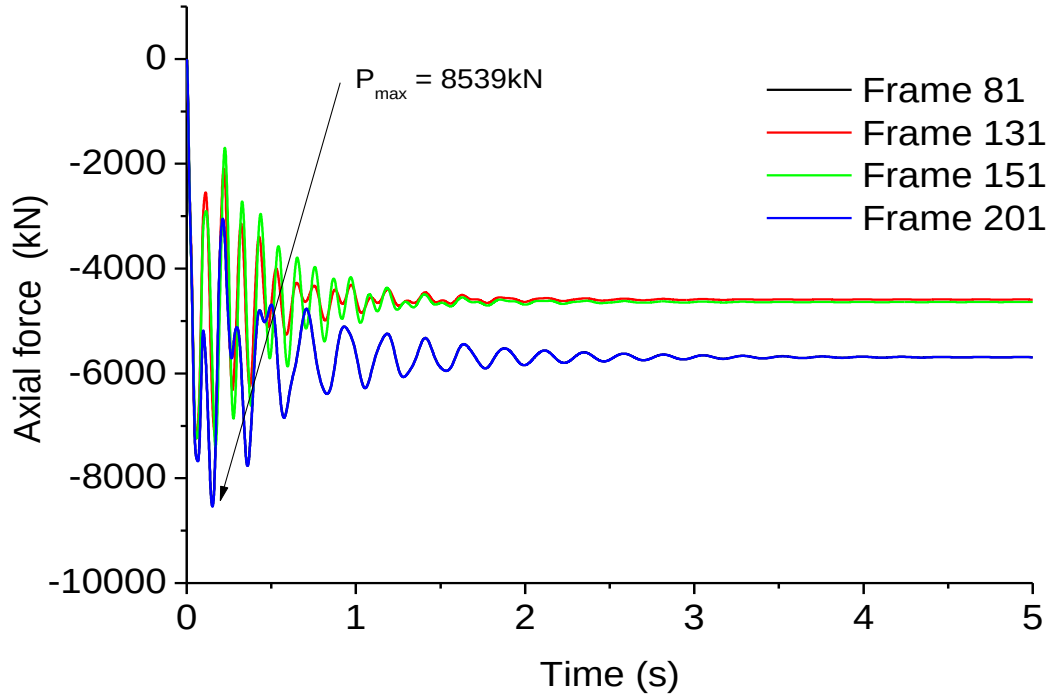

Figure 5-26 Axial force response in columns due to ICRS

:

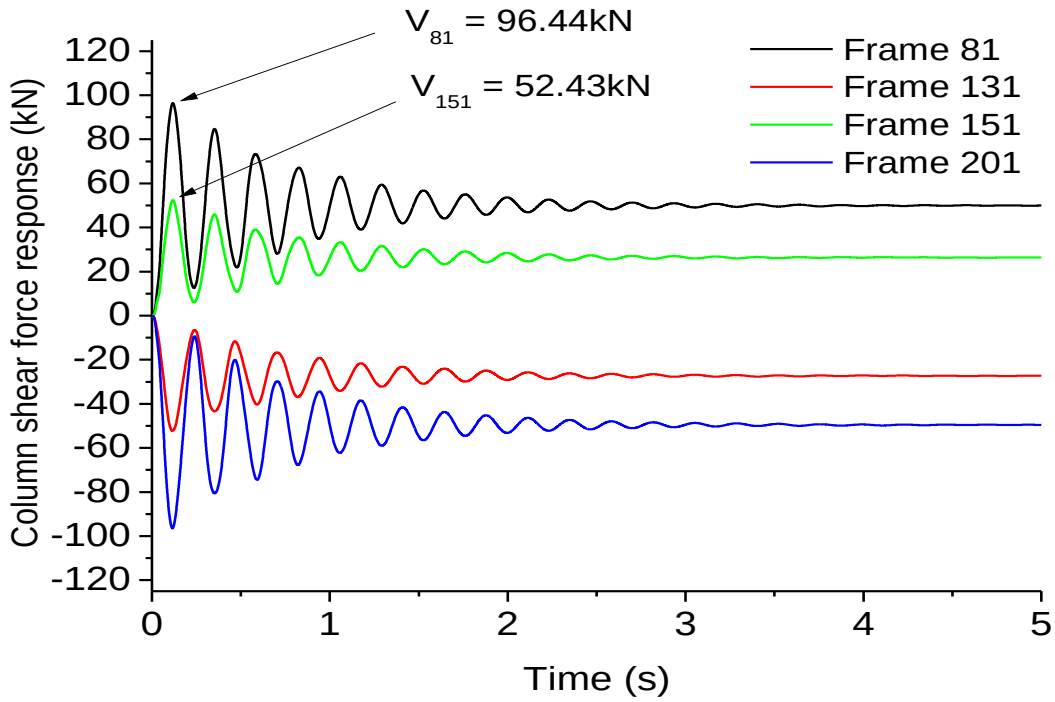

Figure 5-27 Shear force response in columns due to ICRS

The shear force response of the columns linking the beams connecting the removed interior column is presented in Figure 5-27. The maximum shear force response occurs in Frame 81

and Frame 201, which act in opposite direction. A similar behaviour is exhibited in Frame 151 and Frame 131. The maximum dynamic response in frames 81, 201, 151 and 131 are 96.44kN, 52.27kN, 96.55kN and 52.27kN respectively. Comparing the columns on the short span (Frame 81 and Frame 201), the dynamic amplification factor based on the shear force criterion is 1.93; however, when columns (Frame 131 and Frame 151) are compared, the dynamic amplification factor is 1.92. This studies shows that there is a consistent response on the dynamic amplification factor using the shear force criterion for the columns along the short span as well as the long span.

The next plot (Figure 5-28) presents the moment response of the columns as a result of the internal column loss scenario (ICRS). The columns along the short span of the removed column are Frame 81 and Frame 201, while Frame 131 and Frame 151 are on the long span of the removed column. As shown on the plot of Figure 5-28, the maximum moment responses of the columns along the short span are 111.1kNm while the maximum moment response along span is 55.72kNm.

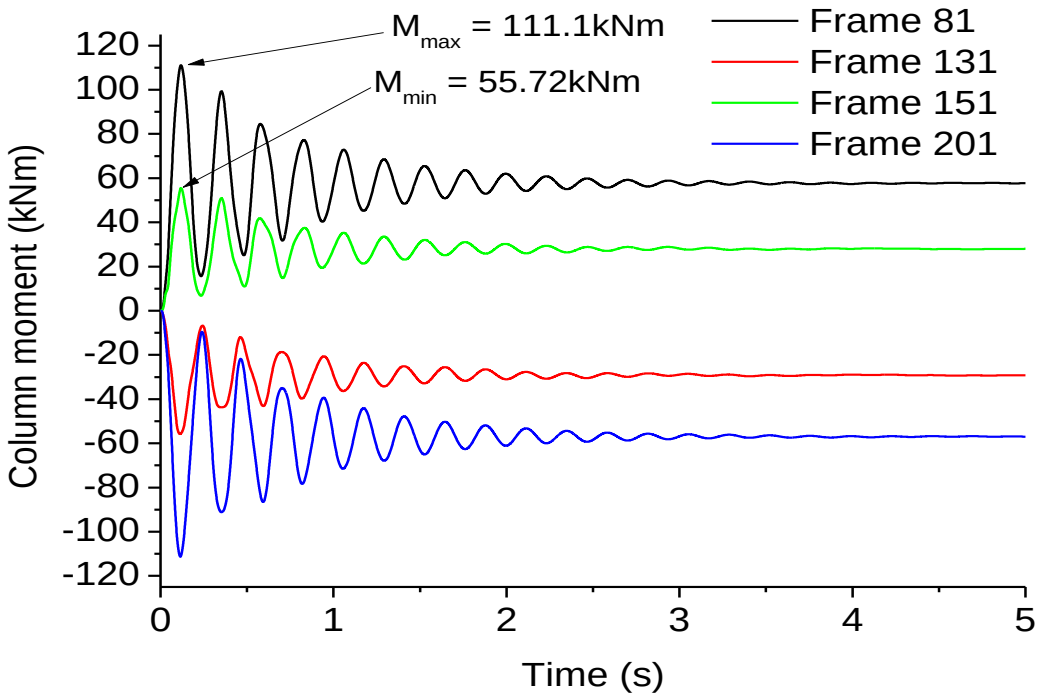

Figure 5-28 Moment response in interior columns due to ICRS

This study shows that the moment criterion used for the dynamic amplification factor does not captures the dynamic response, therefore the axial force and shear force response in

columns can be used to assess the dynamic amplification factor. The shear forces criterion is the most critical relative to the axial force response.

In conclusion for the ICRS, it was observed that the dynamic amplification factor (DAF) based on the catenary force response is 1.93; based on the axial force response criterion in columns, it is 1.5, based on the shear force criterion in columns, it is 1.99 (Col 151). The dynamic effect on the moment response is insignificant. Consequently, this study shows that catenary force response in beams and shear force response in columns are the two key features affected by sudden column loss. The next assessment presents the response of the structure at the eighth floor column removal scenario (EFCRS).

5.5.4 Position four: NLD assessment due to EFCRS

The deformed shape and member descriptions to be investigated are shown in Figure 5-29. The beam connecting the removed columns along the long span is beam 548 which is connected to column 18 at its end. On the transverse direction, beam 308 connects the node of the removed column at one end and column 68 at the other end. Above the node of the removed column (JT 9), the three slab panels would be assessed for the redistribution of principal and shear stresses, and the maximum dynamic amplification factor.

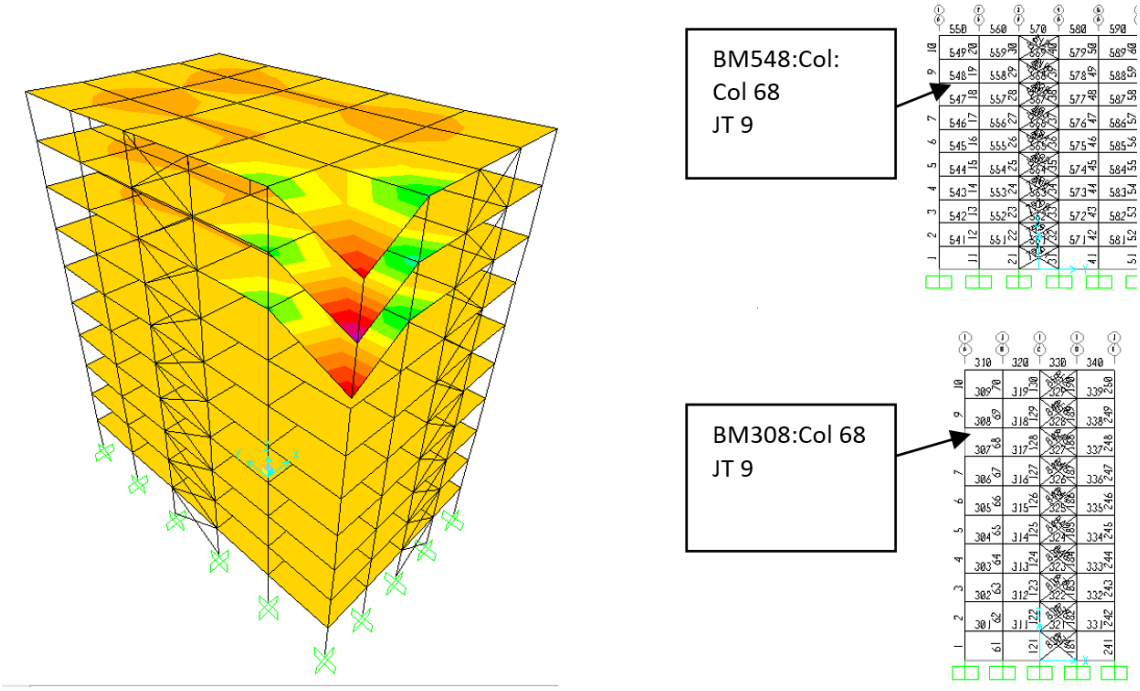

Figure 5-29 Stress distribution and label description under ECRS

The order at which the investigation was carried began with the slab response by considering the panels (141, 161, 181) above the removed column, followed by changes in the stress

redistribution in the beams (BM 308, 548) connecting the removed column, and finally the columns connected to the other end of the beam (Col 18 ,68). Panel 141 corresponds the first panel just above the removed column at the eight floor, panel 161 corresponds to the panel of the slab at the 9th floor while panel 181 is the top most panel at the 10th floor.

The slab response to sudden dynamic response of the structure for principal stresses at the top and bottom of the shell and shear stresses is presented below. The three panels of the slab above the removed column are panel 141, 161 and 181 respectively. Using the maximum principal shell stresses at the top surface of the shell (SMax), sudden removal of the eight floor column shows that the mid panel (Panel 161) is relatively more stressed as compared to panel 141 and 181. The response of panel 141 exceeds panel 181 by 11% while panel 161 exceeds the response of panel 141 and 181 by 27.8% and 35.9% respectively. Figure 5-30 and Figure 5-31 presents the principal stresses at the top and bottom surface of the panel due to EFCRS respectively.

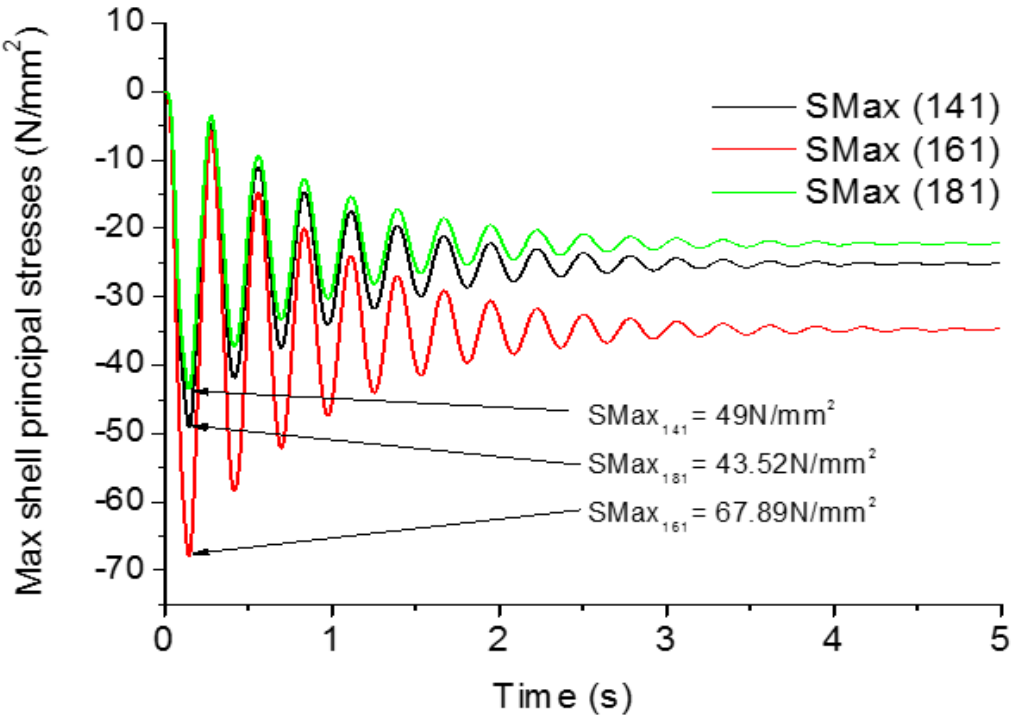

Figure 5-30 Principal stresses vs time at top of shell

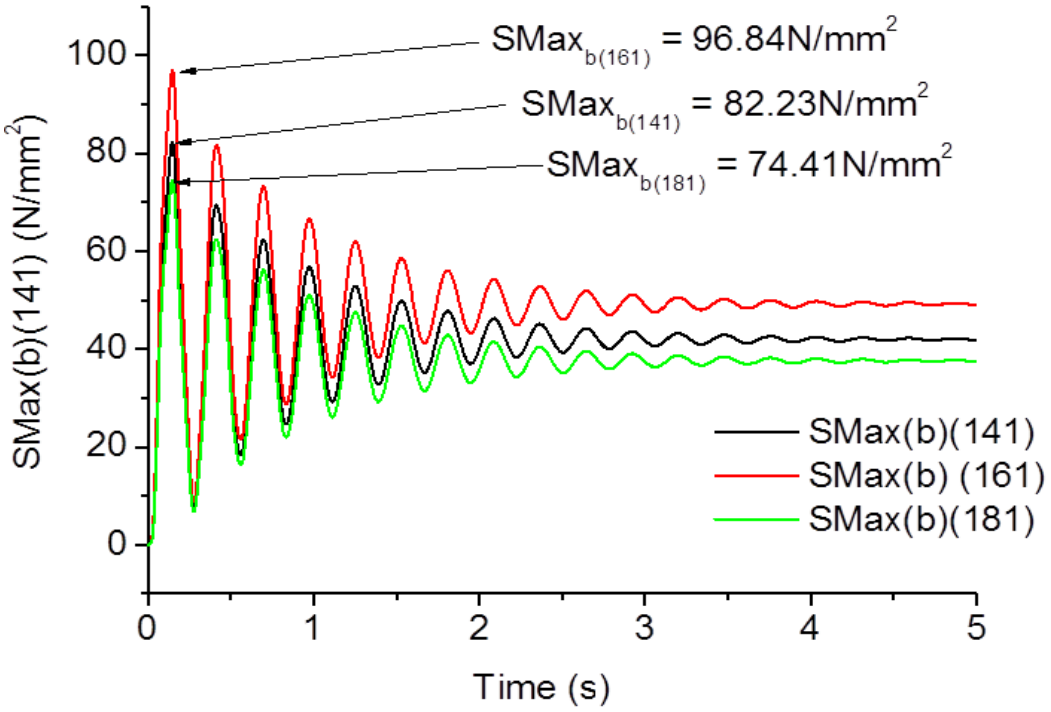

Figure 5-31 Principal stresses vs time at bottom of shell

It is observed that the middle panel response (Panel 161) exceeds panel 141 just above the node of the removed column and panel 181 at the topmost floor by 23.1% and 23.2% respectively. Panel 141 exceeds the response of panel 181 by 9.5%. This investigation shows that the maximum panel response either using the top or bottom principal stress response shows that the mid panel is more stressed relative to the panel just above the node and the topmost panel based on the principal stress response criteria. However, to further ascertain this assertion, the checks were extended to the shear force response of the panels as shown in subsequent plots.

Figure 5-32 presents the maximum shear force response of the panels just above the removed eight floor column. As shown on the plots, the maximum shear force response occurs at the mid panel (Panel 161) with a maximum shear force response of 0.96N/mm^2. This response exceeds the response of panel 141 by 15.6% and 26% respectively. Although, comparing panel 141 and 181, panel 141 just above the removed column exceeds panel 181 at the topmost floor by 12.3%. A summary of the shell responses is presented in table to evaluate the dynamic amplification factor based on the shell responses.

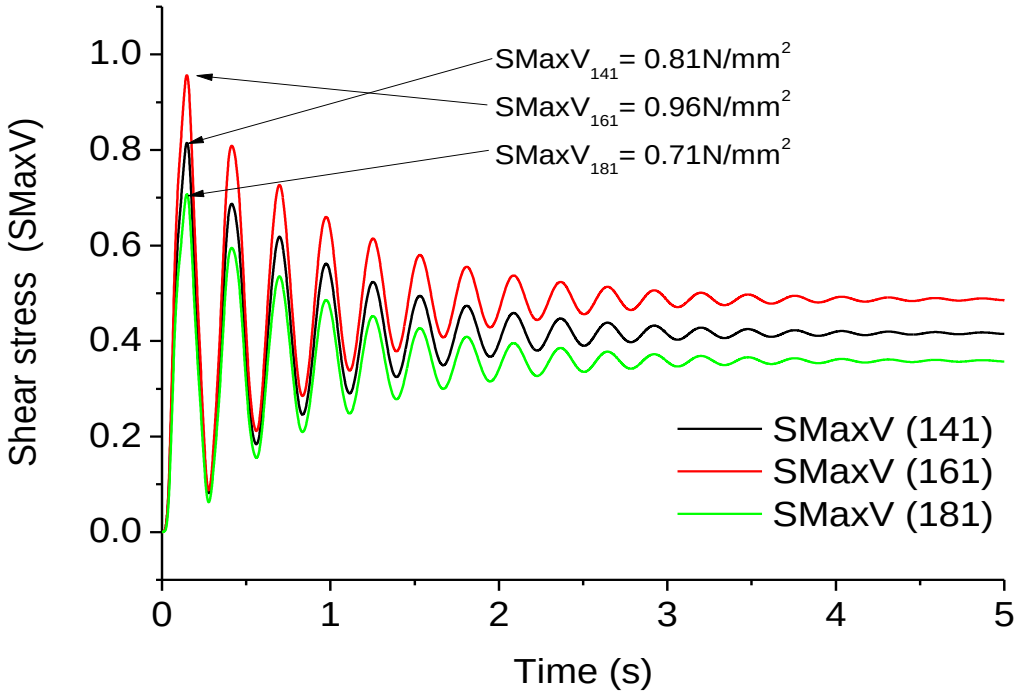

Figure 5-32 Principal shear stresses vs time at shell top surface

Computing the dynamic amplification factor (DAF) using the principal stress criteria and the shear stress criteria, a range of 1.95 to 2.01 was obtained as shown in Table 5-6. The mean DAF is 1.97 with a standard deviation of 0.02.

Table 5-6 Stress redistribution of shells due to EFCRS

H (m)	S-Max (t) N/mm²	S-Max(b) N/mm²	S-MaxV N/mm²	DT N/mm²	DB N/mm²	DS-MaxV N/mm²	DAF-v	DAF-t	DAF-b
28	25.16	41.99	0.416	49	82.23	0.81	1.95	1.95	1.99
31.5	34.78	49.21	0.487	67.89	96.84	0.96	1.97	1.95	1.97
35	22.20	36.96	0.358	43.52	74.41	0.71	1.98	1.96	2.01

The subsequent assessment is based on the behaviour and response of beams to eight floor column removal scenario (EFCRS). The beams assessed as explained earlier are the beams connecting the node of the removed column (BM 584, 308) along the long span and the short span respectively. The beams are assessed for catenary force response criteria as shown below.

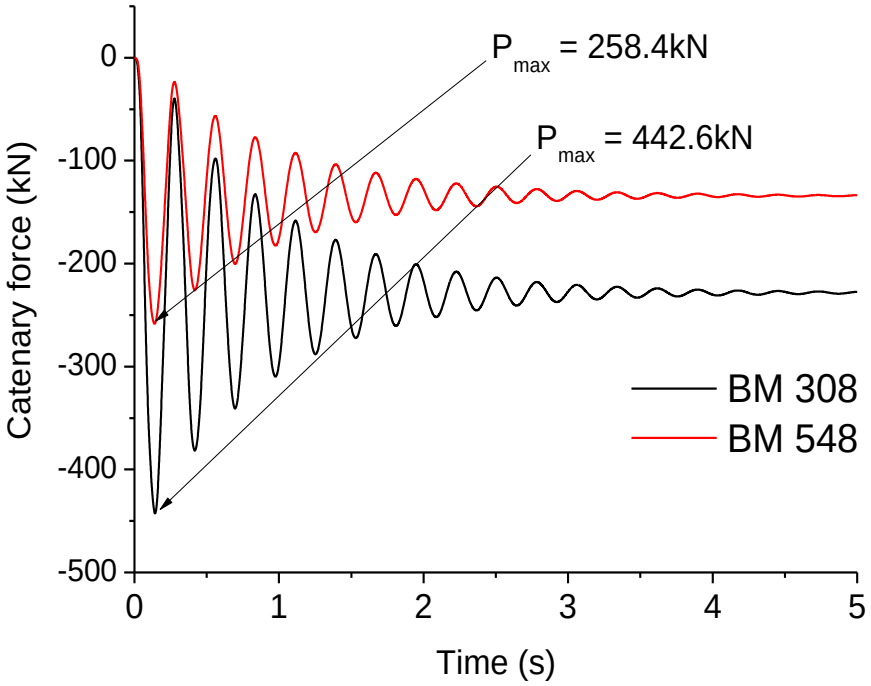

Figure 5-33 Catenary force (kN) vs time at EFCRS

The maximum catenary force response in the beams (BM 308 & BM 548) connecting the node of the removed column are beam are 442.6kN and 258.4kN respectively as shown in Figure 5-33. The ratio of the catenary force response at the short span to the long span is 1.71 which implies that the short beam significantly resist the removed column relative to the beam on the long side.

Using the catenary force response criteria, the dynamic amplification factor for beam 308 and 548 is 1.94 and 1.93 respectively. Using the maximum value of 1.94, it is observed that the recommendation in GSA 2003 is 2% conservative. The columns would be assessed for changes in the axial force response, moment and shear forces in relation to the corresponding static response of the structure. The axial force response, shear and moment are presented in that order in the subsequent plots. Figure 5-34 shows the axial force response of the columns connecting the ends of the beams along the long and short span of the structure. Col 68 which is located on the transverse direction has a maximum axial force response of 2083kN while column 18 has a maximum axial force response of 1670kN. Relatively, Col 68 on the shorter span of the removed column exceeds the response of the column on the longer span with 19.8%. The shear force response of the columns is presented in Figure 5-35.

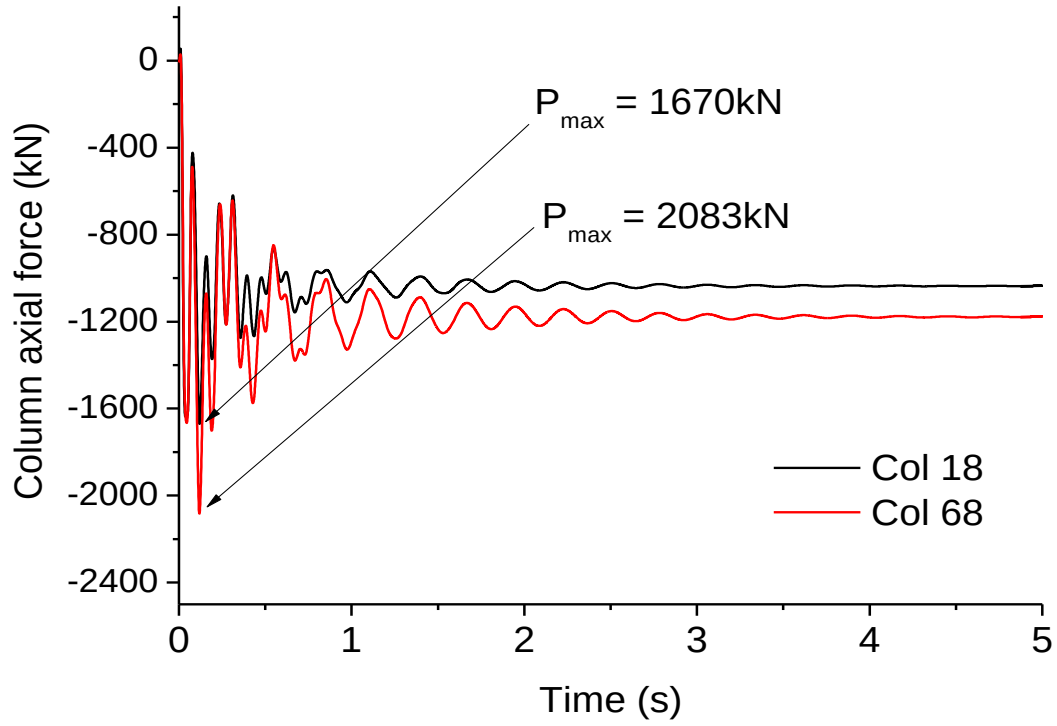

Figure 5-34 Column axial force (kN) vs time

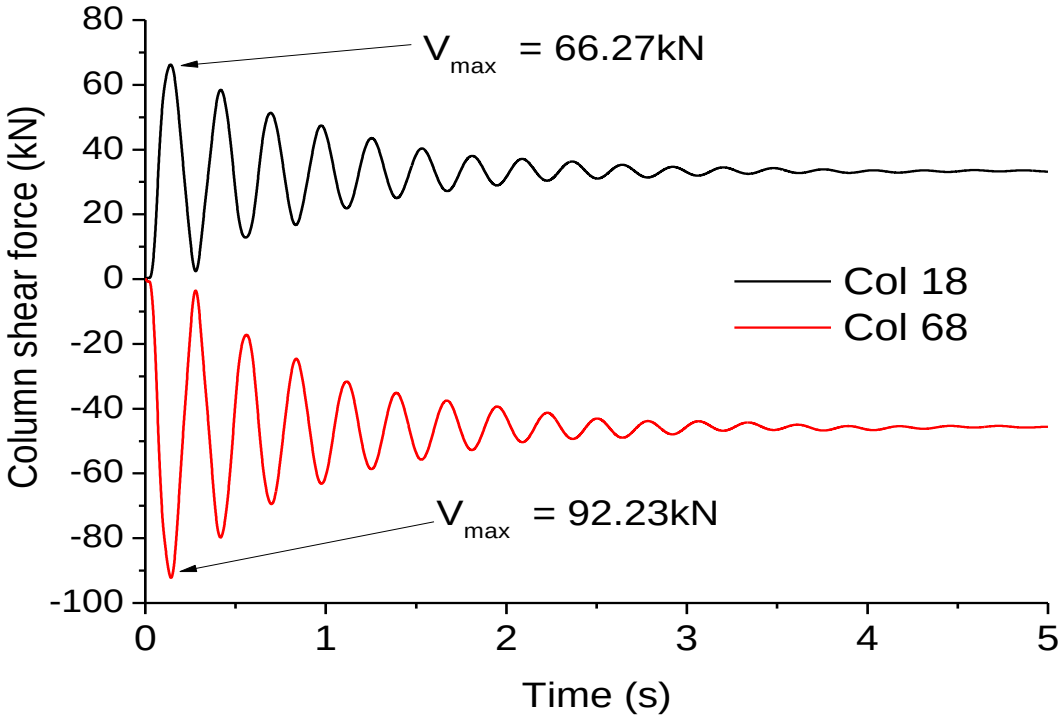

Figure 5-35 Column shear force (kN) vs time

The shear force response of the column 68 is 92.23kN while the shear force response of column 18 is 66.27kN. Comparing the response of the columns, column 68 on the short

span of the removed column exceeds the response of column 18 with 28.14%. Figure 5-36 presents the relative moment response of the columns.

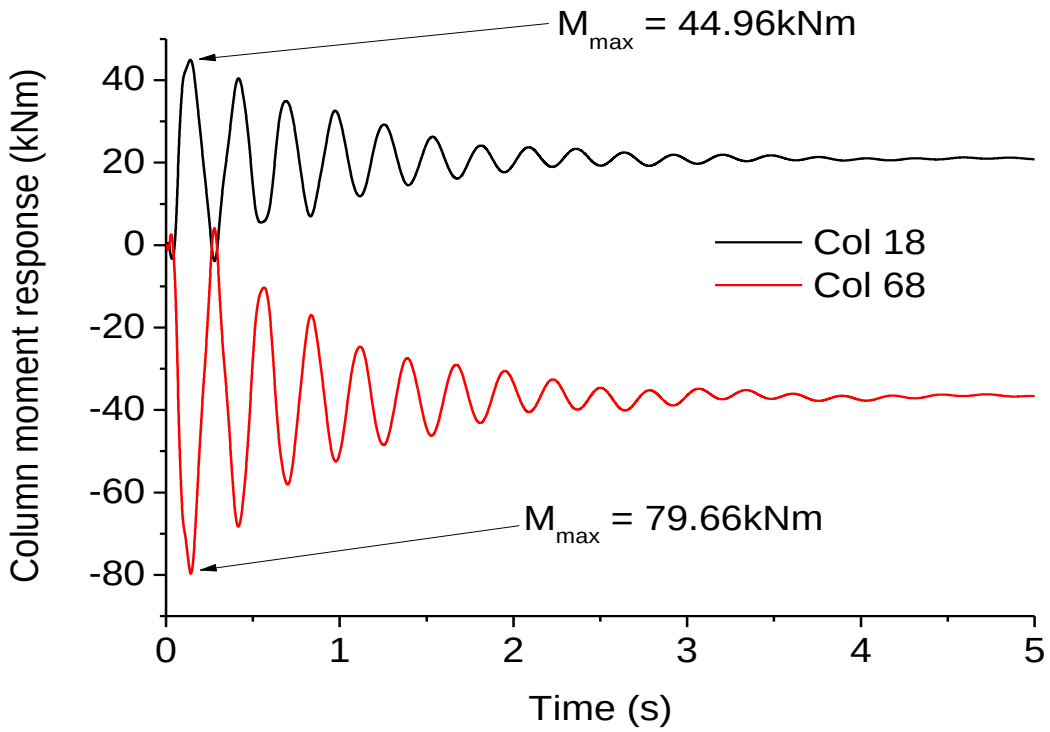

Figure 5-36 Column moment (kNm) vs time response

From observation, column 68 is more critical relative to column 18. The maximum moment response of column 68 is 79.66kNm while that of column 18 was 44.96kNm. This implies that column 68 along the short span of the column exceeds the response of column 18 along the long span with 43.56%.

Since joints are the most important unit in high rise steel structures, it is important to compare the joint responses under sudden column removal scenario. The joint displacement and rotational response are the two criteria used for this assessment and the responses are presented in Figure 3-37 and Figure 3-38. The maximum displacement response of the joints occurs at the eight floor column removal scenario with a maximum displacement of 265mm corresponding to a maximum rotation of 0.0419rads. The interior joint has a minimum displacement and rotational responses relative to the response at the eight floor and corner column removal scenario.

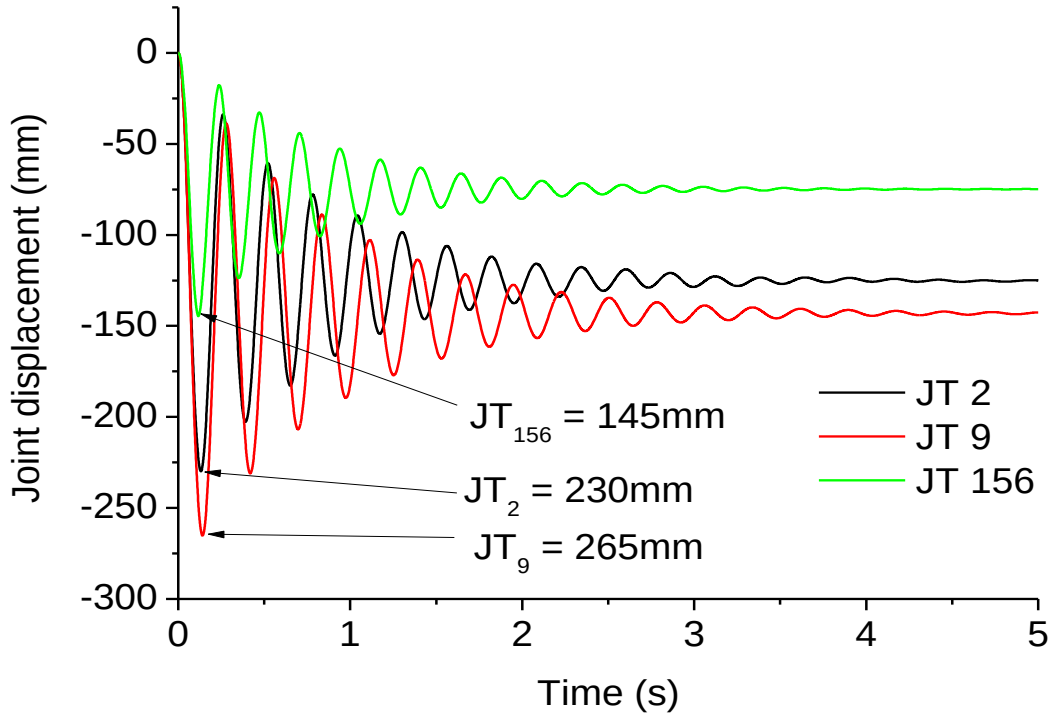

Figure 5-37 Maximum joint displacement (mm) vs time

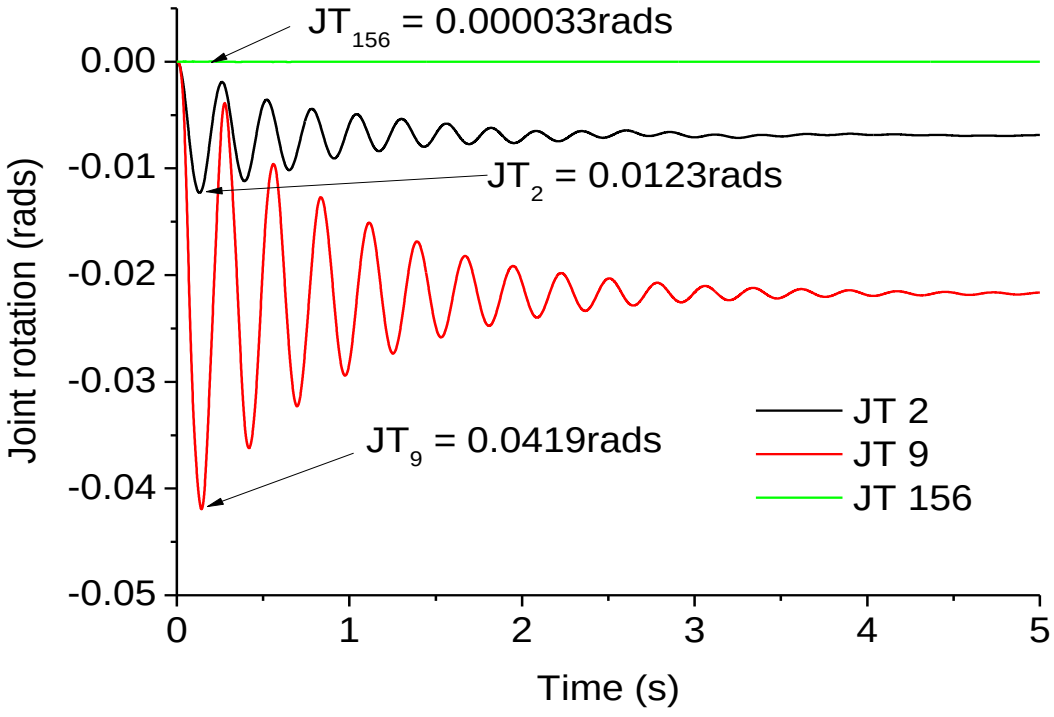

Figure 5-38 Maximum joint rotation (rads) vs time

Evaluating the dynamic amplification factor using the displacement response criteria at JT_9, it was observed that the dynamic amplification factor was 1.85 based on displacement

response and 1.93 based on rotational response. The dynamic amplification factor using the axial force response for columns 68 and 18 are 1.77 and 1.61 respectively.

In summary, at the eight floor column removal scenario it was observed that the most important internal force response in beams is the catenary effects which results to a DAF of 1.94. Using the column responses, it was observed that the shear force is the dominant internal force influence by dynamic effects. The DAF based on the maximum shear force response (Col 68) was 2.01. The next section assessed the response of the brace system to double column loss scenario.

5.6 Multiple column loss investigation

Critical abnormal loads could result in the loss of multiple columns; hence this section investigates the behaviour and response of steel structure to multiple column loss. The assessment will be restricted to the perimeter of the building since it has a potential to external attack relative to the interior of the structure.

5.6.1 Scope of investigation

Figure 5-39 shows the column removal location and the deformed state of the structure under double column removal scenario. Previous study shows that the beam response is the most important criterion, therefore this assessment is focused on the catenary force response. The beams assessed are Beam 541 and Beam 551 in the longitudinal direction of the structure and Beam 301 in the transverse direction. Along the short span, the ends of Beam 301 are connected to column 61 while on the long span, the ends of Beam 551 (BM 551) are connected to Column 21 (Col 21). These columns (Col 21 and Col 61) are evaluated with the columns (Col 2 and Col 12) just above the removed column.

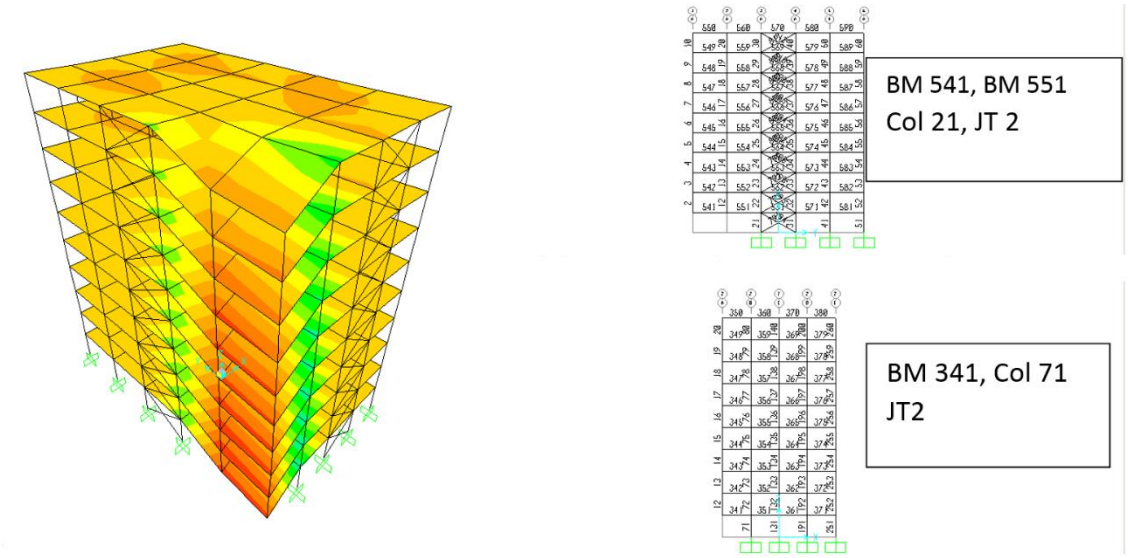

Figure 5-39 Description of model and case study

5.6.2 Catenary beam responses

The beam catenary force response is presented in Figure 5-40. From the assessment, the maximum catenary force response occurs at the short span of the structure. Beam 541 develops a catenary force response of 174.3kN, while the beam (BM 551) connecting it to the bounded column develops a catenary response of 39.8kN. In view of this response, the connection at the ends of Beam 551, showing an axial force response of 39.8kN, may likely not fail due to the catenary effect because it is expected that all connection types should be capable of transferring an axial tension of 75kN based on the provision of Eurocode 3.

Under double column removal scenario, (Col 2 and 12) have a maximum axial response of 434.12kN and 470.2kN respectively. The initial axial forces in these columns were 1715kN and 2762kN respectively. This implies that the loss of the columns beneath it resulted in 75% loss in its initial load for Column (Col 2) and an 83% loss in the axial force of Column 12 (Col 12).

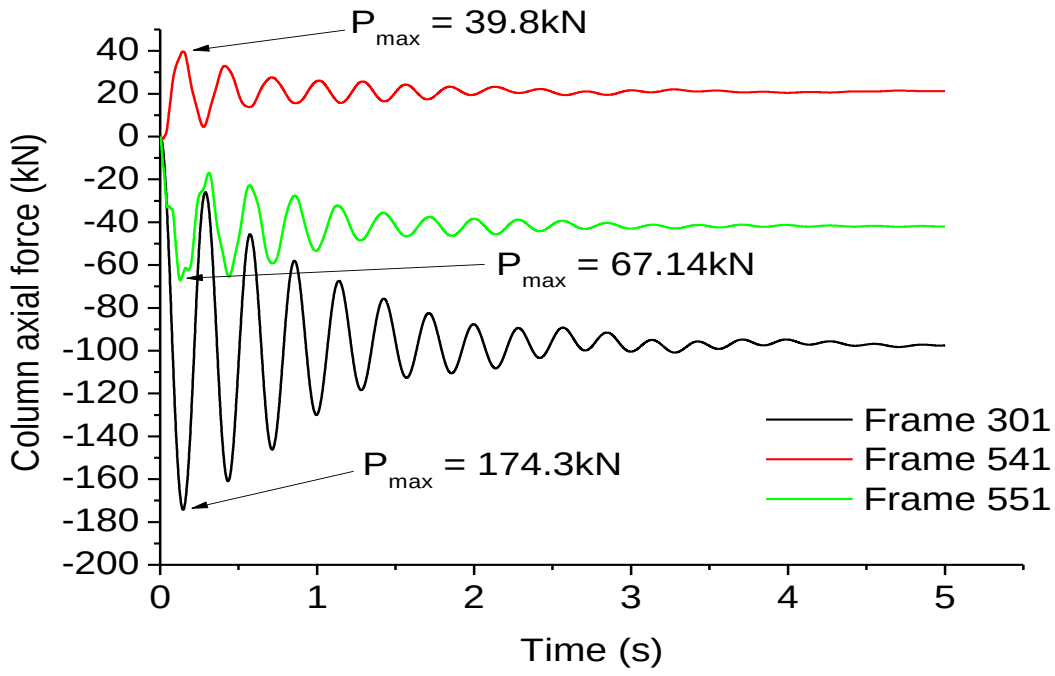

Figure 5-40 Catenary force responses under double column loss

5.6.3 Column responses

The columns just above the joints of the removed columns (Col 12 and Col 2) loss their ability to sustain gravity loads' as presented in Figure 5-41.

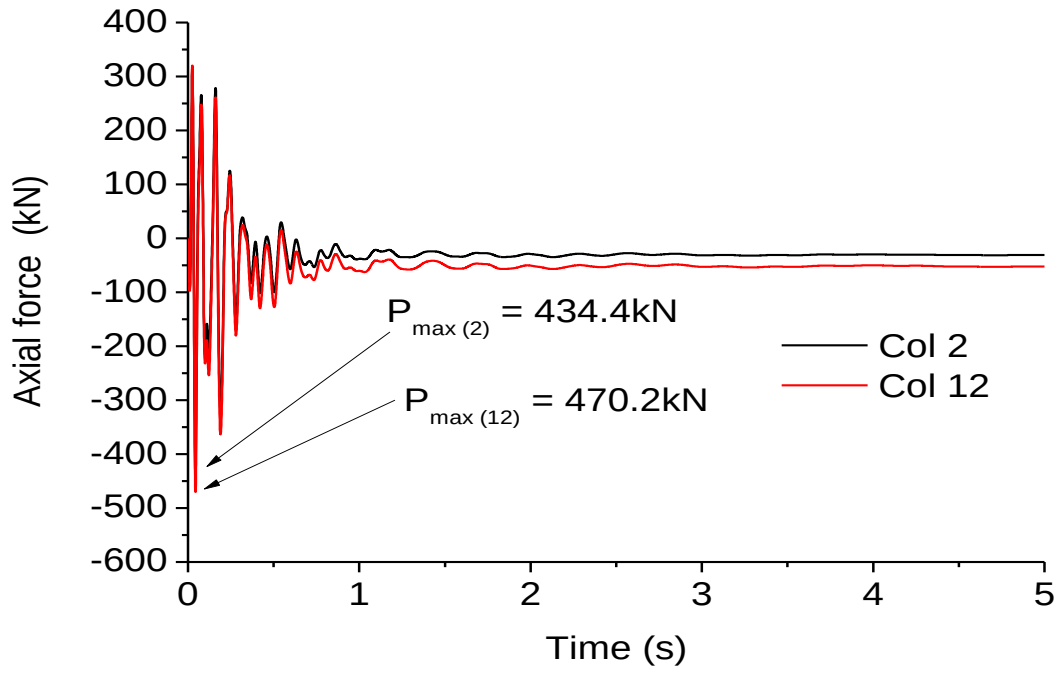

Figure 5-41 Column axial force response above removed column

The initial axial force response in Columns 2 and Columns 12 are 1715kN and 2762kN respectively. For the static analysis, without the double columns, the axial force the axial force of Column 2 and Column 12 are 30.58kN and 51.6kN respectively. Comparing the initial axial force to the static response; it is observed that there is a reduction in the axial force in the columns by 98.2% and 98.13% for Column 2 and Column 12 respectively. Static analyses of the structure without two columns results in the loss in the axial force response of the columns just above the removed columns. The dynamic analysis response of the structure is presented in Figure 5-41. It was observed that the responses of Column 2 and Column 12 are 434.4kN and 470.2kN respectively. The ratio of the dynamic response to the initial static response for columns 2 and 12 are 14.2 and 9.11 respectively. The next plot is to assess the shear force response value of the columns relative to its initial axial force, static response, and dynamic response. Figure 5-42 presents the shear force response of Columns 2 and Column 12 to sudden column loss scenario (DCRS).

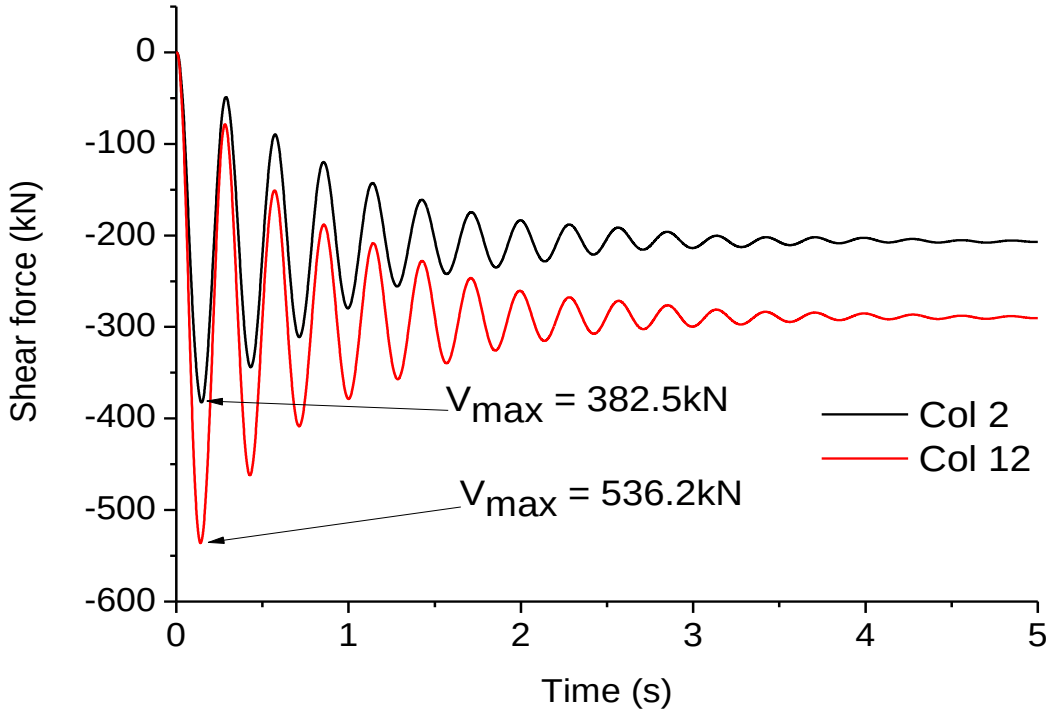

Figure 5-42 Column shear force vs time

These columns are located above the removed columns. The initial shear force in these columns without column removal scenario is 1.95kN. A static analysis was carried out after rebuilding the model without double columns and, it was observed that the shear force responses of the columns above the removed double columns are 205.99kN and 289.09kN for column 2 and 12 respectively. The response of the columns under static analysis is

significant relative to the initial axial force response in the column. The dynamic analysis response of Column 2 and Column 12 are 382.5kN and 536kN respectively. In view of these responses, the dynamic analysis response resulted in an 87% and 85.4% increment in the dynamic response of the structure relative to the linear static response.

Figure 5-43 presents the moment response of Columns 2 and Column 12 under sudden column loss scenario. The maximum moment in Column 2 and Column 12 is 780.6kNm and 1079kNm respectively. At the conventional stage, the maximum moment response of this column before the columns are removed for Column 2 and Column 12 is 1.88kNm and 3.77kNm respectively. After the model is built without the removed columns and the analysis re-run for static case, the moments in the columns are 419.05kNm and 581kNm respectively. A relative comparison between the static and dynamic analysis response based on the moment response of Columns 2 and Column 12, shows that sudden column loss results in 86.3% and 85.7% increase in moment respectively.

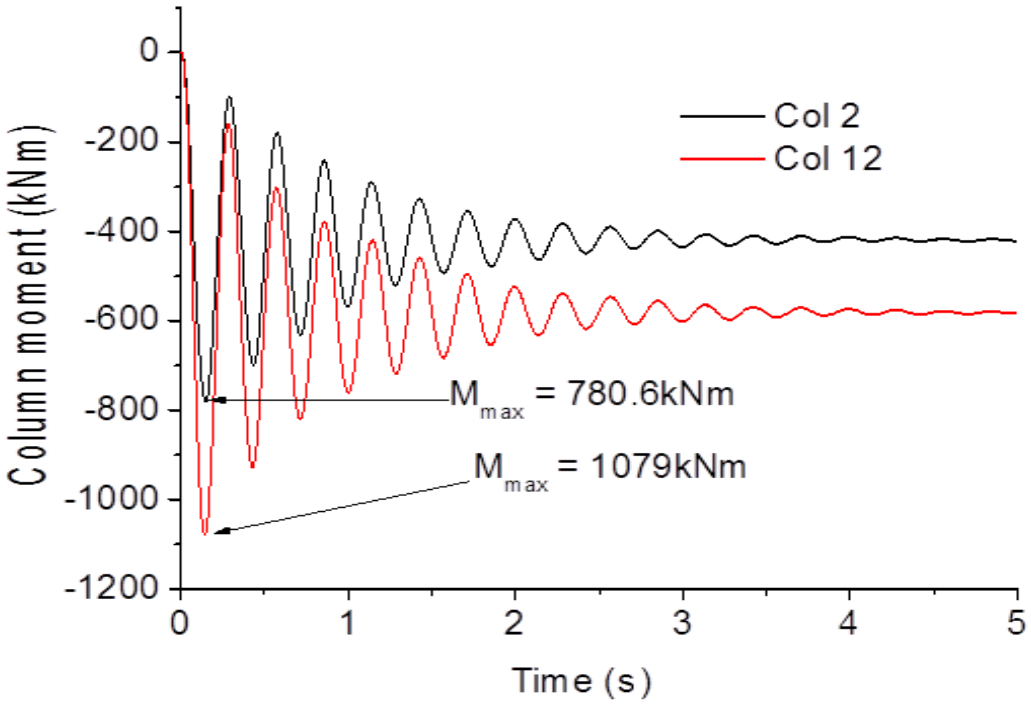

Figure 5-43 Moment response of columns vs time

In summary, the investigation of the columns above the removed double columns (Col 2 and Col 12) shows that the columns lose approximately 98% of their internal axial force with significant shear and moment been developed at the joint connecting the removed column. The internal axial force in these columns were redistributed within the structural

system with significant changes in the shear and moment force responses which were negligible during the conventional design stage of the columns.

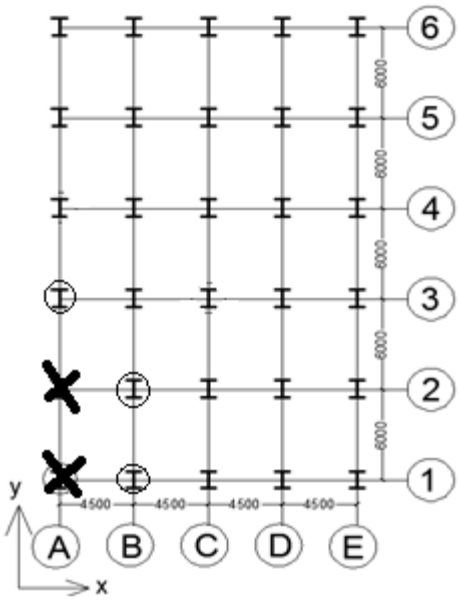

Figure 5-44 Plan layout of double column assessment

Using the plan of Figure 5-44, the columns on grid A-1 and A-2 are the removed columns while the columns investigated are the column on grid A-3 (Col 21), column on grid B1 (Col 71) and interior column on grid B-2 (Col 61).

The beams investigated at the first floor are the beam between grid A1 and A2 (BM 541), the beam at grid A2 and A3 (BM 551) and the beams between grid A and B (BM 301), A and 2 (BM 341). The column response is presented which is followed by the response of the beams under sudden column removal scenario. Figure 5-45 presents the maximum axial force responses of Column 21, Column 61 and Column 71 as they vary with time. The maximum axial force response in Column 21 is 5663kN, that of Column 61 is 7870kN and that of Column 71 is 11360kN. The axial forces in these columns at conventional design stage without column removal are 3066.4kN, 2812.8kN, and 4162.4kN for columns 21, 61 and 71 respectively. After running static analysis without the missing columns, it was observed that the axial force response in Column 21, Column 61 and Column 71 are 3377.8kN, 4936kN and 7003.7kN respectively. The variation between the initial state of the structure and the increment due to stress redistribution shows that Column 21, Column 61 and Column 71 increases by 10.2%, 75.5%, and 18.9% respectively under static response.

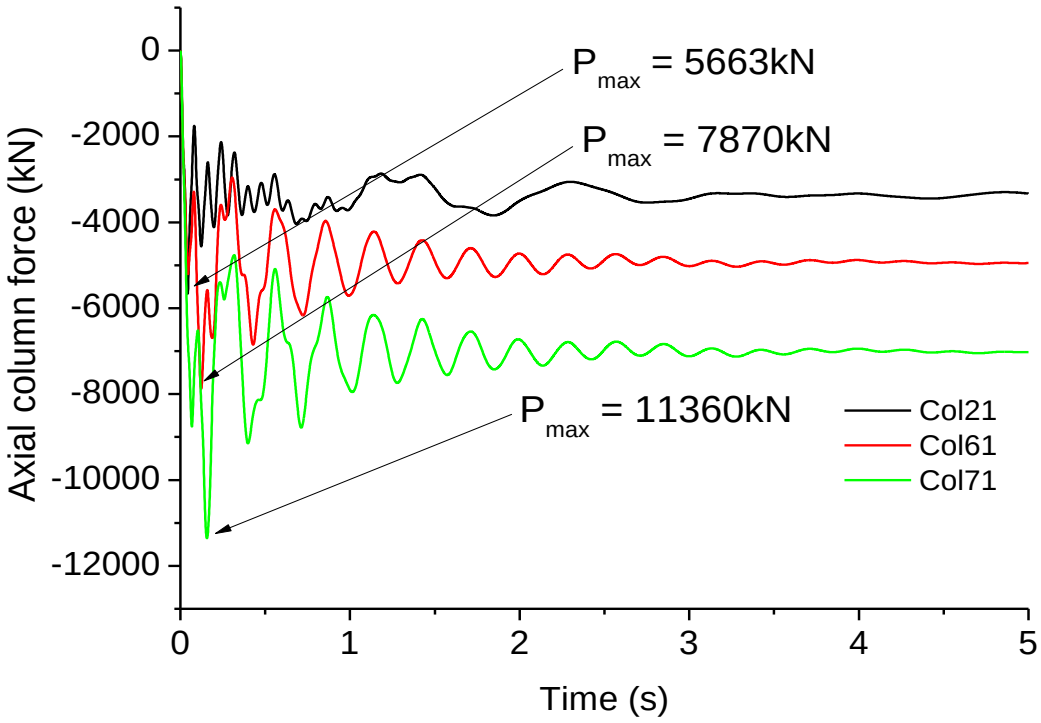

Figure 5-45 Column axial force response (kN)

Comparing the static response with the dynamic response, it was observed that Column 21 increases by 67.7%, Column 61 increases by 59.4% and Column 71 increases by 62.1%. The shear force responses of the columns are presented in Figure 5-46.

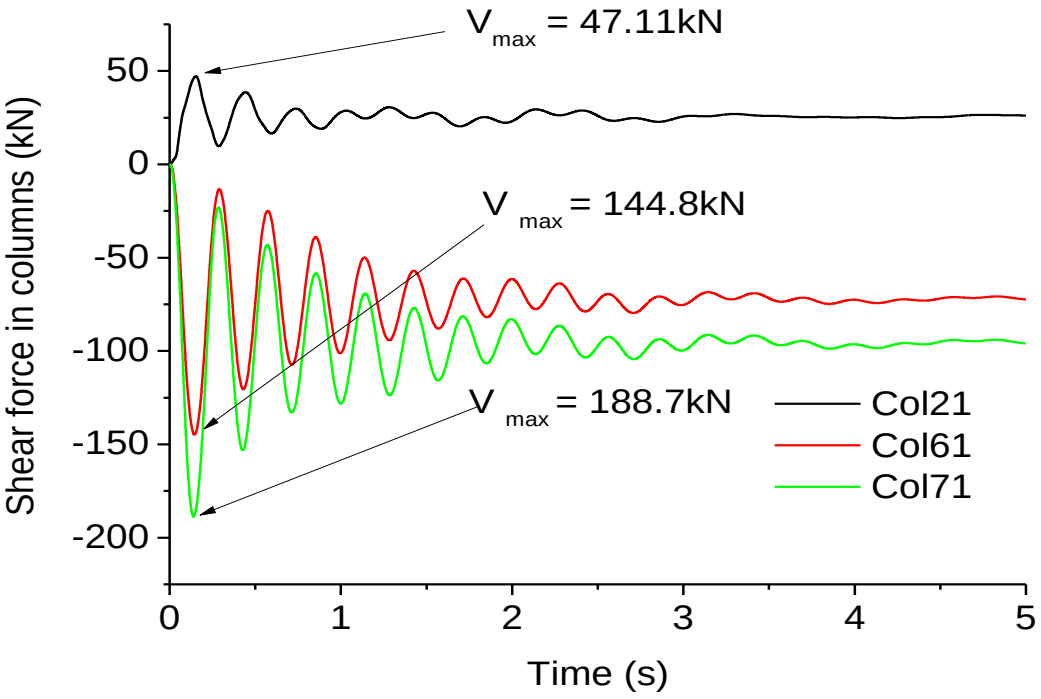

Figure 5-46 Shear force response (kN)

The shear force responses of the columns are presented in Figure 5-46. The maximum shear force response in Column 71 is 188.7kN; Column 61 has a maximum shear force response of 144.8kN while column 21 has a maximum shear force response of 47.11kN. Relatively, Column 71 is more critical relative to Column 21 and Column 61. The initial shear force in columns 21, 61 and 71 before column removal are 0.92kN, 0.866kN, and 0.72kN respectively. After the model was rebuilt without the missing columns for the static analysis case, it was observed that the shear force in the columns 21, 61 and 71 increase to 25.5kN, 72.5kN and 95,9kN respectively. Comparison between the static response and the dynamic response in order to assess the extent at which the sudden column removal affects the structure is important; for the case considered, comparing the static response to the dynamic response of the structure, it was observed that Column 21, Column 61 and Column 71 increases by 85%, 99.7% and 96.8% respectively. Figure 5-47 shows the moment response of Column 21, Column 61 and Column 71 under multiple column removal scenarios.

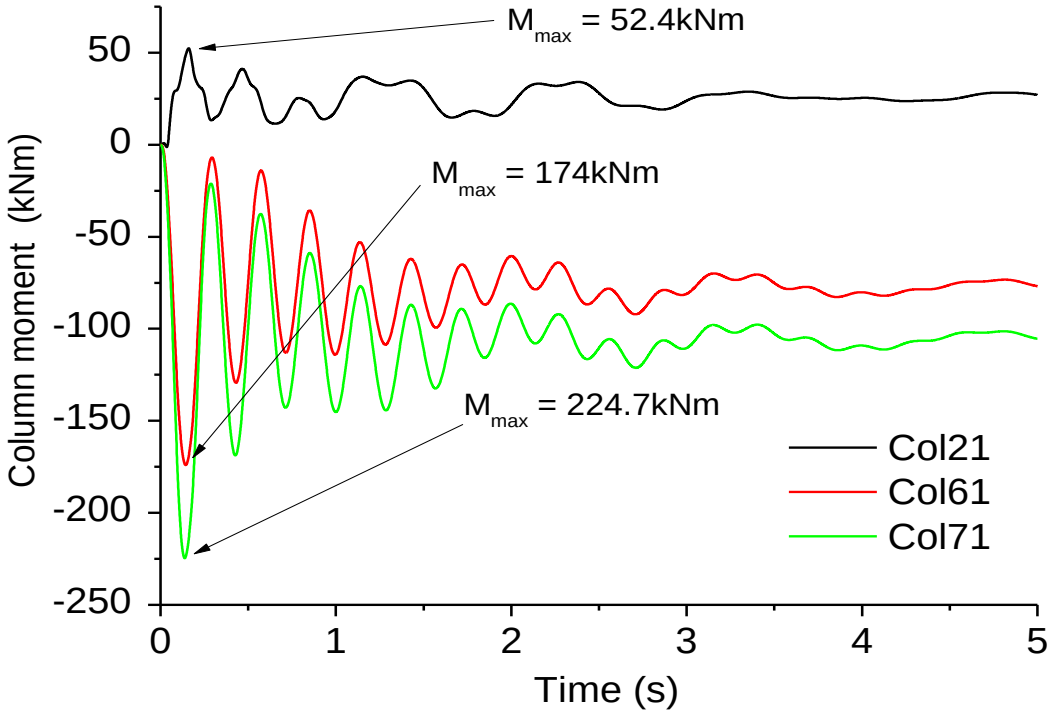

Figure 5-47 Moment force response (kNm)

The initial moment in the columns before double column removal are 2.18kNm, 1.65kNm, and 1.59kNm respectively. This initial state of the column moment is insignificant and can be designed for pure axial loading. The static response in Column 21, Column 61, and Column 71 is 63.8kNm, 175.7kNm, and 229.7kNm respectively, while under dynamic analysis; the responses are 52.4kNm, 174kNm, and 224.7kNm respectively. For the sudden

column removal of double columns, the dynamic increment for Columns 21, Column 61 and Column 71 does not result in an increase in the moment response of the columns.

5.6.4 Joint responses

The two important joint factors that determine the ductility and strength of a joint is its ability to resist vertical displacement under abnormal loading conditions and its rotational capacity. FEMA 350 gives comprehensive recommendations and limits for joint rotations under cyclic or seismic excitations. This subsection presents the maximum joint displacement and rotational response under double column loss scenario. The responses of the joints of the removed columns are presented in Figure 5-48 and Figure **5-49**

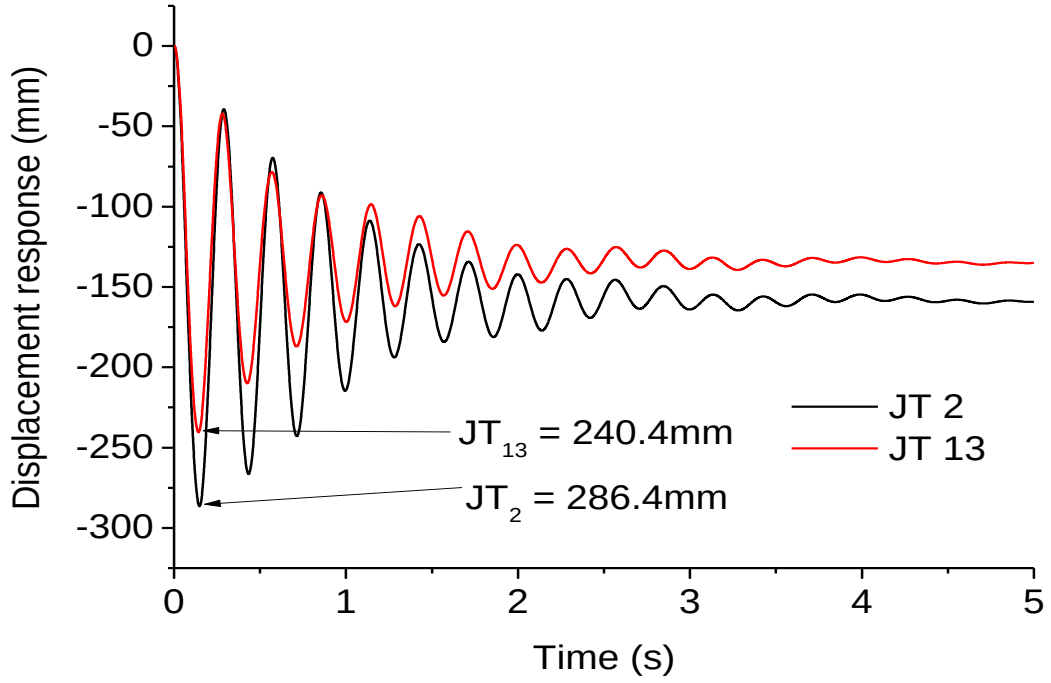

Figure 5-48 joint responses due to multiple column loss

The maximum displacement response occurs at Joint 2 having a value of 286mm relative to Joint 13 having a response of 240mm. When these is compared with the static response, it was observed that joint 2 and joint 13 response increases by 44.8% and 44.1% respectively.

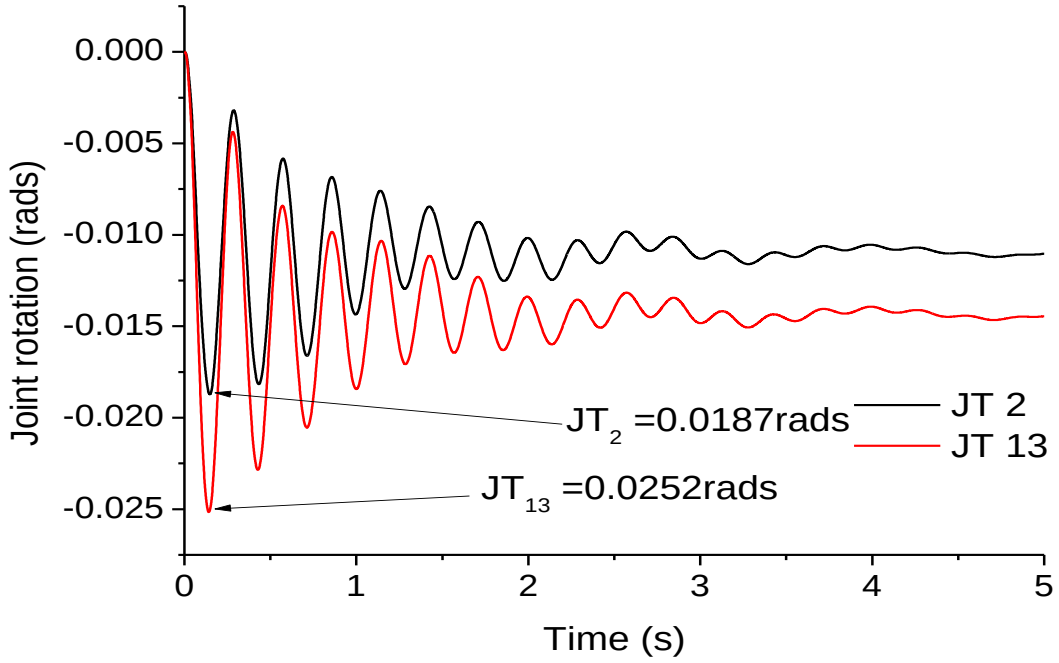

Figure 5-49 Rotational responses due to multiple column loss

The rotational response of the joints is presented in Figure **5-49** above. Maximum joint response occurs at joint 13 having a displacement and rotation of 286.4mm and 0.0252rads respectively. On the other hand, joint 2 has a maximum displacement and rotational response of 240.4mm and 0.0187rads.

5.7 Chapter summary

This chapter assesses the structural brace frame system under progressive collapse scenario. The investigation focused on the internal force redistribution of the braced frame system under progressive collapse scenario.

The catenary force action has been observed to be the main internal force governing the behaviour of braced frame structures under progressive collapse scenario. If the bracing connects the joint of the removed column, the magnitude of the catenary force response significantly reduces because the bracing serves acts as an alternative load redistribution path at the connection.

The author noted that the dynamic amplification factor based on the catenary force response gives a maximum response of 1.94 which is 3% less than the recommendation in GSA 2003. An extension into the response of the slab to progressive collapse, it was observed that the dynamic effect as a result of sudden column removal is a function of the number of floors.

The axial force response, shear force and moment responses are three key internal forces in a column that govern its behaviour under progressive collapse scenario. Relatively, the shear force response is the most important criteria for dynamic amplification factor (DAF) assessment. Comparatively, it was observed that the maximum DAF based on the column shear force criteria was 2.01at the eight-floor column removal scenario. However, at the corner and interior column removal scenario (CCRS: ICRS), it was observed that it was 2.5% less than GSA 2003 recommendation. An extension into stress redistribution of slabs shows that the dynamic effect of sudden column loss is a function of storey height. Consequently, the author correlates the DAF response with the storey height. A minimum response of 1.93 was observed for the slabs which occur on the first floor. The catenary force developed during progressive collapse are actually greater than 75kN recommended in Eurocode 1 EN 1991-1-7 Equation 5-3. At all the locations assessed, it was observed that the eighth-floor column removal scenario is more critical relative to the corner, interior and edge column removal scenarios.

Chapter 6 Comparison of BRF to MRF

6.1 Introduction

This chapter addresses one of the objectives of the thesis; which is to compare the response of moment resisting structural frame system to brace structural frame system. It will focus on comparing the responses obtained from Chapter 4 for moment resisting frame structure to that of Chapter 5 for brace frame system. At the end of this chapter, a basis for the assessment of beam-column connection using finite element analysis is established. The objective is to determine further how progressive collapse loads influence joint standard behaviour.

The choice of frame structures significantly determines the performance of the building system under abnormal loading conditions. Since the collapse of a building is inadvertently a consequence of abnormal loading (blast, earthquake, extreme fire, etc.), the choice of frame structure becomes crucial considering the additional cost required to account for safety requirements incorporating progressive collapse. Building codes around the globe recommend designs that ensure progressive collapse is mitigated, although the codes do not explicitly define performance-based design strategies on how that can be achieved. Consequently, the designer's experience and standard recommendations on optimal structural performance are applied during the normal design stage. One of the key considerations is the choice of a frame structure in the construction of high-rise steel structures that significantly play a unique role in structural performance, completion time and ultimately the project cost. Two fundamental assumptions are often made in the choice of a frame system for high-rise steel structures during the conventional design stage: Pin frame system or Rigid frame system.

Simple braced frame structures are popular in the construction industry as compared to moment resisting frame structure. The choice of this type of frame structure is driven by cost and functionality relative to the moment resisting frame structure. In chapter 4 and 5, an assessment of moment resisting frame structure and braced frame structures were carried out to determine the response of the structure under the column removal scenario. In this study, the percentage increment in the internal forces of the members under the sudden column loss for moment resisting frame structure and braced frame structure are presented. The four locations used in previous chapters would be used for the comparison. It was

observed that irrespective of the structural frame system used for the assessment, column removal at the eighth floor is relatively more critical compared to interior, edge and corner removal scenario.

Furthermore, the previous study reveals that the eighth-floor column removal scenario is relatively more critical as compared to the corner, edge and interior column removal scenarios. The interior column removal scenario is the least vulnerable to progressive collapse based on the responses from the moment resisting frame and the braced frame system.

6.2 Relative comparison of MRF to BFS

This section is aimed at comparing the responses based on the percentage increment of the internal forces under the column removal scenario for moment resisting frame systems and braced frame systems. The comparison is carried out at four different locations: the edge, corner, interior and the eighth-floor column removal scenarios. In addition, the frame structures were compared under multiple column removal scenarios. The subsequent subsection discusses the summary of the investigations to establish the basis for which simple beam-column connections would be assessed in the next chapter.

6.2.1 Eight floor column removal scenario

The structural systems were evaluated based on the response of the internal forces developed under column removal scenario. The dynamic effect of column removal results to 85.3% increment in the joint displacement response of the brace frame system. Using the joint response criteria, the dynamic effect is 93% for braced frame structure. The corresponding dynamic effect using the moment resisting frame structure is 88.4%. This shows that braced frame is prone to progressive collapse as compared to moment resisting frame structure.

6.2.2 Corner column removal scenario

At the corner removal location, the removed corner column bounds column 11 and column 61 at the long and short span respectively for moment resisting and braced frame system. The beams connecting these columns are: Beam 301 on the short span and BM 541 to the long span of the model. Under axial force response of MRF and BFS, it was observed that Col 11 increases by 20.4% for MRF and 44.16% for BFS. Similarly, the axial force in column

61 increased by 23.3% for moment resisting frame while the increment was 54.43% for the brace system.

It was observed column 11 increases by 75.5% in the moment resisting frame (MRF) and 108.6% in the brace frame system (BFS) using the shear force response criteria. Using column 61, it was observed that the shear force response in MRF increases by 93.4% while the response of column 61 in a BFS is 102.6%.

The catenary force action in beams would be used as a standard to compare the percentage increment of the dynamic response to the static response for moment resisting frame structure and Brace Frame System (BFS). It was observed that beam 301 (BM 301) increases by 83.8% for MRF and 112.7% for beam 541 (BM 541). The percentage increment for BM 301 is 84% while for BM 541 is 70.7%. Under corner column removal for joint 2 for moment resisting frame structure (MRF) increases by 72.3% while that of brace system (BFS) increases by 1738.5% when the dynamic response is compared to the static response. Although, the percentage increment in the catenary force for the tie beam of the moment resisting frame structure and the brace frame system is approximately the same.

This relative comparison between the moment resisting frame structure and braced frame system under corner column removal scenario shows that inertia forces triggered by sudden column loss significantly affect the brace frame system (BFS) relative to the moment resisting frame (MRF). Consequently based on the corner column removal scenario, the argument to propose the same dynamic amplification factor for these two forms of structure is conservative, therefore inefficient. Preferably a separate dynamic amplification factor for moment resisting frame structure and braced frame system.

6.2.3 Interior column removal scenario

At the interior column removal scenario, the beams connecting the removed column along the short span is BM 391,401,651 and 661 while the columns binding the removed column is column 81, 201,131 and 151. The axial force response is used to compare the percentage increment of the dynamic to static response for moment resisting frame structure to the braced frame structure. It was observed that column 81 and column 201 increases by 24.6% while column 131 increases by 19.8%, column 151 by 19.2% for moment resisting frame structure. On the other hand, the corresponding response in braced frame system for Col 81, 201, 131 and 151 is 50%, 50%, 58%and 59.5% respectively. Based on the moment criteria,

there is a reduction in the inertia effect on the moment response for braced frame system and moment resisting frame respectively. It was observed that the percentage decrease in column 81, 201,131 and 151 are 15.9%, 17.3%, 31% and 23.1% respectively. On the other hand, for braced frame system, column 81, 201,131 and 151 are 5.1%, 4.5%, 22.19%, 13.9% respectively. Using the shear force response of the braced frame system, it was observed that column 81,201,131 and 151 increases by 93.1%, 94.8%, 91.6%, and 98% respectively. However, that is not the case for moment resisting frame structure. The columns increase by 95.8%, 95.8%, 73.7% and 68% respectively. This studies shows that the inertia effect induced on the structural system as a result of column removal has more effect on the shear force response of a brace system relative to the axial and moment response of the columns for both structural frame systems. However, a relative comparison of the two frames using the column responses shows that brace system are prone to progressive collapse relative to moment resisting system. The next paragraph present a relative comparison of the beam response of the moment resisting frame to braced frame system under interior column removal scenario.

Using the axial force response in the beams to compare the two frame structures, It was observed that the percentage increment in BM 391, BM 401,BM 651 and BM 661 is 95.3%, 91.4%, 84.5% and 88.1% respectively for braced frame system. The corresponding beam response for moment resisting frame structure are 70.1%, 70.1%, 70.3%, 68.5% respectively. Using the joint response criteria, it was observed that the percentage increment in the displacement response of moment resisting frame induced by inertia effect is 67.9% while the corresponding response in braced frame system is 93.7%. Using the beam and the joint displacement response criteria, for the comparison of the inertia effect due to column removal, it can be concluded that the brace system is more susceptible to progressive collapse relative to the moment resisting frame structure. Despite the fact that the interior both frame system has the same moment releases, it was observed that the external frame system significantly influence the response of the structure to sudden column loss. The next subsection compares the relative responses of the braced frame system to the moment resisting frame structure for multiple column loss scenarios.

6.2.4 Relative displacement responses

The relative displacement at the nodes of the removed columns for moment resisting frame structure and the braced frame system is compared as presented in Figure 6-1 below. Joint 2

(JT2) represents the corner column removal scenario, while joint 9 (JT9) represents the eight floor column removal scenario. The interior column removal scenario is represented by joint 156 (JT 156). In all the investigations, joint 9 at the upper floor which corresponds to eight floor column removal scenario is more critical compared to the first floor column removal at the corner and the interior location of the structural system. Most importantly, it's obvious from the relative comparison that brace frame system responds to column removal scenario relative to the moment resisting frame structure. Consequently, the braced frame system is prone to progressive collapse as compared to the moment resisting frame structure.

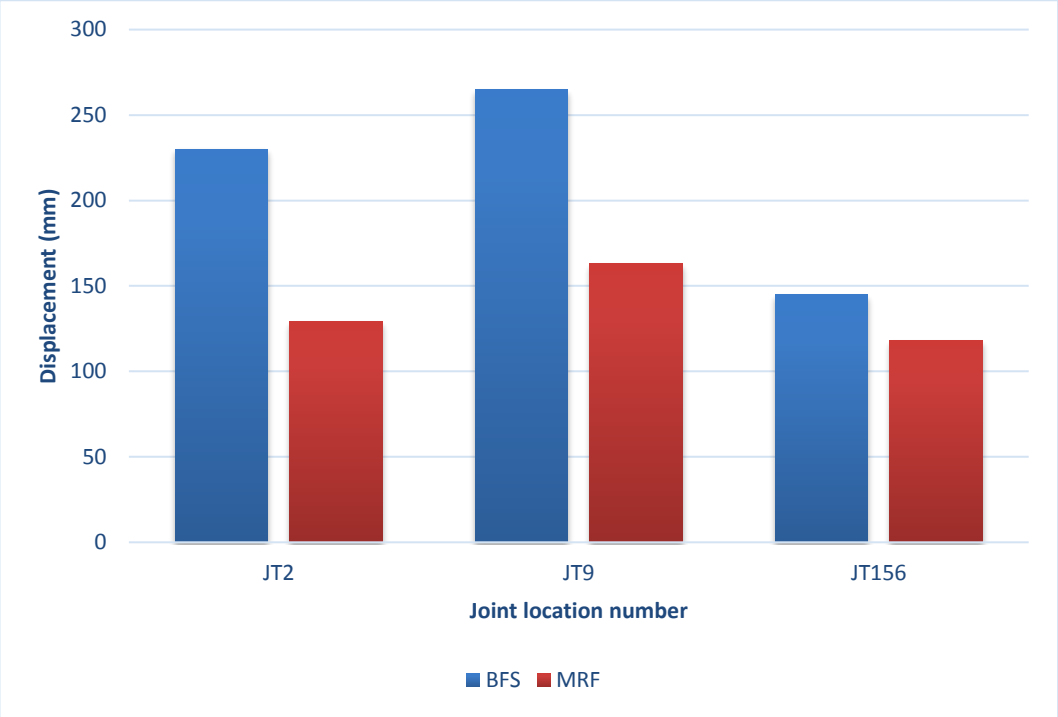

Figure 6-1 Comparison of joint displacement response

Figure 6-2 Comparison of joint rotational response

As shown in Figure 6-1 and Figure **6-2**, Joint 2 (JT 2) represents the corner column removal scenario while Joint 9 (JT 9) and Joint (156) represents the edge and interior column removal scenario. The displacement and rotational responses were compared, at joint 2 (JT2) of the brace and moment resisting frame system, the response of brace frame exceeds that of moment resisting frame system approximately 50% based on the displacement response. However, based on the rotational response the brace frame system responds 16% more than the moment resisting frame structure. At the eight floor column removal scenario (JT 9), the displacement response of JT 9 for brace frame system exceeds the response of moment resisting frame system by 41.5%. However, that is not the case for rotational response which shows a difference of 37.9%. At the interior column removal scenario corresponding to joint 156 (JT 156) the maximum displacement response brace frame system exceeds that of the moment resisting frame system by 31.4%. However, the difference is 46.6% based on the rotational response.

6.3 Chapter summary

This chapter compares the behaviour of the moment resisting frame and the braced frame structure under single column removal scenario. In case of accidental loads, the relative responses of the joints show that the brace system is prone to progressive collapse as

compared to the moment resisting frame structure. A comparison of the joint responses of both structures at different locations shows that the upper floor column removal is more critical relative to the corner, edge and interior column removal scenario. In addition, changes in the internal force of the members were compared at different locations. For the braced frame system, the development of catenary force response is the most important design criterion.

However, under the column removal scenario, changes in the catenary force significantly exceed the minimal recommendation in the design code. The maximum catenary action in the brace frame system is approximate five times the minimum recommendation in Eurocode 3.

Comparing the relative responses of the moment resisting frame structure to the braced frame structure, the moment resisting frame structure develops a higher flexural stress resistance relative to the brace frame system. On the other hand, the bracing in a braced system serves as an alternative path under which some internal forces are been directed. This study agrees with the investigation carried out by Mohamed (2009) which states "Systems with bracing can divert some of the high forces generated by the removed column due to an AP analysis to the bracing system, if the connections are designed to support and transfer additional loads. However, high torsion induced shear forces are generated that can lead to shear failure. Systems with moment resisting frames, on the other hand, experience high flexural stresses for which the structural elements must be designed".

In subsequent chapters, the focus will be on the performance of the connection under conventional design state and the performance of the connection under progressive collapse scenario. Failure of members and connection response will be based on the recommendation of GSA 2003 guidelines, which stipulate a plastic rotation of 0.035 rads. However, DoD recommends 0.02 rads as the collapse prevention limit state corresponding to FEMA-365 seismic load with a return period of 2400 years (Kim et al., 2009).

6.4 Basis for chapter seven

The relative response of moment resisting frame structure to braced frame structure shows that the braced frame system is likely more prone to progressive collapses compared to moment resisting frame structure. The most important change in the internal force of the brace frame system is the catenary force developed under column removal scenario. It significantly exceeds the recommendation in Eurocode 3 for simple connection design. Therefore, there is a need to assess simple beam-column connections under progressive collapse scenario using the geometry at the eight floor column removal location.

Chapter 7 Finite element modelling of a typical connection

7.1 Introduction

This chapter is aimed at investigating the behaviour of simple connections design to Eurocode 3 Part: 1-8 based on the static load response of the brace frame system studied using the SAP 2000 finite element code. In the preceding chapter, the relative response of the moment resisting frame structure and the brace frame structure was compared, and a basis for detailed finite element analysis of the connection using the ABAQUS finite element code was established. This section lays the building block for achieving one the objectives of the thesis: to investigate the response of simple beam-column connection designed to Eurocode 3 Part: 1-8, under progressive collapse scenario. This begins with a detailed introduction which highlights the problem and the need for the research investigation. This followed by a description of the model and basic studies on the shear and catenary effects. The connection model used as a control is assessed, and then the results discussed.

The fundamental principle of the finite element method is to discretise complex geometries into simple forms or shapes called elements. These elements are in a state of equilibrium, that involve solving complex interactive equations correlating nonlinear material and geometric behaviour, boundary condition and applied loads using computer aided engineering. In structural engineering, the application of the finite element method to high-rise steel structures is one of the key research-based interest particularly in the behaviour of connections.

Connections have been the most important unit in high rise steel structures, some inherent challenges in its precise design exist because of the complex interaction of components, loads, material and geometric nonlinearity. At times, it is practically impossible, considering the cost, to achieve a beam-column connection with same stiffness, rotation capacity and strength as the connecting members. In practice, simple connections using end plate connections are mostly popular because of the ease of fabrication and cost considerations. The design principle of this type of connections in the UK is based on the approach recommended in EN1993-1-8.

From analytical and design perspective, the conventional design of these connections is based on a key assumption for moment resisting frame structures and brace frame structures: moment resisting frame structures are assumed to be rigid; that is, they have an infinite

resistance to rotation while the braced system is assumed as a pin with no resistance to joint rotation. Pin connections are not designed to transmit moment through other connecting members. Structures assumed to possess rigid connections are referred to as moment resisting frames while structures assumed to possess pin connections could either be braced frame structure or core frame structure. In the case of rigid frame structures, the connections are assumed to have an infinite stiffness such that joint rotation is not allowed. This assumption restrains the beam deformation due to loading relative to the pin connection that allows joint rotation.

Beams can sustain large deformation if the connections are strong enough to activate full beam catenary action due to the loss of critical structural members. Although connections in practice possess some finite rotational stiffness and can best be described as semi-rigid, this is an ongoing research area. This assumption is necessary to simplify the global analysis of the structure for design purposes. If the connection is assumed to be a pin as in brace or core frame structures, it is commonly designed to transmit shear forces with minimal tensile force. This implies that the connection is not designed to transmit moment and lacks rotational stiffness. However, a fully rigid assumption implies the connections has infinite rotational stiffness and therefore capable of transmitting all stress resultants (Shear, Moment, torsion and axial forces). The assumption of rigid or pin connection is adopted conservatively since in-depth knowledge of the behaviour of semi-rigid connections is currently lacking. In reality, beam-column connection has a finite stiffness and therefore it is semi-rigid.

Since connections are neither pin nor rigid in its actual behaviour, the behaviour and response of a multi-storey building to gravity and unforeseen loads significantly depends on the type of joint used for the construction. The structural robustness and performance of multi-storey buildings significantly depend on the joint design and structural details which determine its strength and ductility. The performance of beam-column connections depends on the contact interaction of the various components, the material, and the geometric nonlinearity. Therefore to effectively capture the behaviour of connections under loading conditions, it is important to incorporate the interaction of contact surfaces, the nonlinearity of the material and the geometric properties in determining the overall performance of the connection. This approach is necessary because it gives a better understanding and appreciation of connection performance in practice as compared to the conservative assumption of either pin or rigid joints. In practice, if the beam connecting the column is designed as pinned connection, a larger section is required for a constant load as compared

to the same beam designed as semi-rigid connection. Similarly, if the same beam is designed and the connection is considered to be rigid, this will yield a smaller section because the ends of the beam are expected to resist moment as well as shear forces.

Under progressive collapse scenario, beam-column connections can be subjected to a concurrent action of axial tension and shear forces for simple connections. Sudden loss of critical columns requires alternative paths for load distribution that results in the development of beam catenary action. These affect the flexural and rotational capacity of the connection under service conditions. Incorporating the behaviour of connections into the design of a multi- storey frame building requires key assumptions considering the complexity of the connection as a structural unit.

This chapter seven is a continuation of chapter six that compares the responses of the moment resisting frame structure to the brace frame system and sets a basis for the connection assessment. This investigation focuses on a detailed finite element modelling of a simple beam-column connection designed to Eurocode 3 Part: 1-8, for static conditions.

In previous chapters, the internal force redistribution due to the loss of columns at different locations was evaluated. Displacement and joint rotational responses were assessed and compared in order to determine the location of the maximum response. Consequently, the eight-floor beam - column connection which develops the maximum response was used as a case study for the connection assessment. A finite element analysis of a 3D model of the beam-column connection initially designed to Eurocode 3 with a consideration of 75kN tensile force was adopted as a control. It is important to note that the maximum shear force response from SAP 2000 is 80.17kN on BM 548 along the long span and a maximum shear force of 34.72kN along the short span. The investigation in this chapter will focus on the stress-components developed as a result of these forces and the critical region checked under various states of stress components. At the end of the investigation, a comprehensive summary of the connection response used as initial condition is presented. This chapter serves as the basis at which the connection will be assessed for a progressive collapse in the next chapter.

7.2 Model validation

In order to validate the accuracy of the proposed model, a 3D connection model was built to replicate the experimental test of Yang and Tan (2013). The objective of the experiment was to investigate the load-deformation characteristics of the connection designed to EC3 British Standards Institution (2005). The finite element result compared to the experimental results shows a good agreement. Figure 7-1 shows the deformed shape of the connection paralleled to the experimental model. The vertical force-displacement response of the joint is shown in Figure 7-2.

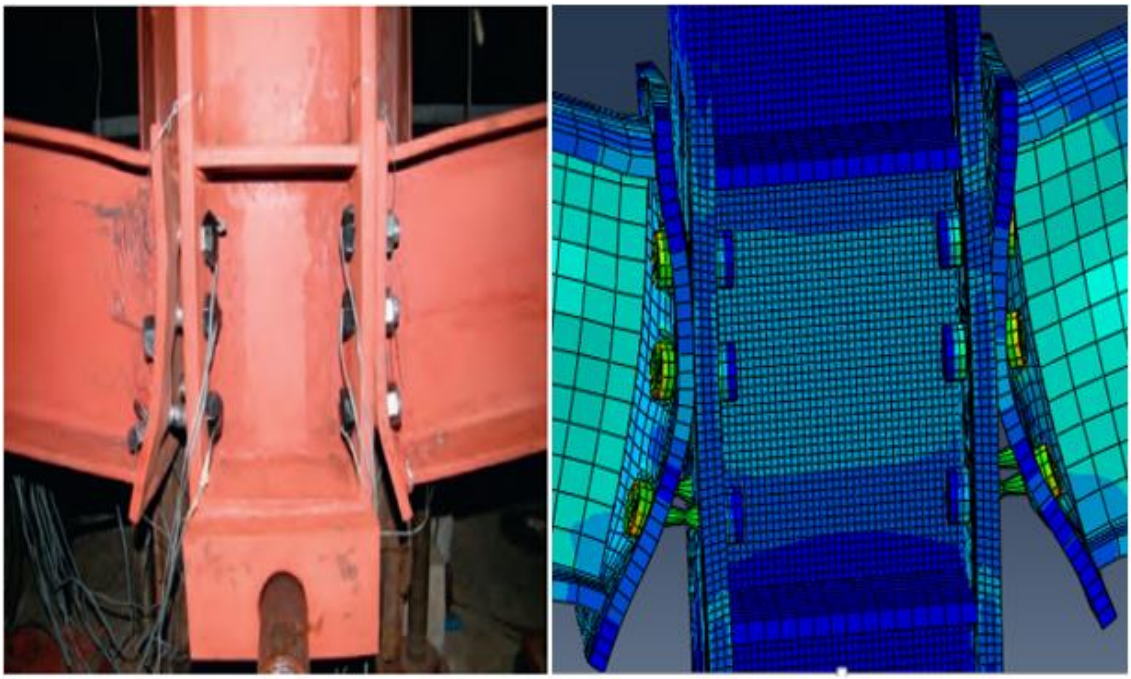

Figure 7-1 Connection geometric deformation (Experimental compared to FEA model)

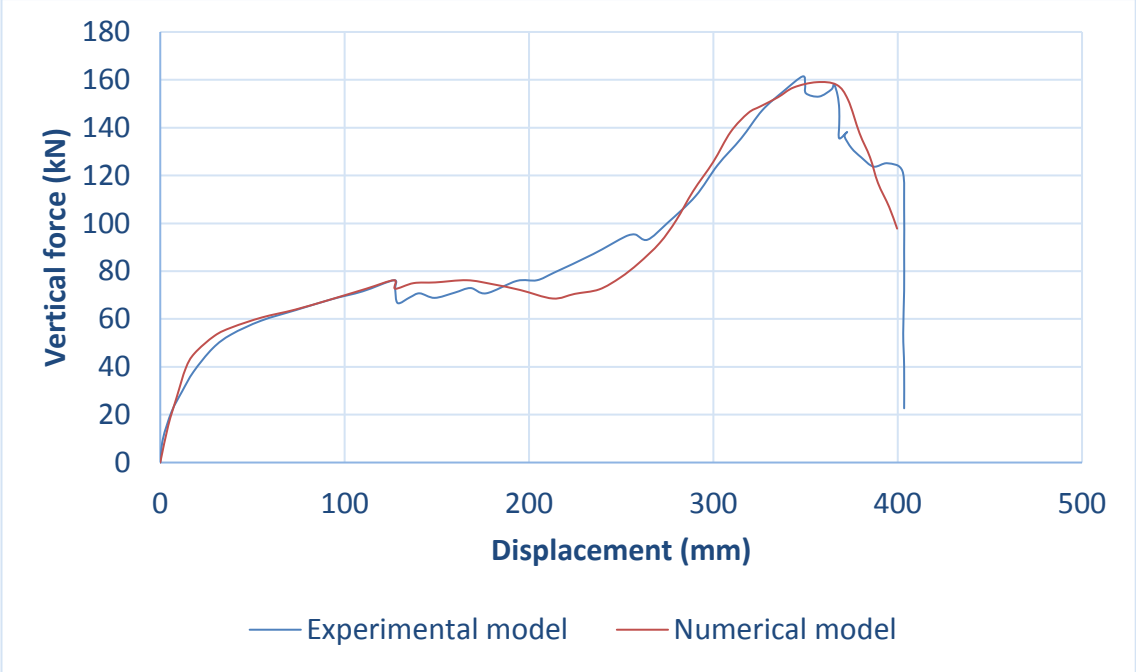

Figure 7-2 Experimental and FEA under CRS.

7.3 Case study connection description

This section presents a brief description of the structural geometry of the beam-column connections while subsequent subsections present basic descriptions of all the factors taken into consideration during the modelling. The column at the eighth floor is UC 254 x 254 x167, the main beam connecting the flange is UB406 x 140 x 39 while the tie beam connecting the web of the column is UB254 x 102 x22. The plate connecting the flange of the column to the main beam is 250mm x 200mm (bw) while the plate connecting the web of the column has a dimension of 160mm x 200mm. The bolts used for the investigation has a diameter of 20mm. The end and edge distance are 50mm while the bolt centre to centre distance (p1) is 150mm. On the other hand, the plate connecting the web of the column has an end and edge distance of 40mm. The finite element beam – column section is shown in Figure 7-3. In this case, the plate height (Ph) is less than the beam section depth (Bh). The design of the header plate is based on Eurocode 3, and the header plate is designed based on the shear force response of the braced frame structure.

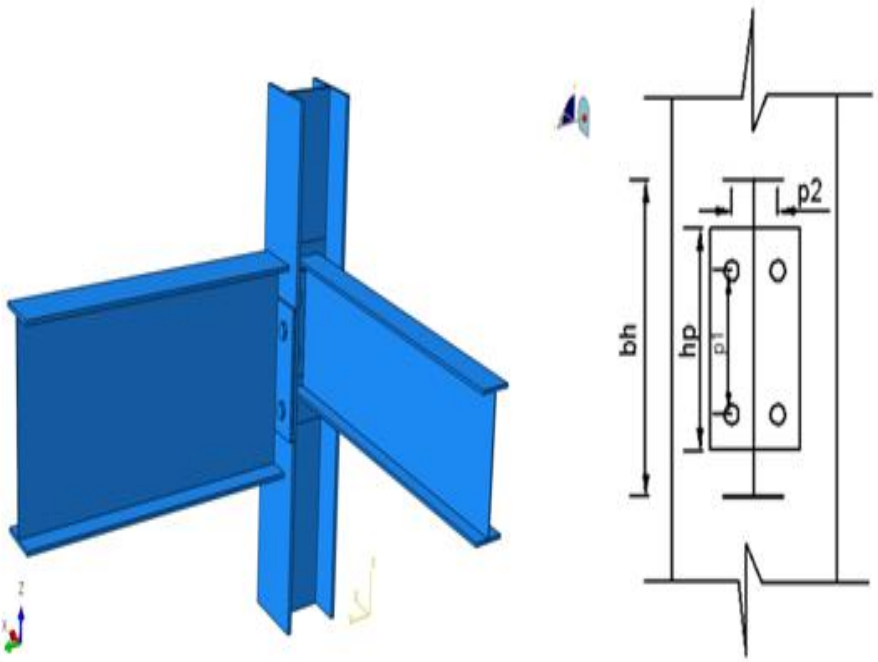

Figure 7-3 3D representation of the control model

7.3.1 Element types

The ABAQUS FEA code provides a wide range of element library depending on the type of investigation and structural geometry. The ABAQUS element library is either standard or explicit with linear or quadratic geometric order with a wide range of family. The basic group classifications of the element types are: Family, Geometric order (number of nodes and degree of freedom), the formulation, and integration. The following subsections briefly describe each of these groups as applied to ABAQUS FEA model.

The family:

The term "family" describes the broad classification of elements that has some common behaviour. For example: continuum, shell, rigid, 3D stress e.t.c describes the unique behaviour of the model under investigation. For the purpose of this investigation, a 3D stress family is adopted since this model represents a typical solid element.

Geometric order

The geometric order can either be linear or quadratic. The basic difference between the linear and quadratic order is in the number of nodes and degree of freedom of the elements. For

instance, a quadratic geometric order in a 3D family of a standard element library has a 20 node quadratic brick (C3D20). However, an element within the same group but having a linear geometric order has 8 node linear brick (C3D8).

Element formulation category

This broad category is a function of mathematical expressions that defines the behaviour of the elements within a group. Typical mathematical formulations are hybrid elements, plain stress, plain strain, and thick and thin shells.

Integration

The behaviour of an element is a function of the integration method used for the assessment. This process requires that the stiffness and mass of the element are computed at sampling points otherwise called integration points. The numerical integration of the variables at these points significantly influences the element behaviour under loading condition. ABAQUS provides two integration methods: 1) Full integration and 2) Reduced integration. Full integration is describes a scenario where minimum integration is required to achieve strain energy of an element in its original form, while reduced integration has an integration point less than the full integration. Considering the wide element library in ABAQUS, the choice of element type depends on the degree of accuracy required and the process under investigation. For the purpose of this investigation, common element types found in literature would be assessed to determine the extent at which choice of element types significantly affect the beam-column connection response.

7.3.2 Material properties

The material property for the bolts is extracted from EN *1993-1-8 Table 3.1 - Nominal values of* f_{yb} *and* f_{ub} as 640N/mm^2 and 800N/mm^2 for grade 8.8 bolt. The grade of steel assumed for this study is S355, the yield strength (f_y) and the ultimate strength (f_u) is based on the nominal thickness of elements (Table 7 of EN 10025-2). Consequently, the values for the yield and ultimate strength are 345N/mm^2 and 470N/mm^2 respectively. The yield strain for steel was obtained as a ratio of fy/E = 0.0018. In conventional design, nominal stress - strain relationship for steel otherwise called engineering stress strain relationships are used. However, under loading conditions the cross-sectional area of the material reduces over a

given period of time. In view of that, the true correlation of stress and strain of the material is expressed as:

$$\sigma_{true} = \sigma_{eng}(1 + \varepsilon_{eng}) \quad \textbf{7-1}$$

$$\varepsilon_{true} = ln(1 + \varepsilon_{eng}) \quad \textbf{7-2}$$

7.3.3 Boundary conditions

The boundary condition was created in the initial step and named "fixed ends". In the edit dialogue box, the displacements and rotations (U1, U2, U3, UR1, UR2 and UR3 = 0) was set to zero to fully constrained the ends of the column from rotation and displacement. The ends of the beams are restrained from lateral and torsional motion while vertical displacement is allowed.

7.3.4 Contact modelling

ABAQUS contact function was used in simulating the interaction between contact pairs. The surface to surface discretisation method with small sliding option was adopted for all the interacting contact pairs. The finite or small sliding allows separation or sliding of surfaces along the elements during analysis although it does not allow overlapping of surfaces. The tied surface is used to simulate welding between components, in this case between the beam and plate, and is used where discontinuity between mesh sizes (dense and coarse) of two components meet. Small sliding was used between the bolt head and the base component or the nut and the base component. For all the components in contact, a master and slave surface interaction was defined. The component with the coarser mesh or having a stiffer body will be the master surface while the other one will be the slave surface (ABAQUS 2011). On the Edit interaction dialogue box, the slave adjustment option to remove over closure option was used for the friction and frictionless contact interaction properties defined. Two interaction contact properties were defined, friction and frictionless. The friction formulation for the tangential behaviour is 'penalty' with a friction coefficient of 0.3 while for normal behaviour, the pressure-over closure was "HARD" contact with penalty constraint enforcement method. The allow separation after contact was allowed to ensure visible deformation of contact bodies during analysis where necessary. The contact surface was

modelled using the surface to surface contact with finite sliding. The surface of the regions considered for contacts are:

- End plate and bolt head
- Column flange and end plate
- Column flange and nut
- Bolt shank and Endplate/column flange hole
- End plate and beam.

The next section presents some preliminary basic investigations including the mesh sensitivity analysis, verification analysis and the investigation of the control model under pure shear and catenary load.

7.3.5 Loading

Shear force loads are applied on the top flange of the beam at 50mm away from the face of the column while catenary forces are simulated as tensile force acting on the end face of the beam.

7.4 Basic investigations

A preliminary investigation was carried out on the effect of shear and catenary force on connection response. These investigations are presented in subsequent subsections. After the preliminary investigations, the model used as the control was assessed for shear force and the initial catenary force developed in the braced frame system presented. Details of the stress contours of the beam column connections are presented to establish the state of stress of the control model before the column removal scenario.

7.4.1 Mesh sensitivity analysis

ABAQUS FEA presents four element shapes in the mesh control dialogue box with multiple techniques for meshing. The free, structured and sweep are the basic techniques commonly used on regular shapes. The choice of the mesh control determines the choice of the element types which could either have a standard geometric or quadratic order. For the purpose of this investigation, the hex element shapes with reduced integration was used to assess the extent at which the number of elements significantly affects the stress state of the element in

an assembly. Figure 7-4 presents the mesh sensitivity analysis on the connection model at varying elements sizes and corresponding maximum von-Mises stress. The results show that for the number of elements above 30000, there is a consistent response in all the structural elements of the model under investigation. Consequently beyond this value, an increase in the number of elements does not significantly affect the component response under constant loading conditions.

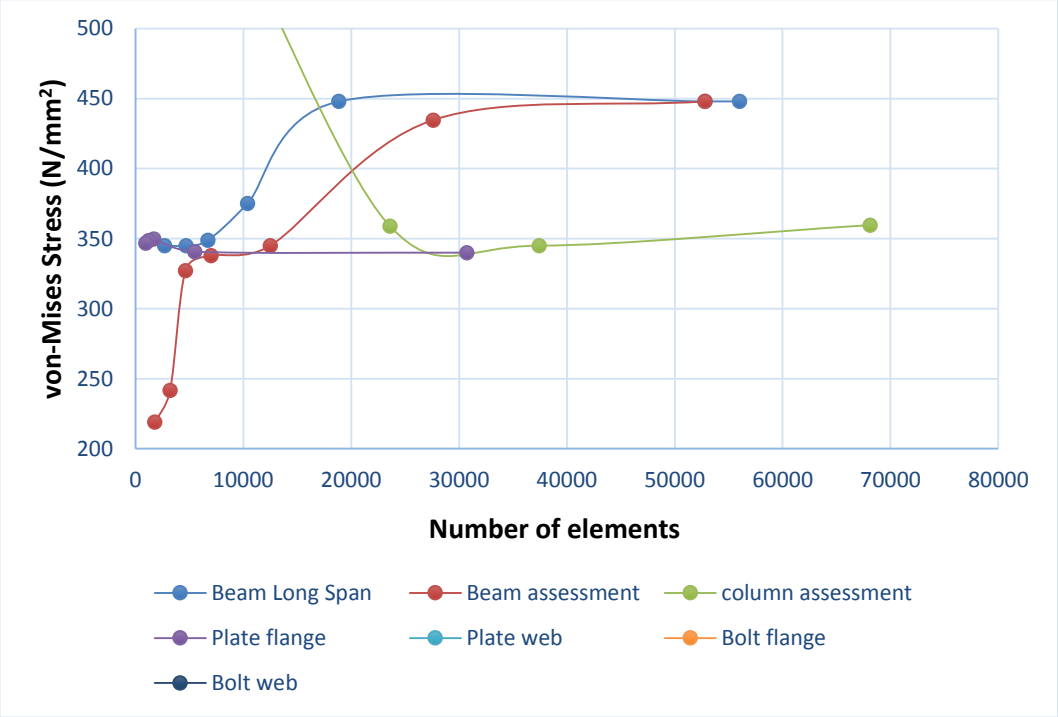

Figure 7-4 Mesh sensitivity analysis

On the other hand, the column exhibits a different trend, though it stabilises when the number of elements exceed 30000. The elements were further verified using ABAQUS standard analysis checks as presented for each component in the next subsection.

7.4.2 Mesh verification analysis

The mesh verification in ABAQUS is shown in Figure 7-5.

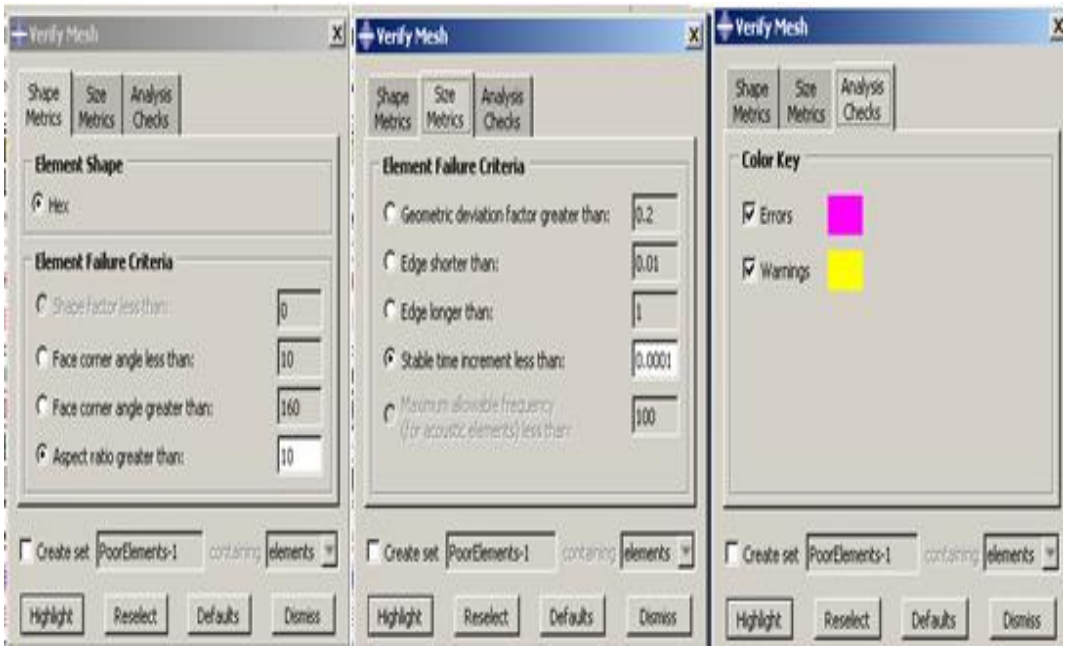

Figure 7-5 Failure criteria checks (ABAQUS 2011)

ABAQUS presents three important verification processes for all elements: The shape metrics, size metrics, and the analysis checks. The analysis checks uses a colour codes under which the elements are checked for analysis warnings and errors when the size metrics presents a failure criteria. The standard element failure criterion defined by the code is presented in Figure 7-5. For all the elements investigated, these checks were carried out to ensure that the elements satisfy standard failure criteria in ABAQUS. The analysis check was carried out on all the elements to ensure there are no warnings or errors in the elements before submitting the job for analysis.

7.4.3 Simple connections investigated as case studies

The simple connection used for this study is an end plate beam column connection. These connections are commonly used in practice in the construction industry to resist shear forces and a tensile force of 75kN. As shown in Figure 7-6, the end plate is connected to the flange and web of the column. The design of the section sizes for the plates and bolt components were based on the static response obtained from SAP 2000.

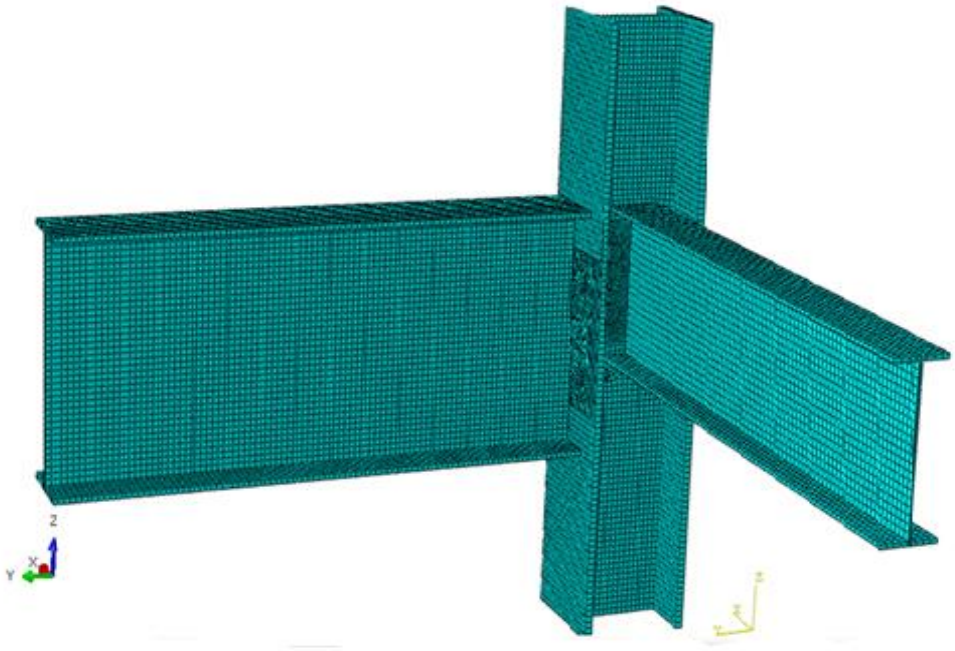

Figure 7-6 Meshing of end plate beam column connection

The beams are assumed welded to the plate, and the plate is bolted to the column. The interaction between the beam and the plate is defined by the tie constraints while the interaction between the plate and the column is defined by the friction constraint. The friction constraint was defined by tangential and normal behaviours based on the penalty friction formulation and "Hard contact" respectively (ABAQUS (2011). The bolt shanks interacting with the plate and column hole are defined by the frictionless contact formulation. This connection was assessed based on static shear force response only to check if the beam lateral restraints significantly affect the response of the structure or not.

7.4.4 Effect of catenary force on connection response

This section presents the results of the investigation of the connection to catenary force only. The objective of this investigation is to assess the response of simple connections to pure catenary force action. The catenary force action in the beam (BM 301) along the short span is 1.06kN, which is equivalent to a pressure of 0.213N/mm^2. Along the long span, the catenary force in the beam (BM 548) is 0.55kN corresponding to a tensile stress of 0.196N/mm^2 Consequently, the connection is assessed for a catenary force of 75kN which corresponds to a pressure of 15.09N/mm^2 in the main beam (BM 548) and 26.78N/mm^2 along the short span (BM 301). As shown in Figure 7-7, the maximum von Mises stress

response is 640N/mm^2 due to catenary action. The maximum stress occurs in the bolt connecting the web of the column, on the other hand, the bolts on the column flange have a maximum response of 358.9N/mm^2.

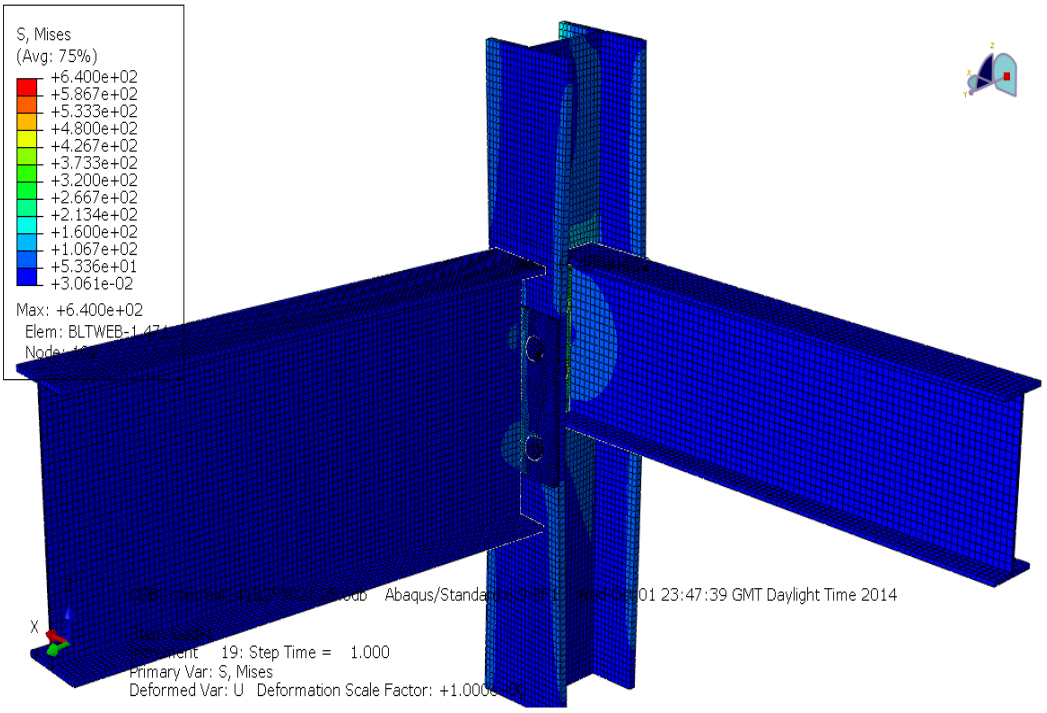

Figure 7-7 Stress contours under catenary force

7.4.5 Effect of shear force on connection response

The plate connecting the flange of the column has a stress value of 263.8N/mm^2 while the plate connecting the web of the column to the tie beam have a stress value of 327N/mm^2. The maximum stress in the column occurs in the column web with a magnitude of 579.2N/mm^2. This implies that for connection designs scenario, the column web is the most important region for design check where the tie beam is connected to the web of the column. In addition to the column web, the bolts at the column web is 78.3% stressed as compared to the bolts located at the flange of the column under the same tensile force loading condition.

This subsection investigates the behaviour of simple connection under pure shear force without consideration for the catenary or tensile force response. The shear force applied on the main beam (BM 548) was 80.17kN which was the static response obtained from the

investigation of the 10 storey building. On the tie beam (BM 301) a shear force response of 34.58kN was applied to the connection. These shear forces were applied at 50mm away from the face of the column. To obtain a pure shear force scenario is unrealistic in modelling, therefore the assumption is to apply the shear force 50mm away from the column face. Global stress contour response of the connection is presented in Figure 7-8. The maximum von Mises stress developed in the connection is 464.8N/mm^2 and it occurs at the column web bolt hole. The maximum stress on the plate connecting the column flange is 345N/mm^2, and this occurs at the base of the plate.

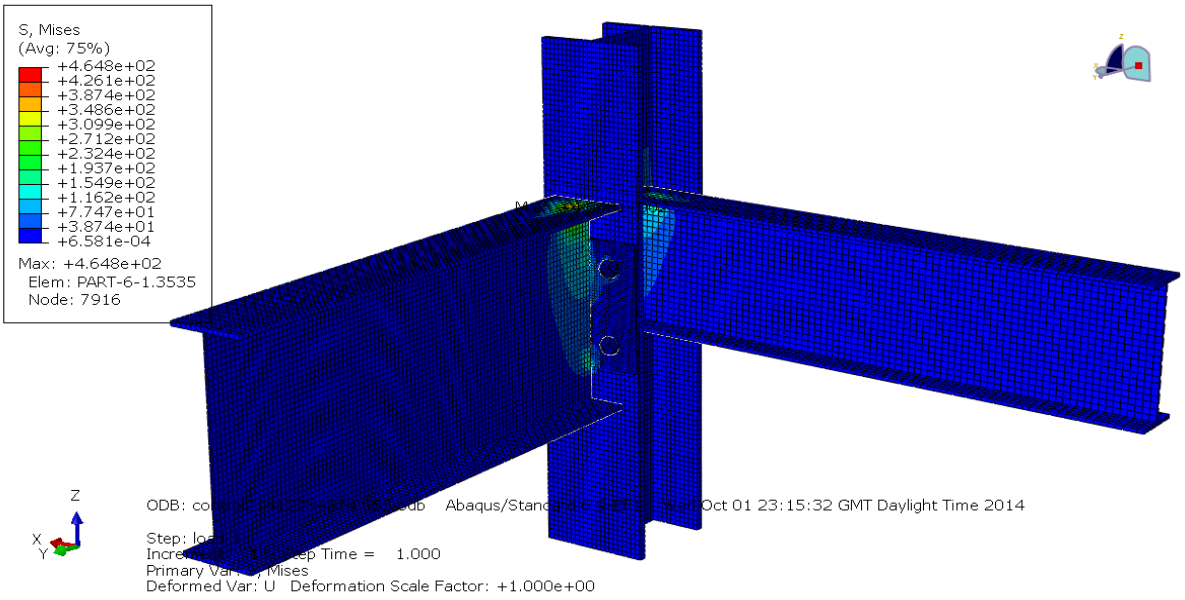

Figure 7-8 Connection response under shear force

The plate connecting the web of the column to the tie beam developed a stress of 296.4N/mm^2. The bolts at the web have a maximum stress of 289.4N/mm^2 that is approximately 2% more that the stress developed in the bolts connecting the flange of the column to main beam. Following a relative comparison of the shear stress components (S12, S13 and S23), it was observed that the maximum shear stress on the plane x-y occurs on the nut having a stress of 151.2N/mm^2.

The maximum shear stress on the x-z plane occurs at the column web with a value of 125.9N/mm^2 while the maximum shear stress on the y-z plane is 180.4N/mm^2. Contour plots for the shear stress components under shear force are presented in

Figure 7-9 through Figure 7-11. The maximum response on plane x-y (S12) is 151.2N/mm^2, on plane x-z (S13) is 125.9N/mm^2 and on plane y-z is 180.4N/mm^2.

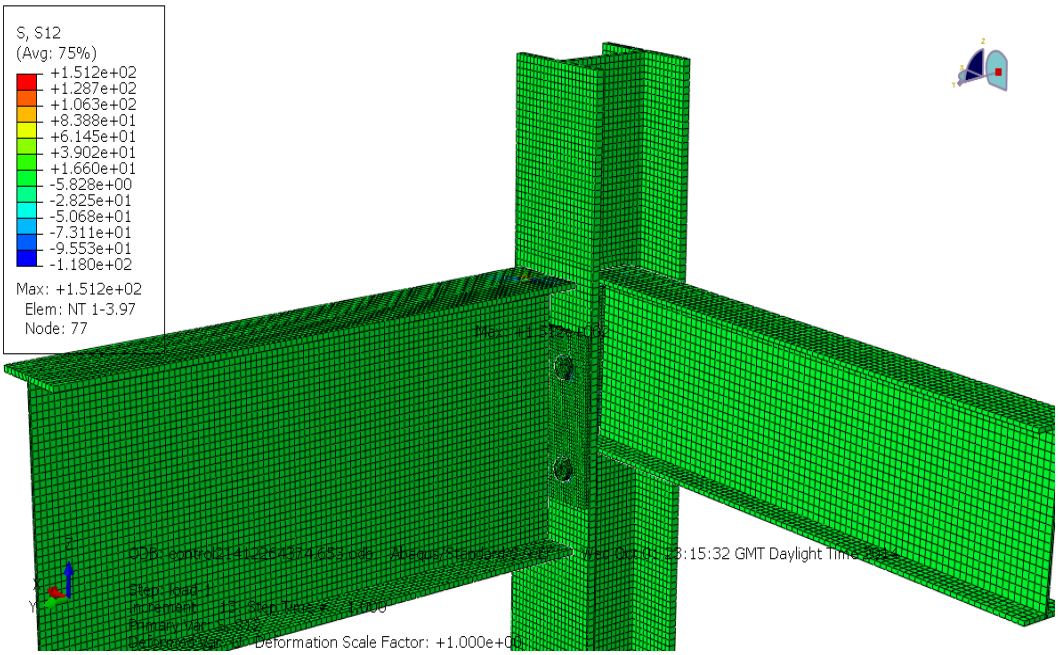

Figure 7-9 Shear stress contours on plane x-y

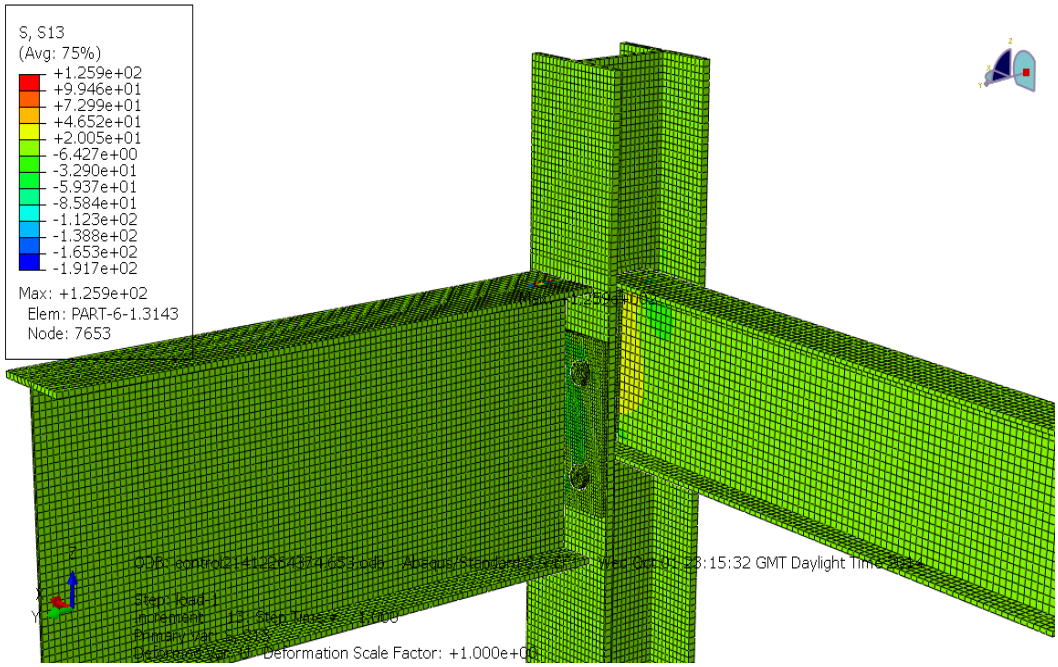

Figure 7-10 Shear stress contour along x-z plane

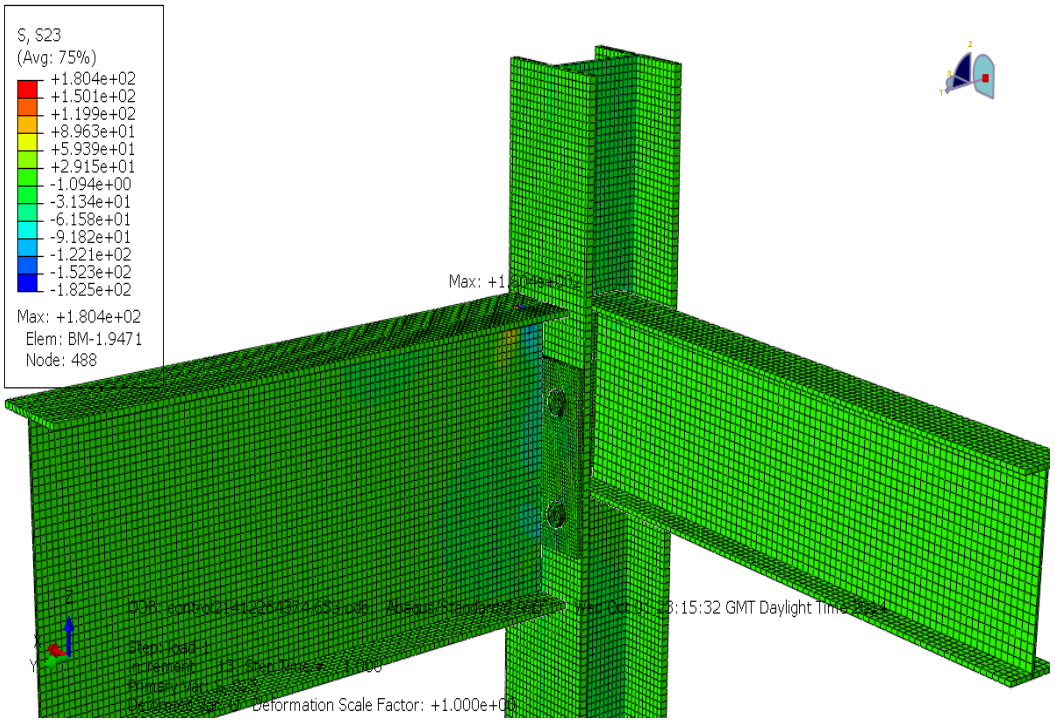

Figure 7-11 Shear stress contour plots on y-z plane

The next section presents the assessment of the connection under static conditions with and without the 75kN tensile force recommended in Eurocode 3 for connection design. Emphasises is based on the consideration of 75kN since it exceeds the initial axial tension in the connection.

7.5 Assessment of beam column connection control

Having investigated the behaviour of these connections under catenary action and shear force action, this section presents the behaviour of the connection under the interaction of shear force and catenary force action. The magnitude of the shear force and catenary force were obtained from the SAP 2000 structural analysis model. The state of stress of these connections under the initial static connection is presented in the following subsection.

7.5.1 Stress contours of model used as control

This subsection describes the simple connections used as controls to determine its behaviour under the static loading conditions obtained from the SAP 2000 structural analysis program. In the previous chapter, a summary of the changes in the internal forces as a result of column removal was presented. This simple connection was assessed for two cases: 1) maximum

shear force (BM 548; 80.17kN, BM 301; 34.58kN) and minimum tensile force (BM 548; 1.06kN, BM 301; 0.55kN) in the beams under static conditions and 2) maximum shear force with consideration for 75kN tensile force for both beams. Figure 7-12 shows the maximum von Mises stress response of 465.2N/mm^2 based on the exact static response of the connection.

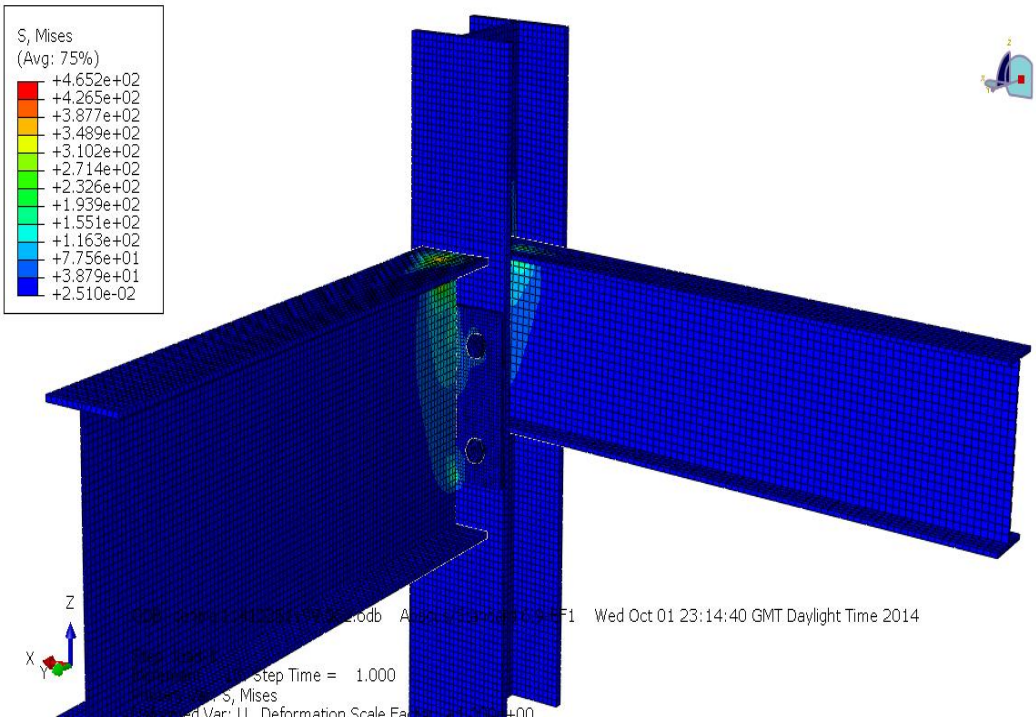

Figure 7-12 VM stress state of the connection

If the minimal tensile force response in the connection is replaced by 75kN, the maximum connection response increases by 37.57% as shown in Figure 7-13.

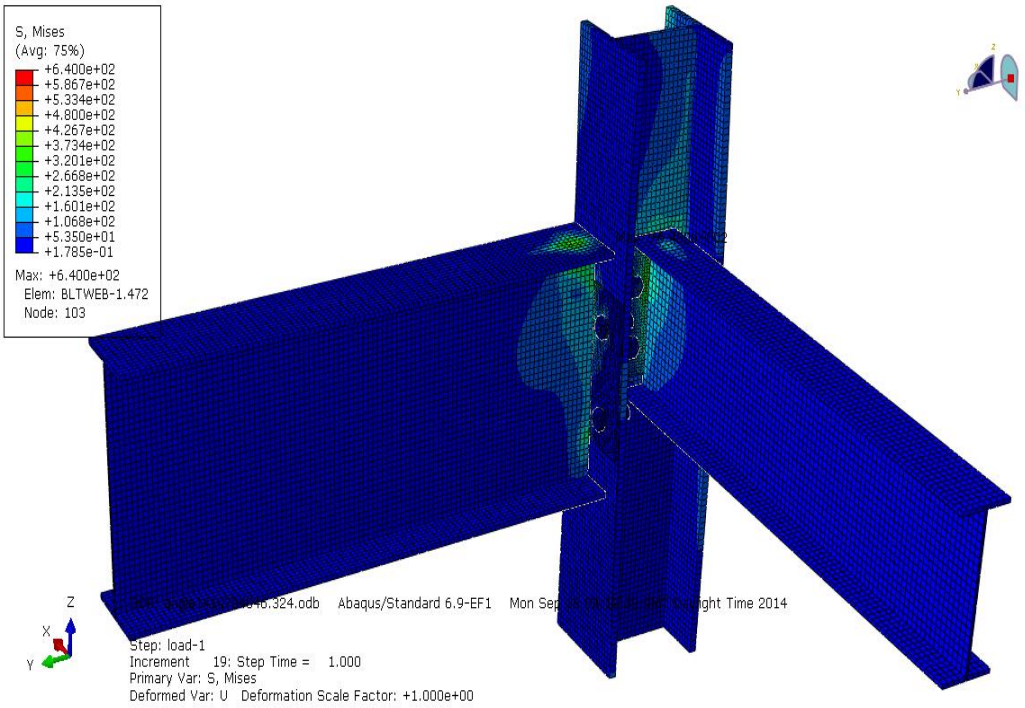

Figure 7-13 Stress state contours under static conditions

As shown above, the maximum stress concentration as a result of the loading is located in the bolt web. Using the von Mises stress-strain criteria, a comparison of the development of stress and strain in each of the component is presented in Figure 7-14.

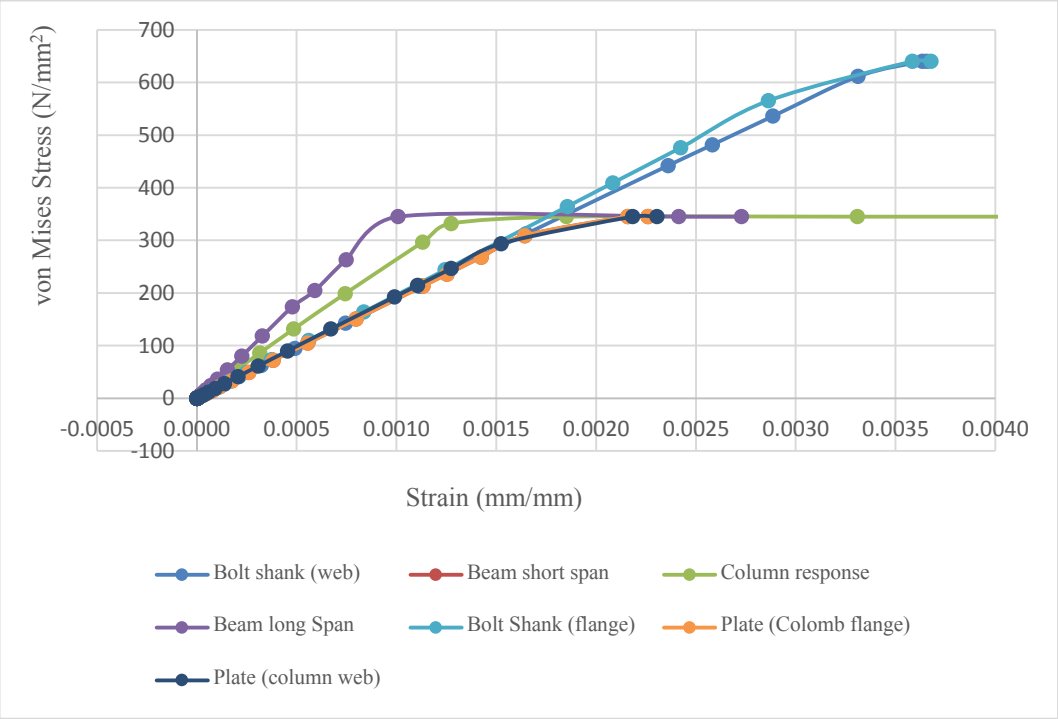

Figure 7-14 Stress state contours under static conditions

It was observed that as the stress increases, the strain increases up to 0.001 for all the components of the beam column connection. However, that is not the case beyond 0.001 for the main beam on the long span. It was observed that the plate connected to the web of the column, the bolts at the flange and the web, the plate connected to the flange to the main beam has an approximate linear stress strain response up to 0.0016 strain. On the other hand, elastic -plastic behaviour was observed for the beam at the long span and the column. Details of the stress distributions of the components are presented in subsequent subsections.

7.5.2 Stress contours in beams

Figure 7-15 presents the stress contour distribution for the beams at the short span and at the long span respectively. The maximum stress occurs at the location of the shear force is applied, which is 50mm from the face of the column for the beams. This state of stress defines the state of the beams before column removal as shown in Figure 7-15.

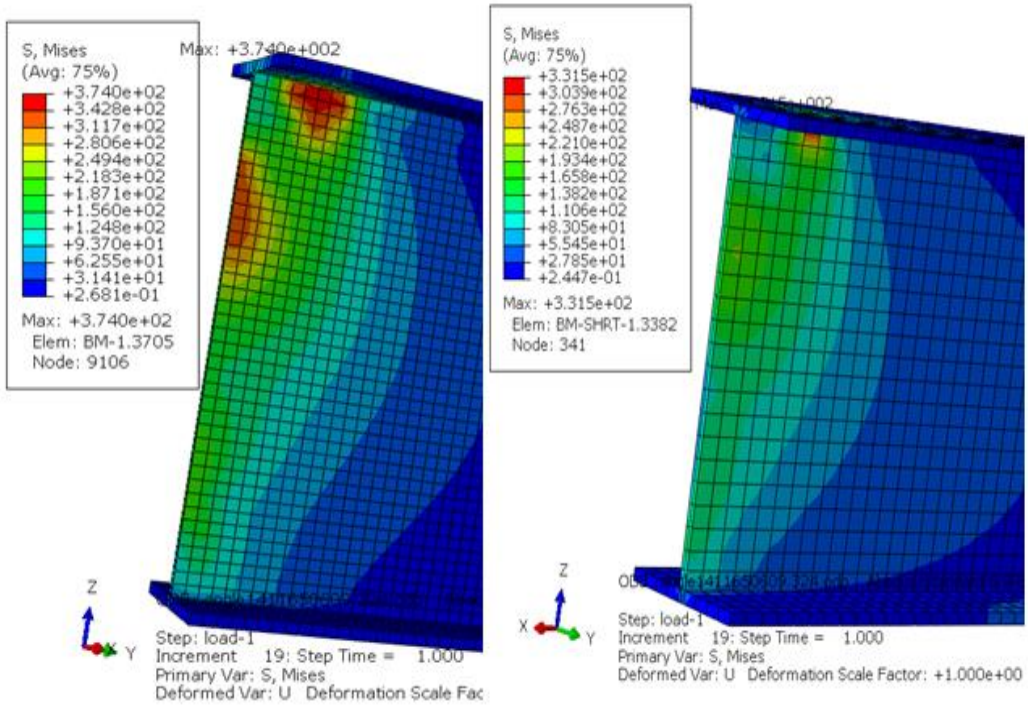

Figure 7-15 VM stress state contour under initial conditions

The maximum stress on the short span beam and long span beam is 331.5N/mm^2 and 374N/mm^2 respectively and occurs at the point of load application. The principal stresses developed in the main and tie beams are presented in Figure 7-16. It was observed that the maximum principal stress along the Y-axis for the main beam is 367.1N/mm^2 while the corresponding principal stress for the tie beam is 45.9N/mm^2 respectively.

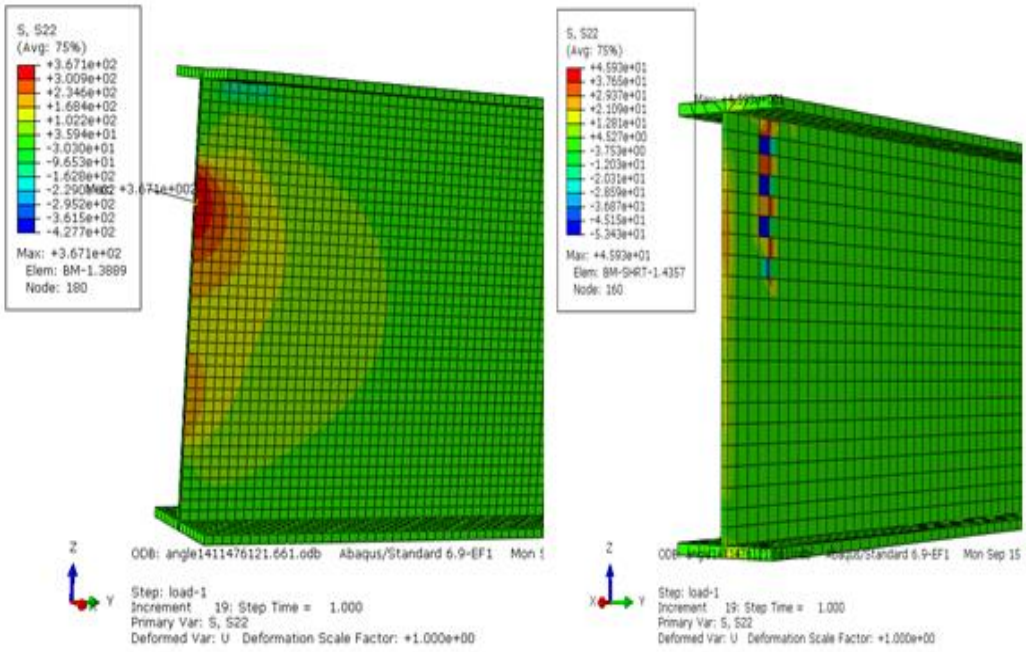

Figure 7-16 Principal stress contour (S22)

The principal stress distributions along the web of the beam propagate from the region of the beam end connection towards the free end of the beam as shown in the contour plots of Figure 7-16. The plot presented in Figure 7-17 shows the principal stress (S11) contours for the main beam and the tie beam respectively.

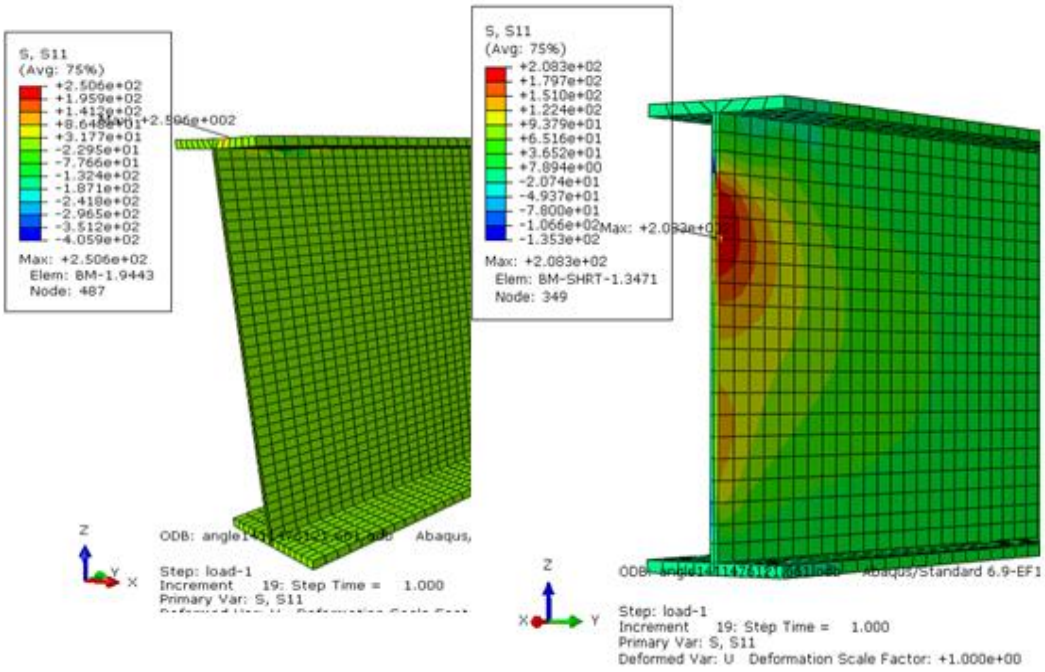

Figure 7-17 Principal stress contour under static conditions (S11)

The principal stresses on the main and tie beams are 250.6N/mm^2 and 208.3N/mm^2 respectively. The beam responses are compared, the principal stress in the main beam along the x-x axis shows that the main beam exceeds the tie beam with 20.3 %.

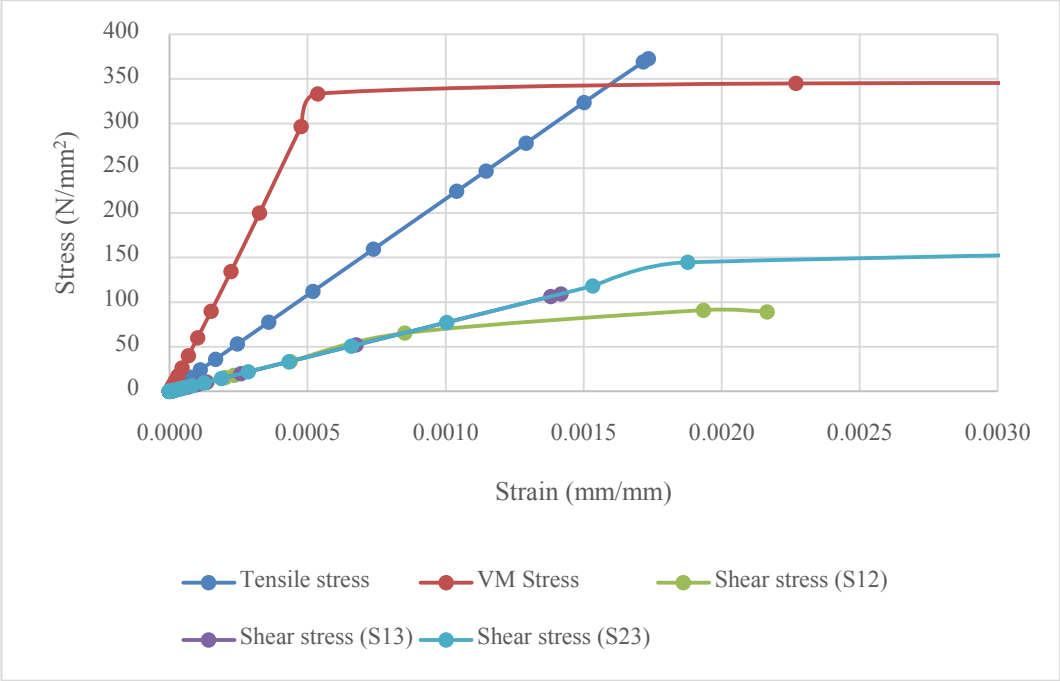

Figure 7-18 Stress vs strain components for main beam

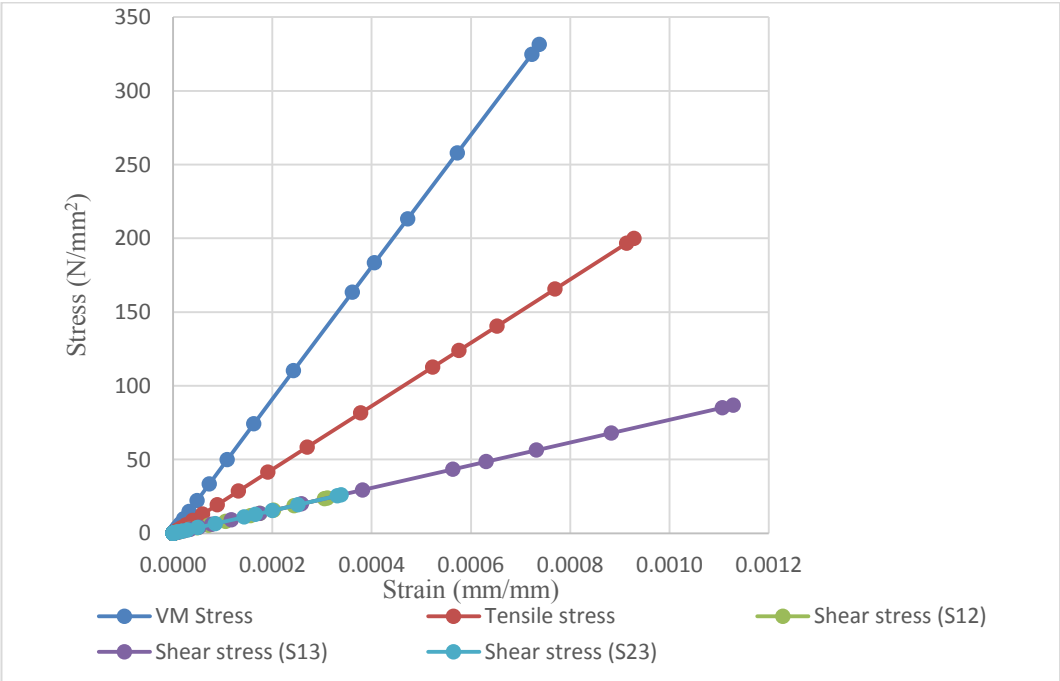

Figure 7-19 Stress components vs strain for tie beam

The development of stress components in relation to the strain for the main and tie beam is presented in Figure 7-18 and Figure 7-19.

From the plots presented in Figure 7-19, at constant strain for the main beam, it was observed that the von Mises stresses exceed the tensile stress in the beam by 109.4% within the maximum elastic limit. At 0.00053 strain point, the von Mises stress becomes relatively stable such that increased in strain does not increase the stress. However, that is not the case for the tensile force variation with strain. The tensile stress increases linearly with the development of tensile strain beyond 0.00053 up to 0.0015.

7.5.3 Stress contours in the bolts

Figure 7-20 shows the stress contours developed in the bolts connecting the flange of column (C'F) and the web (CW) respectively. The maximum stress developed in the bolts occurs on the shank of the bolt which interacts with the plate and column hole. The von Mises stress developed at the bolts connecting the flange of the main beam has a stress of 634N/mm^2 while the stress developed in the bolt shank of connecting the web of the column to the ties beam is 640N/mm^2.

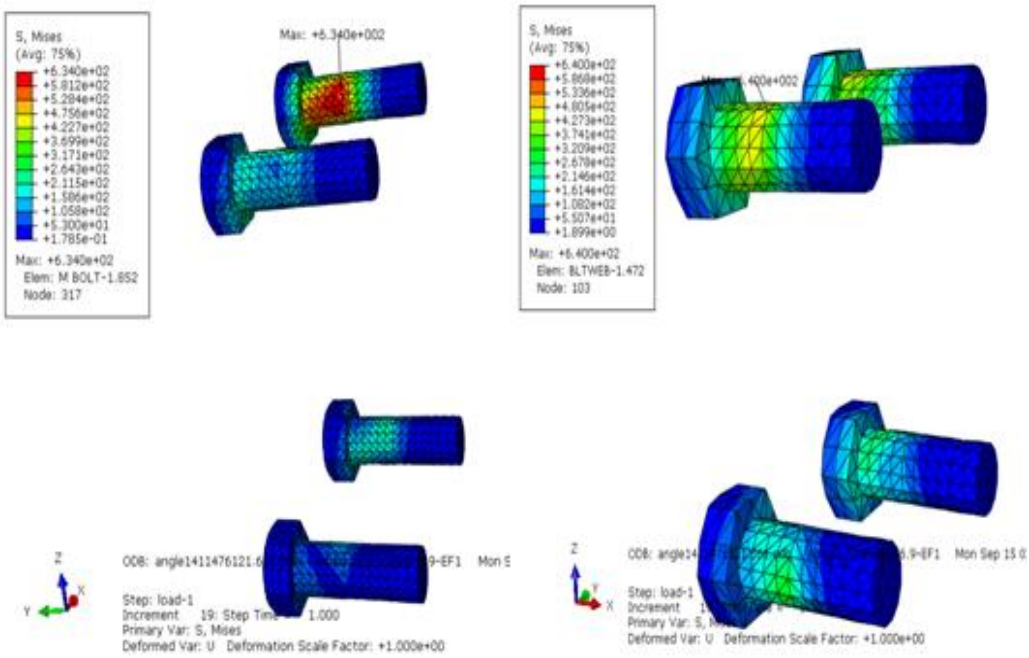

Figure 7-20 VM stress state for the bolts at CF and CW

The principal stresses (S11) developed in the bolts on the flange and web of the column is 234N/mm^2 and 518.5N/mm^2 respectively along the x-x axis. This axis is the main axis of the bolt connecting the plate to the web of the column. However, this x-x axis is the secondary or transverse axis to the bolts connecting the flange of the column through the plate to the main beam. Figure 7-21 presents the tensile stress state for the bolts along the principal axis (x-x).

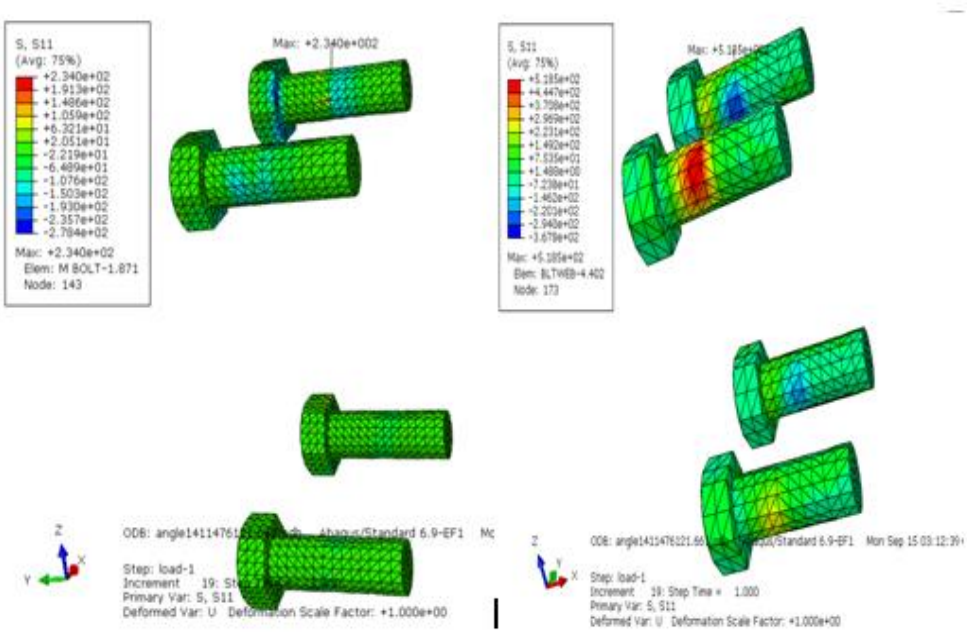

Figure 7-21 Principal stress state of bolts (x-x)

The comparison of these responses shows that the bolts connecting the tie beam to the web of the column exceed the main bolt connecting the flange of the column to the main beam by 121.6%. The stress contour plots for the principal axis (y-y) which is the main axis along the longitudinal direction of the bolts connecting the beam to the flange of the column via the plate are presented in Figure 7-22.

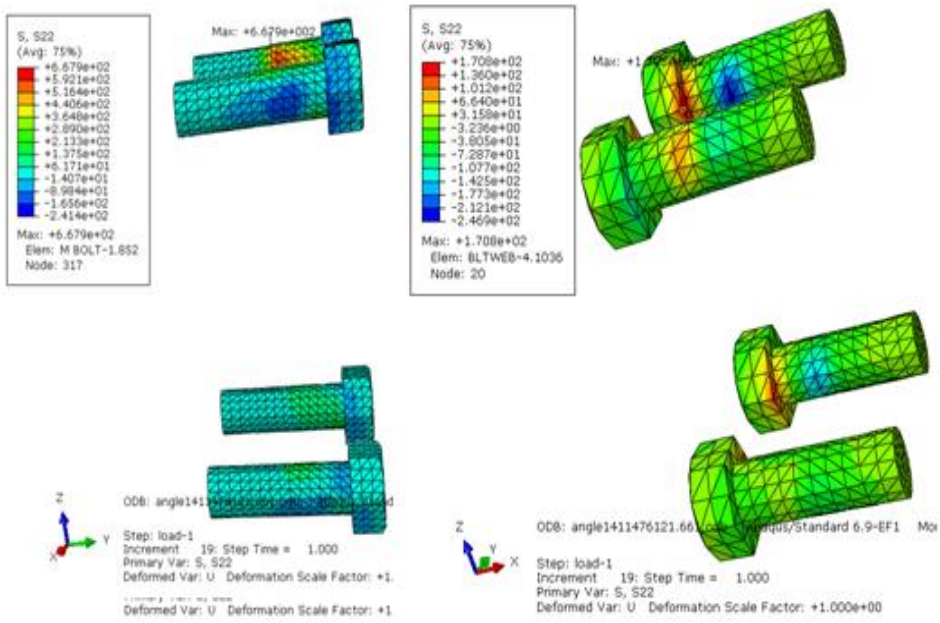

Figure 7-22 Principal stresses at C'F and CW respectively (y-y)

In this case the bolts connecting the main beam through the plate to the flange of the column has its main principal axis along the Y-Y direction while its secondary to the bolts connecting the tie beam to the web of the of the column. The maximum stress in the main bolt is 667.9N/mm^2 while the maximum stress in the bolts connecting the tie beam to the web of the column is 170.8N/mm^2. This implies that the principal stress developed in the main bolts exceeds the corresponding stress developed in the bolts connecting the tie beams by 291%. The stress developed along the vertical axis (z-z) in the bolts are presented in Figure 7-23. Along the vertical axis (z-z), the maximum stress on the main bolt is 319.7N/mm^2 while on the bolts of the web the maximum stress is 136.5N/mm^2.

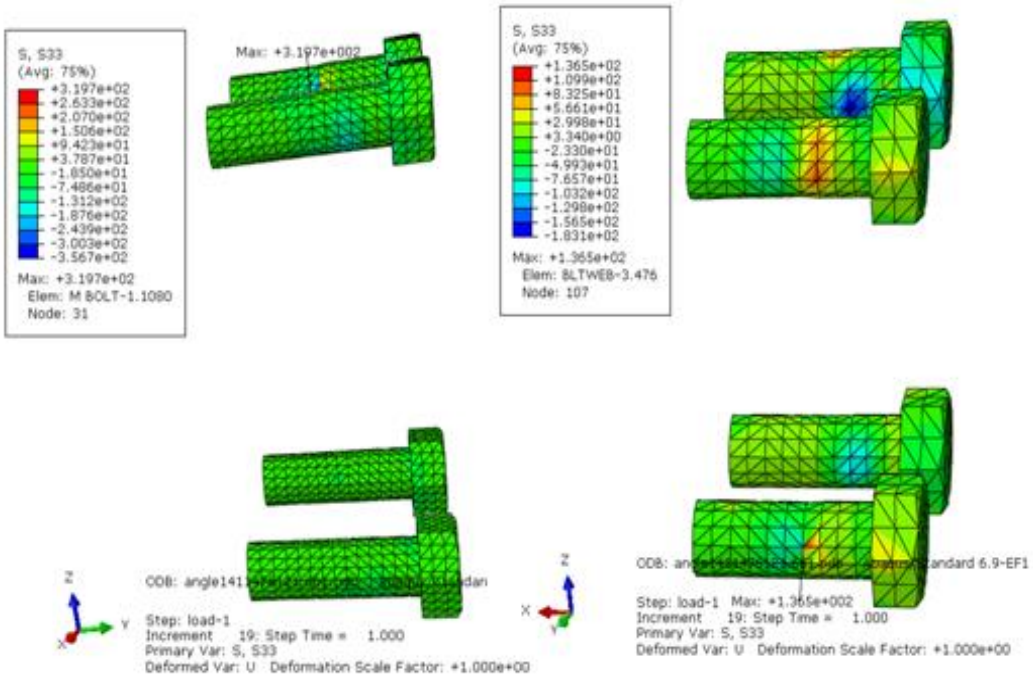

Figure 7-23 Principal stress state of bolts at C'F and CW (z-z)

Figure 7-24 presents the variation of tensile and shear stress corresponding to the strain for the bolts located at the web of the column. The maximum tensile stress developed in the bolts 695.2N/mm^2, this exceeds the yield strength by 8.6% and less than the ultimate yield strength of the bolt by 13.1%. The corresponding strain in the bolt is 0.31%. The maximum shear stress in the bolt is 168.8N/mm^2 and the maximum strain is 0.22%. This implies that along the z-z axis, the main bolts exceeds the bolts at the web of the column connecting the tie beam by 134.2%. The stress - strain progression for the bolts connecting the flange of the column to the main beam is presented in Figure 7-25.

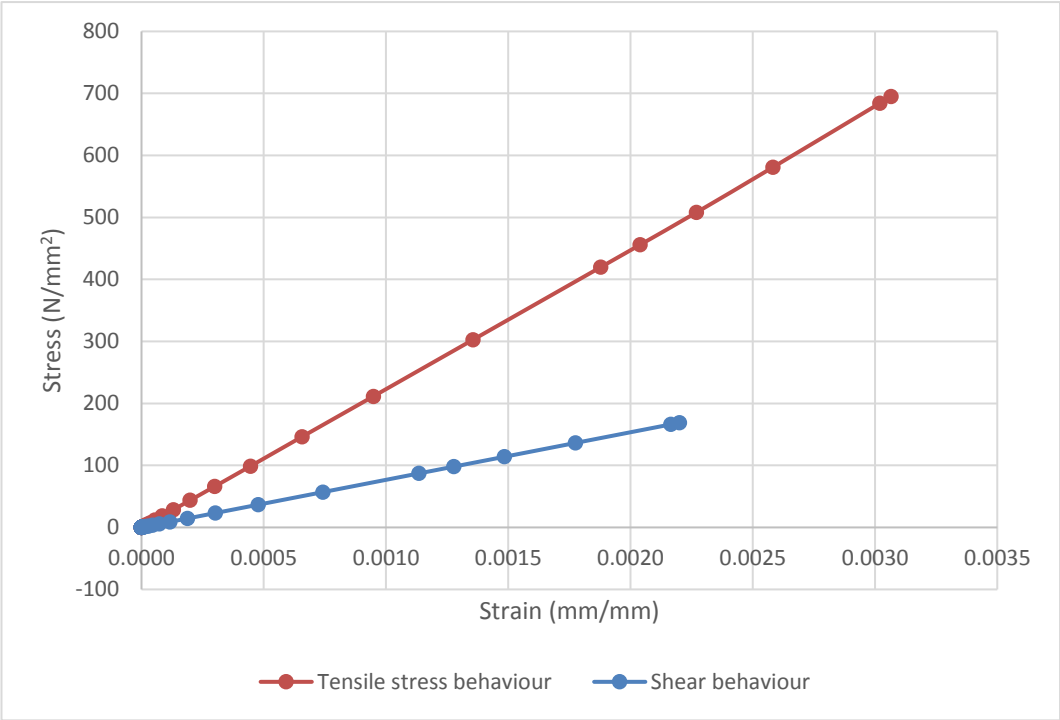

Figure 7-24 Stress vs strain for bolts at column web

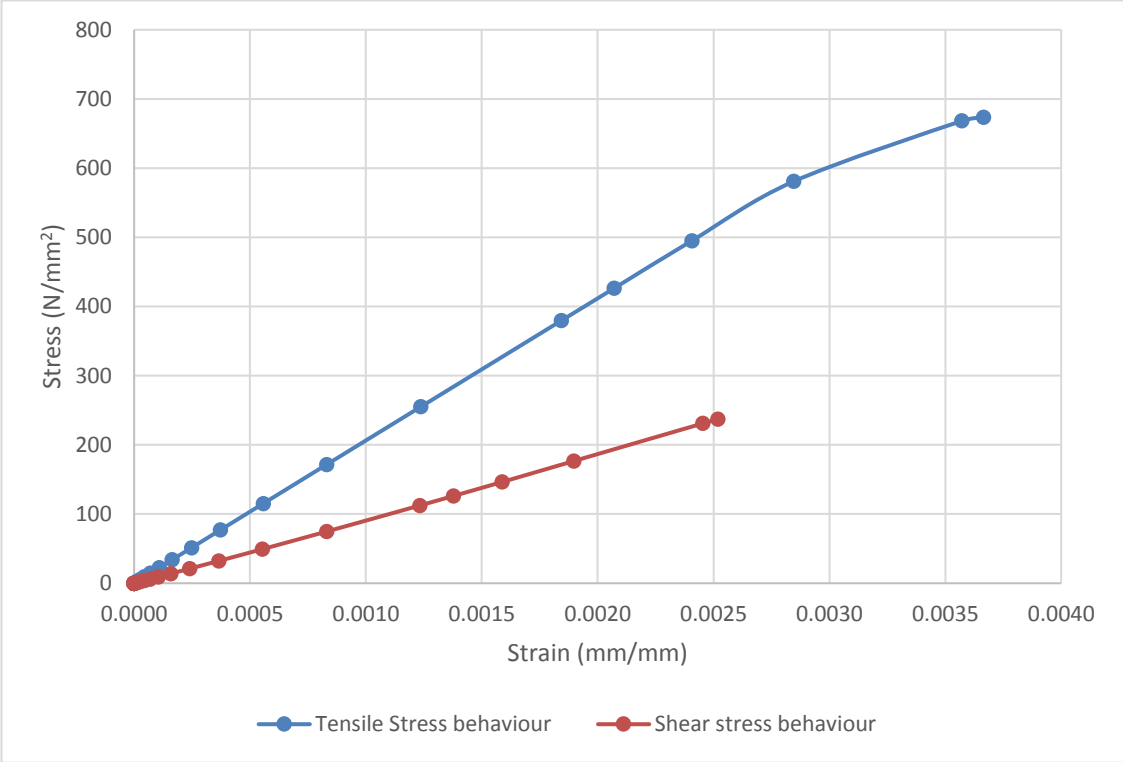

Figure 7-25 Stress vs strain for bolts at column flange

As shown in Figure 7-24 and Figure 7-25 the rate of stress formation corresponding to strain is higher for tensile force responses as compared to shear responses. From Figure 7-25, the maximum tensile stress is 673.5N/mm^2 corresponding to a strain of 0.37%. This exceeds the yield strength of the bolt by 5.2% and less than the ultimate tensile stress by 15.8%. The maximum shear stress in the bolts at the flange is 237N/mm^2 corresponding to a strain of 0.25%. Comparing the response of Figure 7-34 to Figure **3-35**, the study shows that the bolts at the web of the column are likely to fail relative to the bolts at the flange of the beam column connection.

7.5.4 Stress contours in plates

Figure 7-26 presents the response of the plate to static loading conditions.

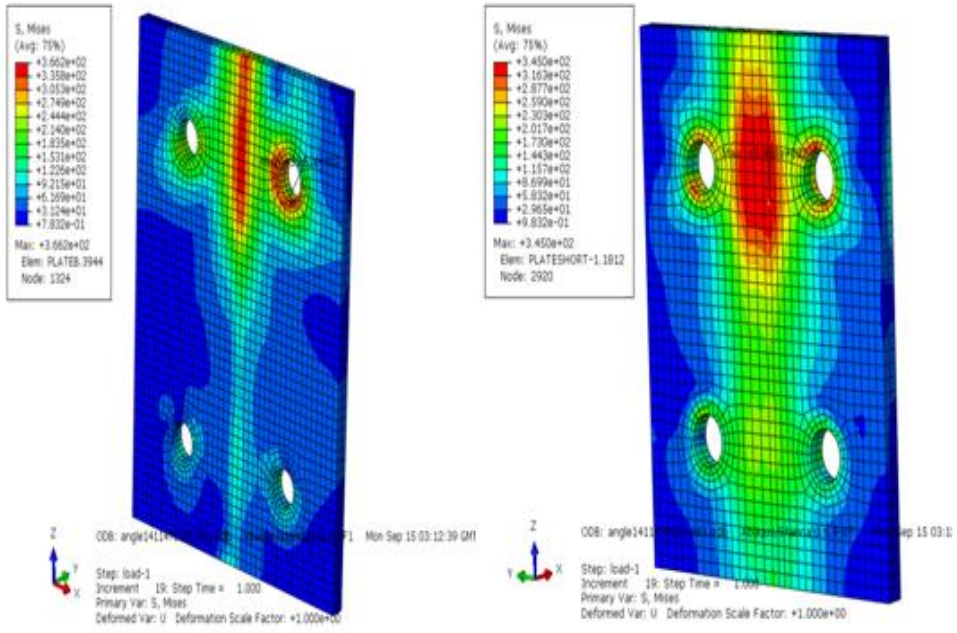

Figure 7-26 VM Stress contours in plates at C'F and CW

The von Mises stress for the plate connecting the web of the column is 345N/mm^2. This implies that the plate connecting the flange of the column is subjected to more stress relative to the plate connecting the web of the column by 6.14%. The plots of Figure 7-27 shows the maximum principal stresses on the plates along the x-x axis. The maximum principal stress along the x-x axis is 462.7N/mm^2 while the principal stress on the web of the column is 73.34N/mm^2 in tension and 243N/mm^2 in compression.

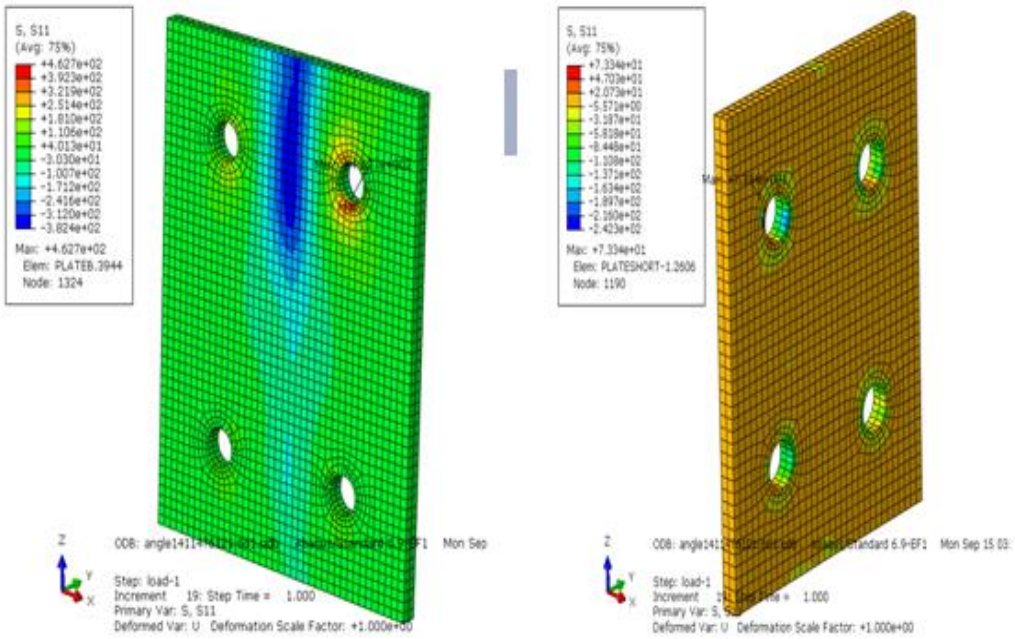

Figure 7-27 Principal stresses at C'F and CW (S11)

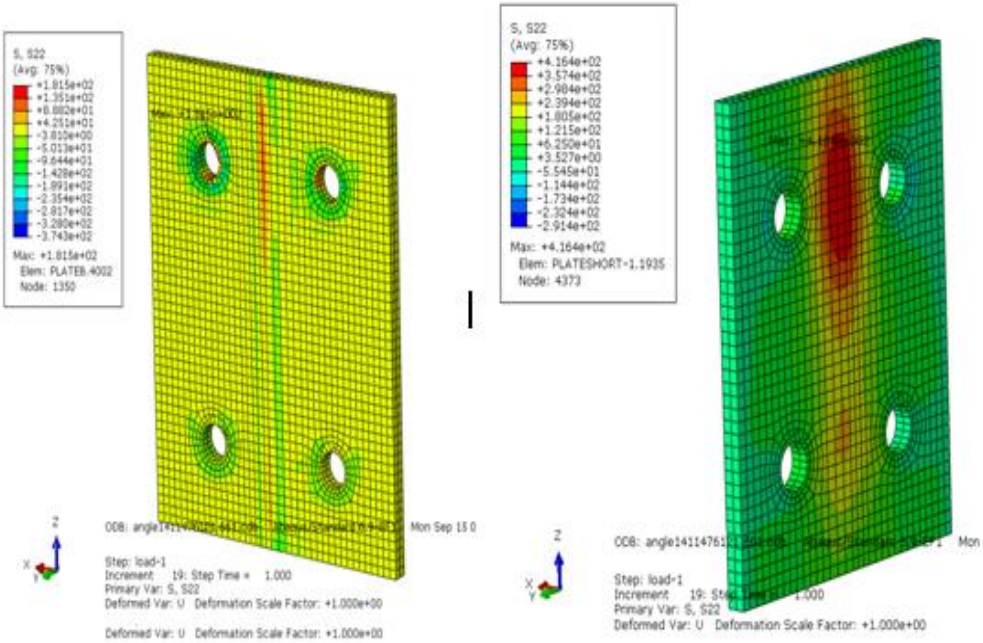

Figure 7-28 Principal stresses at C'F and CW (S22)

As shown in Figure 7-28, the maximum principal stress on the plate along the y-y axis connecting the web of the column is 416.4N/mm^2. However, some part of the plate is in compression with a 30% decline in stress relative to the tensile zones shown in red. On the other hand, the maximum tensile stress in the plate connecting the flange of the column to the main beam is 181.5N/mm^2. The compressive region has a stress increment of 106.2% relative to the tensile stress response for y-y axis. The variation of stress components with strains for the plates are presented in Figure 7-29 and Figure 7-30.

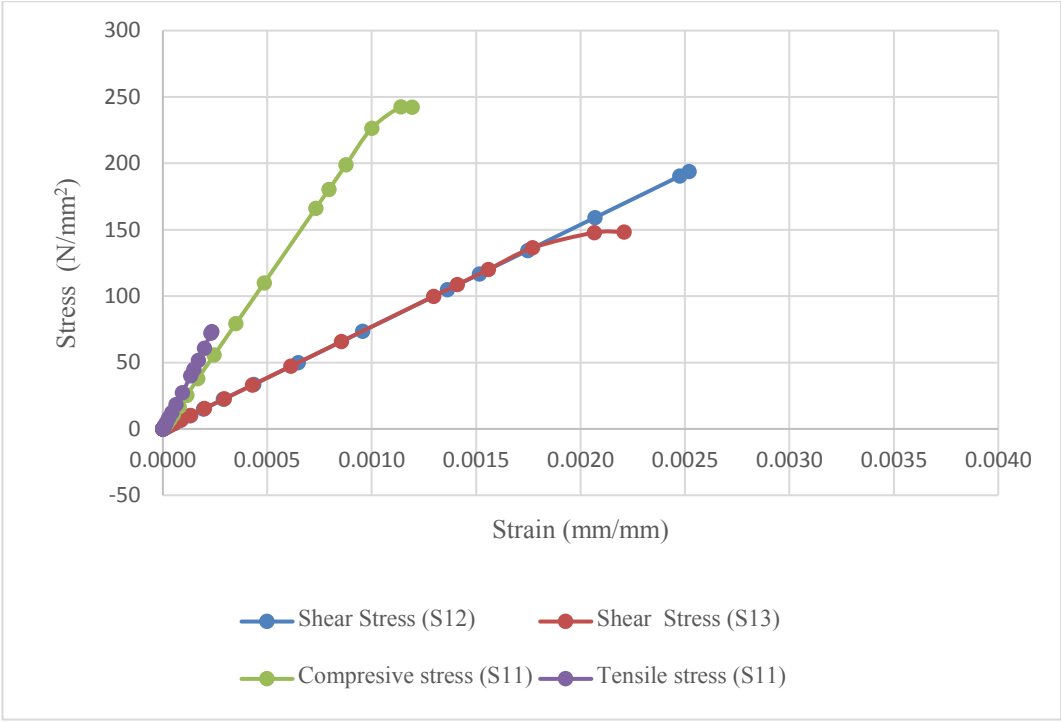

Figure 7-29 Stress components vs strain of plate at column web

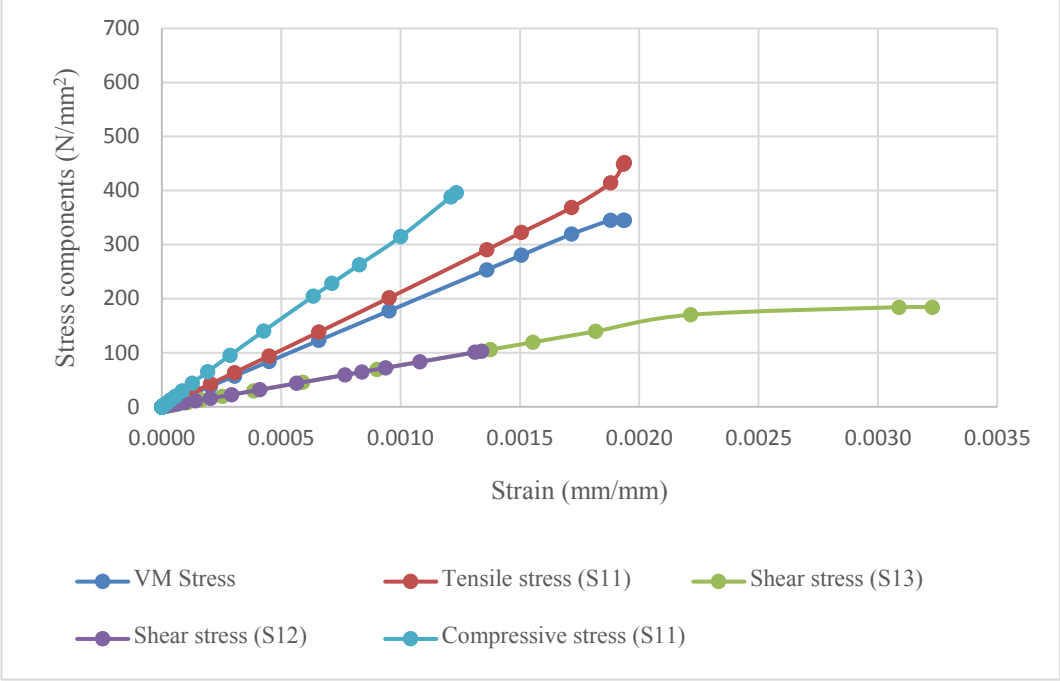

Figure 7-30 Stress components vs strain of plate at the flange

Comparing the tensile behaviour of the plates, it can be seen that along the principal axis (x-x), at 0.005 a maximum tensile stress of 145N/mm^2 is developed while the corresponding stress in the plate at the web is 24.82% lower. The shear stress patterns for the two plates are similar with the column web developing a relatively larger magnitude of shear stress.

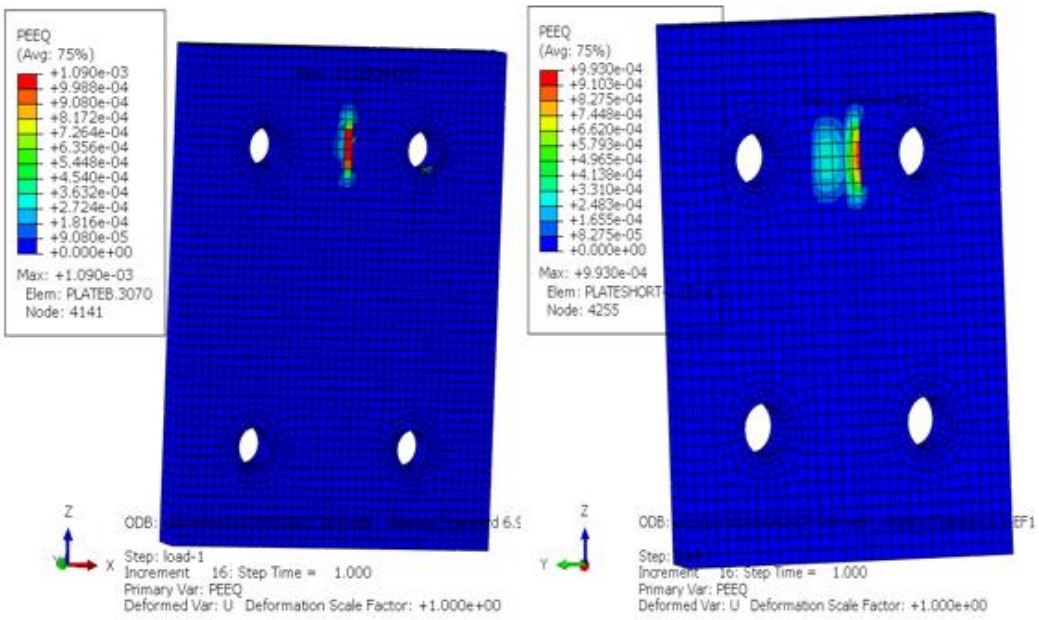

Figure 7-31 Plastic strain distribution in plates

7.5.5 Stress contours in nuts

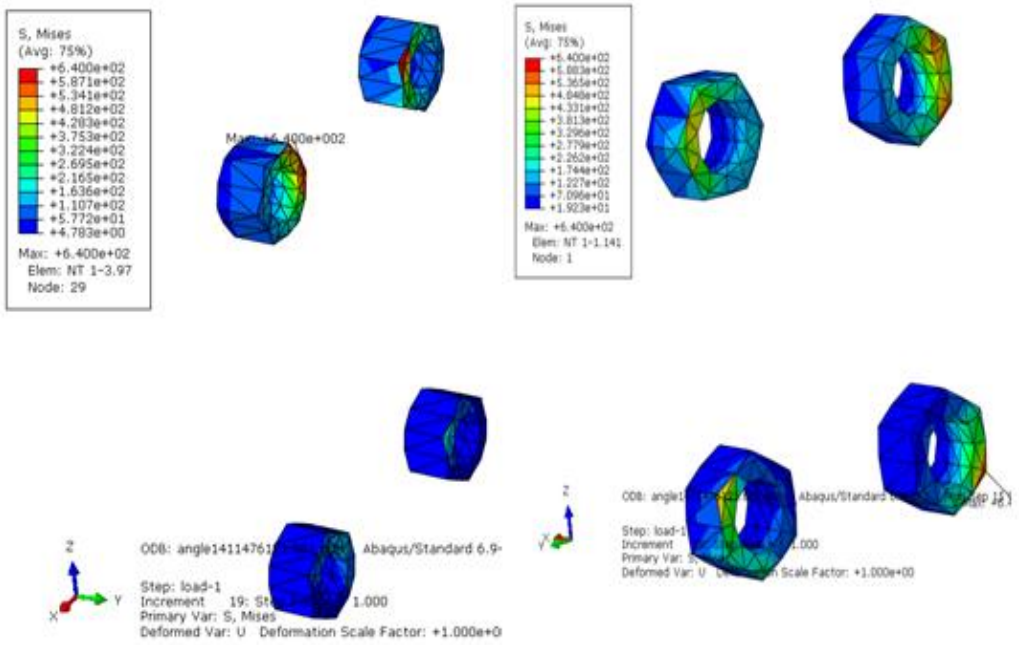

Figure 7-32 Von - Mises stress contours in bolts

Figure 7-32 is the von Mises stress state of the nuts under loading conditions. The maximum von Mises stress occurs at the nuts having a value of 640N/mm^2. The nuts at the web of the column and the nuts at the flange of the column are under the same state of maximum elastic stress. The minimum stress on the nuts is 478.3N/mm^2 which is 25.3% less than the elastic limit of the tensile stress. The details of the variation of the stress components with strain for the nuts is presented in Figure 7-33 and Figure 7-34

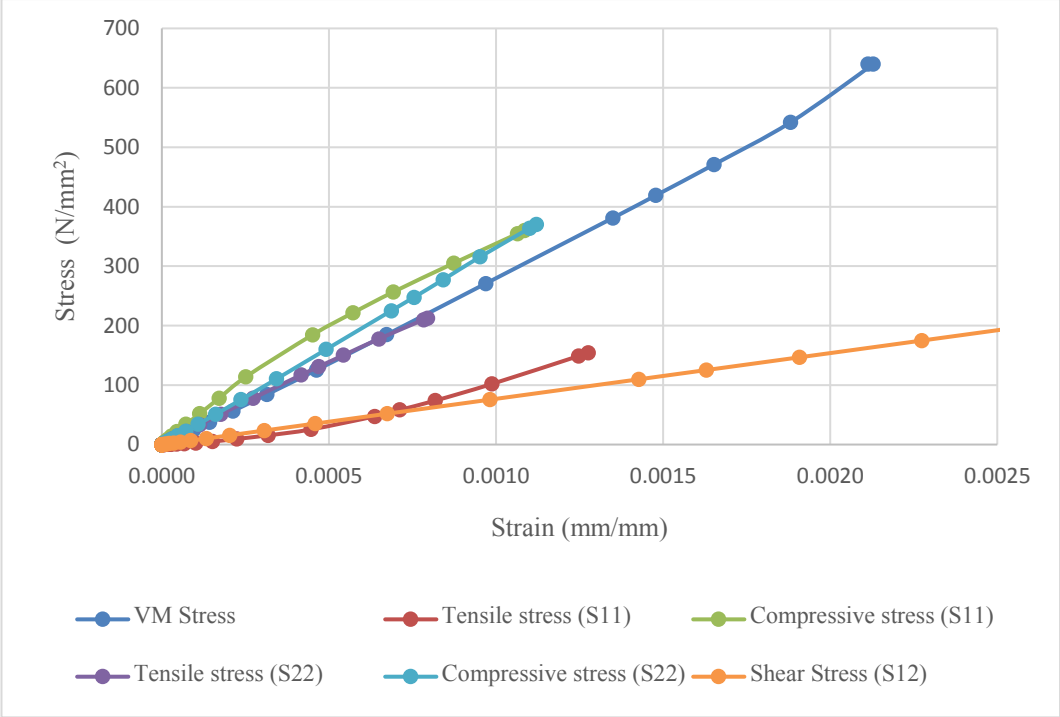

Figure 7-33 Von- Mises stress contours in nuts at column web

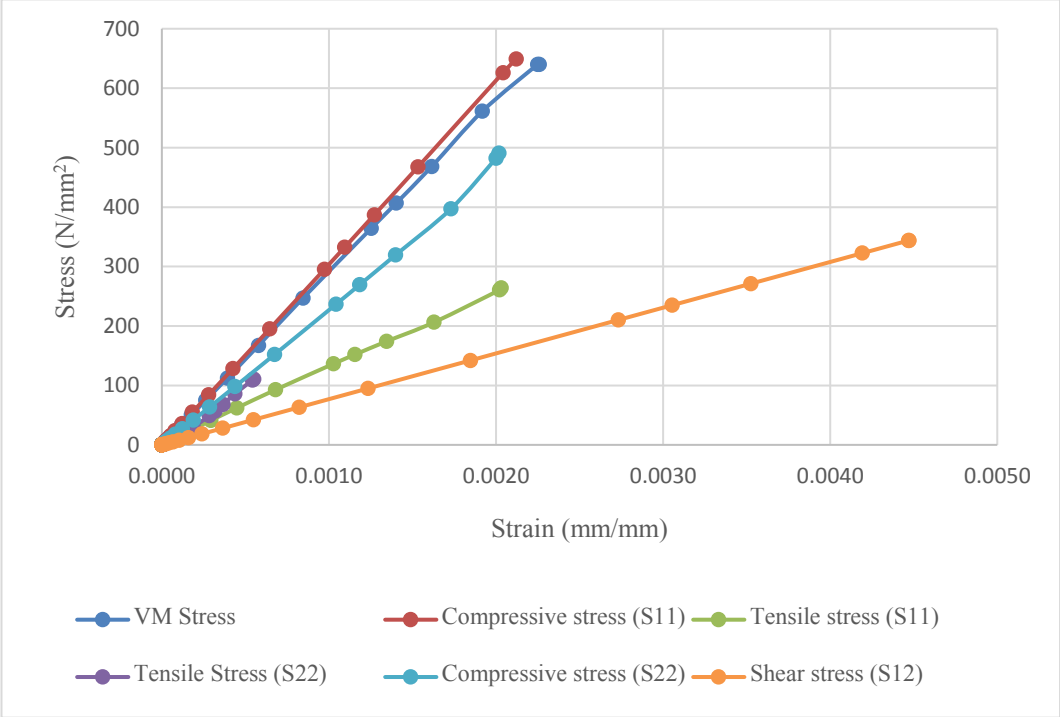

Figure 7-34 Stress components vs strain in nuts at the flange

Figure 7-34 shows the stress state of the nuts for compressive, tensile and shear stresses. Approximately, a linear variation of the stress-strain relationship occurs up to 0.002 strain for all the stress components investigated.

7.5.6 Stress contours in column

This subsection presents the response of the column based on the shear force and catenary force action under static loading conditions.

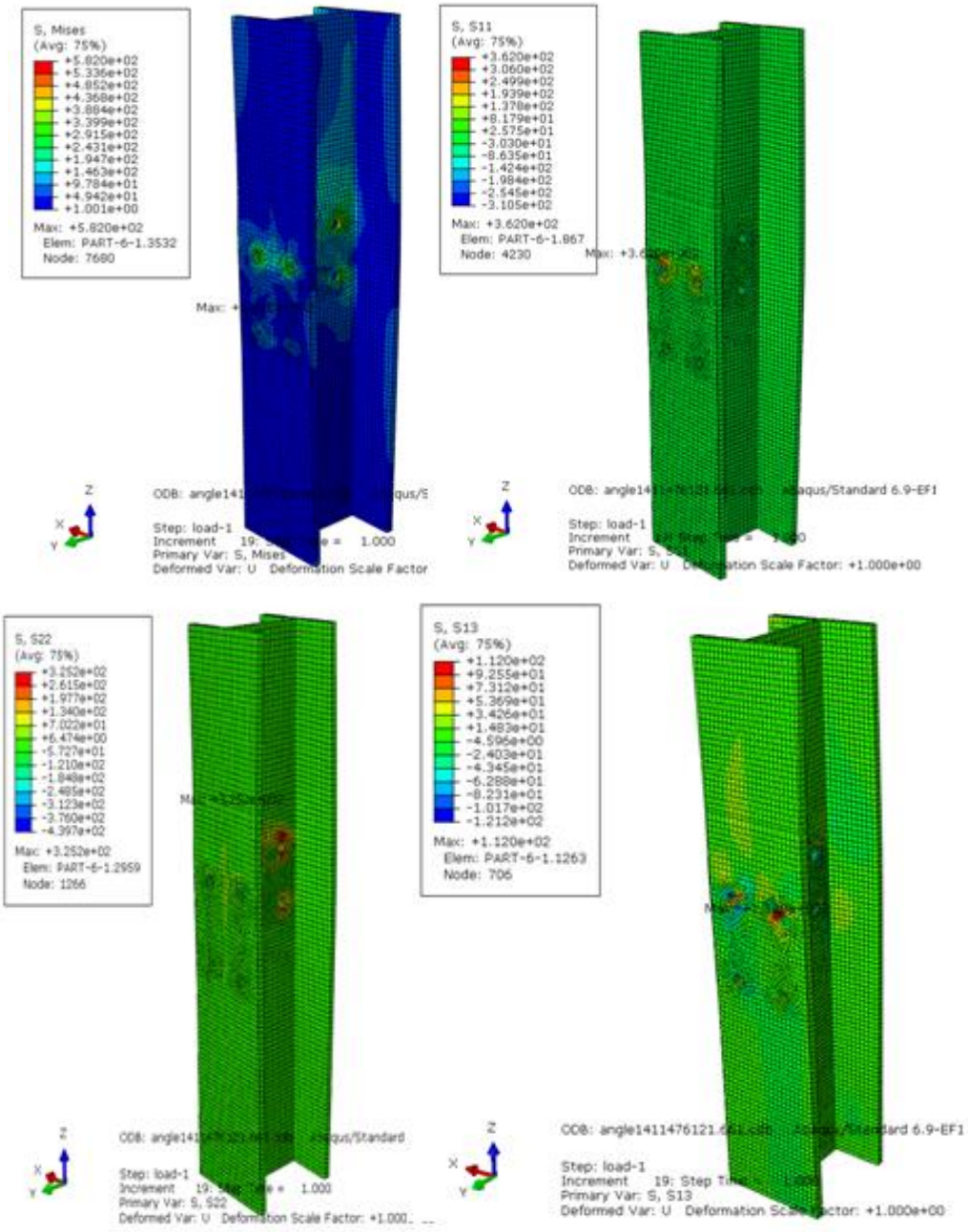

Figure 7-35 Stress components of the column

Figure 7-35 presents the stress distribution of the column under the initial conventional design state of shear and catenary action. It was observed that the maximum stress in the column is 582N/mm^2 which occurs at the compressive region of the column web. The shear stress, on the other hand, along the x-y plane of the column has a maximum value of 119.2N/mm^2 in the positive direction and this occurs at the edge of the hole in the column web. However, at the column flange bolt hole, the maximum shear stress on the x-y plane is 148.2N/mm^2. The initial distance from the outer face of one column flange to the other is 209.6mm before the load application. Applying the shear force and catenary action resulted to an increase of 8.3% as the column flanges bulges outward.

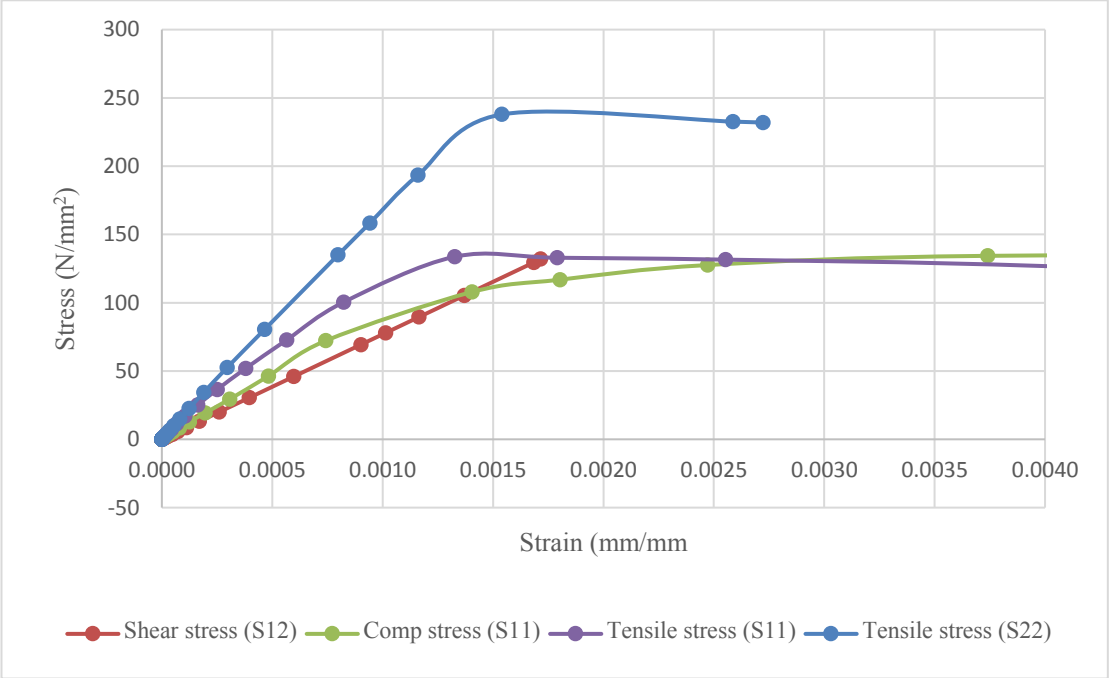

Figure 7-36 Stress components vs strain in column

As shown in Figure 7-36, the tensile resistance of the column at which the main beam is connected (S22), under conventional design scenario is higher as compared to the web of the column under tension as represented by (S11). The maximum tensile stress develop on the flange of the column is 237.92N/mm^2 as compared to the tensile stress of 132N/mm^2 at the web of the column. An approximate tensile stress ratio of the flange to the web under stable condition is 1.8.

7.6 Chapter summary

Figure 7-37 presents the summary of the investigation in establishing the stress values developed in the connection components as a result of the shear force and the applied tensile force on the connection. The variables (VM) refers to the von Mises stress, the shear component along the x-y plane is denoted by number (12) the shear component along the y-z axis is denoted by (2,3) while the principal stress along the x-x axis, y-y axis and z-z axis are denoted by (11), (22) and (33) respectively.

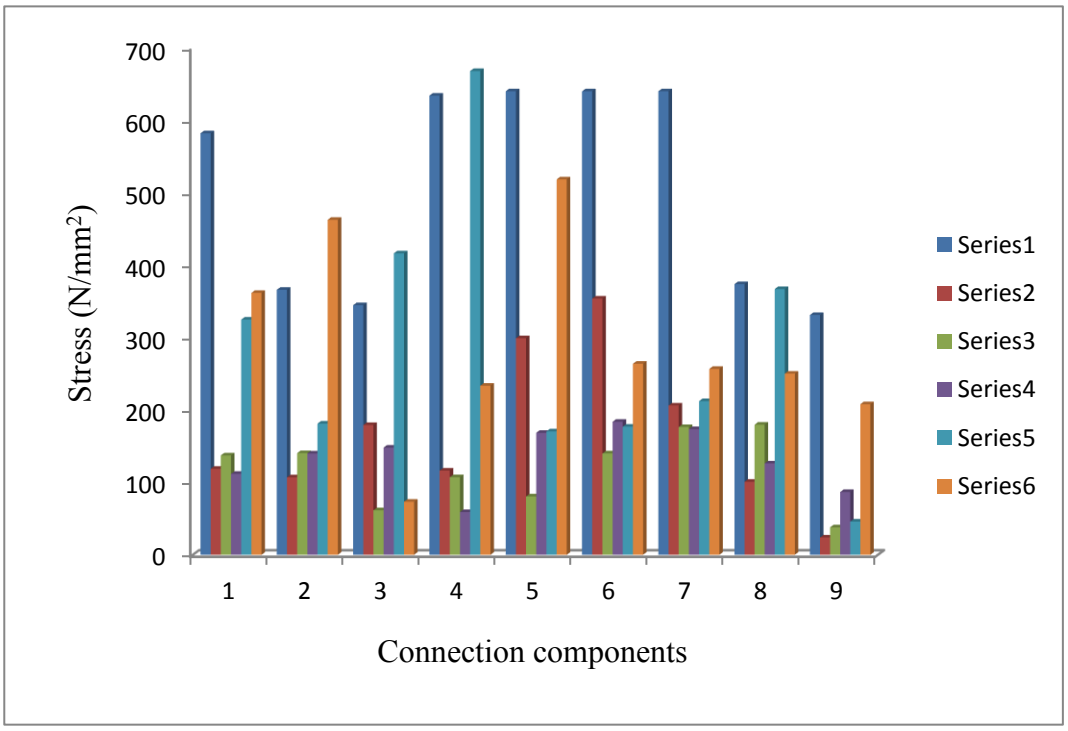

Figure 7-37 Stress responses of connection used as control

The maximum stress responses for each stress component for all the members of the connection are compared. It is obvious that the maximum response is the principal stress along the y-y axis of the bolts. In this case, it is the tensile stress developed in the main bolts of the connection. The studies also present the fact that the type of component under consideration significantly affects the stress response type. This section presents the stress progression and the corresponding strain for each stress component. The bolts and the nuts are the most important connection components that significantly determine the overall behaviour of the connection in tension. The responses of these components will be compared with the responses in the progressive collapse scenario in the next chapter.

7.7 Basis for chapter eight

This chapter presents a study into the behaviour of a simple beam-column connection originally designed using in Eurocode 3 Part: 1-8. The connection was assessed based on a static load response resulting in a shear force of 34.72kN in the tie beam (BM 308), while a shear force of 80.17kN was developed in the primary beam (BM 548). Eurocode 3 recommends that all connections should be able to resist a tensile force of 75kN, this exceeds the initial static response of 0.55kN in the tie beam and 1.06kN in the main beam. Under progressive collapse scenario, a maximum catenary force of 442.6kN was developed in the beam at the eight floors due to a column loss scenario. This corresponds to an increment of 490.1% in catenary force in the tie beam while the main beam increases by 244.5%. This percentage increment as a result of column removal is significant which may likely not be considered in practical conventional designs. Consequently, the next chapter is aimed at investigating the behaviour of the connection under a progressive collapse scenario. The next chapter of the thesis assess the response of the connections with a catenary force of 442.6kN at the tie beam and 258.4kN on the main beam.

Chapter 8 Connection assessment under PC scenario

8.1 Introduction

This chapter of the thesis investigates the behaviour of the connection under progressive collapse loads. Chapter seven establishes the control model, in this study, the state of stress of the beam-column connection under column removal scenario is compared to the control model. The basis of this assessment is to achieve one of the objectives of the thesis, which is: to investigate the behaviour of simple connection under progressive collapse scenario.

In subsequent sections, the author discusses contour plots of the stress and strain in the connection and all its components. The variations between the stresses at the two arms of the beam-column connection at the flange and the web were discussed. The evaluation of the responses in the preceding chapter that serves as control was compared to the responses due to progressive collapse.

As discussed previously, the interaction of beam-column connection under loading conditions is complex and currently a research focus. There is limited data on the semi-rigid behaviour of connection incorporating the beam-column web connection. Most of the experimental and numerically based research works concentrates on the beam column flange connection; this assessment would further enhance the understanding of beam column behaviour with two arm connections. The choice of the finite element approach to investigate the response of connection under progressive collapse is a means of overcoming the inadequate data on the complex behaviour of semi-rigid connections. Besides, it is expensive to investigate some parametric studies experimentally and difficult to determine local effects experimentally. Therefore, the finite element technique is a preferred option for complex investigations.

In chapter seven, an introduction into the basic principles and methodology of modelling simple connections were presented. Consequently, the control model was assessed under static conventional scenario to determine the stresses and shear forces in the various components of the connection. Simple beam connections are often designed to resist shear force only with a minimum tensile force of 75kN as recommended in Eurocode 1 EN1991-1-7. Previous numerical assessment proves this recommendation to be insufficient in mitigating progressive collapse. It is equally observed that the catenary force is the dominant internal forces crucial for a progressive collapse of a brace system.

The initial condition of the connection was first designed for a shear force of 80.17kN along the long span and 34.72kN along the short span. The code requires that simple connections should resist a tensile force of 75kN, it was applied as a pressure force at the ends of the beam. This is equivalent to 5.09N/mm^2 along the long span and 26.79N/mm^2 along the short span. The internal catenary force under the conventional stage was 1.06kN along the long span (BM 548) and a tensile force of 0.55kN along the short span (tie beam). The response corresponds to a pressure force of 0.21N/mm^2 and 0.20N/mm^2 (BM 301 respectively. The cross-sectional area of the beam along the long span (BM 548) and the short span (BM 30) is 4970mm^2 and 2800mm^2 respectively. However, under progressive collapse scenario, the eight floor is more critical as compared to the interior, edge and the perimeter. The maximum catenary force developed in the tie beam is 442.6kN while the primary beam is 258.4kN. The next section presents the stress contour plots in all the connecting components of the structure under the progressive collapse scenario.

8.2 Stress contours under progressive collapse scenario

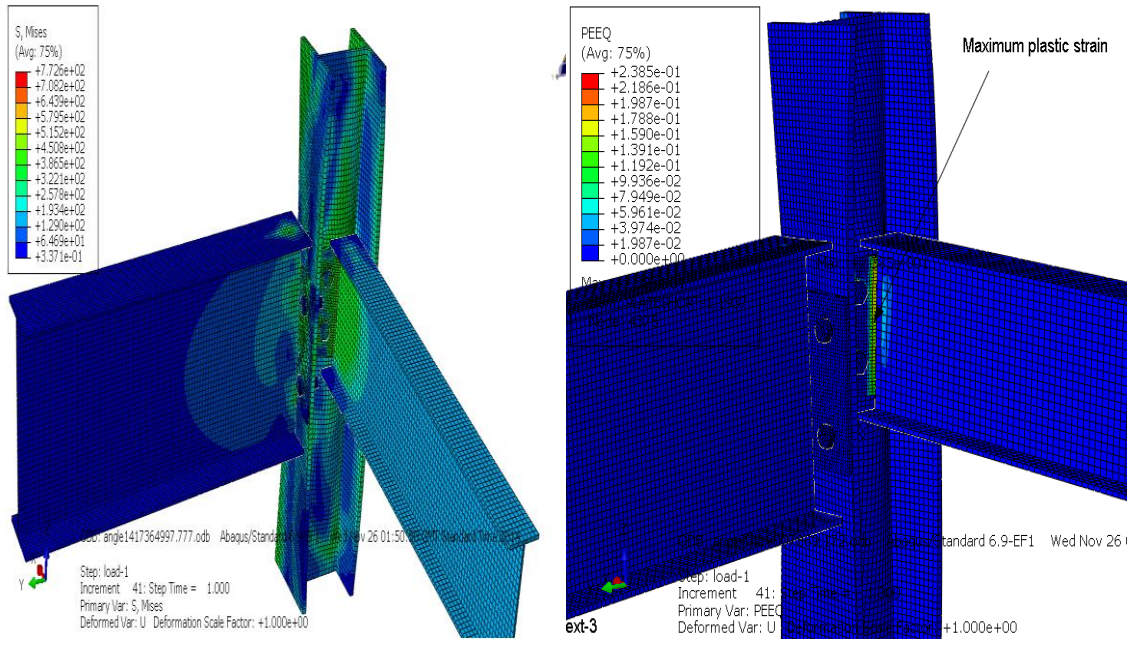

Figure 8-1 VM stress plots with equivalent plastic strain

von Mises (VM) contour plot of the beam-column connection under progressive collapse scenario is shown in Figure 8-1. The maximum von Mises stress redistribution plot for the connection is 772N/mm^2 that exceeds the initial condition by 66.22%. However, if the

tensile force of 75kN is considered as recommended by Eurocode 1 EN1991-1-7, equation 5-3, the percentage increment observed was 20.63%.

The equivalent plastic strain (PEEQ) is 23.9%, and this occurs at the vertical strip of the beam column connection at the web of the column. The large plastic strain is attributed to the catenary force action on the connection. Maximum strain recommendation at based on GSA 2003 at collapse is 3.5%. The assessment carried out in the previous chapter shows a plastic strain of 3.1% that occurs at the main beam connection to the column flange. That is not the case under the progressive collapse scenario. The maximum plastic strain occurs at the strip connecting the tie beam to the plate to the column web as shown in Figure 8-1. Probing the maximum plastic strain at the main beam column connection to column flange is 18.3% relative to 3.1% under conventional design scenario.

Consequently, these studies show that progressive collapse load inherent in the development of catenary force interacting with the shear force significantly affect the response of the connection. This connection does not satisfy the recommendation of GSA 2003 based on the collapse strain recommendation.

As shown in Figure 8-1, the maximum von Mises stress developed in the connection is 772.6N/mm^2 that occurs at the bolts shank. This response exceeds the yield strength by 20.7% although less than the ultimate capacity by 3.4%. The following subsections discuss the stress and strain distribution on the components of the connection relative to the control model.

8.2.1 Stress contours and column deformation

The progressive collapse loads resulted in column buckling and warping as shown in Figure 8-2. The interior un-deformed node to node distance of the column was 181.2mm. It was observed that the column buckled under progressive collapse scenario with the two opposite flanges bulging outwardly in tension and inwardly in compression. The maximum outward deformation of the flanges relative to its original state was 18.6% as shown below while the other inward end suffers compression of 33.38% as shown in Figure 8-2a. This behaviour was attributed to the beam- column connection at the web of the column. Subsequent contour plots show the stress redistributions in the columns under the progressive collapse scenario. Though, the responses are compared with the magnitude obtained in the preceding chapter.

As shown in Figure **8-3**, the maximum von Mises (VM) stress response in the column is 596.4N/mm^2 with a plastic strain of 19.6%. This stress exceeds the ultimate yield stress by 21.2%. Plastic strain response of the column is 5.6 times the maximum recommendation at the collapse in GSA 2003. As shown in the contour plot, the region at which maximum plastic strain occurs in the column web is approximately 23mm away from centre of the top bolts. This strip narrows down towards the centre approximately 34%. This implies that the web of the column within the connection of the bolts fails based on these criteria.

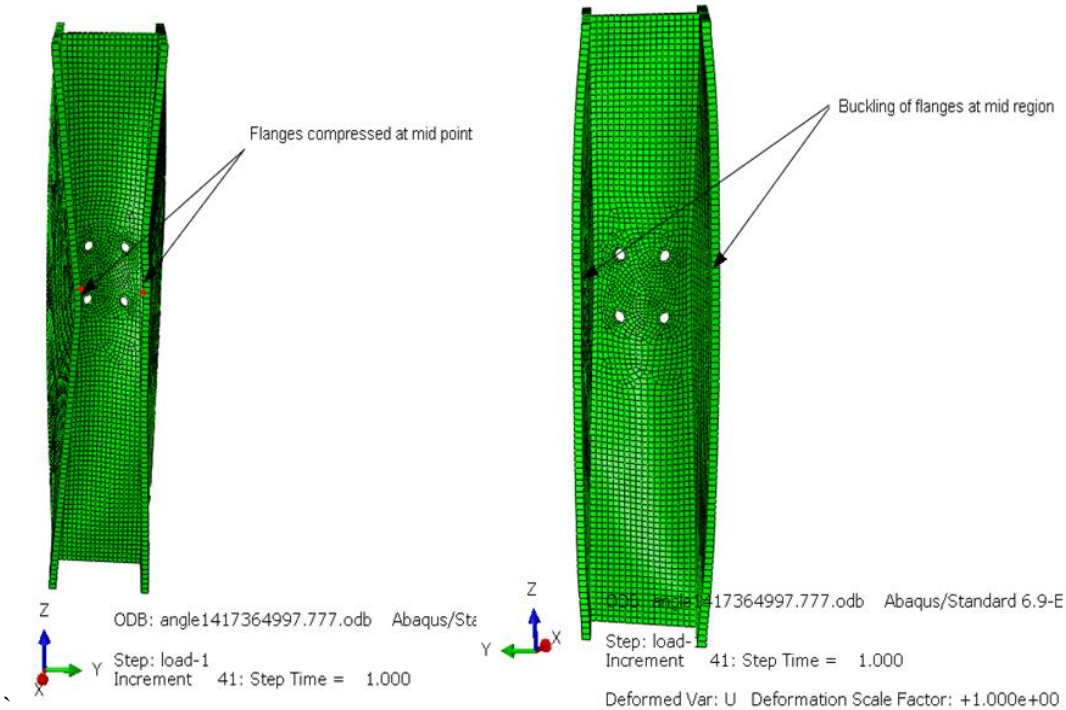

Figure 8-2 Buckling behaviour of column under PC scenario

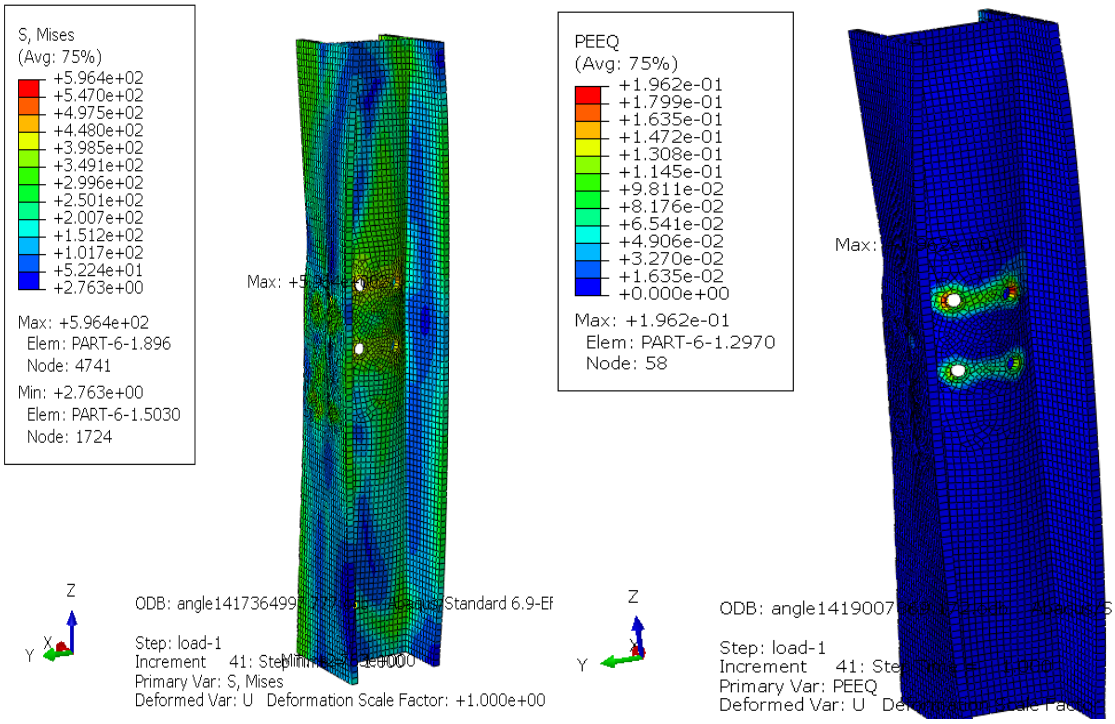

Figure 8-3 Stress and strain contour plots (PC)

Comparing the von Mises stress under column removal and during a conventional stage, an increment of 2.2% was observed. The plastic strain at the conventional design stage was 1.8% while under a progressive collapse scenario was 19.6%, which implies a ratio of 1:11 approximately. The maximum plastic strain before and after a sudden loss of column occurs at the column web. The paragraph discusses the shear and tensile stress response of the column under progressive collapse scenario relative to the control at the preceding chapter.

The shear and tensile stress contour plots of the column are presented in Figure 8-4 below. It was observed that the maximum shear stress was 195.5N/mm^2 (S23) which occurs at the web of the column just by the edge of the bolt hole. Corresponding response of the component shear stress was 25.96% (137.7N/mm^2) for the control model at the preceding chapter

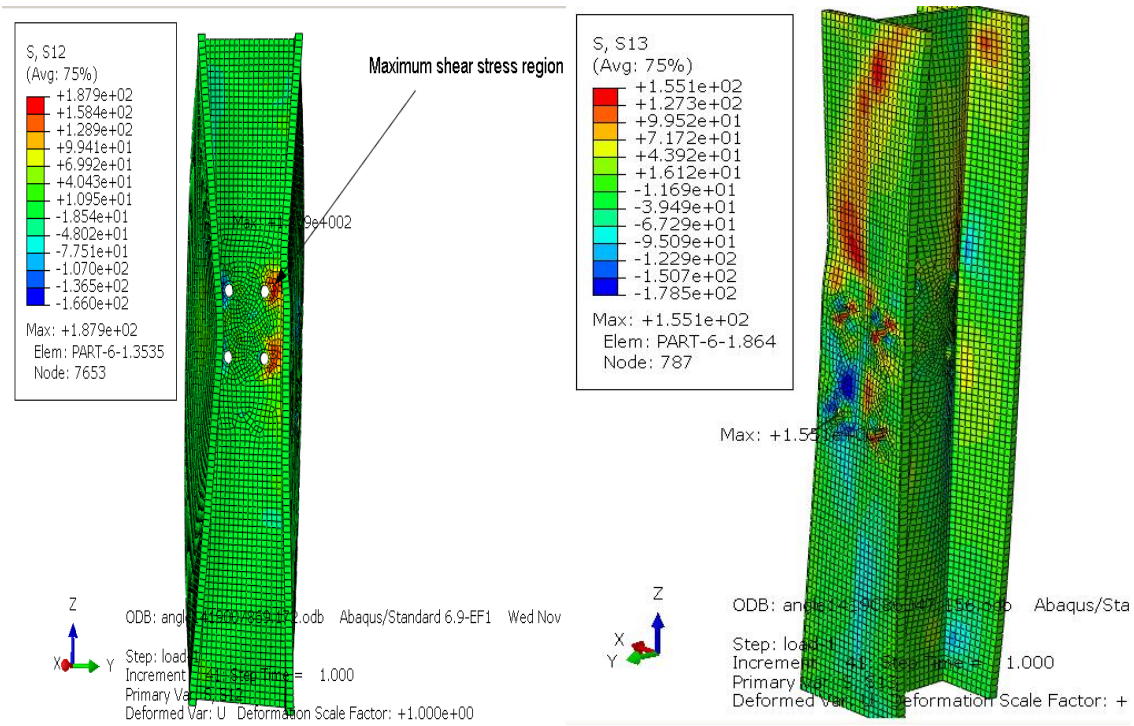

a) Shear stress (S13) contour plots in the columns

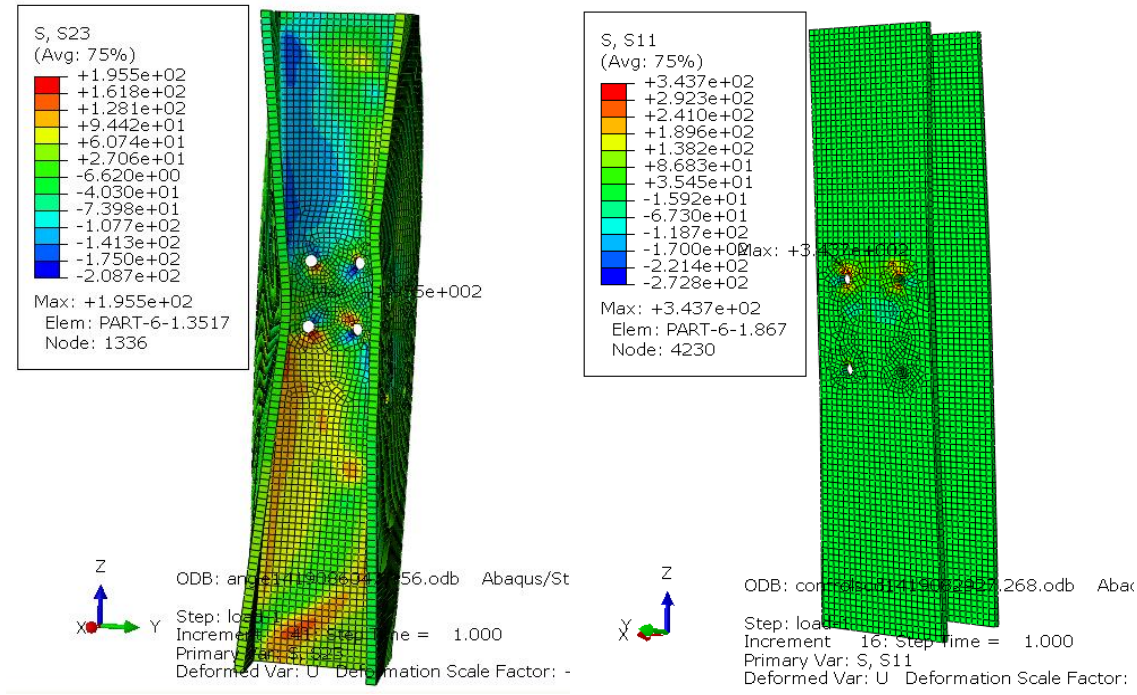

b) Shear (S23) and tensile stress (S11)

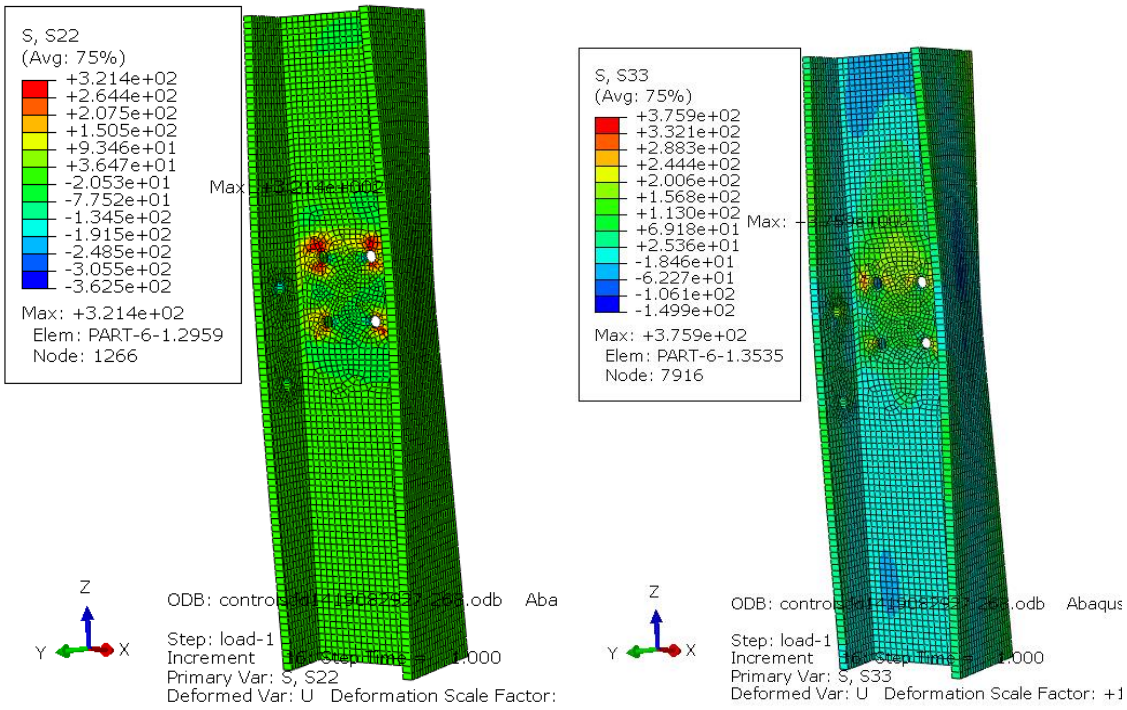

c) Tensile stresses (S22 and S33) in column

Figure 8-4 Tensile and shear stress components under PC

At the preceding chapter, the maximum tensile stress in the column was 375.9N/mm^2. However, under progressive collapse scenario the maximum tensile stress increased by 122.88% (837.8N/mm^2) for the component (S33). However, component stress (S11) at the control has a magnitude of 343.7N/mm^2 that increases by 46.4% (642.2N/mm^2) under the progressive collapse scenario. Component stress, S22, due to progressive collapse scenario exceeds the corresponding component stress at the control by 41.1% (321.4N/mm^2: 545.3N/mm^2).

The maximum stresses in the column occur at the edge of the hole drilled for bolt interacting with the column web. The distortion of the column in the form of buckling and warping resulting to outward and inward opposite sides of the flanges can possibly trigger a progressive collapse. Consequently, column web stiffening to brace up the flanges would increase the overall stiffness of the column joint and limit column deformation. The next section presents the plate response at the web of the column and the flange of the column connecting the tie beam and the main beam.

8.2.2 Stress contour in plates

Under progressive collapse scenario, the von Mises stress contours in the plates connecting the flanges of the column and the web of the column are 422.8N/mm^2 and 470N/mm^2 respectively (Figure 8-5). The plate's response under conventional design state was 366.2N/mm^2 and 340N/mm^2 respectively as presented in the previous chapter. This corresponds to 15.5% and 38.2% increase due to progressive collapse loads.

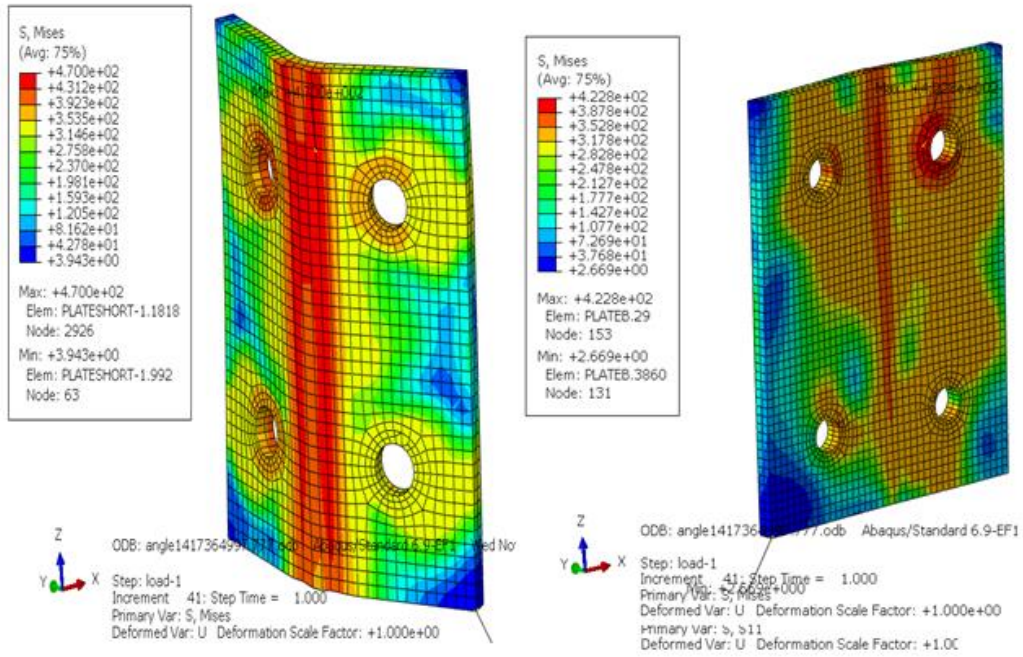

Figure 8-5 VM stress contours of the plates under PC

The tensile stress components of the plates along the x-x axis (S11) are shown in Figure 8-6 while the component tensile stress along the y-y axis (S22) are presented in Figure 8-7. The component stress, S11, for the plate at the flange and web is 2242N/mm^2 and 2877N/mm^2 respectively. The response shows that the stress levels at the plate connecting the web of the column exceeds that of the flange of the column by 28.3%.

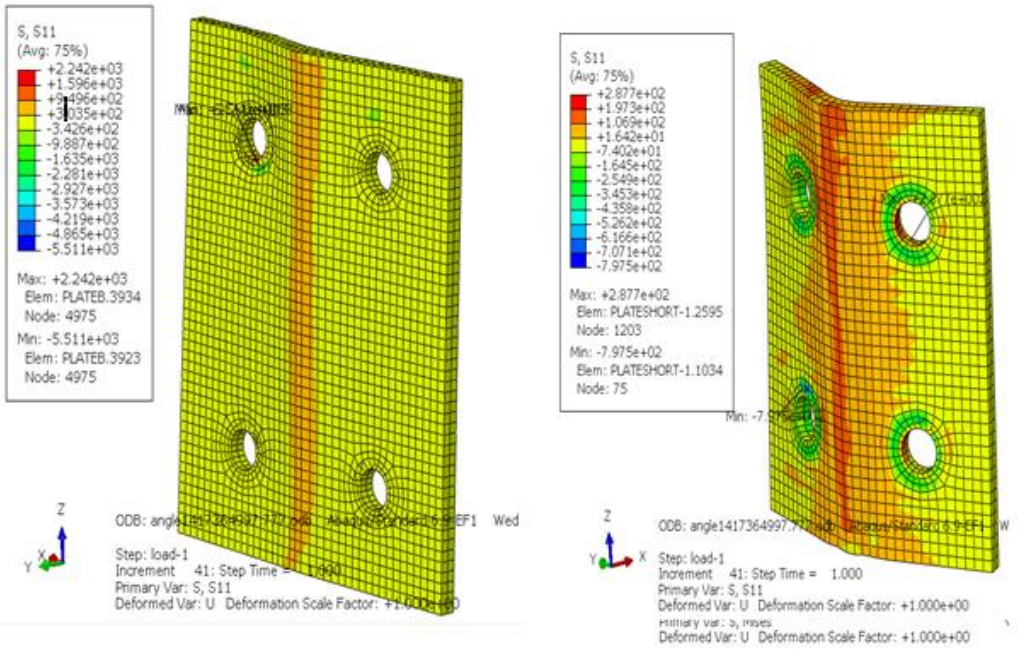

Figure 8-6 Tensile stress distribution (S11) under PC

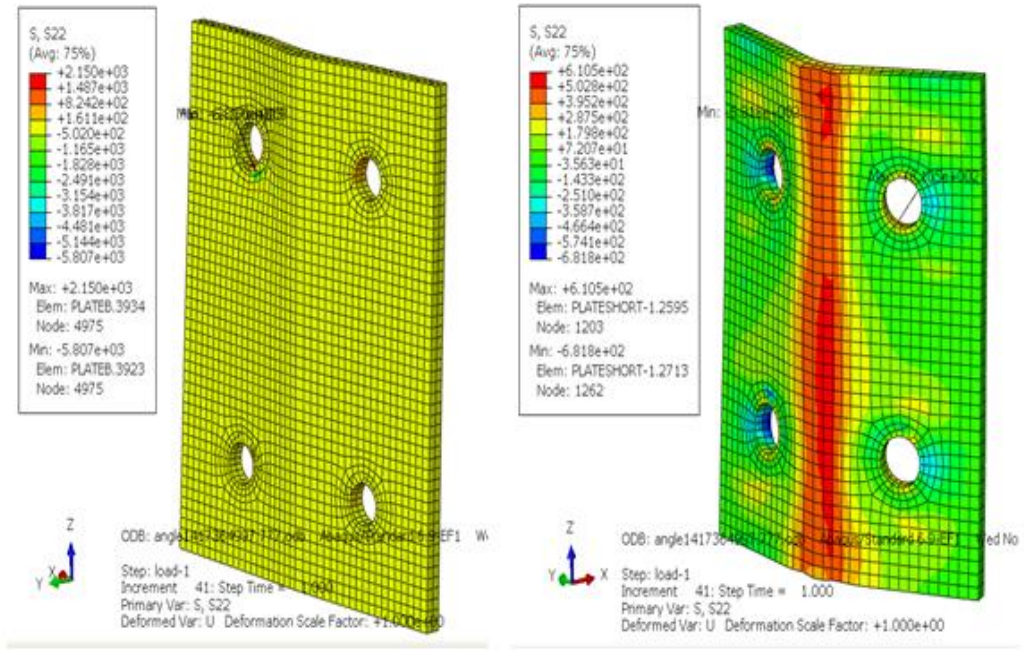

Figure 8-7 Tensile stress response (S22) under PC

However, under the conventional design case, the stress component (S11) is 462.7N/mm^2 at the plate connecting the flange of the column and 73.34N/mm^2 at the web plate. These stresses indicate that that the plate connecting the flange exceeds that of the web by 531%.

The maximum stress (S22) under progressive collapse for the plate connecting the flange of the column is 2150N/mm^2. On the contrary, the stress equivalent on the plate connecting the web is 610.5N/mm^2. Relative to the conventional state, the stress component for the plate at the flange and web of the column are 181.5N/mm^2 and 416N/mm^2.

Figure 8-8 is the equivalent plastic strain developed in the main beam is 18.26% while the maximum plastic strain of the plate at the web of the column is 23.85%. The plate connecting the web of the column to the beam shows a strip exhibits higher deformation relative to the plate at the flange of the column.

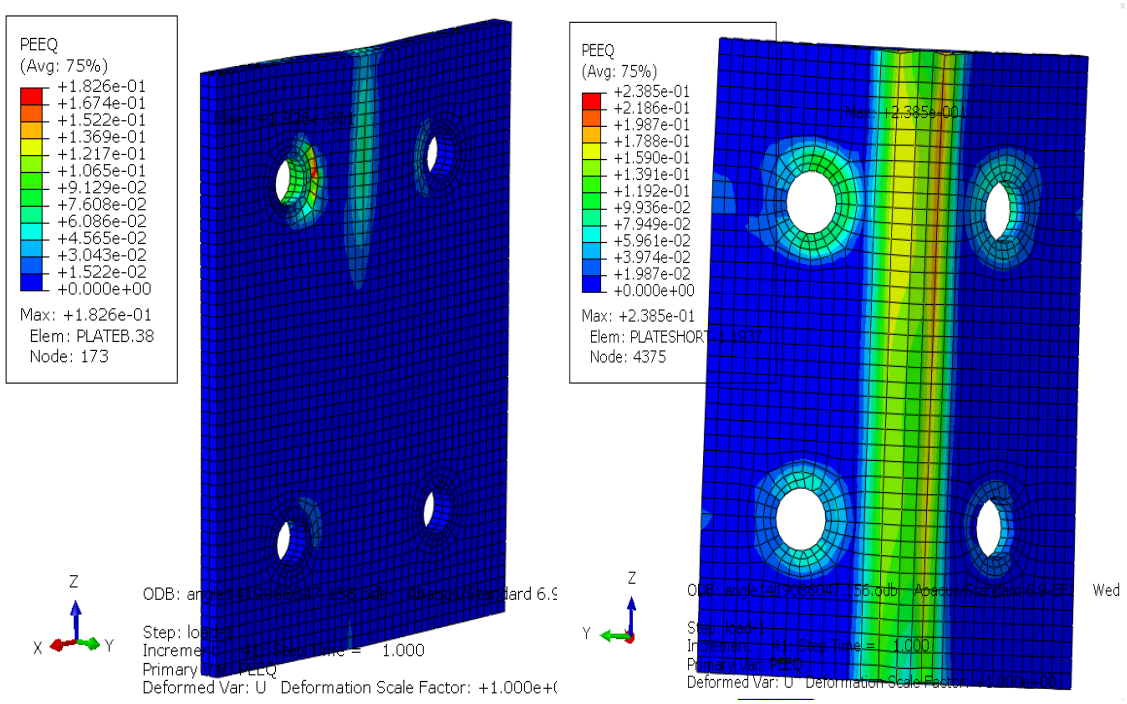

Figure 8-8 Plastic strain redistribution plots

8.2.3 Stress contours in beams

Figure 8-9 through Figure 8-12 shows the stress and strain contour plots of the beams under progressive collapse scenario. The maximum von-Mises stress state in the beam at the column flange is 373.8N/mm^2 and 358.9N/mm^2 at the beam connected to the web of the column. The maximum plastic strain in the main beam is 0.0797 and 0.0569 in the beam connecting the web of the column. The maximum tensile stress developed in the beam connecting the web of the column is 421.7N/mm^2 while the beam at the flange of the column is 468.4N/mm^2.

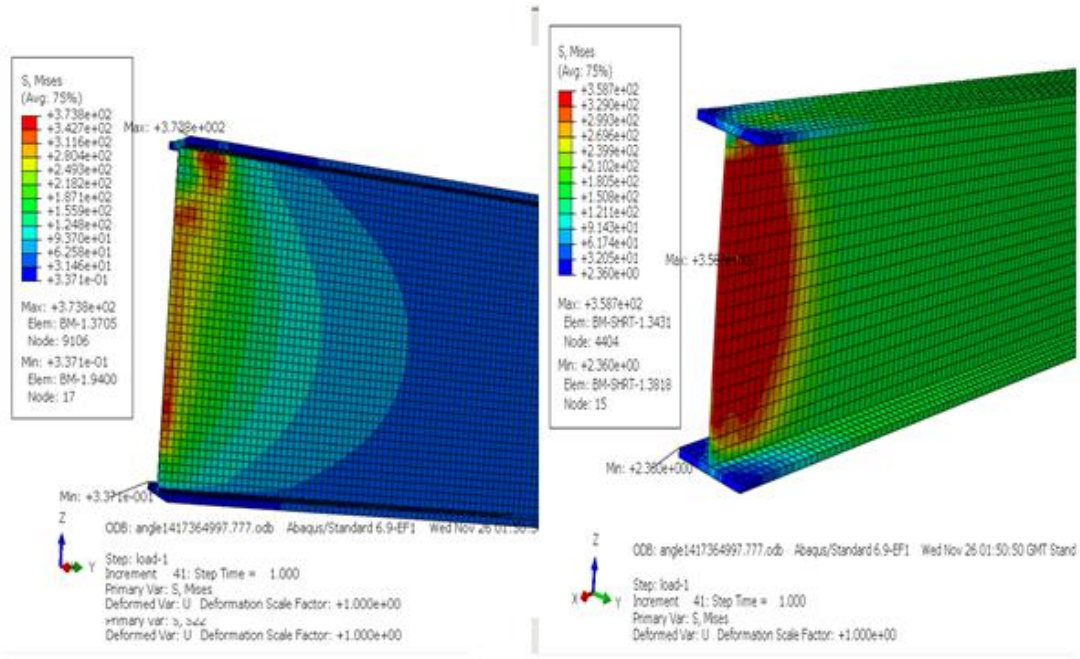

Figure 8-9 VM stress contours of beams connecting the column

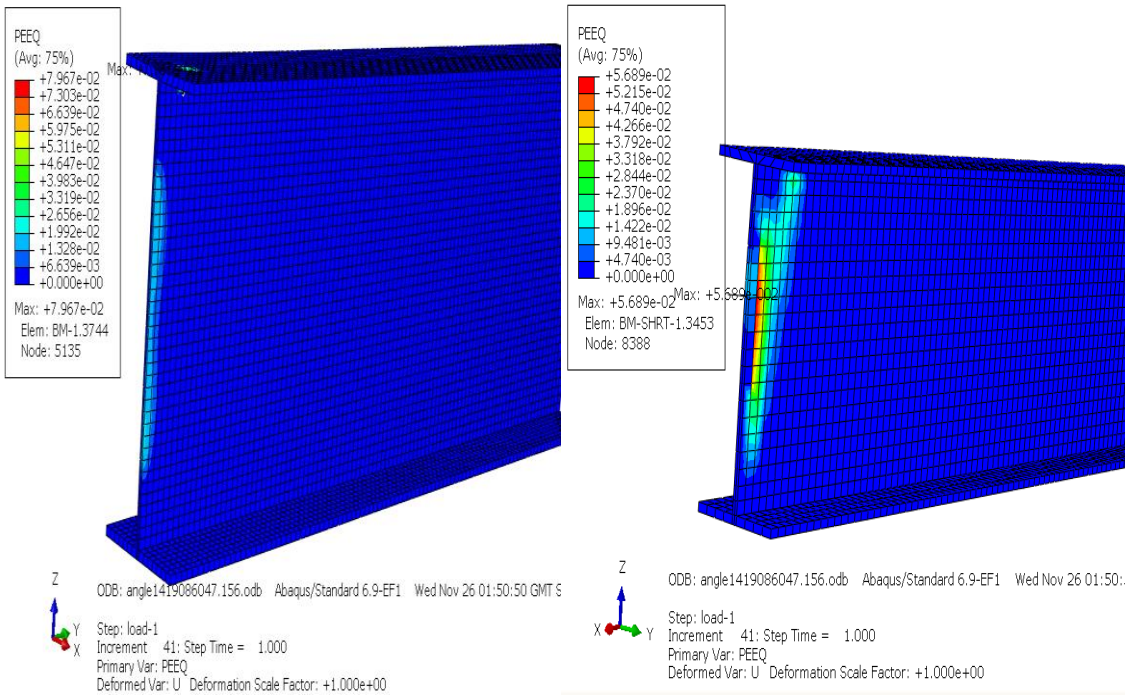

Figure 8-10 Plastic strain distribution under PC scenario

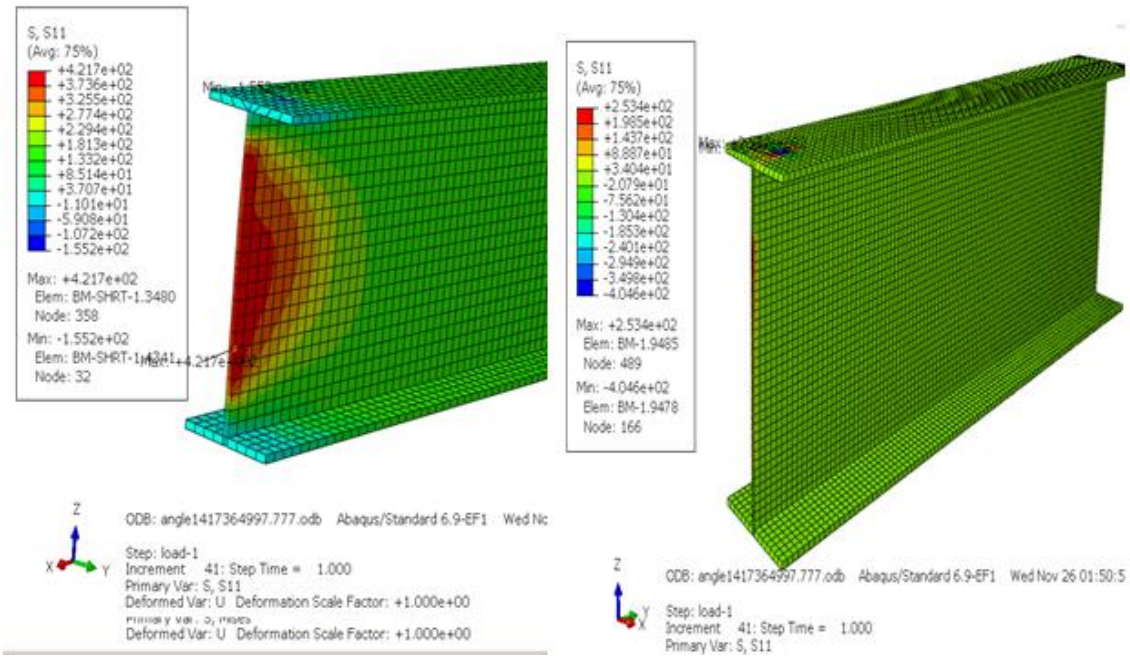

Figure 8-11 Tensile stress contours distribution (S11) in beams

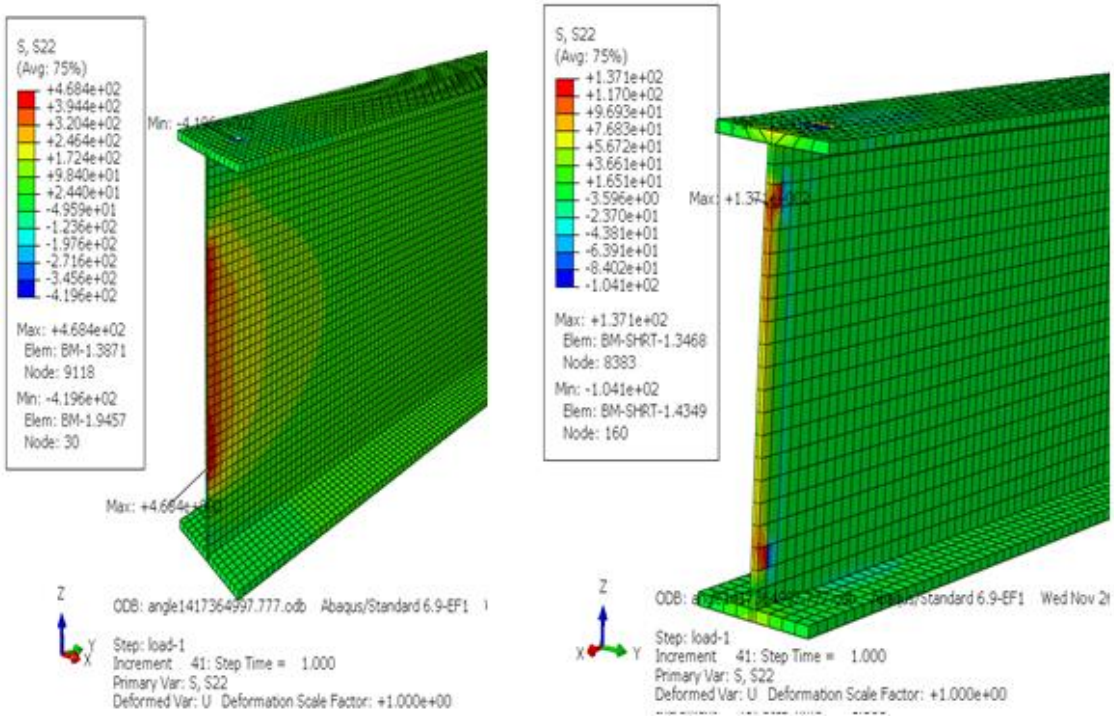

Figure 8-12 Tensile stress contours distribution (S22) in beams

The maximum von Mises stress state of the main and tie beams are 373.8N/mm^2 and 358.7N/mm^2 respectively for the beam connecting the flange of the column and the web of the column. Maximum plastic strains in the beams are 0.059 and 0.053 respectively, and these

occur at the web of the beam connecting the plate to the column. The maximum component tensile stress S11 in the main and tie beams are 253.4N/mm^2 and 421.7N/mm^2 respectively. The stress component, S22, for the main and tie beam under progressive collapse scenario is 468.4N/mm^2 and 137.1N/mm^2 respectively. A comparison of the response with the corresponding control model response shows a 27.56% increase for the main beam and 198.67% increase for the tie beam. Using the component stress (S22), it was also observed that the percentage increment in the contour stress in tie beam is more critical compared to the main beam. On the other hand, the responses show a ratio of 3.42 for the main to the tie beam for S22 and a ratio of 1.66 for the tie to main beam for S11. Stresses contour plots developed in the bolts and nuts under progressive collapse scenario are presented in subsequent subsections.

8.2.4 Stress contours in bolts

Figure 8-13 and Figure 8-14 shows the stress redistribution and plastic strain contour plots for the bolts under the progressive collapse scenario. The maximum von Mises stress on the bolts at column flange and column web are 640N/mm^2 and 772.6N/mm^2 and respectively. When these responses are compared with the control model, it was observed that the stress in the bolts connecting the flange of the column and that of the web increases by 0.9% and 20.72% respectively.

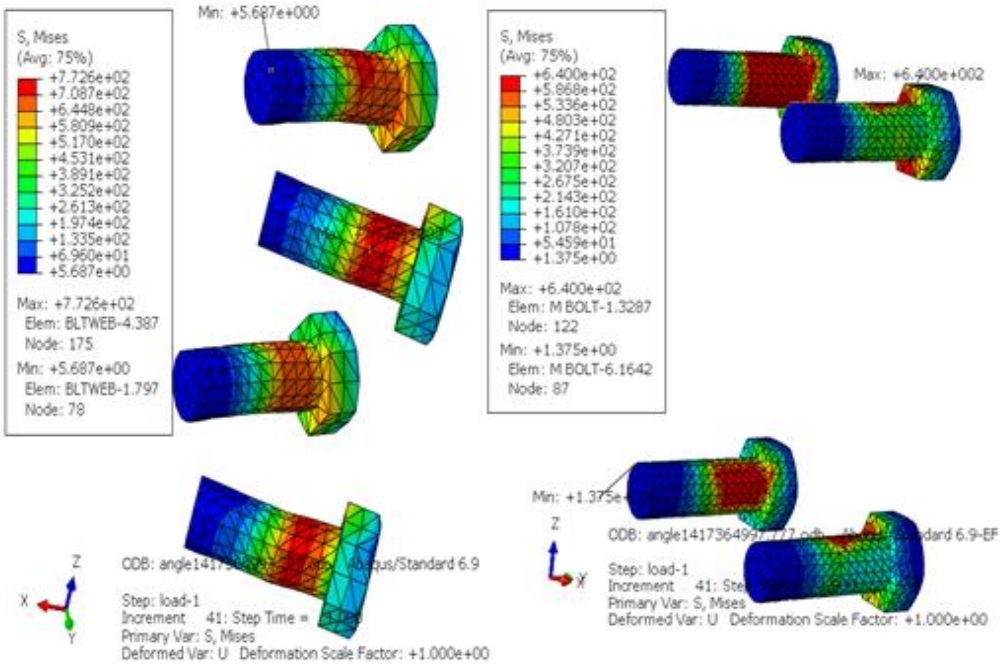

Figure 8-13 Von Mises stress redistribution for the bolts

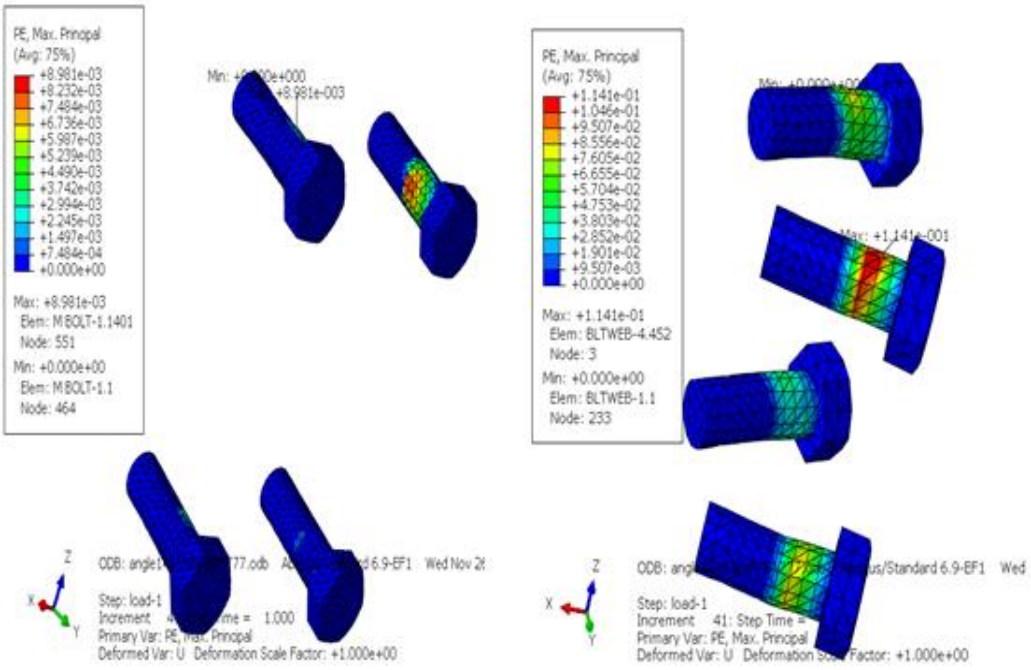

Figure 8-14 Plastic strain distribution for the bolts

The maximum plastic strain response on the bolts connecting the flange of the column is 0.9% while the plastic strain at the column web is 11.41%. Contrary to the control model, the maximum strain response for bolts at the flange of the column is 0.37% while that of the

bolts connecting the web of the column to the beam is 0.32%.,Consequently, the bolts connecting the web of the column are subjected to more strain relative to the bolts connecting the flange of the column. The following subsection presents the tensile component stress (S11) and (S22) response plots for the two principal axes.

Figure 8-15 and Figure 8-16 shows the component stresses redistributions in the bolts connecting the flange and web of the column under progressive collapse. The maximum tensile stress (S22) components in the bolts at the flange and at the web of the column are 780.5N/mm^2 and 3563N/mm^2 respectively. This exceeds the control model initially investigated by 16.9% and 1986% at the column flange and the web respectively. On the other hand, the tensile stress S11 component is 814.2N/mm^2 and 4105N/mm^2 for the bolts connecting the flange and the web of the column respectively.

When this response is compared to the response at the control, an increase of 247.9% and 699.4% for the bolts at the flange and web is observed respectively. Using the component tensile stresses in the bolts, it equally shows that the bolts at the web respond critically to progressive collapse relative to the beam column connection at the flange.

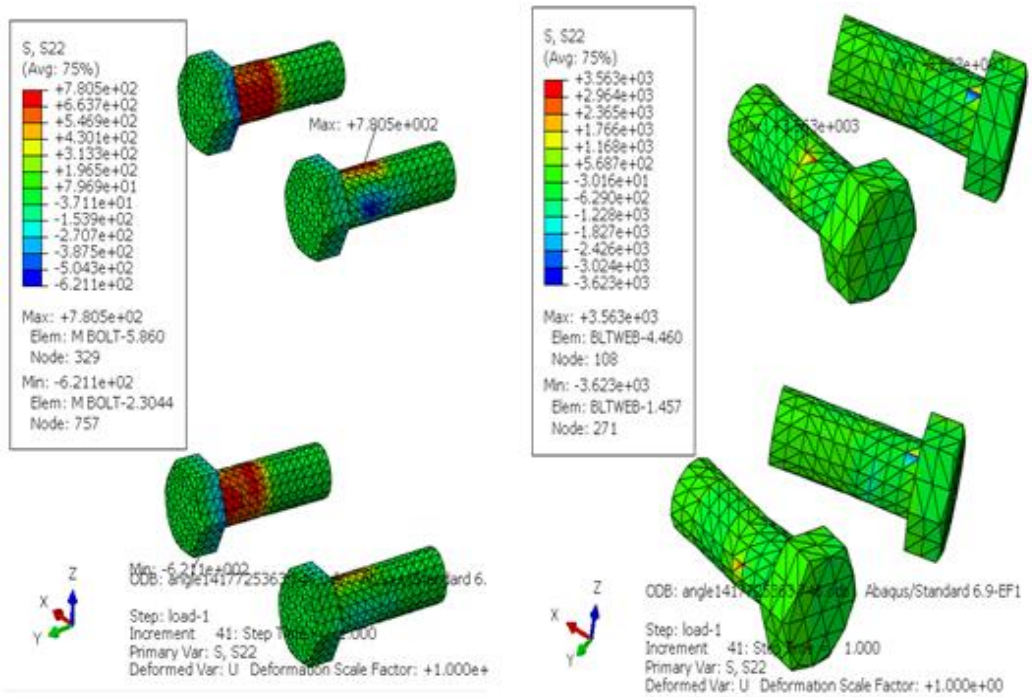

Figure 8-15 Tensile stress component (S22)

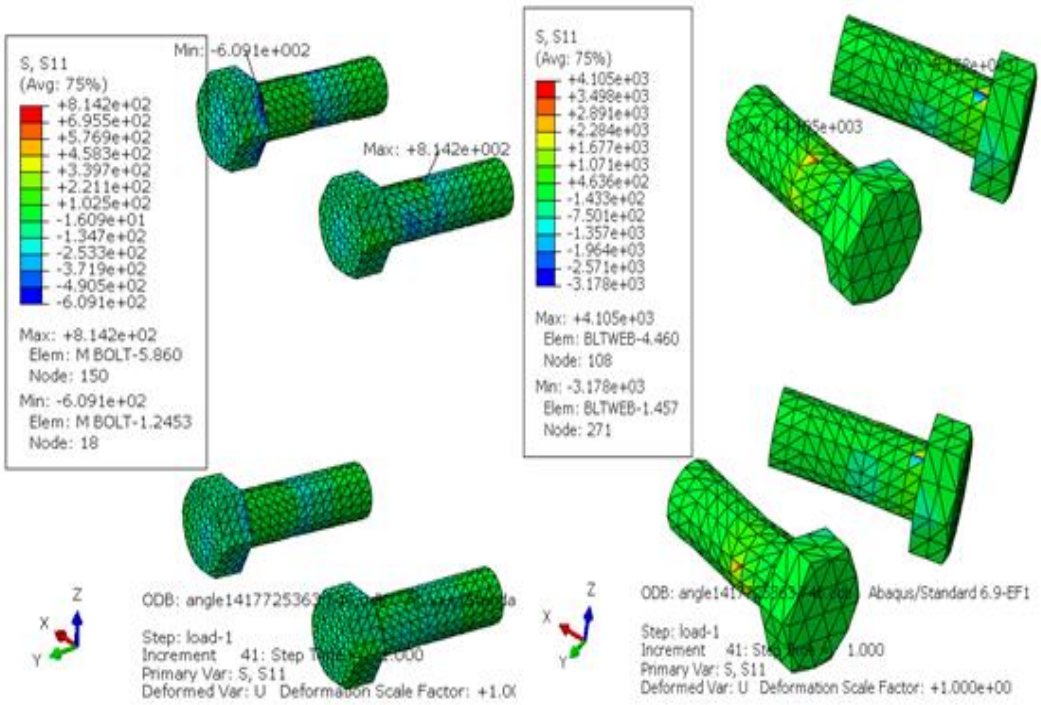

Figure 8-16 Component tensile strain in the bolts

8.2.5 Stress contours in nuts

Failure of nuts under progressive collapse could affect the performance of the beam column connection. This subsection presents the stress state of the nuts under a progressive collapse scenario. These bolts connect the bolts at the flange of the column and the web of the column respectively. As shown in Figure 8-17, the maximum von Mises stress developed in the nuts at the column flange and web is 642.5N/mm^2 and 640N/mm^2 respectively.

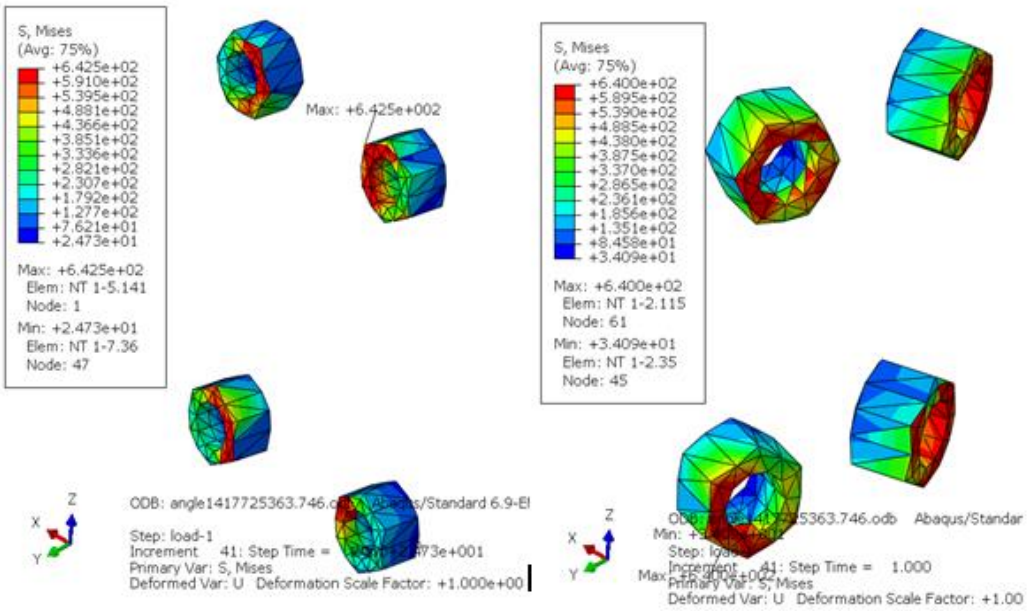

Figure 8-17 VM stress response of the nuts under PC

The increment in the von Mises stress in the nuts relative to the control state is less than 5% that is not significant. Component tensile stresses (S11) response along the principal axis are presented as shown in Figure 8-18. The maximum tensile stress of 1246N/mm^2 occurs in the nuts at the web of the column.

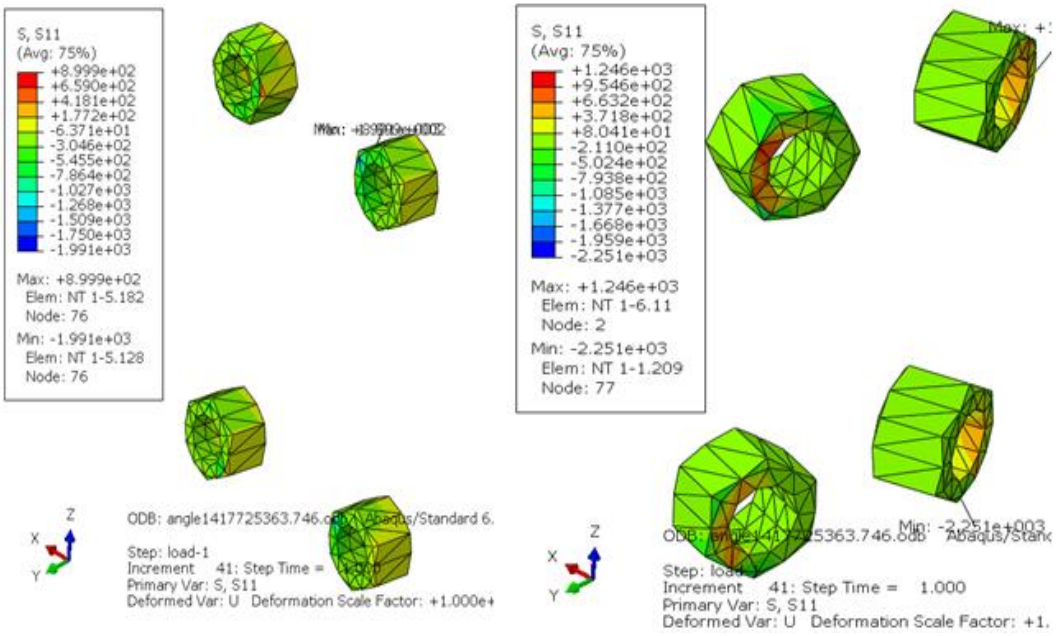

Figure 8-18 Tensile stress component (S11)

Figure 8-19 and Figure 8-20 shows the component tensile stress (S22) and the plastic strain respectively.

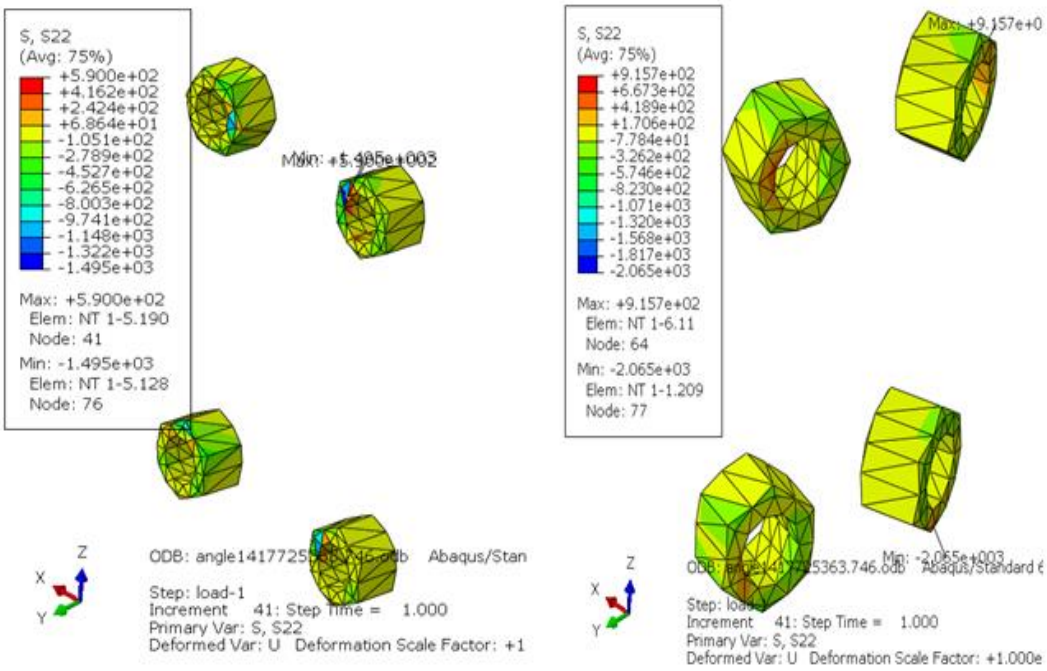

Figure 8-19 Tensile stress component (S22)

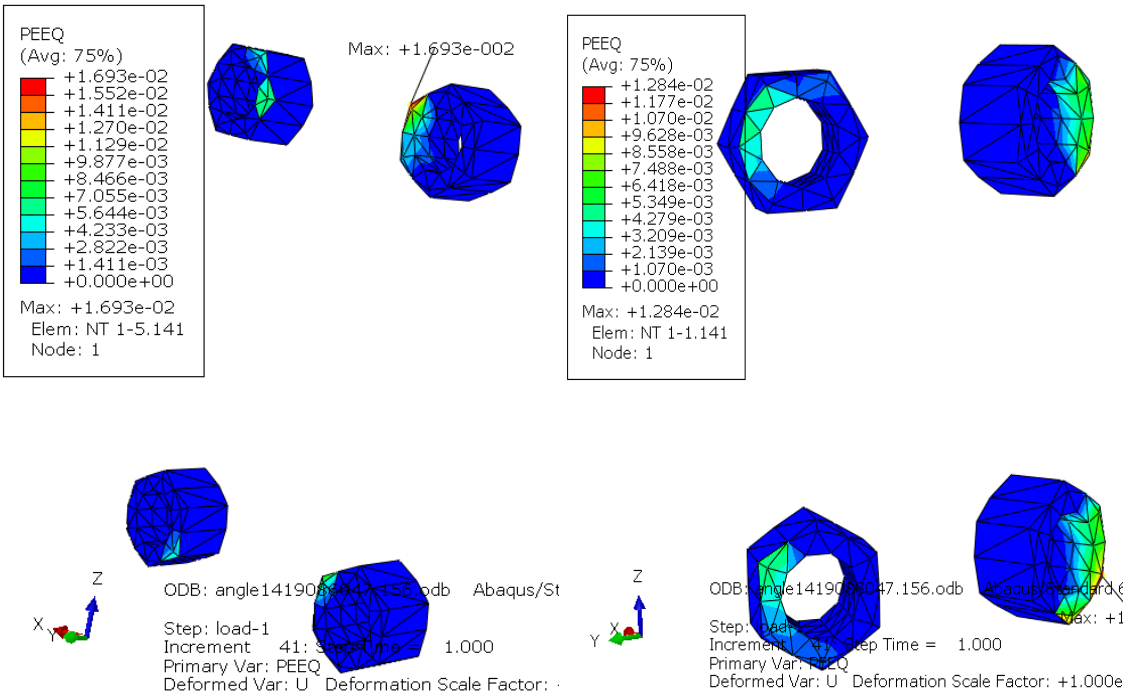

Figure 8-20 Plastic strain contour plots in nuts

The maximum component stress (S11) for the nuts at the column flange is 899.9N/mm^2, and that of the nut connecting the web of the column is 1246N/mm^2. This corresponds to an increase of 40.56% in the nut stress at the column flange and 242.3% at the column web. The maximum plastic strain response at the column flange and the web is approximately 1.7% and 1.3% respectively. The next section presents a summary of the investigation for this chapter, and this concludes the investigations addressing one of the objectives of the thesis.

8.2.6 Chapter summary

This chapter focuses on the assessment of simple connection under progressive collapse scenario. The simple connection in this study designed to the provision of Eurocode 3 Part: 1-8 under standard design conditions does not satisfy progressive collapse loads. Column buckling and warping are an important consideration triggering instability of the connection and likely to cause progressive collapse. The column flange bulges outwardly and inwardly at the opposite sides of the flange face, it is approximately 33.38% and 18.6 % of the interior flange to flange dimension in compression and tension respectively. The maximum von Mises stress in bolts at the column web exceeds the bolt yield stress by 20.7% corresponding to an equivalent plastic strain of 11.41%. The maximum von-Mises stress of the connection under progressive collapse scenario is 772.6N/mm^2 with a plastic strain of 23.9%. This occurs at the bolt shank which exceeds bolt yield strength by 20.7%. Generally, structural components connecting the column web to the tie beam are critically stressed relative to the main beam column flange connection. Geometric deformation of the connection is attributed to the column web connection to the tie beam; this is less research in literature.

Chapter 9 Closure to the thesis

9.1 Research findings

This thesis addresses some of the pertinent questions and observations raised in existing literature on progressive collapse assessment. It describes four techniques for performing column removal analyses and investigates the influence of the length of time over which the column was removed, a parameter common to each method, using a ten storey steel building. At different locations, the techniques were compared to determine the response of the structure under sudden column loss. Since there is no unified standard for modelling and assessing the performance of high rise structures, researchers adopt different modelling techniques/assumptions to model sudden loss of load bearing members. These assumptions determine the results, conclusions and recommendations.

In a progressive collapse, most building codes are moving toward threat-independent load cases for design (e.g., single column removal with reduced gravity loads). Since GSA recommends a column removal time less than a tenth of the period (T) of the structure under vertical vibration mode, the author observes that several values satisfies this criterion. However, maximum response due to instantaneous column loss occurs when the length of column removal time is within the range $(\frac{T}{1000}s) \leq R_t \leq (\frac{T}{100}s)$. The author addresses one of the research needs observed at structures congress 2009 which focuses on the relevant features in modelling for progressive collapse (Ellingwood et al., 2009). The loading path and column removal time were identified as key features of progressive collapse modelling of high rise structures.

The author observed that the dynamic amplification factor (DAF) of 2.0 recommended in GSA 2003 depends on the modelling technique, column removal time, structural member type (column, beams, etc.) and the stress resultants considered (shear, moment or axial force). The recommendation of 1.5 for a dynamic analysis response for moment resisting frame structure by Ruth et al., (2006) is misleading. This recommendation only accounts for the axial force response in columns but does not satisfy shear force criteria.

This study further highlights the fact that the tie force recommendation to progressive collapse in Eurocode 1 EN1991-1-7, Equation 5-3 is unsatisfactory if progressive collapse load is considered. Recently published numerical studies carried out by Tohidi et al. (2014b) and Tohidi et al. (2014a) further corroborate the shortcomings in the tie force

recommendation. Consequently, the author proposes five times the recommendation in EN1991-1-7, Equation 5-3; a further numerical and experimental research based investigation is required. The author observes that braced frame system is prone to progressive collapse by up to 35% using the displacement and rotational response criteria relative to the moment resisting frame structure. The author observes that warping and buckling of a column are significant geometric deformations under progressive collapse loads. These deformations are attributed to the beam-column web connection action, which is less researched in the literature.

9.2 Proposals for future investigations

The connection of structural members is the most important unit in the design of high-rise steel structures. Most researchers on connection performance focus on the beam to column flange connection relative to the beam to column web connection. Limited research-based work is done on the beam-column web connection that significantly influences the deformations of the column causing it to warped and buckle under progressive collapse scenario. It is crucial to consider the choice of using angle irons relative to end plates to harness the post-yield ductile behaviour of angle irons relative to endplates.

9.3 Limitations of research

This research work is within the context of a ten storey structural model and the corresponding simple connection designed to Eurocode 3 Part 1-8. The choice of a ten storey was based on the recommendation of GSA 2003 which limits the application of static loading to ten storey buildings. The common and most popular connection type in practice is the end plate connection because of its simplicity in fabrication and cost effectiveness. Consequently, a simple header plate that satisfies the shear and tension requirement of the code was used and checked under progressive collapse to determine the effect of progressive collapse loading on the stress redistribution of the connection.

9.4 Conclusion and recommendation

This thesis presents a holistic investigation of a structural model for progressive collapse scenario and a detailed examination of the beam -column connection using ABAQUS finite element code. The author observes that the dynamic amplification factor of 2 recommended in GSA 2003 depends on the structural member investigated, the internal force criterion used and the joint moment releases, which determine the structural configuration type. Some researchers who have proposed 1.5 for the moment resisting frame structure do not consider the shear force criteria in the column, although the recommendation holds for the axial force response. However, in this study, different recommendations were made based on the structural system and force criteria considered. Response from the slab structural element shows that the DAF is a function of story height; therefore, a correlation of DAF with story height was derived. During the progressive collapse of structures, the corner column removal scenario is more critical as compared with the interior, edge or perimeter location of the column for symmetrical structural layout. At higher elevations, it was observed that the EFCRS is more critical than the first-floor corner column removal scenario. It is noted that the column above the removed column loses its ability to sustain gravity load and redistribute it to other structural members. Other findings are:

Bracing of a structural building for lateral loads significantly serves as an alternative path for load redistribution during a progressive collapse.

- Progressive collapse assessment of high-rise structures is crucial and should be incorporated into the conventional design stage of high rise structures. These studies highlight the need to increase tie force recommendation for progressive collapse mitigation.
- Using stiffeners in beam-column structural configurations to brace up the flanges of the column should limit the inward and outward deformation of the flanges and improve the stiffness of the connection.
- Column web stiffening within the zone of the connection may likely improve the overall stiffness of the connection since stress concentration occurs at the web of the column.
- As a minimum consideration, the beam-column connection along the secondary span should be the same as that of the primary beam-column connection at the corner of the building.

- For this case study considered, simple connections designed to Eurocode 3 Part:1-8 does not satisfy progressive collapse scenario. Therefore, further research based investigation is required for connection design under a progressive collapse scenario.

Since progressive collapse assessment tends towards a threat independent assessment, an assumption which does not incorporate column removal time but results to a corresponding or maximum response is suggested. Therefore, the author proposes the sudden application of gravity loading on the structure for modelling sudden column loss for progressive collapse. To account for the column removal time, the author suggests a hundredth of the period of the structure in the vertical vibration mode. From a practical viewpoint, it may not be necessary to have column removal times in fractions of a second which obviously have no physical meaning. However, since maximum structural response occurs as column removal time tends to zero, the author recommends a hundredth of the period of the structure in the vertical vibration mode for column removal time.

Finally, steel structures have a complex behaviour under the progressive collapse scenario. Assessment of the prototype model used in this study shows that the redistribution of internal forces under accidental loads is intricate, though key features likely to trigger failure mechanisms were identified. To rely on a tie force provision in current UK guidelines to account for the disproportionate collapse is a huge risk. The critical response observed within the structural system is approximately five times the recommendation in Eurocode 1 (EN1991-1-7). Column Shear force and beam catenary actions are key features in determining the dynamic amplification factor (DAF) of structural systems.

REFERENCES

ABAQUS (2011). *ABAQUS Documentation, Dassault Systèmes, Providence, RI ,USA.*

Abolmaali, A., Matthys, J.H., Farooqi, M. and Choi, Y. (2005). Development of moment–rotation model equations for flush end-plate connections. *Journal of Constructional Steel Research.* 61(12), pp.1595-1612.

Abruzzo, J., Matta, A. and Panariello, G. (2006). Study of Mitigation Strategies for Progressive Collapse of a Reinforced Concrete Commercial Building. *Journal of Performance of Constructed Facilities.* 20(4), pp.384-390.

Adey, B.T., Grondin, G.Y. and Cheng, J.J. (2000). Cyclic loading of end plate moment connections. *Canadian Journal of Civil Engineering.* 27(4), pp.683-701.

Agarwal, A. and Varma, A.H. (2014). Fire induced progressive collapse of steel building structures: The role of interior gravity columns. *Engineering Structures.* 58, pp.129-140.

Agarwal, J. and England, J. (2008). Recent developments in robustness and relation with risk. In: *Proceedings of the ICE - Structures and Buildings*, pp.183-188.

Aggarwal, A.K. (1994). Comparative tests on endplate beam-to-column connections. *Journal of Constructional Steel Research.* 30(2), pp.151-175.

Alashker, Y. and El-Tawil, S. (2010). Design Model for Collapse Capacity of Composite Floors. In: *Structures Congress 2010*. pp.1160-1170.

Alexander, S. (2004). New approach to disproportionate collapse. *The Structural Engineer.* 7(23), pp.14 - 18.

Ang, K.M. and Morris, G.A. (1984). Analysis of three-dimensional frames with flexible beam–column connections. *Canadian Journal of Civil Engineering.* 11(2), pp.245-254.

Aristizabal-Ochoa, J.D. (2010). Second-order slope–deflection equations for imperfect beam–column structures with semi-rigid connections. *Engineering Structures.* 32(8), pp.2440-2454.

Arros, J. and Doumbalski, N. (2007). Analysis of aircraft impact to concrete structures. *Nuclear Engineering and Design.* 237(12–13), pp.1241-1249.

Ashraf, M., Nethercot, D.A. and Ahmed, B. (2007). Sway of semi-rigid steel frames, part 2: Irregular frames. *Engineering Structures.* 29(8), pp.1854-1863.

Azizinamini, A., Bradburn, J.H., Radziminski, J.B. (1985). Static and Cyclic Behavior of Semi-rigid Steel Beam-column Connections: *Final Report : a Report of an Investigation Conducted by the Civil Engineering Department, University of South Carolina.* University of South Carolina.

Baker, J.W., Schubert, M. and Faber, M.H. (2008). On the assessment of robustness. *Structural Safety.* 30(3), pp.253-267.

Bao, Y., Kunnath, S., El-Tawil, S. and Lew, H. (2008). Macromodel-Based Simulation of Progressive Collapse: RC Frame Structures. *Journal of Structural Engineering.* 134(7), pp.1079-1091.

Bayo, E., Cabrero, J.M. and Gil, B. (2006). An effective component-based method to model semi-rigid connections for the global analysis of steel and composite structures. *Engineering Structures.* 28(1), pp.97-108.

Bažant, Z. and Zhou, Y. (2002). Why Did the World Trade Centre Collapse?—Simple Analysis. *Journal of Engineering Mechanics.* 128(1), pp.2-6.

Beeby, A.W. (1999). Safety of structures, and a new approach to robustness. *The Structural Engineer.* 77(4), pp.16-19.

Bennetts, I.D. and Thomas, I.R. (2002). Design of steel structures under fire conditions. *Progress in Structural Engineering and Materials.* 4(1), pp.6-17.

Biondini, F., Frangopol, D.M. and Restelli, S. (2008). On Structural Robustness, Redundancy, and Static Indeterminacy. In: *Structures Congress 2008* pp.1-10.

Bjorhovde, R., Colson, A. and Brozzetti, J. (1990). Classification System for Beam-to-Column Connections. *Journal of Structural Engineering.* 116(11), pp.3059-3076.

Bose, B., Wang, Z. and Sarkar, S. (1997). Finite-Element Analysis of Unstiffened Flush End-Plate Bolted Joints. *Journal of Structural Engineering.* 123(12), pp.1614-1621.

Braham, M. and Jaspart, J.-P. (2004). Is it safe to design a building structure with simple joints, when they are known to exhibit a semi-rigid behaviour? *Journal of Constructional Steel Research.* 60(3–5), pp.713-723.

British Standards Institution. (2005).European committee for standardization. Eurocode 3: design of steel structures-Part1-1: general rules and rules for buildings, BS EN 1993-1-1:2005. UK.

BS5950. (2001). Structural use of steelworks in building. Part 1: Code of practice for the design of simple and continuous costruction: Hot rolled section. London.

BS 8110. (1997). The structural use of concrete in building - Part 1: Code of practice for design construction. London, UK

Bursi, O.S. and Jaspart, J.P. (1998). Basic issues in the finite element simulation of extended end plate connections. *Computers and Structures.* 69(3), pp.361-382.

Buscemi, N. and Marjanishvili, S. (2005). SDOF Model for Progressive Collapse Analysis. In: *Structures Congress* pp.1-12.

Cabrero, J.M. and Bayo, E. (2005). Development of practical design methods for steel structures with semi-rigid connections. *Engineering Structures.* 27(8), pp.1125-1137.

Cabrero, J.M. and Bayo, E. (2007). The semi-rigid behaviour of three-dimensional steel beam-to-column steel joints subjected to proportional loading. Part II: Theoretical model and validation. *Journal of Constructional Steel Research.* 63(9), pp.1254-1267.

Cabrero, J.M. and Bayo, E. (2007). The semi-rigid behaviour of three-dimensional steel beam-to-column joints subjected to proportional loading. Part I. Experimental evaluation. *Journal of Constructional Steel Research.* 63(9), pp.1241-1253.

CEN. (1994).General Actions - Accidental actions *Eurocode 1 - Actions on structures - Part 1-Basis of Design, European Pre Standard ENV 1991-1, Comite Europeen de Normalaization 250.*Brussels, Belgium.

Chen, W. and Kishi, N. (1989). Semirigid Steel Beam-to-Column Connections: Data Base and Modeling. *Journal of Structural Engineering.* 115(1), pp.105-119.

Choi, H.-J., Magallanes, J.M. and Crawford, J.E. (2007). Incorporating Uncertainties in the Blast-Resistant Design. In: *New Horizons and Better Practices*, pp.1-9.

Corley, W., Sr., P., Sozen, M. and Thornton, C. (1998). The Oklahoma City Bombing: Summary and Recommendations for Multihazard Mitigation. *Journal of Performance of Constructed Facilities.* 12(3), pp.100-112.

da S. Vellasco, P.C.G., de Andrade, S.A.L., da Silva, J.G.S., de Lima, L.R.O. and Brito Jr, O. (2006). A parametric analysis of steel and composite portal frames with semi-rigid connections. *Engineering Structures.* 28(4), pp.543-556.

da Silva, J.G.S., de Lima, L.R.O., da S. Vellasco, P.C.G., de Andrade, S.A.L. and de Castro, R.A. (2008). Nonlinear dynamic analysis of steel portal frames with semi-rigid connections. *Engineering Structures.* 30(9), pp.2566-2579.

Díaz, C., Martí, P., Victoria, M. and Querin, O.M. (2011). Review on the modelling of joint behaviour in steel frames. *Journal of Constructional Steel Research.* 67(5), pp.741-758.

Department of Defence (DoD), (2005). "Design of building to resist progressive collapse." Unified Facility Criteria, UFC 4-023-03, Washington, DC.

Department of Defence (DoD), (2009). "Design of building to resist progressive collapse." Unified Facility Criteria, UFC 4-023-03, Washington, DC.

Dusenberry, D. (2002). Review of existing guidelines and provisions related to progressive collapse In: *Worshop on prevention of progressive collapse, National Institute of Building Science, Washington, D.C,.*

Dusenberry, D. and Hamburger, R. (2006). Practical Means for Energy-Based Analyses of Disproportionate Collapse Potential. *Journal of Performance of Constructed Facilities.* 20(4), pp.336-348.

Duthinh, D., Phan, L. and Simiu, E. (2013). Discussion of "Review of Methods to Assess, Design for, and Mitigate Multiple Hazards" by Yue Li, Aakash Ahuja, and Jamie E. Padgett. *Journal of Performance of Constructed Facilities.* 27(2), pp.215-216.

Ellingwood, B. (2005). Strategies for Mitigating Risk of Progressive Collapse. In: *Structures Congress 2005*: American Society of Civil Engineers, pp.1-6.

Ellingwood, B. (2006). Mitigating Risk from Abnormal Loads and Progressive Collapse. *Journal of Performance of Constructed Facilities.* 20(4), pp.315-323.

Ellingwood, B., Marjanishvili, S., Mlakar, P., Sasani, M. and Williamson, E. (2009). Disproportionate Collapse Research Needs. In: *Structures Congress* pp.1-12.

Ellingwood, B.R. and Dusenberry, D.O. (2005). Building Design for Abnormal Loads and Progressive Collapse. *Computer-Aided Civil and Infrastructure Engineering.* 20(3), pp.194-205.

Ellingwood. B.R and Leyendecker E. V. (1978). Approaches for Design against Progressive Collapse. *Journal of the Structural Division.* 105(1), pp.413-423.

Elsanadedy, H.M., Almusallam, T.H., Alharbi, Y.R., Al-Salloum, Y.A. and Abbas, H. (2014). Progressive collapse potential of a typical steel building due to blast attacks. *Journal of Constructional Steel Research.* 101, pp.143-157.

EN1991 -1-7: (2006). *Action on Structures - Part 1-7: General actions -accidental action.* London, UK

EN 1990: (2002). *Eurocode: Basis for structural design.*

EN 1993-1-8. (2005).*Design of steel structures.* Brussels.

England, J., Agarwal, J. and Blockley, D. (2008). The vulnerability of structures to unforeseen events. *Computers and Structures.* 86(10), pp.1042-1051.

Faber, M. (2006). Robustness of structures: an introduction. *Structural Engineering International.* 16(2), pp.101-107.

FEMA 356. (2000).Prestandard and commentary for the seismic rehabilitation of buildings.Reston, Virginia.

FEMA 427. (2003).Primer for Design of Commercial Buildings to Mitigate Terrorist Attacks. *Risk Mangement Series.*

Feng, J. and Cai, J. (2009). Progressive Collapse of Cable-Stayed Bridges. In: *International Conference on Transportation Engineering* pp.2483-2489.

Fontaine, M. and Steinemann, A. (2009). Assessing Vulnerability to Natural Hazards: Impact-Based Method and Application to Drought in Washington State. *Natural Hazards Review.* 10(1), pp.11-18.

Formisano, A., Landolfo, R. and Mazzolani, F.M. (2015). Robustness assessment approaches for steel framed structures under catastrophic events. *Computers and Structures.* 147, pp.216-228.

Fu, F. (2010). 3-D nonlinear dynamic progressive collapse analysis of multi-storey steel composite frame buildings — Parametric study. *Engineering Structures.* 32(12), pp.3974-3980.

Fu, F. (2012). Response of a multi-storey steel composite building with concentric bracing under consutive column removal scenarios. *Journal of Constructional Steel Research.* 70, pp.115-126.

Galvão, A.S., Silva, A.R.D., Silveira, R.A.M. and Gonçalves, P.B. (2010). Nonlinear dynamic behaviour and instability of slender frames with semi-rigid connections. *International Journal of Mechanical Sciences.* 52(12), pp.1547-1562.

Garlock, M., Ricles, J. and Sause, R. (2003). Cyclic Load Tests and Analysis of Bolted Top-and-Seat Angle Connections. *Journal of Structural Engineering.* 129(12), pp.1615-1625.

General Service Administration (GSA). (2003). Progressive collapse analysis and design guidelines for new federal office buildings and major modernization projects, U.S. General Service Administration, Washington, DC.

Gerasimidis, S. and Baniotopoulos, C.C. (2011). Steel moment frames column loss analysis: The influence of time step size. *Journal of Constructional Steel Research.* 67(4), pp.557-564.

Ghobarah, A., Korol, R. and Osman, A. (1992). Cyclic Behaviour of Extended End-Plate Joints. *Journal of Structural Engineering.* 118(5), pp.1333-1353.

Godschalk, D. (2003). Urban Hazard Mitigation: Creating Resilient Cities. *Natural Hazards Review.* 4(3), pp.136-143.

Goel, R.K. (1997). Period Formulas for Moment-Resisting Frame Buildings. *Journal of Structural Engineering.* 123(11), pp.1454-1461.

Goverdham, A.V. (1983). *A collection of experimental moment rotation curves and evaluation of prediction equations for semi rigid connections, In partial fulfilment for the award of Master of Science.* Master of Science thesis, Vanderbilt University, at Nashville, Tenn.

Goverdhan, A.V. (1983). *A collection of experimental moment-rotation curves and evaluation of prediction equations for semi-rigid connections.* M. Sc. thesis, Vanderbilt University.

Griffiths, H., Pugsley, A. G., and Saunders, O. (1968). Report of the inquiry into the collapse of flats at Ronan Point, Canning Town. Her Majesty's Stationery Office,. In: *London.*

Gross, J. and McGuire, W. (1983). Progressive Collapse Resistant Design. *Journal of Structural Engineering.* 109(1), pp.1-15.

GSA. (2013).*General Service Admnistration, Alternate Path Analysis and Design Guidelines for Progressive Collapse Resistance.*

Hadi, M.N.S. and Alrudaini, T.M.S. (2011). Preventing the Progressive Collapse of Reinforced Concrete Buildings. In: *Proceedings of the thirteenth international conference on civil, structural and environmental engineering computing, UK.* Civil-Comp Press, Stirlingshire.

Hadianfard, M.A. and Razani, R. (2003). Effects of semi-rigid behaviour of connections in the reliability of steel frames. *Structural Safety.* 25(2), pp.123-138.

Hartmann, D., Breidt, M., Nguyen, V., Stangenberg, F. and Höhler, S., Schweizerhof, K. (2008). Structural collapse simulation under consideration of uncertainty - Fundamental concept and results. *Computer Structure.* 86, pp.2064-2078.

Hueste, M.B.D. and Bai, J.-W. (2007). Seismic retrofit of a reinforced concrete flat-slab structure: Part I — seismic performance evaluation. *Engineering Structures.* 29(6), pp.1165-1177.

Humay, F.K. and Baldridge, S.M. (2005). Multi Hazard Approach to Progressive Collapse Mitigation. In: *Structures Congress* pp.1-12.

Izzuddin, B.A., Vlassis, A.G., Elghazouli, A.Y. and Nethercot, D.A. (2008). Progressive collapse of multi-storey buildings due to sudden column loss — Part I: Simplified assessment framework. *Engineering Structures.* 30(5), pp.1308-1318.

Jaspart, J.-P. (1988). Extending of the merchant-rankine formula for the assessment of the ultimate load of frames with semi-rigid joints. *Journal of Constructional Steel Research.* 11(4), pp.283-312.

Jaspart, J.-P. and Maquoi, R. (1990). Guidelines for the design of braced frames with semi-rigid connections. *Journal of Constructional Steel Research.* 16(4), pp.319-328.

Jenkins, W.M., Tong, C.S. and Prescott, A.T. (1986). Moment transmitting endplate connections in Steel construction, and a proposed basis for flush endplate design. *The structural Engineer.* 64A(5), pp.121-131.

Jeong, S.-H. and Elnashai, A.S. (2007). Fragility relationships for torsionally-imbalanced buildings using three-dimensional damage characterization. *Engineering Structures.* 29(9), pp.2172-2182.

Kim, J. and Park, J., (2008). Design of steel moment frames considering progressive collapse. *Steel and Composite Structures*, *8*(1), pp.85-98.

Kim, J., Ghaboussi, J. and Elnashai, A.S. (2010). Mechanical and informational modeling of steel beam-to-column connections. *Engineering Structures.* 32(2), pp.449-458.

Kaewkulchai, G. and Williamson, E.B. (2004). Beam element formulation and solution procedure for dynamic progressive collapse analysis. *Computers and Structures.* 82(7–8), pp.639-651.

Khandelwal, K., El-Tawil, S., Kunnath, S. and Lew, H. (2008). Macromodel-Based Simulation of Progressive Collapse: Steel Frame Structures. *Journal of Structural Engineering.* 134(7), pp.1070-1078.

Khandelwal, K., El-Tawil, S. and Sadek, F. (2009). Progressive collapse analysis of seismically designed steel braced frames. *Journal of Constructional Steel Research.* 65(3), pp.699-708.

Kim, H.-S., Kim, J. and An, D.-W. (2009). Development of integrated system for progressive collapse analysis of building structures considering dynamic effects. *Advances in Engineering Software.* 40(1), pp.1-8.

Kim, J. and Choi, H. (2004). Behaviour and design of structures with buckling-restrained braces. *Engineering Structures.* 26(6), pp.693-706.

Kim, J. and Kim, T. (2009a). Assessment of progressive collapse-resisting capacity of steel moment frames. *Journal of Constructional Steel Research.* 65(1), pp.169-179.

Kim, T. and Kim, J. (2009b). Collapse analysis of steel moment frames with various seismic connections. *Journal of Constructional Steel Research.* 65(6), pp.1316-1322.

Kishi, N. and Chen, W. (1990). Moment-Rotation Relations of Semirigid Connections with Angles. *Journal of Structural Engineering.* 116(7), pp.1813-1834.

Kokot, S., Anthoine, A., Negro, P. and Solomos, G. (2012). Static and dynamic analysis of a reinforced concrete flat slab frame building for progressive collapse. *Engineering Structures.* 40, pp.205-217.

Kwasniewski, L. (2010). Nonlinear dynamic simulations of progressive collapse for a multistory building. *Engineering Structures.* 32(5), pp.1223-1235.

Lee, C.-H., Kim, S., Han, K.-H. and Lee, K. (2009). Simplified nonlinear progressive collapse analysis of welded steel moment frames. *Journal of Constructional Steel Research.* 65(5), pp.1130-1137.

Lee, K., Kim, J., Hall, B.E., Karns, J.E. and Houghton, D.L. (2007). Analytical Verification of Blast Testing of Steel Frame Moment Connection Assemblies. *Structural Engineering Research Frontiers.* pp.1-19.

Lew, H., Main, J., Robert, S., Sadek, F. and Chiarito, V. (2012). Performance of Steel Moment Connections under a Column Removal Scenario. I: Experiments. *Journal of Structural Engineering.* 139(1), pp.98-107.

Lew, H., Main, J., Robert, S., Sadek, F. and Chiarito, V. (2013). Performance of Steel Moment Connections under a Column Removal Scenario. I: Experiments. *Journal of Structural Engineering.* 139(1), pp.98-107.

Li, Y., Ahuja, A. and Padgett, J. (2012). Review of Methods to Assess, Design for, and Mitigate Multiple Hazards. *Journal of Performance of Constructed Facilities.* 26(1), pp.104-117.

Li, Y. and Padgett, J. (2013). Closure to "Review of Methods to Assess, Design for, and Mitigate Multiple Hazards" by Yue Li, Aakash Ahuja, and Jamie E. Padgett. *Journal of Performance of Constructed Facilities.* 27(2), pp.216-216.

Liu, J.L. (2010). Preventing progressive collapse through strengthening beam-to-column connection, Part 2: Finite element analysis. *Journal of Constructional Steel Research.* 66(2), pp.238-247.

Liu, M. (2013). A new dynamic increase factor for nonlinear static alternate path analysis of building frames against progressive collapse. *Engineering Structures.* 48, pp.666-673.

Liu, R., Davison, B. and Tyas, A. (2005). A Study of Progressive Collapse in Multi-Storey Steel Frames. *Structures Congress* pp.1-9.

Liu Y, Xu L and Grierson D.E. (2010). Influence of Semi-Rigid Connections and Local Joint Damage on Progressive Collapse of Steel Frameworks. *Computer - Aided Civil and Infrastructural Engineering.* 25(3), pp.pp184-204.

Lu, L.-W., Ricles, J.M., Mao, C. and Fisher, J.W. (2000). Critical issues in achieving ductile behaviour of welded moment connections. *Journal of Constructional Steel Research.* 55(1–3), pp.325-341.

Maggi, Y.I., Gonçalves, R.M., Leon, R.T. and Ribeiro, L.F.L. (2005). Parametric analysis of steel bolted end plate connections using finite element modeling. *Journal of Constructional Steel Research.* 61(5), pp.689-708.

Mahin, S.A. (1998). Lessons from damage to steel buildings during the Northridge earthquake. *Engineering Structures.* 20(4–6), pp.261-270.

Malla, R.B., Agarwal, P. and Ahmad, R. (2011). Dynamic analysis methodology for progressive failure of truss structures considering inelastic postbuckling cyclic member behaviour. *Engineering Structures.* 33(5), pp.1503-1513.

Marjanishvili, S. (2004). Progressive Analysis Procedure for Progressive Collapse. *Journal of Performance of Constructed Facilities.* 18(2), pp.79-85.

Marjanishvili, S. and Agnew, E. (2006). Comparison of Various Procedures for Progressive Collapse Analysis. *Journal of Performance of Constructed Facilities.* 20(4), pp.365-374.

Marjanishvili, S. and Buscemi, N. (2005). SDOF Model for Progressive Collapse Analysis. *Structures Congress.* pp.1-12.

Mark Adom-Asamoah and Ankamah, N.O. (2016). Effect of Design Ductility on the Progressive Collapse Potential of RC Frame Structures Designed to Eurocode 8. *American Journal of Civil Engineering.* 4(2), pp. 40-49.

Mashaly, E., El-Heweity, M., Abou-Elfath, H. and Osman, M. (2011). Finite element analysis of beam-to-column joints in steel frames under cyclic loading. *Alexandria Engineering Journal.* 50(1), pp.91-104.

McKay, A., Marchand, K. and Diaz, M. (2012). Alternate Path Method in Progressive Collapse Analysis: Variation of Dynamic and Nonlinear Load Increase Factors. *Practice Periodical on Structural Design and Construction.* 17(4), pp.152-160.

Mitchell, D. and Cook, W. (1984). Preventing Progressive Collapse of Slab Structures. *Journal of Structural Engineering.* 110(7), pp.1513-1532.

Mlakar, P. (2005). The Pentagon Building Performance Study. *Journal of Performance of Constructed Facilities.* 19(3), pp.188-188.

Mohamadi-Shoore, M.R. and Mofid, M. (2011). New modeling for moment–rotation behaviour of bolted endplate connections. *Scientia Iranica.* 18(4), pp.827-834.

Mohamadi-Shooreh, M., Mofid, M. and McCabe, S.L. (2013). Empirical Model of the Moment-Rotation Curve of Beam-to-Beam Bolted Flush Endplate Connections. *Journal of Structural Engineering.* 139(1), pp.66-72.

Mohamadi-shooreh, M.R. and Mofid, M. (2008). Parametric analyses on the initial stiffness of flush end-plate splice connections using FEM. *Journal of Constructional Steel Research.* 64(10), pp.1129-1141.

Mohamed, O. (2006). Progressive Collapse of Structures: Annotated Bibliography and Comparison of Codes and Standards. *Journal of Performance of Constructed Facilities.* 20(4), pp.418-425.

Mohamed, O.A. (2009). Assessment of progressive collapse potential in corner floor panels of reinforced concrete buildings. *Engineering Structures.* 31(3), pp.749-757.

Möller, B., Liebscher, M., Schweizerhof, K., Mattern, S. and Blankenhorn, G. (2008). Structural collapse simulation under consideration of uncertainty - Improvement of numerical efficiency. *Comput Struct.* 86, pp.1875-1884.

Morris, G.A. and Packer, J.A. (1987). Beam-to-column connections in steel frames. *Canadian Journal of Civil Engineering.* 14(1), pp.68-76.

Nair, R. (2006). Preventing Disproportionate Collapse. *Journal of Performance of Constructed Facilities.* 20(4), pp.309-314.

Nair, R.S. (2004). Progressive collapse basics,. In: *The Steel Conference, Mordern Steel Construction, North America.* pp.1-3.

Neal, M., Garlock, M., Quiel, S. and Marjanishvili, S. (2012). Effects of Fire on a Tall Steel Building Designed to Resist Progressive Collapse. *Structures Congress* pp.246-256.

NEHRP. (1994) Building Seismic Safety Council. *Recommended provisions for the development of seismic regulations for new buildings.*Washington. D.C.

Nethercot, D.A. (2011). Design of Building Structures to Improve their Resistance to Progressive Collapse. *Procedia Engineering.* 14, pp.1-13.

NIST. (2007).Best Practices for Reducing the Potential for Progressive Collapse in Buildings. *National Institute of Standards and Technology (NIST)* Washinton, D.C: Technology Administration, Department of Commerce, U.S

Osteraas, J. (2006). Murrah Building Bombing Revisited: A Qualitative Assessment of Blast Damage and Collapse Patterns. *Journal of Performance of Constructed Facilities.* 20(4), pp.330-335.

Park, J. and Kim, J. (2010). Fragility analysis of steel moment frames with various seismic connections subjected to sudden loss of a column. *Engineering Structures.* 32(6), pp.1547-1555.

Pearson, C. and Delatte, N. (2003). Lessons from the Progressive Collapse of the Ronan Point Apartment Tower. *Forensic Engineering* pp.190-200.

Pearson, C. and Delatte, N. (2005). Ronan Point Apartment Tower Collapse and its Effect on Building Codes. *Journal of Performance of Constructed Facilities.* 19(2), pp.172-177.

Picard, A., Giroux, Y.-M. and P.Brun. (1976). Analysis of flexibly connected steel frames: Discussion. *Canadian Journal of Civil Engineering.* 3(2), pp.350-352.

Powell, G. (2005). Progressive Collapse: Case studies Using Nonlinear Analysis. In: *Structures Congress 2005,* pp.1-14.

Prabha, P., Marimuthu, V., Saravanan, M. and Arul Jayachandran, S. (2010). Evaluation of connection flexibility in cold formed steel racks. *Journal of Constructional Steel Research.* 66(7), pp.863-872.

Prater, C. and Lindell, M. (2000). Politics of Hazard Mitigation. *Natural Hazards Review.* 1(2), pp.73-82.

Pujol, S. and Paul Smith-Pardo, J. (2009). A new perspective on the effects of abrupt column removal. *Engineering Structures.* 31(4), pp.869-874.

Qian, J., Yu, H., Yan, F., Dong, H., Li, J. and Liu, Y. (2005). Experimental study on full-scale steel beam-to-column moment connections. *Earthquake Engineering and Engineering Vibration.* 4(2), pp.311-323.

Richard R. M. and Abbot B. J. (1975). Versatile elastic-plastic stress-strain formula. *Journal of the Engineering Mechanics Division.* 101(4), pp.511-515.

Ruth, P., Marchand, K. and Williamson, E. (2006). Static Equivalency in Progressive Collapse Alternate Path Analysis: Reducing Conservatism while Retaining Structural Integrity. *Journal of Performance of Constructed Facilities.* 20(4), pp.349-364.

Sadek, F., Main, J., Lew, H. and El-Tawil, S. (2012). Performance of Steel Moment Connections under a Column Removal Scenario. II: Analysis. *Journal of Structural Engineering.* 139(1), pp.108-119.

Salama, I.M. (2015). Estimation of period of vibration for concrete moment-resisting frame buildings. *HBRC Journal.* 11(1), pp.16-21.

Samuel Tan and Astaneh-Asl, A. (2003). Use of steel cables to prevent progressive collapse of existing buildings. In: *Proceedings of sixth conference on tall buildings in seismic regions, Los Angeles, California,*. pp.1-20.

SAP 2000.Integrated software for structural analysis and design. Computers and Structures. Berkeley, California.

SEI/ASCE 7-05. American Society of Civil Engineers. *Minimum Design Loads for Building and Other Structures* Reston (VA, USA).

Sherbourne, A. and Bahaari, M. (1994). 3D Simulation of End-Plate Bolted Connections. *Journal of Structural Engineering.* 120(11), pp.3122-3136.

Sherbourne, A. and Bahaari, M. (1997). Finite Element Prediction of End Plate Bolted Connection Behaviour. I: Parametric Study. *Journal of Structural Engineering.* 123(2), pp.157-164.

Shi, Y., Chan, S. and Wong, Y. (1996). Modeling for Moment-Rotation Characteristics for End-Plate Connections. *Journal of Structural Engineering.* 122(11), pp.1300-1306.

Simões da Silva, L., Santiago, A. and Vila Real, P. (2001). A component model for the behaviour of steel joints at elevated temperatures. *Journal of Constructional Steel Research.* 57(11), pp.1169-1195.

Sozen, Thornton, C., Corley, W. and Sr. (1998). The Oklahoma City Bombing: Structure and Mechanisms of the Murrah Building. *Journal of Performance of Constructed Facilities.* 12(3), pp.120-136.

Starossek, U. and Haberland, M. (2009). Evaluating Measures of Structural Robustness. In: *Structures Congress 2009,* pp.1-8.

Stephen, D., Ye, J. and Lam, D. (2011). Realistic Modelling of High Rise Steel Structures subjected to progressive collapse. In: *Thirteenth International Conference on Civil, Structural and Environmental Engineering Computing,* UK: Civil Comp Press,Stirlingshire UK.

Stephen, D., Ye, J. and Lam, D. (2012). Progressive Collapse Evaluation of High Rise Steel Structures due to Sudden Loss of Structural Members. In: *10th International Conference on Advances in steel Concrete Composite and Hybrid Structures, Singapore*. pp.1179-1186.

Stephen, O.D., Lam, D. and Toropov, V.V. (2013). Assessment of column removal time for progressive collapse evaluation of high rise structures. *Research and Applications in Structural Engineering, Mechanics and Computation.* CRC Press, pp.699-704.

Stevens, D., Crowder, B., Sunshine, D., Marchand, K., Smilowitz, R., Williamson, E. and Waggoner, M. (2011). DoD Research and Criteria for the Design of Buildings to Resist Progressive Collapse. *Journal of Structural Engineering.* 137(9), pp.870-880.

Tohidi, M., Yang, J. and Baniotopoulos, C. (2014b). Numerical evaluations of codified design methods for progressive collapse resistance of precast concrete cross wall structures. *Engineering Structures.* 76, pp.177-186.

Tsai, M.-H. (2010). An analytical methodology for the dynamic amplification factor in progressive collapse evaluation of building structures. *Mechanics Research Communications.* 37(1), pp.61-66.

Tsai, M.-H. (2012). A performance-based design approach for retrofitting regular building frames with steel braces against sudden column loss. *Journal of Constructional Steel Research.* 77, pp.1-11.

Tsai, M.-H. and Lin, B.-H. (2009). Dynamic amplification factor for progressive collapse resistance analysis of an RC building. *The Structural Design of Tall and Special Buildings.* 18(5), pp.539-557.

Türker, T. and Bayraktar, A. (2011). Experimental and numerical investigation of brace configuration effects on steel structures. *Journal of Constructional Steel Research.* 67(5), pp.854-865.

Usmani, A.S., Chung, Y.C. and Torero, J.L. (2003). How did the WTC towers collapse: A new theory. *Fire Safety Journal.* 38, pp.501-533.

Vlassis, A.G., Izzuddin, B.A., Elghazouli, A.Y. and Nethercot, D.A. (2006). Design Oriented Approach for Progressive Collapse Assessment of Steel Framed Buildings. *Structural Engineering International.* 16(2), pp.129-136

Vlassis, A.G., Izzuddin, B.A., Elghazouli, A.Y. and Nethercot, D.A. (2008). Progressive collapse of multi-storey buildings due to sudden column loss—Part II: Application. *Engineering Structures.* 30(5), pp.1424-1438.

Vlassis, A.G., Izzuddin, B.A., Elghazouli, A.Y. and Nethercot, D.A. (2009). Progressive collapse of multi-storey buildings due to failed floor impact. *Engineering Structures.* 31(7), pp.1522-1534.

Wada, A., Ohi, K., Suzuki, H., Kohno, M. and Sakumoto, Y. (2004). A Study on the Collapse Control Design Method for High-Rise Steel Buildings. *Structural Engineering International.* 16(2), pp.137-141.

Xu, G. and Ellingwood, B.R. (2011). Disproportionate collapse performance of partially restrained steel frames with bolted T-stub connections. *Engineering Structures.* 33(1), pp.32-43.

Yang, B. and Tan, K. (2012a). Robustness of Bolted-Angle Connections against Progressive Collapse: Experimental Tests of Beam-Column Joints and Development of Component-Based Models. *Journal of Structural Engineering.* 139(9), pp.1498-1514.

Yang, B. and Tan, K.H. (2012b). Numerical analyses of steel beam–column joints subjected to catenary action. *Journal of Constructional Steel Research.* 70, pp.1-11.

Yang, B. and Tan, K.H. (2013). Experimental tests of different types of bolted steel beam–column joints under a central-column-removal scenario. *Engineering Structures.* 54, pp.112-130.

Yang, B., Tan, K.H. and Xiong, G. (2015). Behaviour of composite beam–column joints under a middle-column-removal scenario: Component-based modelling. *Journal of Constructional Steel Research.* 104, pp.137-154.

Yee, Y. and Melchers, R. (1986). Moment-rotation curves for bolted connections. *Journal of Structural Engineering.* 112(3), pp.615-635.

Yu, H., Burgess, I.W., Davison, J.B. and Plank, R.J. (2009). Tying capacity of web cleat connections in fire, Part 2: Development of component-based model. *Engineering Structures.* 31(3), pp.697-708.

Yu, M., Zha, X. and Ye, J. (2010). The influence of joints and composite floor slabs on effective tying of steel structures in preventing progressive collapse. *Journal of Constructional Steel Research.* 66(3), pp.442-451.